An investigation of the products formed through oxidative transformations of some antibiotics using Nuclear Magnetic Resonance spectroscopic and chromatographic/mass spectrometric techniques

Sahar Radi

BSc (Honours)

Thesis submitted for the fulfilment of the requirement for the degree of
Doctor of Philosophy (PhD)

Victoria University, Australia
Institute for Sustainable Industries and Liveable Cities (ISILC)

August 2025

Abstract

Antibiotics are increasingly recognized as emerging pollutants due to their continual release into aquatic environments, where they contribute to antimicrobial resistance and generate transformation products with uncertain toxicity. This study investigated the degradation behaviour of three representative antibiotics, Penicillin G, Amoxicillin, and Ciprofloxacin, under an oxidative treatment, with an initial assessment of UV irradiation and a detailed investigation of treatment sodium hypochlorite solution, a widely used water disinfectant.

Preliminary experiments tested UV irradiation on both solid and solution forms of the antibiotics using spectroscopic means (FTIR and NMR), but no measurable structural changes were observed under the experimental conditions. Based on these findings, the study focused on oxidation using sodium hypochlorite solution, which showed clear and measurable degradation for the target antibiotics.

A dual analytical approach combined ^{1}H, $^{13}C$and ^{19}F Nuclear Magnetic Resonance (NMR) spectroscopy with High-performance liquid chromatography/ Mass spectrometry (HPLC/MS) to provide complementary insights into the degradation process. Initially, FTIR spectroscopy (ATR mode) was also employed as a supporting technique to characterise the pristine antibiotics and their oxidised forms after UV and sodium hypochlorite solution treatment. The FTIR spectra revealed notable band shifts and intensity changes, suggesting functional group modifications in case of modified versions through sodium hypochlorite solution treatment, though the information was limited and could not conclusively resolve specific degradation pathways.

The NMR spectroscopic analyses revealed real-time functional group changes, including β-lactam ring opening, side-chain rearrangements, and piperazine ring oxidation, while HPLC/MS identified and tracked the parent compounds and their key transformation products over time. For the β-lactam antibiotics, Penicillin G and Amoxicillin, NMR and HPLC/MS together confirmed rapid and extensive degradation, with the parent ions (m/z 365 and m/z 364) disappearing quickly and products such as penicilloic acid, penilloic acid, and other lower-mass fragments forming sequentially. In contrast, Ciprofloxacin showed partial, slower degradation, where the piperazine ring was oxidised (producing m/z 306 and 362), but the parent ion (m/z 332) persisted after 24 hours, and the cyclopropyl ring remained intact.

By correlating NMR and LC/MS data, this thesis provides a detailed picture of antibiotic behaviour under sodium hypochlorite solution treatment, demonstrating that β-lactams degrade readily, while fluoroquinolones are more resistant. These findings have important implications for water disinfection strategies, highlighting both the effectiveness of sodium hypochlorite solution for some antibiotic classes and the need for further treatment processes for more persistent compounds.

Declaration of Authenticity

I, Sahar Radi, declare that the PhD thesis entitled, *An investigation of the products formed through oxidative transformations of some antibiotics using Nuclear Magnetic Resonance spectroscopic and chromatographic/mass spectrometric techniques*, is no more than 80,000 words in length including quotes and exclusive of tables, figures, appendices, bibliography, references and footnotes. This thesis contains no material that has been submitted previously, in whole or in part, for the award of any other academic degree or diploma. Except where otherwise indicated, this thesis is my own work.

I have conducted my research in alignment with the Australian Code for the Responsible Conduct of Research and Victoria University's Higher Degree by Research Policy and Procedures.

Signature 11 August 2025

Acknowledgements

Firstly, I greatly acknowledge my principal supervisor, Dr Paul Joseph, for accepting me as his student and for his enduring guidance and constant encouragement, without which this thesis would not have been possible. I am also grateful to my associate supervisor, Professors Andrew Smallridge, for his constant help and support throughout my PhD programme. I also greatly acknowledge the technical support from various people at Victoria University; Stacey Lloyd; Nishantha Illangantilaka; Larruceo Bautista and Vanessa Barriga. In addition, I am greatly indebted to Victoria University for the provision of a Research Scholarship for my doctoral study.

My family has always been my pillars of support, and I am forever indebted and deeply register my heartfelt gratitude towards my both parents, my sisters, Nada and Noha, especially my mum, Sana, for her unfailing love and support from the very beginning. I am who I am, because I am apart of you, and no words could ever express how blessed I am to have you all in my life.

Last but never the least, I express my profound gratefulness to my teachers, past and present and all my friends, close relatives, husband and my kids who helped and supported me in every way possible during this doctoral journey!

Planned research outputs relating to the PhD programme

I. Peer-reviewed papers

Sahar Radi, Paul Joseph and Andrew Smallridge, “A review of wastewater treatment strategies for mitigating the problem of antibiotic resistance”, *Environmental Science: Water Research and Technology*, (Elsevier, Q1: under review).

List of abbreviations

With a view to simplifying the main text, the following abbreviations are used:

AOP – Advanced Oxidation Process

ARB – Antibiotic-Resistant Bacteria

AGR – Antibiotic Resistance Genes

ca. – Approximately

DBPs – Disinfection By-Products

EAOP – Electrochemical Advanced Oxidation Process

EO – Electrochemical Oxidation

FTIR – Fourier-transform Infrared Spectroscopy

HPLC – High-performance Liquid Chromatography

HPLC/MS – High-performance Liquid Chromatography/Mass Spectrometry

m/z – Mass-to-Charge Ratio

MS/MS – Tandem Mass Spectrometry

NMR – Nuclear Magnetic Resonance

PCDD – Polychlorinated Dibenzo-p-dioxins

PDS – Peroxydisulfate (Persulfate)

PMS – Peroxymonosulfate

PPCs – Pharmaceutical and Personal Care Products

ROS – Reactive Oxygen Species

SR-AOPs – Sulfate Radical-Based Advanced Oxidation Processes

TIC – Total Ion Chromatogram

UHPLC – Ultra High-performance Liquid Chromatography

UV – Ultraviolet

UV-Vis – Ultraviolet–Visible Spectroscopy

UWTPs – Urban Wastewater Treatment Plants

WWTP – Wastewater Treatment Plants

WHO – World Health Organisation

Contents

List of Figures

List of Tables

CHAPTER 1: INTRODUCTION

This chapter, predominantly, discusses the relevant literature precedents pertaining to the thesis in detail. Here, firstly, the subject matter of the PhD programme is introduced, followed by an in-depth analysis of its various facets, which include: different ways to disinfecting wastewater in general and advanced oxidation processes, in particular. This has led to identifying some research gaps, and their respective rationale Finally, the overall aim and the individual objectives of the research programme are described.

1. General background and literature review

1.1 Introduction

It is now well recognized that the discovery of antibiotics is one of the greatest achievements that led to effective treatments against bacterial infection, and thus improving the quality of life of patients worldwide. However, over time, a serious problem has emerged, mainly through the widespread use, and often misuse, of antibiotics. Over the decades, this has resulted in the emergence of antibiotic-resistant pathogens. The development of antibiotic resistance is a major problem for humans and has resulted in serious and fatal consequences on a daily basis across the globe (Elder et al., 2016, Manaia et al., 2018(Sanganyado and Gwenzi, 2019, Shah, 2009, Manaia, 2017, Levy and Marshall, 2004)

Antibiotic resistance is generally referred to the ability of bacteria to survive in the presence of antibiotics (Wang et al., 2020). Resistance to antibiotics is determined in segments of DNA called antibiotic-resistance genes (ARGs), which enable bacteria to fight antibiotics by employing different mechanisms, such as modifying the cellular target, degrading, or modifying the antibiotic and preventing uptake of the cell (Levy and Marshall, 2004). The main problem here is that antibiotic-resistant bacteria can survive and multiply better than those usually fail in the presence of antibiotics, thus resulting in the proliferation of the populations of resistant strains during the course of treatment (Manaia et al., 2018, Pruden, 2014).

As stated above, especially, in recent years the enhanced prevalence of antibiotic resistance has become a major problem for humans and has resulted in fatal consequences on a daily basis across the globe (Elder et al., 2016, O'Neil, 2015, Le Page et al., 2017). The resistant strains of antimicrobial pathogens are always referred to as ‘superbugs’ and they are a growing concern worldwide (Alpert, 2017). ‘Superinfections’, also known as secondary infections, is the condition whereby an individual is infected by a secondary bacterial infection while the person is being treated for a primary infection, usually caused by a virus, which is increasing now-a-days. Secondary bacterial infections, especially in older adults can be potentially fatal (Jones et al., 2008). Worldwide, it is estimated that there are more than 700,000 deaths annually caused by antimicrobial resistance infections and predicted that this figure could reach 10 million by 2050 if no action will be taken (O'Neil, 2015, Sanganyado and Gwenzi, 2019). This growing threat has drawn attention not only to the clinical misuse of antibiotics but also to the environmental pathways through which resistance can emerge and spread (O'Neil, 2015)(L. Riaz, 2020, Manaia et al., 2018, Neth et al., 2019).

The use of antibiotics in animal husbandry, poultry, and other areas has been also associated in increasing the emergence of resistant strains of pathogenic bacteria that is capable in impacting human health (Bound and Voulvoulis, 2004). One of the main concerns for the release of antibiotics into the environment is related to the development of antibiotic-resistance genes (ARGs) and antibiotic-resistance bacteria (ARB) (Rizzo et al., 2013). Most effluents from urban wastewater treatment plants (UWTPs) are the main anthropogenic sources for the spread of bacterial resistance into the environment (Manaia et al., 2018). As a consequence, the increasing environmental problem of antimicrobial resistance can compromise the therapeutic effectiveness of commonly used drugs for the treatment of human and animal infections (Rizzo et al., 2013). A recent study by the World Health Organization (WHO) reported the speed at which bacteria develop antimicrobial resistance overtakes the discovery and development of the drugs resulting in untreatable infections (Venter, 2019). This highlights the need to consider not only clinical antibiotic use but also the environmental pathways, particularly wastewater systems, that facilitate the persistence and spread of resistance.

The significant effects of antibiotic resistance are beginning to play out worldwide (O'Neil, 2015, Venter, 2019). The WHO, the US Centre for Disease Control and Prevention, and many other global and national agencies have recognized antibiotic resistance as a crucial challenge of our time (Venter, 2019, Alpert, 2017). The global rate of resistance among many disease-causing bacteria continues to rise (Venter, 2019, Pruden, 2014).

There are several contributing factors to this growing crisis, including the increased movement of people through international travel and health tourism, as well as the overuse of antibiotics and the inappropriate or ineffective use of antimicrobial drugs in both human and veterinary medicines (Elder et al., 2016). Recent studies have also shown that sub-inhibitory concentrations of antibiotics may have more extensive and complex effects on bacterial populations than previously understood, owing to the adaptive capacity of bacterial communities (Santos-Lopez et al., 2019). This also gradually leads to a decrease in the general efficiency of antibiotics, and that in return threatens their ability to fight infectious diseases. Therefore, when it becomes more difficult to treat a pathogen, the possibility of emergence of a newer-type of antibiotic-resistant bacterium is also enhanced (Elder et al., 2016).

Moreover, antibiotic concentrations have also been detected in various aquatic environments, such as surface water and wastewater (Keen and Linden, 2013). Urban wastewater treatment plants (UWTPs) are commonly designed to cleanse urban wastewater so that the treated wastewater satisfies the quality requirements for recycled water and controls urban water

pollution (Michael et al., 2013). UWTPs can be considered as hotspots for antibiotic resistant bacteria, spread of genes and the associated gene transfer into the environment (Michael et al., 2013).

This happens as UWTPs holds several favorable factors, such as: a high cell density sustained by a nutrient rich environment and a regular contamination with both antibiotics and resistant bacteria (Michael et al., 2013). Furthermore, UWTPs normally involves many different processes, such as mechanical, biological, physical, and chemical. These processes affect the fate of antibiotics, Antibiotic Resistance Bacteria (ARB) and Antibiotic Resistance Genes (ARGs) in different ways (Michael et al., 2013, Rizzo et al., 2013). As a result, resistant strains and resistance genes may persist through treatment and ultimately be released into the environment (Sanganyado and Gwenzi, 2019, Michael et al., 2013).

The method for the classification and evaluation of ARB, ARGs and genes transfer are well documented in the literature in a comprehensive way to enable the understanding of the effect of wastewater treatment processes on ARB and ARGs (Michael et al., 2013, Ferreira et al., 2020, Yuksek et al., 2016). Apparently, it is very clear now that human activities, including WWTPs, have a strong impact on the distribution of ARGs in the aquatic environment (Allen et al., 2010, Pruden, 2014). This growing awareness has led to increased research into wastewater discharges from different sources within the sewerage system. Hospital effluents typically enter municipal wastewater treatment plants and can contribute to the overall presence of antibiotic-resistant bacteria and resistance genes in treated wastewater. As a result, studies have examined both the effectiveness of disinfection processes in reducing microorganisms and the role of advanced treatment processes in addressing antibiotic residues that are not removed by disinfection alone (Alpert, 2017).

Additionally, hospital effluents are known to contain high concentrations of antimicrobial-resistant bacteria and residual antibiotics, which are discharged into aquatic and soil environments following wastewater treatment (Berendonk et al., 2015). These effluents, primarily resulting from antibiotic use by patients, contribute significantly to the environmental load of resistance genes and compounds (Berendonk et al., 2015, Rizzo et al., 2013).

Wastewater treatment plants are considered the primary systems responsible for treating these effluents before environmental release. However, treating hospital wastewater that contains antimicrobial agents can itself promote the development of resistant bacterial strains, especially if the treatment is incomplete, or suboptimal (Rizzo et al., 2013). In Fact, a number of studies have been performed that supports the connection between wastewater treatment plants'

effluent discharge and the presence of antibiotic-resistant micro-organisms in the environment (Rizzo et al., 2013, Manaia et al., 2018, Wang et al., 2020, Herraiz-Carboné et al., 2021, Elder et al., 2016). These findings highlight the need for advanced treatment strategies to minimize the release of both parent antibiotics and their resistant derivatives from hospital sources.

Several processes for the degradation or removal of antibiotics from the environment have been investigated in order to mitigate the associated environmental risks. Existing approaches for the treatment of antibiotics in aqueous media include conventional wastewater treatment processes, such as primary and secondary biological treatment, chemical oxidation using sodium hypochlorite, advanced oxidation processes, adsorption and membrane separation techniques, as well as combinations of these methods (Homem and Santos, 2011). All the above-mentioned methods can be only considered as a partial solution bringing about only a limited degree of mitigation. Therefore, there remains an urgent need to develop more effective and environmentally sustainable treatment solutions.

Excluding the antibiotics that are known to be present in wastewater, other active compounds with antibacterial activity could be formed when antibiotics undergo chemical reactions during wastewater treatment process (Kennedy Neth et al., 2017, Kennedy Neth et al., 2019). Most of the chemical transformations occurring during wastewater treatment arise from the exposure of antibiotics to disinfectants; however, it is important to recognise that other biological and physical processes can also contribute to their transformation.It is now known that photosensitized processes during wastewater disinfection might well explain the reasons behind creating anti-bacterially active transformation products from some common antibiotics (Keen and Linden, 2013, Kennedy Neth et al., 2017). This will even pose more threats as the transformed derivatives make the microbes more resistant and virulent. Even trace levels of antibiotics in treated wastewater effluents can certainly pose a definite risk factor to humans and could potentially result in the rise of anti-bacterial activity in our immediate environment (Bound and Voulvoulis, 2004). Although advanced oxidation technologies show promise in degrading trace antibiotic residues, the residual or enhanced antibacterial activity of the transformation products remains a critical concern (Kennedy Neth et al., 2017, Krasner et al., 2006).

Advanced oxidation processes (AOPs) have gained considerable attention as promising treatment technologies for the removal of organic pollutants, including antibiotics, from wastewater (Elder et al., 2016, Chen et al., 2021). These processes involve the generation of highly reactive oxidative species, primarily hydroxyl radicals ($\cdot OH$), which are capable of non-selectively degrading a wide range of organic contaminants (Chen et al., 2021). Unlike conventional treatment methods, AOPs are designed to achieve complete mineralisation, or

transformation of pollutants into less harmful compounds. A variety of AOP techniques exist, including photolysis (UV-based), ozonation when combined with additional oxidants or catalysts that enhance hydroxyl radical generation, such as UV/H_2O_2, O_3/H_2O_2, or catalytic ozonation, Fenton and photo-Fenton reactions.

In addition to these, other oxidation treatments, such as hydrogen peroxide alone and sodium hypochlorite solutions, although not strictly classified as AOPs, are commonly employed in wastewater treatment and can still lead to significant oxidative transformation of antibiotics. (Chen et al., 2021). These methods are increasingly applied in both pilot and full-scale water treatment facilities due to their high efficiency in degrading micropollutants (Chen et al., 2021). The following sections provide an overview of key AOPs, with a focus on their mechanism, applicability to antibiotic degradation, and limitations.

1.2 Advanced oxidation processes (AOPs)

Advanced oxidation process is now considered to be an effective wastewater treatment method in the environmental research field (Ezeuko et al., 2021).

Figure 1. Classifications of advanced oxidation process (Adapted from Mishra N. S, 2017).

The advanced oxidation processes (AOPs) can be defined as oxidation technologies based on the production of large amounts of highly reactive species that are directly involved in the destruction of target pollutants (Venieri et al., 2020). Hydroxyl radicals are among the most powerful oxidants (standard electrode potential, E^0 = +2.86 V) and can non-selectively attack a wide range of intractable organic compounds and microorganisms found in wastewater effluents. In wastewater treatment applications, advanced oxidation processes are primarily employed as tertiary or quaternary treatment steps to remove contaminants of emerging concern, including antibiotics, thereby reducing their release into the receiving environment

(Ezeuko et al., 2021).

Advanced oxidation processes (AOPs) are commonly classified as homogeneous or heterogeneous based on the phase of the catalyst or reactive components involved in the process (Kamali et al., 2023). Homogeneous AOPs involve the formation of radicals from fully dissolved chemical species within the effluent, while heterogeneous AOPs rely on solid catalysts to initiate radical production.

Additionally, AOPs may also be grouped based on whether UV irradiation or other external energy sources are required to drive the reaction. (Kamali et al., 2023, Ezeuko et al., 2021, Chen et al., 2021).

For disinfection purposes, hydrogen peroxide (H_2O_2) been mainly used as it is a powerful oxidant (E^0: +1.78 V) (Garcia-Munoz et al., 2023). It is considered as a cleaner reagent since H_2O_2 is usually decayed in oxygen and water, avoiding the generation of unwanted by-products (Herraiz-Carboné et al., 2021). Depending on the initial concentration, the bactericidal effect can be limited, and therefore the activation of H_2O_2 with other oxidants, or catalysts, to improve the processes efficiencies has been extensively tried and are reported in the literature (Chen et al., 2021, Liu et al., 2018, Herraiz-Carboné et al., 2021). The combined effect of H_2O_2 and ozone (O_3) enhances the generation of reactive oxygen species, particularly hydroxyl radicals ($^{\cdot}OH$) and superoxide radical anions ($O_2^{\cdot -}$), which play a key role in microbial inactivation and contaminant degradation (equation 1) (Nahim-Granados et al., 2020). This process (H_2O_2/O_3) has been intensely investigated for the disinfection of water and wastewater (Mishra N. S, 2017, Garcia-Munoz et al., 2023) (Nahim-Granados et al., 2020).

$$O_3 + H_2O + hv \rightarrow H_2O_2 + O_2 \quad \text{.....(1)}$$

Several classes of AOPs are also known to generate powerful oxidative agents capable of degrading persistent organic pollutants and microbial contaminants. These agents include Fenton and Fenton like oxidation, photo catalytical oxidation, electrochemical advanced oxidation, ozonation and sonolysis (Chen et al., 2021, Herraiz-Carboné et al., 2021, Prada-Vásquez et al., 2021).

1.2.1 Fenton and Fenton-like processes

The Fenton oxidation process (H_2O_2/Fe^{2+}) is one of the most extensively studied advanced oxidation processes for water and wastewater treatment, with applications reported primarily at laboratory and pilot scales rather than widespread full-scale implementation (Chen et al.,

2021, Herraiz-Carboné et al., 2021, Cheng et al., 2018, Ziembowicz and Kida, 2022). It is based on the generation of highly reactive hydroxyl radicals (*OH) through the activation of hydrogen peroxide in the presence of ferrous iron (Fe^{2+}) acting as a catalyst. The core reaction proceeds via a redox cycle where Fe^{2+} reacts with hydrogen peroxide to form ferric iron (Fe^{3+}), hydroxide ions, and hydroxyl radicals, as shown in the reaction below (equation 2) (Chen et al., 2021, Herraiz-Carboné et al., 2021, Neyens and Baeyens, 2003, Pignatello et al., 2006, Ziembowicz and Kida, 2022).

$$Fe^{2+} + H_2O_2 \rightarrow Fe^{3+} + OH^- + *OH \quad \text{..... (2)}$$

The process is sustained through further reactions, where Fe^{3+} is reduced back to Fe^{2+} by reacting with additional hydrogen peroxide and its reactive intermediates (Chen et al., 2021, Gamarra-Güere et al., 2022).

$$Fe^{3+} + H_2O_2 \rightarrow Fe^{2+} + HO_2 + H^+ \quad \text{.....(3)}$$

$$Fe^{3+} + HO^2 \rightarrow Fe^{2+} + O^2H^+ \quad \text{.....(4)}$$

These reactions allow continuous generation of hydroxyl radicals, ensuring high oxidation efficiency for the degradation of organic contaminants (Chen et al., 2021, Herraiz-Carboné et al., 2021)

Catalytic efficiency in the Fenton process is affected by mobile operating parameters including H_2O_2 concentration, Fe^{2+} concentration and temperature (Chen et al., 2021). The method is known for its high degradation efficiency and relatively simple operation. However, its practical application is limited by the requirement for a strictly acidic environment (optimal at pH = 3) as well as the formation of large volumes of iron-containing sludge, which can result in secondary pollution and increase operational costs (Chen et al., 2021, Hodges et al., 2018).

In contrast, persulfate-based advanced oxidation processes (SR-AOPs), which function via sulfate radicals, are considered Fenton-like reactions that can operate over a broader pH range (Chen et al., 2021, Xiao et al., 2020, Wang and Wang, 2018, Wang and Wang, 2022). Solid-

phase oxidants such as peroxydisulfate (PDS) are often used in these systems. Compared to H_2O_2, PDS is more stable, safer to transport, and more cost-effective, making it suitable for on-site storage and use (Wang and Zhuan, 2020, Wang and Wang, 2022).

In addition to the above-mentioned chemical oxidation method, photochemical-based AOPs have also gained increasing attention, especially due to their ability to generate reactive species using light, offering a more environmentally friendly and catalyst-driven approach for the breakdown of pollutants (Chen et al., 2021).

Despite their proven effectiveness, Fenton and Fenton-like processes still face several practical restrictions that limit large-scale implementation, including sensitivity to water matrix composition and the need for careful control of operating conditions. These challenges highlight the need for continued research into oxidation strategies that are effective under milder, environmentally relevant conditions and that minimise secondary waste generation and chemical consumption. Such considerations support the motivation for investigating alternative oxidants and treatment approaches in this thesis.

1.2.2 Photochemical oxidation

Photochemical oxidation-based AOPs have attracted considerable attention due to their effectiveness in degrading organic pollutants in water, while also being considered more environmentally friendly (Ezeuko et al., 2021, Vallejo et al., 2015). These processes typically rely on semiconductor catalysts that, upon irradiation, generate reactive oxygen species (ROS) through photocatalytic reactions. Commonly reported ROS include hydroxyl radicals ($^{\cdot}OH$), superoxide radical anions ($O_2^{\cdot-}$) formed via one-electron reduction of dissolved oxygen, and, in some cases, singlet oxygen ($^1O_2$), all of which contribute to the oxidation and degradation of organic contaminants (Chen et al., 2020b, Chen et al., 2020a).

Although there are numerous catalysts with photocatalytic properties (i.e., TiO_2, WO_3 or ZnO), research has mainly concentrated on using the TiO_2 catalyst. In this context, TiO_2 is a benchmark photocatalysts used in water treatment, owing to its low cost, high oxidative potential, high photostability, and chemical strength (Chen et al., 2021). However, its use also presents some limitations. The high recombination rate of electron–hole (e^-/h^+) pairs significantly reduce its photocatalytic efficiency, and its wide bandgap 3.2 eV also restricts photoactivation to the ultraviolet region of the electromagnetic spectrum (Varma et al., 2020, Linsebigler et al., 1995, Etafa Tasisa et al., 2024, Mao, 2007). Although hundreds of photocatalytic materials have been developed, TiO_2 remains widely used as a UV-active

benchmark material against which the performance of alternative and modified photocatalysts is commonly evaluated (Mao, 2007).

In addition to photocatalytic systems, electrochemical advanced oxidation processes (EAOPs) have also emerged as an effective and flexible AOP strategy for degrading persistent organic pollutants in wastewater.

1.2.3 Electrochemical advanced oxidation

Electrochemical oxidation (EO) refers to a process in which harmful substances are transformed into harmless compounds through the application of electrical potential (Wang and Zhuan, 2020, Chen et al., 2021). In the context of wastewater disinfection, EO operates via two primary mechanisms: indirect oxidation, involving the electrochemical generation of reactive oxygen species (ROS), and direct oxidation, which involves charge transfer at the electrode surface (Chen et al., 2021, Sirés et al., 2014, Vecitis et al., 2011). In direct oxidation, microorganisms are adsorbed onto the anode, where they undergo electron loss, ultimately resulting in their inactivation (Chen et al., 2021). This two-step mechanism interrupts transmembrane electron transport and induces oxidative stress, leading to microbial cell damage (Vecitis et al., 2011, Chen et al., 2021). Alternatively, indirect oxidation relies on specific electrode materials to generate highly reactive ROS, such as chlorine radicals (e.g. $Cl^{\cdot}$ or $Cl_2^{\cdot-}$) (and hydroxyl radicals ($^{\cdot}OH$), which contribute to efficient microbial inactivation in treated water (Chen et al., 2021).

The main advantages of the electrochemical advanced oxidation process (EAOP) include high energy efficiency, minimal secondary pollution, simple operational requirements, a compact system footprint, and environmentally safe operating conditions due to the use of mild reaction parameters (Chen et al., 2021). Despite these strengths, several limitations exist. These include concerns about the long-term stability of the process, the potential formation of harmful disinfection by-products (DBPs), the high cost of electrode materials, and restricted mass transfer between the bulk solution and electrode surface, all of which can compromise overall treatment performance (Hodges et al., 2018, Chen et al., 2021, Herraiz-Carboné et al., 2021).

Another widely researched AOP technique for wastewater treatment is ozonation, which has demonstrated strong oxidative capabilities and broad-spectrum antimicrobial efficacy (Issaka et al., 2022).

1.2.4 Ozonation

Ozone (O_3), also known as trioxygen, is an inorganic molecule widely recognised for its strong oxidative properties and effectiveness as a disinfectant (Prado and Esplugas, 1999, Prada-Vásquez et al., 2021). Ozonation-based oxidation mechanisms can generally be categorised into two types: direct and indirect. In the direct pathway, ozone molecules react directly with micropollutants. In contrast, the indirect mechanism involves the formation of hydroxyl radicals (*OH), that are generated during the decomposition of ozone in water and are responsible for the secondary radical-mediated oxidation of contaminants (Von Sonntag and Von Gunten, 2012).

The treatment efficiency of ozone in wastewater applications is influenced by several factors, including ozone concentration, contact time, pH, temperature, and the presence of carbonates (Chen et al., 2021, Zhuang et al., 2015). However, conventional ozonation is associated with several limitations, such as ozone's low solubility in water, limited utilisation efficiency, high operational cost, and the potential for incomplete oxidation of certain organic pollutants. Additionally, this process may result in the formation of toxic disinfection by-products (DBPs). To address these challenges, catalytic ozonation has been developed as an advanced alternative to enhance disinfection performance (Chen et al., 2021). The use of catalysts facilitates the decomposition of ozone into highly reactive free radicals, thus improving the mineralisation of organic matter (Yang and Wu, 2019). A variety of materials, such as metal oxides, minerals, activated carbon, and other metallic catalysts, have been explored to improve pollutant removal efficiency (Chen et al., 2021, Issaka et al., 2022). Overall, catalytic ozonation is regarded as a more environmentally friendly and effective method for wastewater treatment (Wang and Bai, 2017, Issaka et al., 2022).

In addition to chemical-based AOPs like ozonation, physical methods such as sonolysis have also been explored for their potential in degrading organic pollutants in wastewater.

1.2.5 Sonolysis

Sonolysis is a physical AOP technique that utilises the mechanical effects of ultrasound, specifically audio cavitation, to generate reactive species. In systems where iron is present, these conditions may also promote the formation of iron oxide nanoparticles (Torres-Palma and Serna-Galvis, 2018, Chowdhury and Viraraghavan, 2009). The cavitation bubbles collapse under ultrasonic irradiation, generating extreme local conditions (high temperature and pressure) that facilitate the formation of hydroxyl radicals (·OH), which are capable of degrading persistent organic pollutants in water. Because of this, ultrasound-based treatment is considered an advanced oxidation process. Sonolysis is currently being explored as an alternative AOP for

tertiary wastewater treatment, although reported treatment efficiencies are generally low, particularly when applied as a standalone process for the removal of chemical and microbiological contaminants. This technique offers several benefits over other AOPs, including simple operation, no chemical additives, and the ability to selectively degrade compounds based on their physicochemical properties (Xiao et al., 2014, Chen et al., 2021).

The above technique makes use of high-frequency ultrasound waves, typically in the range of 20 kHz to 10 MHz, to induce cavitation and generate highly reactive species in solution. One of the main advantages of sonolysis is that it does not require any hazardous chemical mediators, making it a clean and environmentally friendly process (Chowdhury and Viraraghavan, 2009, Joseph et al., 2009). Studies have shown that ultrasonic treatment can target the active nucleus of β-lactam antibiotics, leading to their structural transformation and reducing their antimicrobial activity. As a result, this method may also help lower the risk of developing antibiotic-resistant bacteria (Joseph et al., 2009, Torres-Palma and Serna-Galvis, 2018, Chen et al., 2021).

Despite these advantages, sonolysis also presents several limitations that restrict its practical application. These include relatively low energy efficiency, limited treatment volumes, high electrical power consumption and reduced effectiveness in complex water matrices where radical sifting can occur. In addition, sonolysis alone often provides incomplete mineralisation of organic contaminants, meaning it is frequently more effective when combined with other oxidation processes. These limitations highlight the need for continued research into alternative oxidation approaches that are more energy-efficient and suitable for large-scale wastewater treatment.

While AOPs offer advanced and often highly effective strategies for degrading pollutants, conventional and widely practiced disinfection methods still remain central to wastewater management specifically for the inactivation of microorganisms and the reduction of pathogen loads.

1.3 Disinfection of wastewater through conventional methods

Apart from advanced oxidation technologies, conventional disinfection methods continue to play a crucial role in wastewater treatment systems. During water treatment processes, disinfection techniques and their mechanisms are always considered to be an essential pathway, as it reduces the risk of pathogen transmission and the number of bacteria in wastewater (Ezeuko et al., 2021). Commonly, the disinfection of wastewater is achieved using different

methods, including physical (for example, ultraviolet radiation); chemical (for example, chlorination, ozonation); and biological (for example, detention lagoons) methods (Pichel et al., 2019, Krasner et al., 2006, Yuksek et al., 2016, Voukkali and Zorpas, 2015).

Among these, chlorine remains the most widely used chemical disinfectant worldwide (Kennedy Neth et al., 2017). Chlorine is used to disinfect wastewater in either the hypochlorite salts/solutions or the gaseous form (Cl_2). Its disinfection action primarily involves the oxidation, or inactivation, of key functional sites on microbial cell surfaces and disruption of cell wall integrity, ultimately leading to cell lysis and death (Fan et al., 2010, Kennedy Neth et al., 2017). The overall effectiveness of chlorine disinfection depends on both the dosage and the contact time, typically expressed as "chlorine exposure" (Hiller et al., 2019).

However, it is now well recognised that chlorine can also react rapidly with pharmaceuticals and other organic micropollutants present in wastewater, often resulting in the formation of a wide range of disinfection by-products (DBPs)(Simazaki D, 2008, Kennedy Neth et al., 2017, Kennedy Neth et al., 2019). For example, studies have shown that chlorination of quinolone antibiotics leads to the generation of genotoxic by-products (Li et al., 2016). Similarly, chlorination of levofloxacin was reported to produce transformation products more toxic than the parent compound itself (El Najjar et al., 2013). In addition, a recent study by researchers from USA showed that the transformation of doxycycline (a common pharmaceutical pollutant in wastewater effluent (see for examples, (Kennedy Neth et al., 2017) and (Keen and Linden, 2013)), resulted in the emergence of anti-bacterially active products during water disinfection using chlorine gas that raises concerns over the potential contribution of such by-products to the development of antimicrobial resistance.

Another widely used chemical disinfectant is ozone (O_3) (Von Sonntag and Von Gunten, 2012). As discussed in the previous section, the oxidative mechanisms of ozonation have been described in detail and are not repeated here (Voukkali and Zorpas, 2015, Huber et al., 2005, Juárez, 2021). While ozonation is often more effective than chlorine against viruses and bacteria, its efficiency is influenced by operational conditions such as ozone dosage, pH, temperature, and the presence of competing compounds (Chen et al., 2021). Major limitations of ozonation include its low solubility in water, high operational costs, and the potential formation of toxic or persistent oxidation by-products (Dodd et al., 2009, Gomes et al., 2017). Previous studies also have demonstrated the main disadvantage of ozonation, as their decomposition controls the formation of low molecular by-products with stronger behavioural activity towards radical degradation or towards further ozone oxidation (Gomes et al., 2017). Similar conclusions were reached with other study as when sulfamethoxazole was used as a

target molecule (Willach et al., 2017). This may be a disadvantage of ozone application in wastewater treatment while the products formed might present stronger toxic characteristics than the initial pollutants (Willach et al., 2017, Gomes et al., 2017, Zhuang et al., 2015).

Ultraviolet (UV) radiation is also commonly used as a physical disinfection method (Chen et al., 2021). It is widely implemented in water treatment plants due to its ability to inactivate pathogens without producing chemical by-products, being environmentally friendly and the easy operation parameters (Zhuang et al., 2015, Keen and Linden, 2013). Ultraviolet irradiation is a disinfection method that uses short-wavelength ultraviolet light to deactivate or kill microorganisms by damaging the nucleic acids and interfering their DNA, causing them incapable of performing important cellular functions (Cutler and Zimmerman, 2011, Ashok and Khedikar, 2016). High-energy UV lamps are used to irradiate wastewater as it flows past the source. UV is broadly effective against most waterborne pathogens (Hijnen et al., 2006b), and studies have shown its potential for inactivating *Escherichia coli* and *Bacillus subtilis* spores, particularly when using pulsed UV light (Uslu et al., 2015). The major disadvantage of UV disinfection is the cost efficiency, energy consumption, short wavelength and the ability to recover and repair damaged DNA to prevent the reactivation of antibiotic-resistance bacteria (ARB) (Chen et al., 2021). In contrast, UV/H_2O_2 systems are advanced oxidation processes designed primarily for the degradation of chemical contaminants rather than for disinfection. Recent studies have shown that UV-based AOPs may not always effectively eliminate antibiotics and, in some cases can transform them into active by-products with retained or altered antibacterial properties (Keen and Linden, 2013).

In conclusion, antibiotics are increasingly recognised as emerging pollutants due to their continual release and persistence in aquatic environments, even at low concentrations (Homem and Santos, 2011). Growing evidence indicates that wastewater effluents are often enriched with antibiotics, antibiotic-resistant bacteria (ARB), and antibiotic resistance genes (ARGs), potentially contributing to the global rise of antibiotic resistance in human infections (Pruden, 2014). Several processes to degrade/remove antibiotics have been identified to prevent this contamination. Some of the current state of knowledge regarding the degradation and removal processes of antibiotics from aqueous media include, chlorination, advanced oxidation processes, ozonation, semiconductor and photocatalysis (Homem and Santos, 2011). However, these methods generally provide only partial mitigation and may themselves generate transformation products with unknown or enhanced toxicity (Kennedy Neth et al., 2019). This highlights the urgent need for more effective and environmentally sustainable treatment strategies.

In recent years, the combined use of Nuclear Magnetic Resonance (NMR) spectroscopy and high-performance liquid chromatography–mass spectrometry (HPLC/MS) has become a powerful approach in the analysis of pharmaceutical degradation. In this context, NMR spectroscopy, particularly ^{1}H and ^{19}F NMR, allows for real-time, non-destructive monitoring of molecular structures, enabling the identification of functional group changes, ring cleavage events, and intermediate formation (Branch et al., 1987, Vafaei et al., 2020). Its ability to provide detailed structural information makes it invaluable in tracking the breakdown pathways of antibiotics, especially for detecting transformations such as β-lactam ring opening and side chain rearrangement (Dr. Holzgrabe, 2010, Holzgrabe, 2015). In parallel, HPLC/MS offers high sensitivity and selectivity for detecting low-concentration degradation products (Aldeek et al., 2015). It is particularly useful for identifying small or transient fragments that may not be visible in NMR spectra. The use of quadrupole-based mass spectrometry allows for precise determination of mass-to-charge (m/z) ratios, facilitating the identification of transformation products even at trace levels (Pérez-Parada et al., 2011(Petrovic et al., 2005, Matta et al., 2018)). When used together, NMR and HPLC/MS provide complementary and comprehensive insights into both structural and compositional changes during oxidative treatment, forming the core analytical platform applied in this study to investigate the degradation of selected antibiotics under sodium hypochlorite exposure.

Several studies have reported the successful application of NMR spectroscopy for investigating pharmaceutical degradation pathways and identifying major transformation products formed during oxidation and photolytic processes (Petrovic et al., 2005, Branch et al., 1987, Dr. Holzgrabe, 2010, Mitsumori et al., 1977, Holzgrabe, 2015, Daletos et al., 2017). However, a known limitation of NMR with comparatively lower sensitivity, which can restrict detection of low-abundance or short-lived intermediates. Accordingly, the integration of NMR with LC/MS is widely recognised as an effective strategy, whereby LC/MS provides sensitive detection and molecular mass information, while NMR offers definitive structural elucidation (Zięba et al., 2004, Samanidou et al., 2007). This combined approach supports comprehensive characterisation of pharmaceutical breakdown products and strengthens confidence in product identification.

Given the persistence of antibiotics and their transformation products in aquatic environments, along with the limitations of existing treatment strategies, there is a clear need for detailed investigations into their chemical fate under realistic disinfection strategies. The complementary strengths of NMR spectroscopy and HPLC/MS analysis provide a unique opportunity to address this knowledge gap. The following section presents the rationale for the present study, which is grounded in the environmental urgency to mitigate antimicrobial resistance and supported by the analytical precision of these techniques.

1.4 Rationale behind the current programme

As discussed in the previous sections, advanced oxidation techniques have demonstrated promising potential for the treatment of trace levels of antibiotics in wastewater effluents. However, the formation of residual or newly generated antibacterial transformation products remains a significant concern. These by-products may contribute to the spread of antimicrobial resistance and pose additional environmental and health risks.

The current study was therefore designed to systematically investigate the chemical transformations of selected antibiotics under oxidative disinfection conditions. This was primarily achieved through detailed investigations using high-field NMR spectroscopy and HPLC/MS techniques, which together provide superior capability for confident identification of unknown transformation products. NMR offers definitive structural information, while HPLC/MS provides high sensitivity and selectivity, enabling detection of degradation products down to trace concentrations where quantification is required. The results obtained through these analyses were then correlated with a view to identifying the by-products of oxidative transformations and to monitor their phenomenological evolution and fate. It was anticipated that the insights gained from this work will contribute to broader efforts to mitigate the consequences of antibiotic resistance and support the development of more informed water treatment strategies.

1.5 Overall aim of the project

The overall aim of the project is to systematically investigate the chemical transformations occurring in selected common antibiotics belonging to the β-lactam and fluoroquinolone classes, specifically Penicillin G, Amoxicillin, and Ciprofloxacin, as a result of oxidative disinfection of effluent water, and to generate new knowledge on potential degradation pathways and transformation products that may affect antimicrobial activity and antimicrobial resistance.

1.6 Individual objectives

In order to realize the overall aim of this project, we have systematically broken down the overall programme into the following individual objectives:

1) Selection of key antibiotics (for example, Penicillin G, Amoxicillin and Ciprofloxacin). Penicillin G and Amoxicillin were selected as representative β-lactam antibiotics due to their common detection in wastewater, widespread clinical use and well-documented susceptibility of the β-lactam ring to oxidative and hydrolytic transformations. Ciprofloxacin was selected as a representative fluoroquinolone antibiotic because of its environmental persistence, extensive prescription and structural features known to influence degradation behaviour. Together, these compounds represent different antibiotic classes with contrasting chemical structures and reactivities, allowing comparative assessment of oxidative transformation behaviour.

2) Implementation of laboratory-scale oxidative disinfection treatments, using sodium hypochlorite solution and UV irradiation.

   Sodium hypochlorite solution and UV irradiation were selected because they represent widely used disinfection processes in conventional wastewater treatment. These treatments were implemented at laboratory scale to allow controlled investigation

of antibiotic transformation under clear conditions, including known reagent concentrations, analytical monitoring and exposure times. A laboratory-scale approach was implemented to ensure experimental reproducibility and to enable detailed mechanistic interpretation of degradation behaviour.

3) Development of analytical methodologies for detecting both the parent antibiotics and their transformation products, using nuclear magnetic resonance (NMR) spectroscopy, high-performance liquid chromatography coupled to mass spectrometry (HPLC/MS).

4) Identification and identification, where possible, use of major degradation products through the protocol developed by using NMR and HPLC/MS

5) Elucidation of degradation mechanisms by integrating the spectral and chromatographic data to propose plausible transformation pathways under oxidative treatment conditions.

The above objectives were expressed based on a combination of existing research gaps identified in the literature, practical limitations related to time and resources, and the availability of analytical instrumentation and expertise. The selection of antibiotics was guided by their widespread use, environmental relevance, and representation of different antibiotic classes. The choice of sodium hypochlorite and UV irradiation reflects their common application in wastewater disinfection practices. The importance on NMR and HPLC/MS analysis was driven by their complementary capabilities for structural elucidation and sensitive detection of transformation products. Together, these objectives provide a focused and achievable framework for addressing the overall aim of the study.

CHAPTER 2: MATERIALS AND METHODS

Chapter 2 predominantly describes the sources and chemical natures of the antibiotics that were employed in the present study, as well as other laboratory reagents and chemicals used for oxidative transformations and for instrumental analyses (NMR and HPLC/MS studies). Initially, the solubility tests on the antibiotics were carried out to identify suitable solvents and solvent systems for sample preparation in NMR and HPLC/MS analyses and to ensure complete dissolution prior to oxidative treatment experiments. This was followed by the development of procedures for oxidative transformations (i.e. treatment with sodium hypochlorite solution and UV irradiation). This section also narrates the instrumentation, experimental parameters, including typical operating conditions of the NMR and HPLC/MS instruments.

2.1 Materials

All antibiotics were obtained as certified reference materials with stated purities from Aldrich® Chemical Company, and all reagents and solvents were of analytical or LC/MS grade and used as received. The antibiotics that were used for the present study included Penicillin G (β-lactam antibiotic, sodium salt), Amoxicillin (β-lactam antibiotic, trihydrate form), and Ciprofloxacin (fluoroquinolone antibiotic), all supplied as certified reference materials with stated purities. The solvents used for chromatographic studies were of ultra-high purity LC/MS grade, including LC/MS-grade water, methanol, and acetonitrile. The chemical structures of the antibiotic are given in Figure 2.

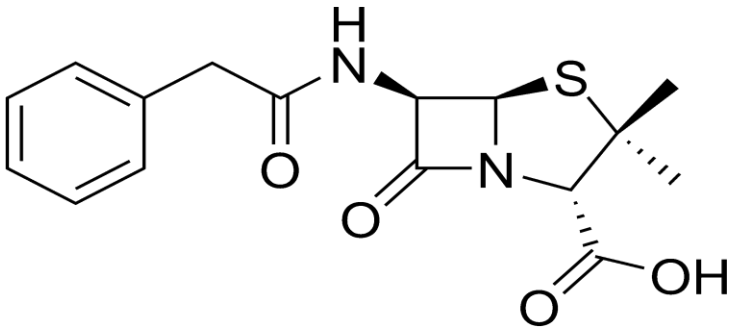

a. Penicillin G

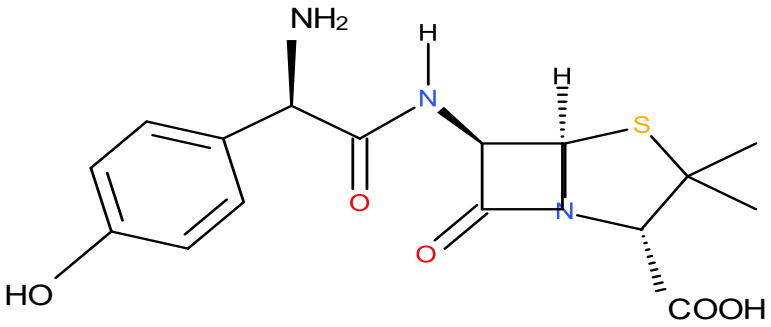

b. Amoxicillin

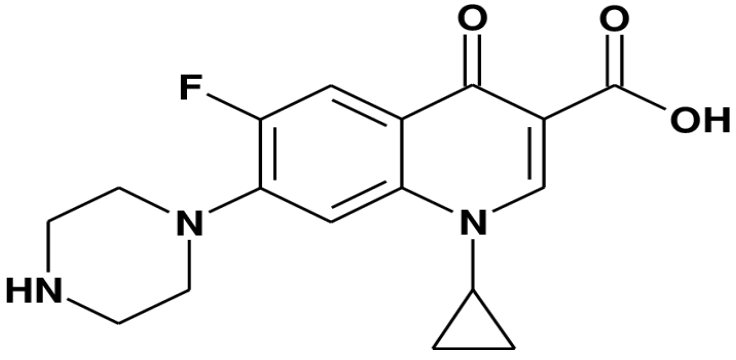

c. Ciprofloxacin.

Figure 2.1. Chemical structures of: a. Penicillin G, b. Amoxicillin and c. Ciprofloxacin (adapted from PubChem).

2.2 Methods

2.2.1 Solubility tests for the antibiotics

The solubilities of the chosen antibiotics were first tested using different including deionised water; dipolar-aprotic solvents (dimethyl sulfoxide, dimethylformamide, acetonitrile); protic solvents (methanol, ethanol); chlorinated aliphatic solvent (dichloromethane); aromatic solvents (toluene, xylene); and carboxylic acid (acetic acid). The main impetus behind these tests was to identify possible solvent/mixtures for the chromatographic (HPLC/MS) and to record NMR spectra. The tests were carried out as follow follows: *ca.* 0.05 mg of the antibiotic sample was placed in 1.5 mL vials and different solvents (*ca.* 1.00 mL) were added and the resultant mixtures were shaken vigorously. The table below shows the test results (Table 1).

Table 2.1. Results from the solubility tests

Solubility was assessed qualitatively based on visual observation, with results recorded as soluble, partially soluble, or insoluble under the tested conditions. The test results are summarised in Table 1.

Solvents	**Penicillin G**	**Amoxicillin**	**Ciprofloxacin**
Deionised water	Slightly soluble	Partially soluble	Partially soluble
Acetonitrile	Soluble	Soluble	Not soluble
Methanol	Soluble	Slightly soluble	Not soluble
Ethanol	Soluble	Slightly soluble	Not soluble
Dimethyl sulfoxide	Soluble	Soluble	Partially soluble
Dimethyl formamide	Soluble	Soluble	Partially soluble
Dichlomethane	Soluble	Soluble	Slightly soluble
Toluene	—	—	Not soluble
Xylene	—	—	Not soluble
Acetic acid	—	—	Soluble

2.2.2 Procedures for oxidative transformations of the antibiotics

In this set of experiments, the antibiotics (i.e. Penicillin G, or Amoxicillin, or Ciprofloxacin) were irradiated with UV rays within the germicidal range (200–280 nm, centred at 254 nm),, or were treated with sodium hypochlorite solution (12.5 vol%), as follows:

a. *Procedure for irradiation with UV rays*

The required amount of the antibiotic samples (*ca.* 50 mg each of Penicillin G, Amoxicillin and Ciprofloxacin) was taken in separate quartz cuvettes. The cuvettes were then placed in an accelerated weatherability chamber (Heraeus SUNSET CPS ®), which was used as a controlled UV irradiation source. UV exposure was applied at different irradiance levels controlled by the chamber settings. As absolute UV intensity was not directly measured, irradiance is reported in arbitrary units to indicate relative exposure levels Prior to use, the accelerated weatherability chamber was verified in accordance with the manufacturer's operating procedures. Lamp performance and irradiance output were checked using the instrument's internal monitoring system to ensure stable and reproducible operation. Routine maintenance and lamp replacement were conducted by technical staff according to scheduled service intervals The test samples were taken through the following cycle (Table 2).

Table 2.2. Accelerated weatherability test regime

Sl. No.	Irradiance level (arbitrary units)	Exposure time-duration (hours)	Exposure time-cumulative (hours)
1	0	0	0
2	3	8	8
3	3	24	33
4	3	23	56
5	5	47	152
6	7	48	200

In addition to the above, another route for UV-irradiation was employed using the internal UV light source of a Shimadzu® UV–Visible spectrophotometer (UV-1900). In this procedure, antibiotic solutions were placed in quartz cuvettes and irradiated in situ within the spectrophotometer sample compartment over the wavelength range 190–450 nm for defined exposure periods (as specified in Table 2.3). The spectrophotometer was wavelength-calibrated using the manufacturer's internal calibration routines prior to analysis, ensuring wavelength accuracy and reproducibility. This approach enabled

controlled low-intensity UV exposure while simultaneously allowing spectral monitoring of the samples. For UV irradiation experiments, antibiotic solutions were prepared by dissolving a fixed mass of compound in solvent and exact solvent volumes were not recorded and therefore concentrations are reported on a mass basis. Here a reference sample with Deuterium oxide (D_2O) (with and without 0.1% formic acid, as the case may be) was used in conjunction with the solution of the antibiotic in D_2O (it may be noted that 0.1 % of formic acid was also used in the cases of Ciprofloxacin and Amoxicillin to ensure complete dissolution). The details such as the applied UV irradiance, exposure duration, and irradiated area (spot size) were defined and quantified, with full experimental parameters reported in Table 2.3.

Table 2.3. Irradiation using a UV-Visible spectrophotometer

Sl. No	**Antibiotic**	**Reference**	**Sample (mg)**	**Wavelength (nm)**	**Duration of UV exposure (min)**
1	Penicillin G	D_2O	D_2O/30 mg	190- 300	30; 60; 120
2	Amoxicillin	D_2O/methanol (5 drops)	D_2O/methanol/30 mg	250- 450	30; 60; 120
3	Ciprofloxacin	D_2O/formic acid (9 drops)	D_2O/formic acid/30 mg	275- 430	30; 60; 120

Once the samples were irradiated to the required time intervals, the solutions were immediately transferred into NMR tubes, and the proton spectra were run in each case (for Ciprofloxacin, ^{19}F were also recorded). In all cases, after the irradiation interval of 120 minutes, the NMR spectra of the samples were run after *ca.* 16 hours (without any further irradiance). Here it is relevant to note that the ensuing NMR spectra (^{1}H, ^{13}C and ^{19}F, as the case may be). did not reveal any discernible changes in chemical shift, signal intensity, or peak pattern. These observations indicated that, under the UV irradiation conditions employed in this study, no detectable structural transformations had occurred. On this basis, the UV-treated samples were not subjected to further analysis by HPLC/MS, and subsequent degradation studies were focused on oxidation using sodium hypochlorite solution.

b. *Procedure for oxidation using sodium hypochlorite*

It should be noted that, in the oxidation experiments using sodium hypochlorite described below, the oxidant was applied at a nominal level based on volume addition of a commercial stock solution. The free chlorine concentration was not independently quantified, and the experiments were therefore designed to assess qualitative oxidative transformation rather than precise dose/response behaviour.

Prior to sample analysis, the NMR spectrometer was locked on the deuterium (^2H) signal of D_2O to ensure magnetic field stability. Standard tuning and shimming procedures were performed before each batch of measurements to optimise spectral resolution and reproducibility. Chemical shift referencing for ^1H spectra was performed using the residual HDO/H_2O signal of the solvent. Here, an in-situ of sodium hypochlorite used for oxidation method just to prior to the NMR runs was carried out as follows: Initially, *ca.* 10 mg of the antibiotics were run as neat in 0.75 mL and 0.25 mL of D_2O and deionized water (DI) respectively (note: for Amoxicillin and Ciprofloxacin about two drops of formic acid were added for better dissolution). This was followed by NMR runs, where 0.25 mL of sodium hypochlorite solution (12.5 vol%) added with 0.75 mL of *ca.*10 mg of each antibiotic, and the solution were run over two days to check the effect of the sodium hypochlorite on the three different antibiotics.

The pH was not controlled during the in-situ addition of sodium hypochlorite chlorination experiments; however, commercial sodium hypochlorite solutions are typically strongly alkaline (pH > 11), under which conditions hypochlorite (OCl^-) predominates over hypochlorous acid (HOCl). Consequently, the degradation observed is considered to arise mainly from hypochlorite-driven oxidation.

For the HPLC/MS analyses, a stock solution was first prepared by dissolving 10 mg of Penicillin G in 100 mL of commercially supplied LC/MS-grade water. To initiate oxidative degradation, two drops of sodium hypochlorite solution (12.5 vol%) were added to the solution under gentle stirring. Subsequently,1 mL of this reaction mixture was then diluted with 99 mL of commercially supplied LC/MS-grade water, yielding a final concentration of 1 ppm, which was identified to provide optimal chromatographic and spectrometric responses.

Chromatographic separation was performed using a Waters Acquity ® UPLC BEH C18 column (100 × 2.1 mm, 1.7 µm particle size). The mobile phase consisted of:

Solvent A: commercially supplied LC/MS-grade water with 0.1% (v/v) formic acid and
Solvent B: commercially supplied LC/MS-grade acetonitrile with 0.1% (v/v) formic acid

The gradient began with 1% solvent B, creating a highly aqueous environment suitable for retaining polar degradation products. The injection volume was 1 µL, with a flow rate of 0.2 mL/min and a total run time of 7 minutes per sample. The prepared sample was analysed using an LC/MS system operating in negative ionisation mode. A total of six sequential runs were conducted at 1-hour intervals, followed by a final run at 24 hours to monitor longer-term degradation of Penicillin G under oxidative conditions.

The oxidative degradation of Amoxicillin by sodium hypochlorite solution was also investigated using HPLC/MS in negative ion mode. For this, a stock solution was prepared by dissolving 10 mg of Amoxicillin in 100 mL of LC/MS-grade water, followed by the addition of two drops of methanol to assist with solubility. The solution was then sonicated for 10 minutes to ensure complete dissolution and for achieving Amoxicillin final concentration of 0.1 ppm. To initiate the degradation process, two drops of sodium hypochlorite solution (12.5 vol%) were added to the solution. This mixture was subsequently and serially diluted to a final concentration of 0.1 ppm: i.e. first, 1 mL of the treated solution was added to 99 mL of LC/MS-grade water; then, 1 mL of that diluted solution was added to 9 mL of LC/MS grade water. This final concentration was selected based on preliminary trial injections, which showed that it provided optimal peak intensity, signal-to-noise ratio, and chromatographic resolution without detector saturation This final concentration was selected as it produced the most consistent and informative chromatographic results. The chromatic procedure was repeated as it was done in case of Penicillin G.

The HPLC/MS runs were performed hourly over the first 6 hours after the addition of sodium hypochlorite solution, with a final run at 24 hours. Each run was conducted over a total of 7 minutes, but the retention time window was cropped to 0–2.5 minutes for analysis and figure presentation, as all significant peaks appeared within this timeframe. This adjustment improved visual clarity and allowed for more focused comparison of changes in the early eluting regions. Prior to analysis, the HPLC/MS system was calibrated and tuned using manufacturer-recommended procedures to ensure accurate

mass assignment, stable ionisation, and consistent chromatographic performance.

For following the oxidative degradation of Ciprofloxacin by sodium hypochlorite, the HPLC/MS analyses were done in a positive ion mode. As before, the analyses were aimed to characterize degradation behaviour over time and identify transformation products resulting from the treatment with sodium hypochlorite solution.

Firstly, a stock solution was prepared by dissolving 10 mg of Ciprofloxacin in 100 mL of a pre-sonicated standard solution consisting of 500 mL of commercially supplied LC/MS-grade acetonitrile and 0.5 mL of formic acid. Two additional drops of formic acid were added to assist the solubility, and the solution was sonicated for 10 minutes to ensure full dissolution. The degradation reaction was initiated by adding two drops of sodium hypochlorite solution (12.5 vol%). Following this, a serial dilution was performed to achieve a final concentration of 1 ppm (i.e. by adding 1 mL of the treated solution to 99 mL of the standard solution), which provided optimal chromatographic results.

Chromatographic separation was carried out using a Waters Acquity ® UPLC BEH C18 column (100 × 2.1 mm, 1.7 μm), with solvent A as LC/MS-grade water (0.1% formic acid) and solvent B as LC/MS-grade acetonitrile (0.1% formic acid). The gradient began at 20% solvent B, favouring retention of polar degradation products. The injection volume was 2 μL, with a flow rate of 0.4 mL/min, and each sample run lasted 6 minutes. Samples were analysed at 1-hour intervals during the first 6 hours after the addition of sodium hypochlorite, followed by a final run at 24 hours to monitor time-dependent degradation trends.

2.2.3 Analytical instrumentation and tests

All analytical instruments used in this study were operated in accordance with manufacturer-recommended procedures and were verified to be fit for purpose prior to sample analysis. The FTIR spectrometer was checked using standard polystyrene film to verify wavenumber accuracy, resolution, and signal response across the mid-infrared region. Background spectra were collected prior to each batch of measurements to ensure baseline stability.

The NMR spectrometer was calibrated using the residual solvent signal of deuterium oxide (D_2O) as an internal chemical shift reference. Routine tuning, matching, and shimming procedures were performed prior to data acquisition to ensure optimal magnetic field homogeneity, reproducibility and spectral resolution. The HPLC/MS system was calibrated and tuned using manufacturer-

supplied calibration solutions to ensure accurate mass assignment across the relevant m/z range. System suitability was verified through test injections to confirm stable retention times, consistent peak shape, and sensitivity prior to analysis of samples. These procedures ensured that all instruments were operating within acceptable performance limits and were suitable for the analytical objectives of this study.

c. *Fourier-transform Infrared Spectroscopy (FTIR)*

FTIR spectroscopy was initially employed in the present study with a view to interpreting information regarding specific functionalities in the antibiotic molecules. A Perkin Elmer® spectrometer was used, and the spectra were recorded in the attenuated total reflectance mode (ATR). Through these analyses the important function groups in the antibiotics and the transformed versions were identified. This is expected to provide complementary information regarding the functional group transformations accompanying oxidative disinfection processes. The other operating parameters included: number of scans: 32; resolution: 4 cm^{-1}; range: 4000 to 400 cm^{-1}.

d. *Nuclear Magnetic Resonance spectroscopy (NMR)*

Nuclear Magnetic Resonance (NMR) spectroscopy is a powerful analytical technique that is very commonly used to investigate molecular structures, chemical reactivities, and dynamic processes in a non-destructive and non-invasive manner (Daletos et al., 2017, Acosta). The technique is widely applied in chemical, environmental, pharmaceutical and biomedical research due to its ability to provide detailed information about atomic environments in molecules.

Modern high-field NMR spectrometers contain three primary hardware components: the console, which controls pulse sequence generation and data acquisition; the probe, which emits radiofrequency pulses and detects the resulting signals; and the superconducting magnet, which generates a strong, stable magnetic field to polarize nuclear spins. When nuclei are placed in this magnetic field and exposed to specific radiofrequencies, they resonate and emit detectable signals. Analysis of these signals yield detailed molecular insights(Acosta, Daletos et al., 2017).

In this study, a Bruker 600 MHz NMR instrument was used to investigate the structural changes in three antibiotics-Penicillin G, Amoxicillin, and Ciprofloxacin- where these compounds underwent oxidative transformations. Deuterium oxide (D_2O) was used as the primary solvent for all samples. Due to solubility limitations, a drop of 0.1% ammonium

hydroxide was added in the case of Amoxicillin, and a few drops of 0.1% formic acid were added to Ciprofloxacin, to ensure dissolution. Penicillin G dissolved readily in D_2O and required no additives. Here, apart from the routine ^{1}H and ^{13}C spectra, two-dimensional (homo-and hetero-nuclear) correlation spectra were also recorded. In addition, ^{19}F spectral recording was carried out.

Generally, for each run, *ca.* 30 wt.% solution was used, and the spectra were collected at ambient-temperature probe conditions. The raw spectra were then processed using a proprietary software (Bruker TopSpin 4.0.10), and the residual solvent signals were used to calibrate the spectrum. In the case of spectra that were recorded in D_2O, a 'water peak suppression' was affected through an appropriate spectral editing technique.

In summary, the NMR experiments on each of the three antibiotics (Penicillin G, Amoxicillin and Ciprofloxacin) can be given as follows:

^{1}H water suppression;

^{1}H-^{1}H correlation spectroscopy (COSY);

^{13}C with proton decoupling;

^{1}H-^{13}C COSY (Heteronuclear Single Quantum Coherence (HSQC)

Here, COSY runs showed coupling patters between protons (as cross peaks), and this is often referred to as homonuclear correlation spectroscopy, whereas, the HSQC stands for Hetero-nuclear Single Quantum Coherence, that shows the proton-carbon coupling.

The effect of the oxidant, sodium hypochlorite solution, was also studied on the three chosen antibiotics over time, using an *in-situ* method. In order to achieve this, 10 mg of both Amoxicillin and Ciprofloxacin were treated with *ca.* 0.75 cm^3 of D_2O and 0.25 cm^3 of DI water and two drops of formic acid. However, formic acid was not needed for complete dissolution when preparing the Penicillin G solution for the NMR runs. The three antibiotics were run first as neat (i.e., without addition of sodium hypochlorite or other oxidants), followed by the versions treated with the hypochlorite solution, with repeated runs over a specified time interval (i.e. 30 min, 40 min, 50 min, 60 min, 120 min, etc.). The chlorinated samples of each of the antibiotics were run for approximately two days with a view to studying the effect of chorine on these antibiotics over time.

e. *High Performance Liquid Chromatography / Mass Spectrometry (HPLC/MS)*

Liquid Chromatography Triple Quadrupole Mass Spectrometry HPLC/MS instrument (Shimadzu) was used for analysing the chosen antibiotics and their treated versions. A maximum pressure of 9000 psi, at an operating temperature of 35^{o}C, was set during the runs. The eluent (i.e. the mobile phase) for Penicillin G, Amoxicillin and Ciprofloxacin consisted of HPLC grade water with 0.1% formic acid and HPLC grade acetonitrile with 0.1% formic acid (50%/50% by volume). Injection volume for Penicillin G and Amoxicillin was 1µl, and 0.2 mL/min was the flow rate, whereas in case of Ciprofloxacin and its treated samples, 2µl sample was used with a flow rate of 0.4 mL/min. A C18 Acquity ® UPLC BEH 100 x 2.1 mm, 1.7 µm, column was used for all the analysis.

All the three antibiotics and their treated samples (i.e. chlorinated and UV irradiated) were tested using HPLC/MS by employing the above-mentioned method. Each aliquot from the treated samples was run through the high-performance liquid chromatography instrument (HPLC) coupled to a Shimadzu® ion trap mass spectrometer (MS) with a view to determining the residual concentrations of the parent antibiotics and the major transformed products. The mass spectra obtained will be analysed using known degradation pathways, and the detailed information will be retained in the Shimadzu® LabSolutions ® mass spectral database' of the instrument.

CHAPTER 3: RESULTS AND DISCUSSION

This chapter reflects the main thrust of the PhD programme, where the complementary information from the two main analytical techniques (i.e. HPLC/MS and NMR) are collated, and correlations are drawn with a view to identifying the main products formed through oxidative transformations of the chosen antibiotics. Subsequently, the plausible pathways leading to the formation of these products are deduced, and where possible, the actual mechanisms are sought.

3.1 Fourier-transform Infrared spectroscopy (FTIR)

Fourier-transform infrared (FTIR) spectra were acquired using a Perkin Elmer® spectrometer was used, and the spectra were recorded in the attenuated total reflectance mode (ATR). During the initial phases of the investigations, FTIR spectroscopic runs were performed on both the pristine and those samples that underwent UV-irradiation. In these experiments, the antibiotics were exposed to ultraviolet radiation using the accelerated weatherability chamber described in the Materials and Methods section, operating as a controlled UV source. The primary purpose was to follow the changes in vibrational frequencies of the individual antibiotics upon UV-irradiations. Prior to sample analysis, FTIR wavenumber accuracy and instrument performance were verified using a standard polystyrene film, and background spectra were collected to ensure baseline stability. The corresponding FTIR spectra are presented in Figures 3.1–3.6, allowing direct comparison between untreated and UV-irradiated samples.

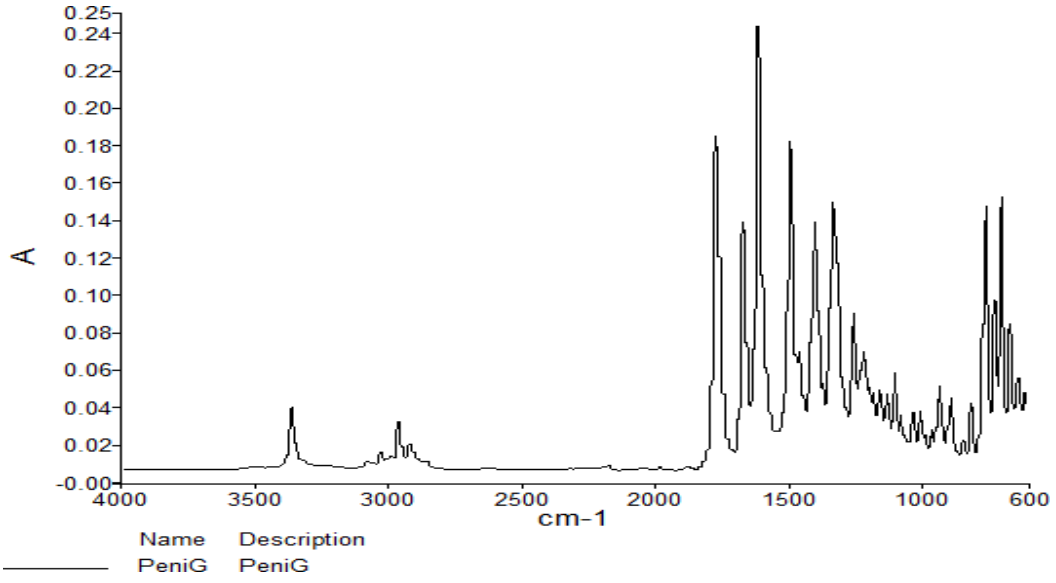

Figure 3.1. FTIR spectrum of Penicillin G (ATR mode)

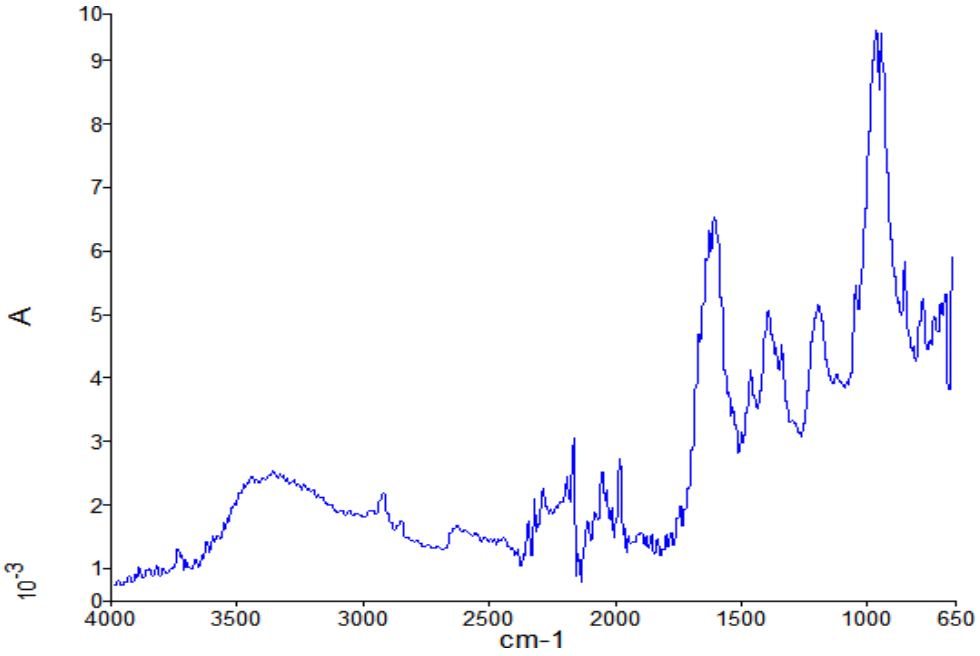

Figure 3.2. FTIR spectrum of Penicillin G, after UV irradiation in the solid-state (ATR mode)

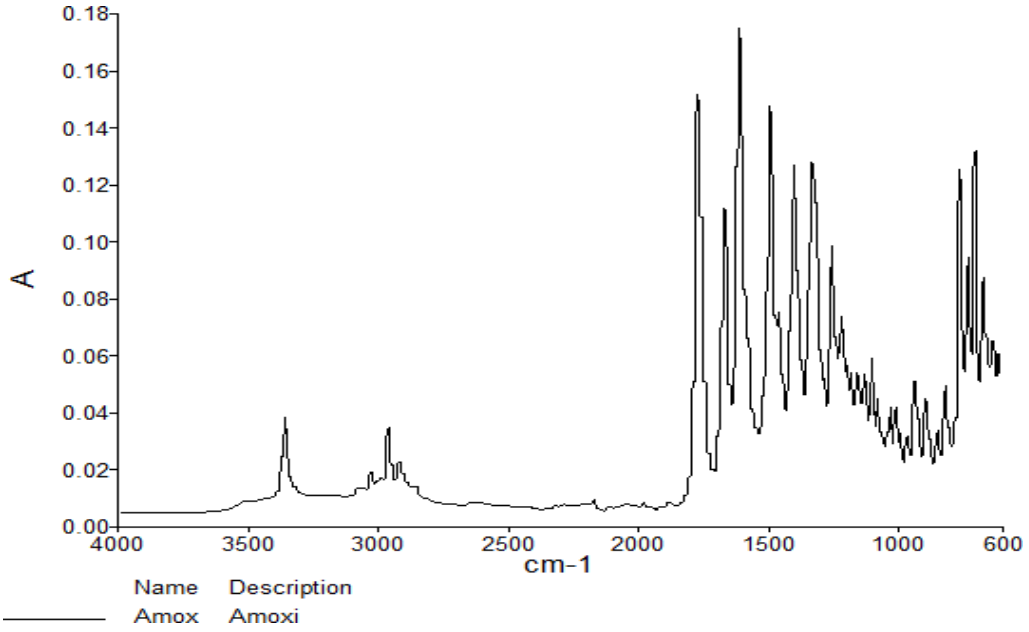

Figure 3.3. FTIR spectrum of Amoxicillin (ATR mode)

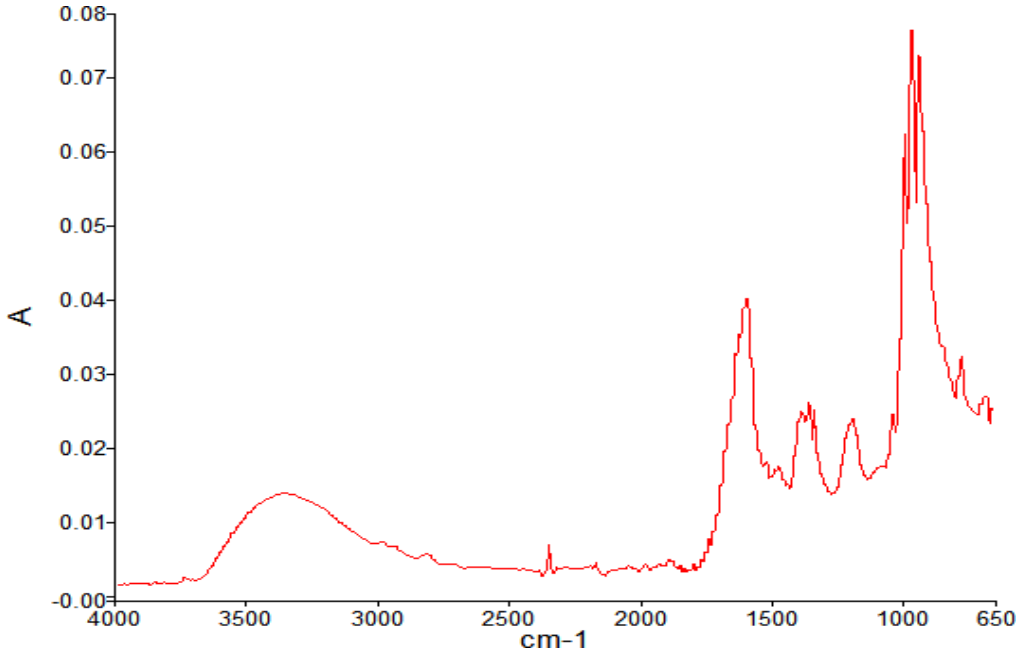

Figure 3.4. FTIR spectrum of Amoxicillin, after UV irradiation in the solid-state (ATR mode)

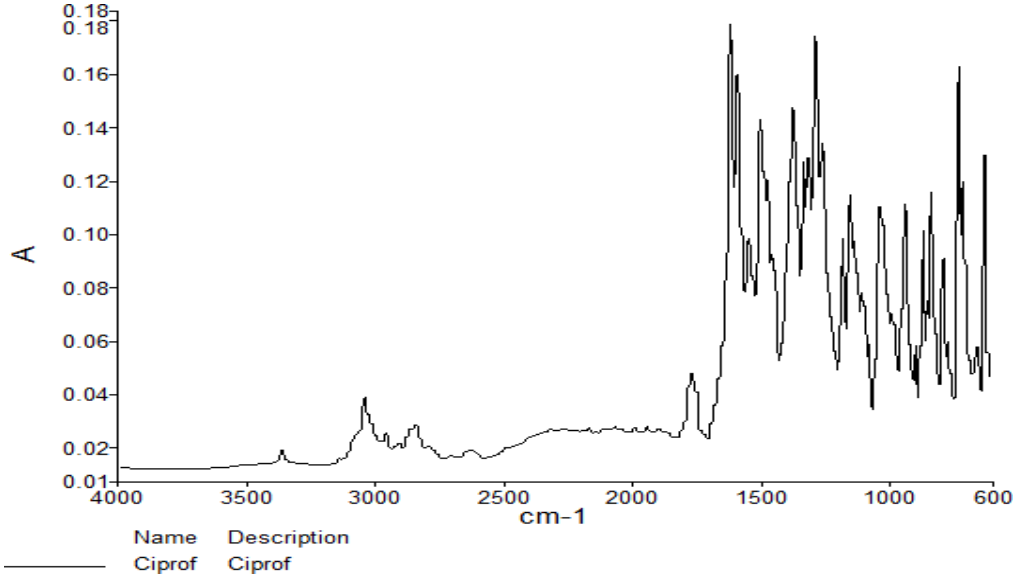

Figure 3.5. FTIR spectrum of Ciprofloxacin (ATR mode)

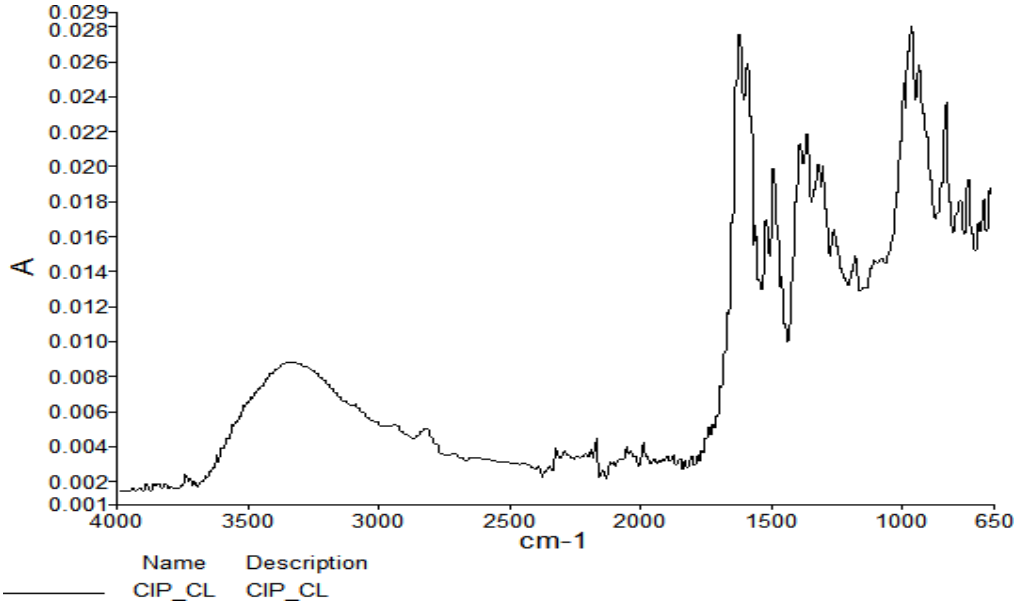

Figure 3.6. FTIR spectrum of Ciprofloxacin, after UV irradiation in the solid state (ATR mode)

In all cases, it is very clear that that there are discernible changes, especially, the in region of –C-H stretching region (where broader peaks possibly owing to water present in the sample), it is not very straight forward to interpret the changes in the fingerprint region. It is, therefore, to be concluded that FT-IR spectra of only very limited use in the context of overall identification of chemical species owing to oxidative transformations of the compounds in question. When the FTIR spectra of the three antibiotics following solid-state UV irradiation were compared with those of the corresponding pristine samples, no significant spectral differences were observed under the specific UV wavelength and irradiance conditions employed in this study, as described in the Materials and Methods section. It should be noted that

the extent of UV-induced photochemical transformation is strongly dependent on the irradiation wavelength and intensity. Therefore, the absence of detectable structural changes in the FTIR spectra reflects the particular UV exposure conditions applied rather than a general lack of photochemical reactivity. Hence, the focus of the program was shifted to NMR and HPLC/MS investigations, where a smaller scale in situ oxidative transformations was tried out.

3.2 Nuclear Magnetic Resonance (NMR) analyses of Penicillin G, Amoxicillin and Ciprofloxacin

Nuclear Magnetic Resonance (NMR) spectroscopy was employed as an analytical technique to investigate structural changes in the selected antibiotics following oxidative treatment. In contrast to FTIR analysis, which showed limited sensitivity to indirect molecular alterations, NMR enabled detailed examination of changes in the chemical environments of key functional groups. The NMR results presented below provide insight into oxidative transformation pathways of penicillin G, amoxicillin, and ciprofloxacin under the experimental conditions applied.

For each sample, ^{1}H and ^{13}C NMR spectra were recorded, and optionally two-dimensional experiments such as ^{1}H–^{1}H COSY and ^{1}H–^{13}C HSQC analyses were also carried out. Additionally, ^{19}F NMR runs were used to monitor structural changes in Ciprofloxacin, which contains a fluorine atom. Prior to sample analysis, the NMR spectrometer was calibrated using the residual solvent signal of deuterium oxide (D_2O) as an internal chemical shift reference, and routine tuning, matching, and shimming procedures were performed to ensure optimal field homogeneity and spectral resolution. As given earlier, an approximately 30 wt.% solutions were used, and all spectra were recorded at ambient probe temperature, in all cases.

Spectra were processed using Bruker® TopSpin 4. 4.10, and chemical shifts were automatically calibrated as described in Section 2.2.3. Water suppression was achieved using standard pre-saturation pulse sequences provided within the TopSpin software, where required.

The NMR methodology in this study was designed to monitor chemical degradation resulting from environmental treatments. Two oxidative reagents were employed: UV irradiation and sodium hypochlorite solution. The UV exposure experiments were carried out in both solid and solution states using irradiation conditions selected for each compound based on published photochemical studies and implemented as described in the Materials and

Methods section, with antibiotic solutions prepared by dissolving approximately 10 mg of antibiotic in 1.0 mL of solvent (Ou et al., 2016, Jung et al., 2012, Han et al., 2024, Zhang et al., 2019, Uslu et al., 2015). The NMR spectra were recorded at intervals and carried over up to overnight exposures to assess any structural changes.

In parallel, time-resolved NMR experiments were performed to assess the effect of sodium hypochlorite solution, a disinfectant widely used in water and wastewater treatment. As detailed in the experimental section, Amoxicillin and Ciprofloxacin (*ca.* 10 mg each) were dissolved in 0.75 mL D_2O and 0.25 mL DI water, with added formic acid as needed due to their solubility issue. Penicillin G was dissolved directly in D_2O without additives. The parent compounds were first recorded as untreated, followed by repeated NMR scans after the addition of sodium hypochlorite. Spectra were collected at various time points (e.g., 30 min, 60 min, 120 min, etc.) for up to two days.

This approach enabled real-time observation of molecular changes under oxidative conditions, including the appearance, disappearance, and evolution of characteristic proton signals associated with specific functional groups. The NMR results were used to identify time points at which significant spectral changes occurred and to indicate which regions of the molecule were most affected by oxidation. These observations were then used to select appropriate sampling times and to target specific mass-to-charge (m/z) values during further HPLC/MS analyses for the detection and identification of corresponding transformation products.

In summary, this chapter presents the detailed NMR analyses of, Penicillin G, Amoxicillin, and Ciprofloxacin under two oxidative conditions (i.e. UV irradiation and sodium hypochlorite solution treatment). As mentioned earlier, time-resolved ^{1}H, ^{13}C, and ^{19}F NMR spectra were also used to monitor degradation processes and identify major structural changes. The findings provided molecular-level insight into the stability and reactivity of these antibiotics and served as a foundation for the complementary HPLC/MS analyses, that are presented in the follow-on chapter.

3.2.1 Penicillin G

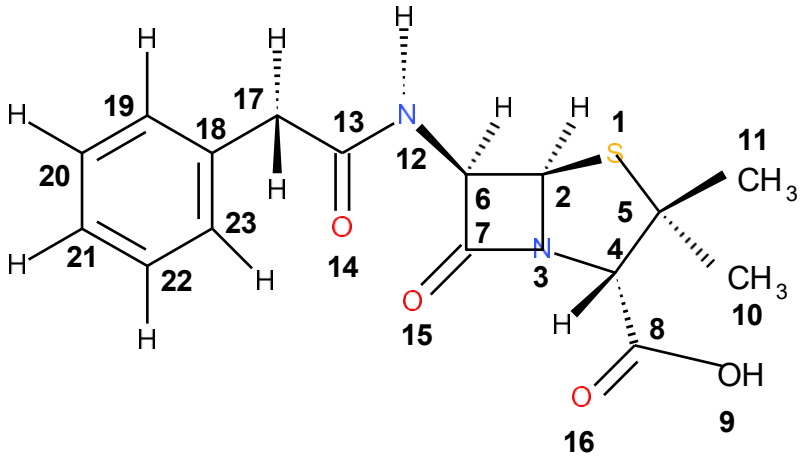

Figure 3.7. Detailed structure of Penicillin G
(structure drawn by the author)

The generic structure of penicillins consists of a thiazolidine ring (i.e. a five-membered ring), connected to a β-lactam ring (a four-membered ring) to which an aminoacyl side chain is attached, and end-tethered with an aromatic ring (Padfield and Kellaway, 1974). The peak assignments of protons, which are of particular interest in the current study were investigated using the Nuclear Magnetic Resonance spectrometry instrument.

a. Nuclear Magnetic Resonance (NMR) spectra for Penicillin G

A range of NMR spectra of Penicillin G in water were run as follows, ^{1}H water suppression; ^{1}H-^{1}H correlation spectroscopy (COSY); ^{13}C with proton decoupling; ^{1}H-^{13}C (Heteronuclear Single Quantum Coherence (HSQC) that can be seen below in Figures 3.8 to 3.11.

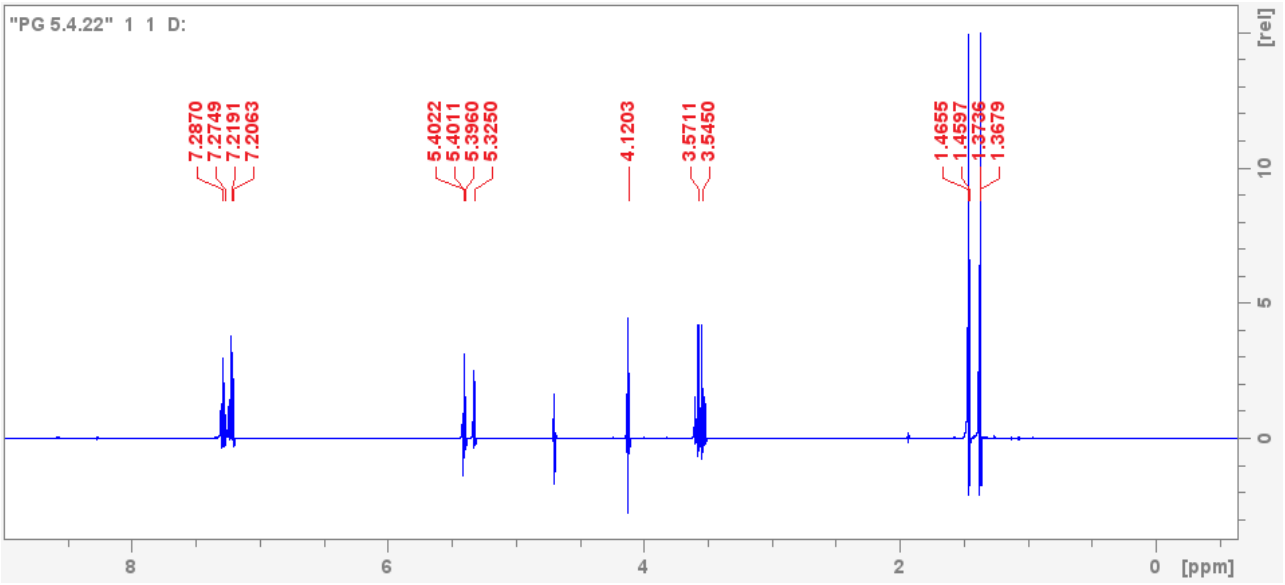

Figure 3.8. ^{1}H NMR of Penicillin G in D_2O (with water suppression NMR spectra)

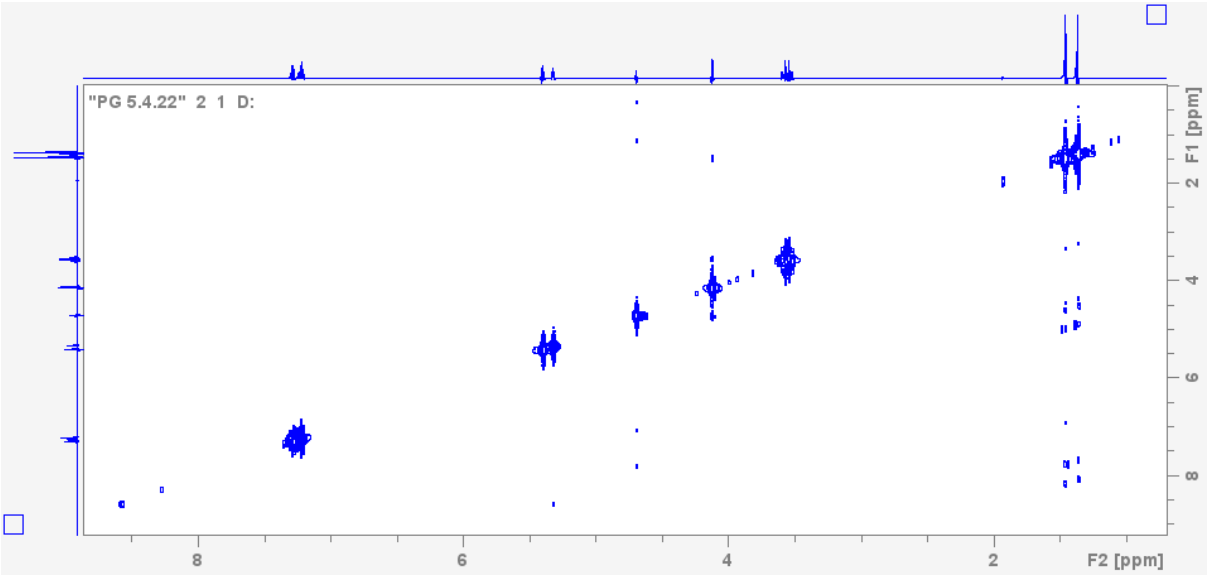

Figure 3.9. ^{1}H-^{1}H COSY NMR spectra of Penicillin G in D_2O (with water suppression)

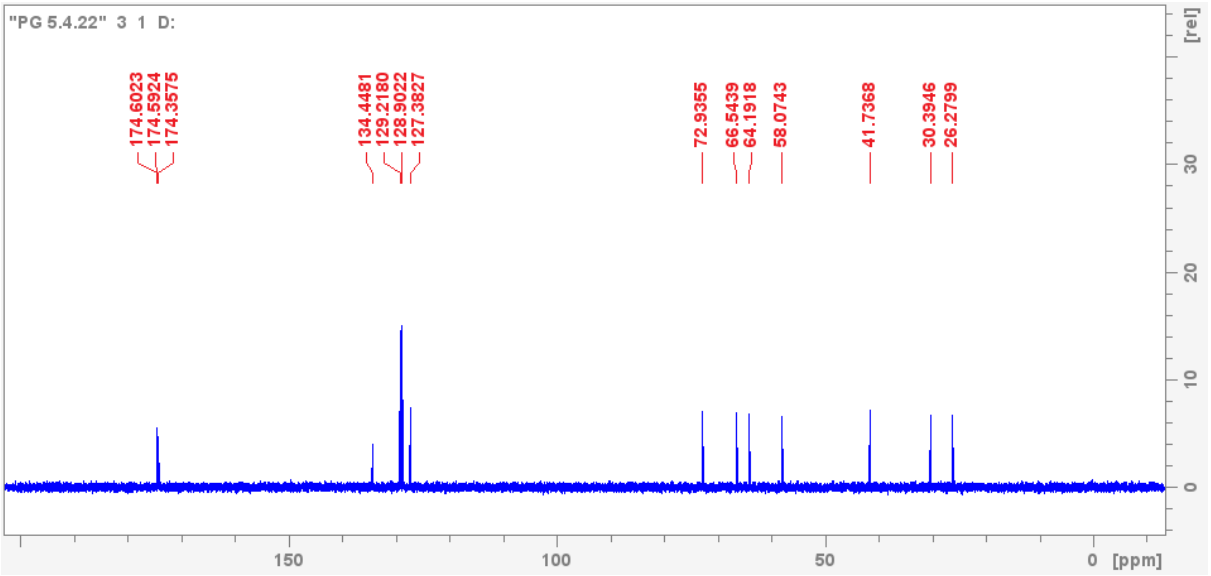

Figure 3.10. ^{13}C NMR spectra of Penicillin G in D_2O

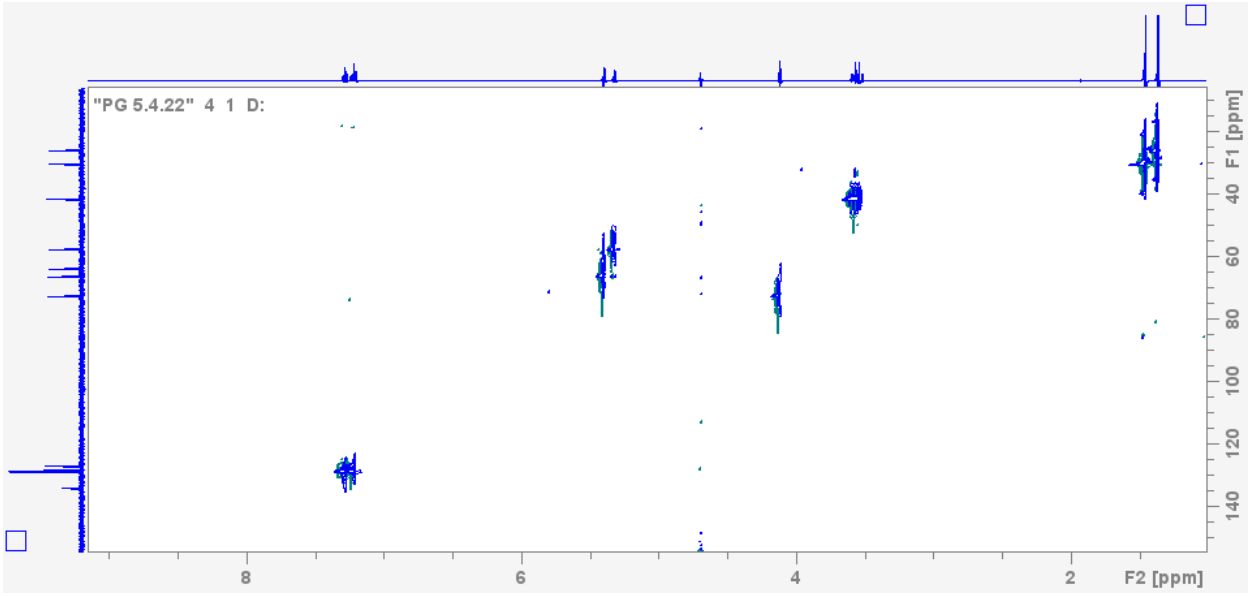

Figure 3.11. ^{1}H-^{13}C COSY (HSQC) NMR spectrum of Penicillin G in D_2O

Figure 3.8 shows various signals of all the protons found in Penicillin G structure. Generally, signals from protons on the beta-lactam ring, the side chains, the thiazolidine ring and the aromatic ring are clearly distinguishable. In Penicillin G, the main features include, the protons of the methyl group usually depending on the environment can be seen as singlets or sometimes as doublets. The amide hydrogens always appear as singlets. Aromatic protons that can always be seen around 7 to 8 ppm due to the magnetic induction of the aromatic ring, and finally the methylene and the methine protons that usually appear as multiples due to coupling.

Figure 3.9 shows the Correlation Spectroscopy (COSY) of Penicillin G. This is a two-dimensional (2D) NMR spectroscopy that is used for studying and analyzing the structures of different compounds like Penicillin G. In the ^{1}H - ^{1}H COSY spectrum, both the horizontal and vertical axes represent ^{1}H chemical shifts. The diagonal peaks correspond to the conventional one-dimensional ^{1}H spectrum, while the off-diagonal cross-peaks indicate scalar (through-bond) coupling between protons. This experiment therefore enables identification of coupled proton pairs and enables the assignment of spin systems within complex molecules such as Penicillin G (Andersen et al., 1988, Sawa et al., 1994, Deimel et al., 2023). Furthermore, it helped in identifying the protons that are coupled to each other, which provides useful information regarding the connectivity of hydrogen atoms in the molecule.

Moreover, Figure 3.10 shows various peaks of the signals of all the carbon atoms found in Penicillin G structure. Generally, peaks for the carbons in beta-lactam ring, the side chains, the thiazolidine ring and the aromatic ring are distinguishable. In Penicillin G, the main features include, the aromatic carbons usually appear between 120 -140ppm, the

carbonyl carbons appearing between 170-180 ppm in the downfield region and the aliphatic carbons that can be seen around 0-50 ppm in the upfield region of the molecule depending on the environment.

Finally, Figure 3.11 shows the Heteronuclear Single Quantum Coherence, or HSQC, Spectroscopy of Penicillin G. This is a two-dimensional (2D) NMR spectroscopy that is used for studying and analysing the structures of different compounds like Penicillin G. This helped in identifying the protons that are bonded directly to carbon atoms, which provides useful information when assigning the carbons in Penicillin G.

After running NMR spectroscopy of Penicillin G using different methods, it was possible to assign the peaks for both the hydrogens and the carbons in Penicillin G and that can be seen in the tables, 3.1 and 3.2, given below.

Table 3.1. Assignments of protons NMR peaks for Penicillin G

Assignments	**Protons in Penicillin G (δ ppm)**
Aromatic protons (19-23)	7.28 - 7.20
Methine protons of the lactam ring (2 and 6)	5.4 - 5.3
Methine proton of the thiazolidine ring (4)	4.12
Benzylic protons (17)	3.54 – 3.57
Methyl protons attached to the thiazolidine ring (10 and 11)	1.46 – 1.36

Table 3.2. Assignments of ^{13}C peaks for Penicillin G

Assignments	**Carbons in Penicillin G (δ ppm)**
Carbonyl carbon of amide (13)	174.6
Carbonyl carbon of the lactam ring (7)	174.59
Carbonyl carbon of the carboxylate group (8)	174.36
Aromatic carbons (18-23)	134.45 -127.38
Methylene carbon of the thiazolidine ring (4)	72.93
Methine carbon common to the lactam and thiazolidine ring (2)	66.54
Quaternary carbon of the thiazolidine ring (5)	64.19
Methine carbon of the lactam ring adjacent to the amide group (6)	58.07
Methylene carbon adjacent to the aromatic ring (17)	41.73
Methyl carbons attached to the thiazolidine ring (10 and 11)	26.28 – 30.39

Penicillin G has been studied extensively using NMR spectroscopy (Daletos et al., 2017, Chang and Hem, 1979, Branch et al., 1987, Degelaen et al., 1979, Kan et al., 1973). In case of ^{1}H NMR of Penicillin G, the frequency ranges of ^{1}H resonances are observed in the range of chemical shifts from 0 to 8ppm. Obvious functionalities, such as the aromatic protons (~7-8 ppm), methyl (~1-2 ppm) and methoxy (~3.5-4 ppm) ones were identified. Whereas, in case of ^{13}C NMR spectrum of Penicillin G the frequency shifts range from 0 to 220 ppm. Due to ^{13}C inherent low sensitivity and the low isotopic abundance, the signals are obviously weaker than those of ^{1}H, and therefore more time for spectra acquisition was needed (Daletos et al., 2017).

Obvious functionalities such as carbonyl, methoxy, aromatic, and methyl groups were identified. The tables above show all the peak assignments of the protons and the carbons in Penicillin G. The NMR data was consistent with that previously reported (Ben Salem et al., 2016, Padfield and Kellaway, 1974, Chang and Hem, 1979), confirming the structural integrity of the parent compound. Minor variations in chemical shift values were observed, which are attributed to differences in concentration, solvent systems, and experimental conditions; however, no opposing structural features were identified.

b. The effect of UV irradiation on Penicillin G in the solid state

The effect of UV light on Penicillin G (solid state) was studied in order to determine if it causes degradation of the antibiotic. Penicillin G in quartz cuvettes was left in a UV irradiation chamber (300-800 nm) using an accelerated weatherability instrument for 2 days. This wavelength range corresponds primarily to UVB and UVA radiation rather than UVC, which is more commonly employed for photolysis and disinfection processes. An ^{1}H NMR spectrum was then run on the irradiated sample in order to determine if any degradation had occurred (Figure 3.12).

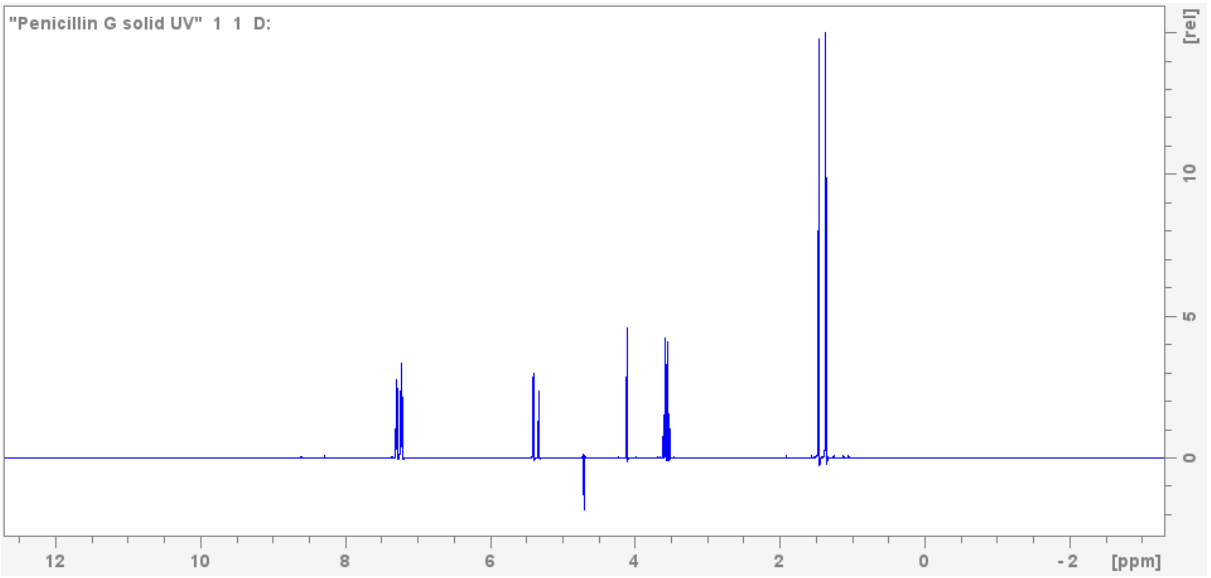

Figure 3.12. ^{1}H NMR spectra of Penicillin G after UV irradiation using accelerated weatherability chamber over 2 days.

The ^{1}H spectrum of Penicillin G after irradiation using the UV source was identical with that of the pure antibiotic which clearly indicated that under the applied UVB/UVA irradiation conditions, no significant degradation of penicillin G was detected, indicating photostability of the compound within this spectral range with no observable degradation had occurred.

Given that no degradation was observed using the Penicillin G when it was irradiated with UV in the solid state, the primary focus of this research shifted to investigation of penicillin G under aqueous conditions that is more relevant to wastewater treatment employing UV irradiation.

c. The effect of UV irradiation on Penicillin G in solution

As described earlier, UV irradiation is widely used as a disinfection method in water treatment when applied at germicidal wavelengths (Pullerits et al., 2020). Furthermore, unlike other disinfection methods, such as ozonation, or chlorination, UV irradiation requires no addition of chemicals, and generally low-pressure UV produces insignificant amounts of unwanted byproducts (Hijnen et al., 2006a, Reckhow et al., 2010).

Moreover, UV irradiation is also an attractive method for efficient disinfection of water, given that this method is more environmentally friendly (Kim et al., 2022). Even though, many studies have been conducted on the removal of antibiotics using Advanced

Oxidation Processes (AOPs) (i.e. using UV in combination with other reagents), there are no reports on degradation of Penicillin G using UV radiation alone.

In this experiment, the UV irradiation of Penicillin G in solution was conducted using the internal UV light source of a UV-visible spectrophotometer (wavelength range of 190-300 nm). Penicillin G (30 mg) was dissolved in D_2O and irradiated under UV radiation for up to 24 hours. It should be noted that spectrophotometer-based UV irradiation involves relatively low light intensity and a limited irradiated area, defined by the optical path and beam dimensions. Consequently, the experiment represents low-fluence UV exposure conditions, and the observed effects reflect the response of penicillin G under these specific irradiation constraints rather than high-intensity UV disinfection scenarios. ^{1}H NMR spectra of the sample were run at intervals of: 30 minutes, then after one hour, two and 24 hours of UV irradiation (Figure 3.13).

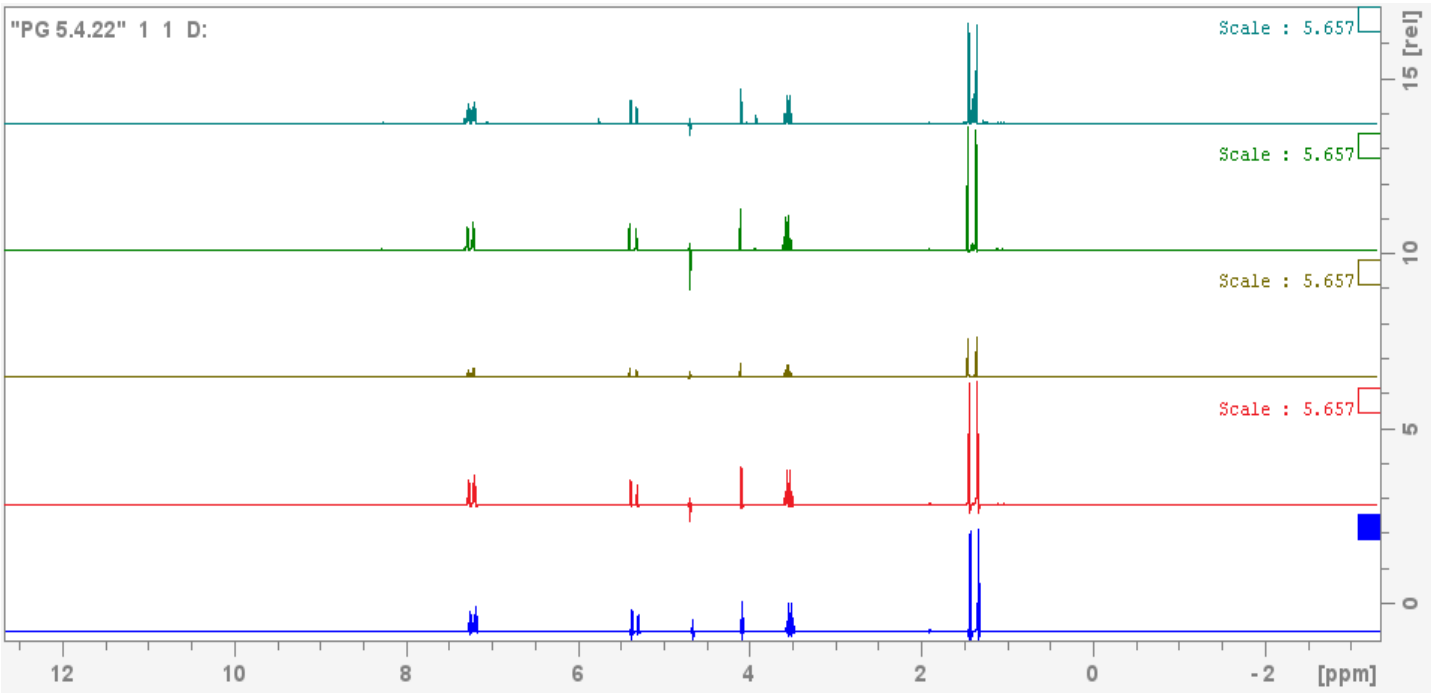

Figure 3.13. ^{1}H NMR spectra of Penicillin G under UV irradiation using the UV visible spectrophotometer instrument with wavelength ranging from 190-300 nm over time. (Blue line showing the standard Penicillin G, red 30 minutes after irradiation, brown 1 h, green 2 h and teal 24 h after irradiation)

The ^{1}H NMR spectra were unchanged at each of the time periods and were identical to that of the pure Penicillin G. Here again, the obvious functionalities, such as the aromatic protons (~7-8 ppm), methyl (~1-2 ppm) and methoxy (~3.5-4 ppm) protons in Penicillin G remained effectively the same even after 24 hours of irradiation. This clearly shows that no measurable degradation of penicillin G occurred after 24 hours of irradiation under the low-irradiance conditions of the spectrophotometer-based experimental setup employed.

In conclusion, given that no observable degradation of Penicillin G was identified in both solid form and in solution after UV irradiation using different instruments, wavelengths and exposure times, it was decided to study the effect of sodium hypochlorite on Penicillin G. Sodium hypochlorite is widely employed as a disinfectant in wastewater treatment for microbial inactivation rather than for the removal of organic contaminants. This investigation of hypochlorite-induced transformations of penicillin G is environmentally relevant in the context of wastewater disinfection practices. This observation is consistent with previous studies reporting that UV irradiation alone often results in limited degradation of β-lactam antibiotics in the absence of additional oxidants or radical-generating systems. Conversely, some studies have reported enhanced UV-driven degradation when higher irradiance, combined UV–oxidant processes or germicidal wavelengths are employed, highlighting that photodegradation efficiency is strongly dependent on irradiation conditions. The present results therefore reflect the limitations of the UV systems employed in this study rather than opposing the broader literature.

d. The effect of sodium hypochlorite on Penicillin G

Sodium hypochlorite solution, or bleach, is a relatively strong oxidizing agent that has been widely applied for microbial inactivation during water and wastewater disinfection. While oxidation using sodium hypochlorite is not employed with the primary objective of degrading organic contaminants, previous studies have shown that antibiotic compounds can undergo chemical transformation when exposed to hypochlorite-based oxidants during disinfection processes (Zhang et al., 2017b, Daletos et al., 2017); however, to the best of our knowledge no studies have been reported on its use for the degradation of Penicillin G. In order to monitor the degradation of Penicillin G, 10 mg of Penicillin G was dissolved in 0.75 mL of deuterium oxide (D_2O), followed by the addition of 0.25 mL of sodium hypochlorite solution. ^1H NMR spectra of the Penicillin G solution were recorded at regular intervals (Figure 3.14).

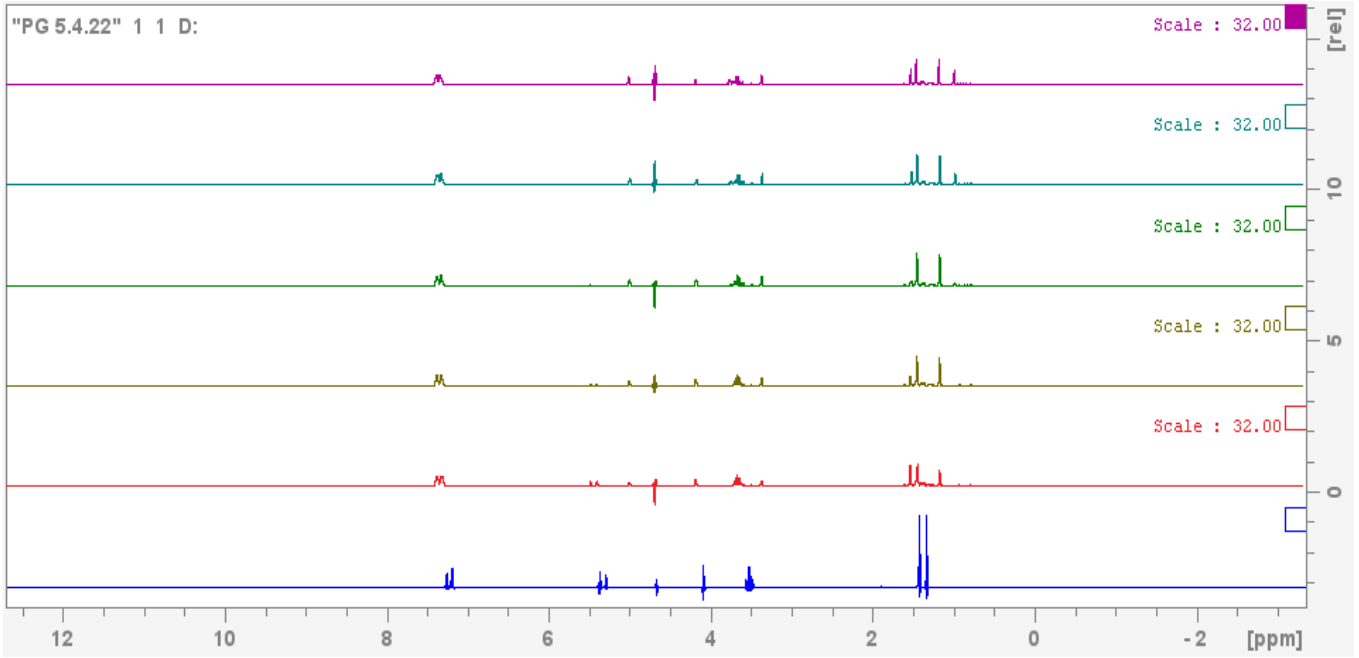

Figure 3.14. ^{1}H NMR of Penicillin G in 0.75 cm^3 of D_2O and 0.25 mL of sodium hypochlorite solution (with water suppression NMR spectra) over two days (blue is the standard prior to addition of sodium hypochlorite, starting from red that shows half an hour after the addition of sodium hypochlorite, brown 1 h, green is 7 h, teal 19 h and purple 27 h).

The ^{1}H NMR spectra of the solution after the addition of sodium hypochlorite under the nominal conditions described in the Materials and Methods section shows pronounced differences compared to the untreated reference spectrum, with significant changes between 1-2 ppm and 5-5.5 ppm (Figure 3.14). These spectral changes reflect time-dependent chemical transformation of the compound under hypochlorite oxidation conditions, rather than a defined dose-response associated with a quantified free or residual oxidant concentration. Interestingly, an immediate change can be observed upon addition of the hypochlorite solution, indicating a very rapid degradation of the antibiotic. ~~The~~ signals in the aromatic region remained the same as did the peak due to the benzylic protons at 3.5 ppm.

It is also clear from the NMR analysis that more than one product is formed during the degradation process as evidenced by the new peaks appearing at 1.2 and 1 ppm (Figure 3.15). Almost immediately after the addition of the hypochlorite a peak appears at 1.2 ppm indicating the formation of a degradation product and then after 5 hours a second peak appears at 1ppm indicating the formation of a second degradation product.

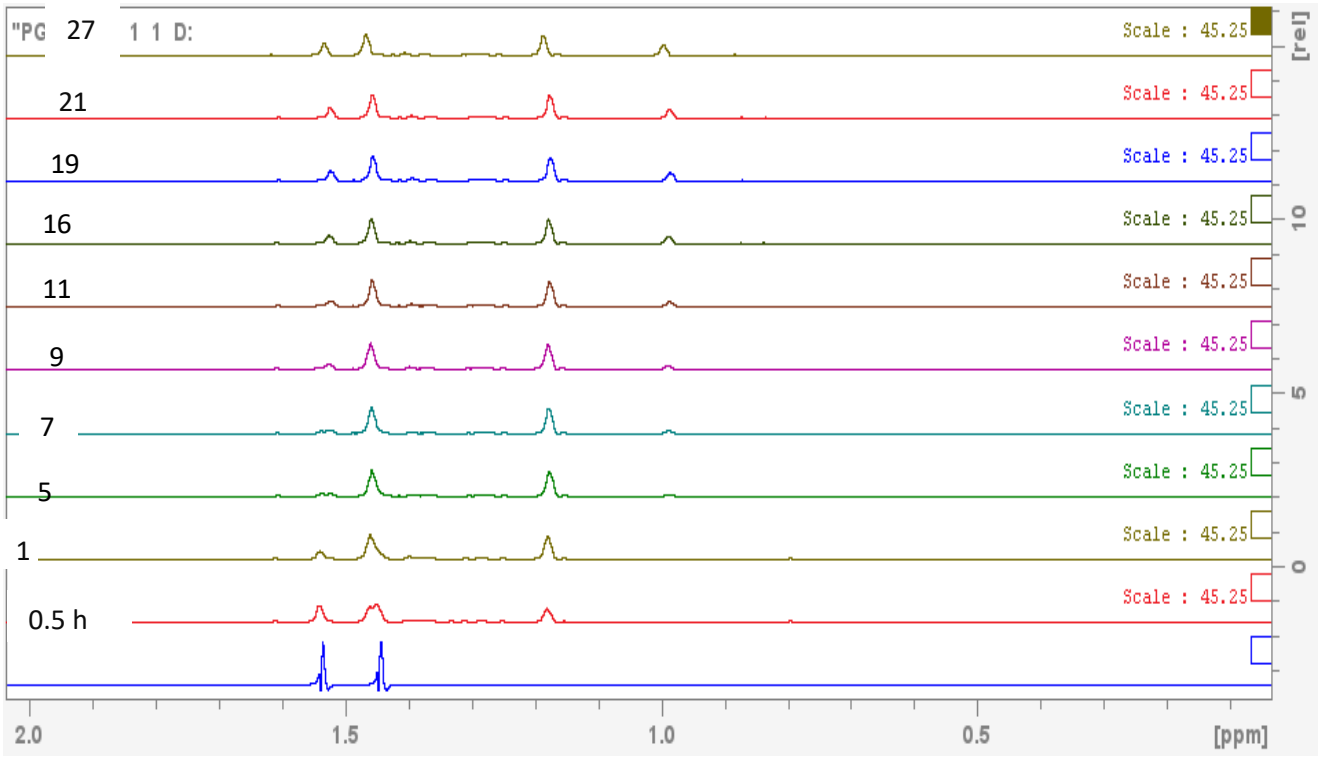

Figure 3.15. NMR spectra of the methyl region of Penicillin G after the reaction with sodium hypochlorite solution (blue is the standard prior to addition of sodium hypochlorite solution, and the others show the respective spectra after specific time periods).

Figure 3.15 shows the peaks of methyl protons attached to the thiazolidine ring (within a range 0- 2 ppm) and the degradations products formed after the addition of sodium hypochlorite solution.

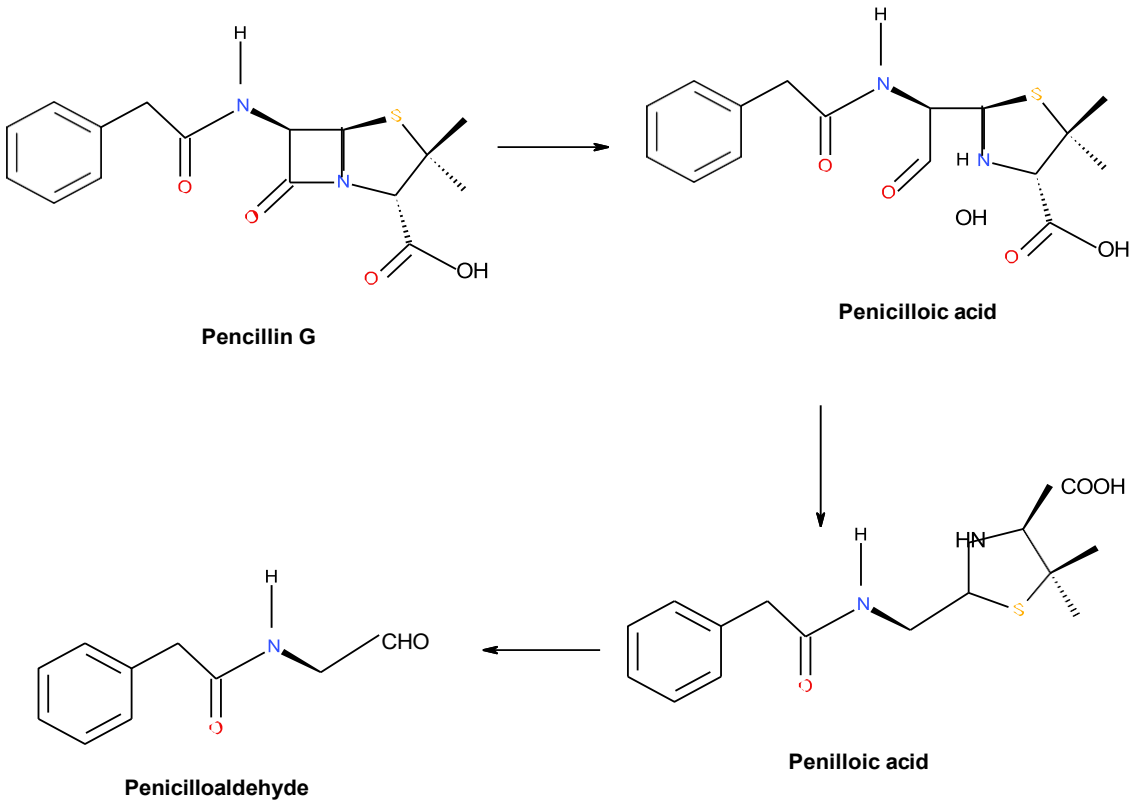

Figure 3.16 Penicillin G main degradation products/derivatives (structure drawn by the author)

Previous studies have reported that exposure of penicillin G in aqueous solution can lead to structural transformation and cleavage of the β-lactam ring. Depending on experimental conditions, reported transformation products include penicilloic acid, penilloic acid and penicilloaldehyde formed through oxidative and hydrolytic pathways rather than intentional contaminant removal. (Figure 3.16) (Lima et al., 2020, Batchelor et al., 1965, Weltzien and Padovan, 1998, Ariza et al., 2015, Li et al., 2008a, Hou and Poole, 1971, Aldeek et al., 2016, Szabó et al., 2016, Kheirolomoom et al., 1999, Branch et al., 1987).

It is likely that exposure of penicillin G to sodium hypochlorite induces oxidative transformation rather than simple degradation. It should be noted that oxidation using sodium hypochlorite may also lead to the formation of chlorinated transformation products under certain conditions. However, within the resolution and sensitivity of the NMR analysis employed in this study, no distinct signals attributable to chlorinated derivatives were clearly identified. The observed spectral features therefore most likely reflect non-chlorinated oxidative transformation pathways of penicillin G under the experimental conditions applied.

Based on the ^{1}H NMR data, the initial transformation is consistent with formation of penicilloic acid, followed by further rearrangement to penilloic acid. The peak which

appears at1.2 ppm is consistent with the methyl group of penicilloic acid which has a reported chemical shift of 1.185 ppm. (Mitsumori et al., 1977). The secondary degradation product which appears at 1 ppm has previously been assumed to be penilloic acid although this was not confirmed (Mitsumori et al., 1977). Other work (Degelaen et al., 1979) has reported that the methyl group of penilloic acid appears at 1.5 ppm. In addition, the formation of penicilloaldehyde degradation product is very unlikely to take place in this case as strong oxidising agent was used for Penicillin G reaction. Further analysis is needed for confirmation of this identity of the second degradation product.

Reaction of Penicillin G with sodium hypochlorite solution also resulted in changes to the signals from protons of the β-lactam ring (5-6 ppm) that is due to the opening of the β-lactam ring (Figure 3.17). Immediately after exposing Penicillin G to the hypochlorite solution, a new peak at 5.0 ppm appears in the NMR spectra. This peak is between the reported peaks for penicilloic acid (5.3ppm) and penilloic acid (4.8ppm) (Mitsumori et al., 1977, Degelaen et al., 1979). Based on the analysis of the methyl groups (Figure 3.15), it is expected that this peak at 5 ppm could be due to penicilloic acid and the difference in chemical shift is likely to arise owing to differences in the pH of the NMR solution, as this study was conducted in aqueous as opposed in an acidic solution (Mitsumori et al., 1977, Degelaen et al., 1979).

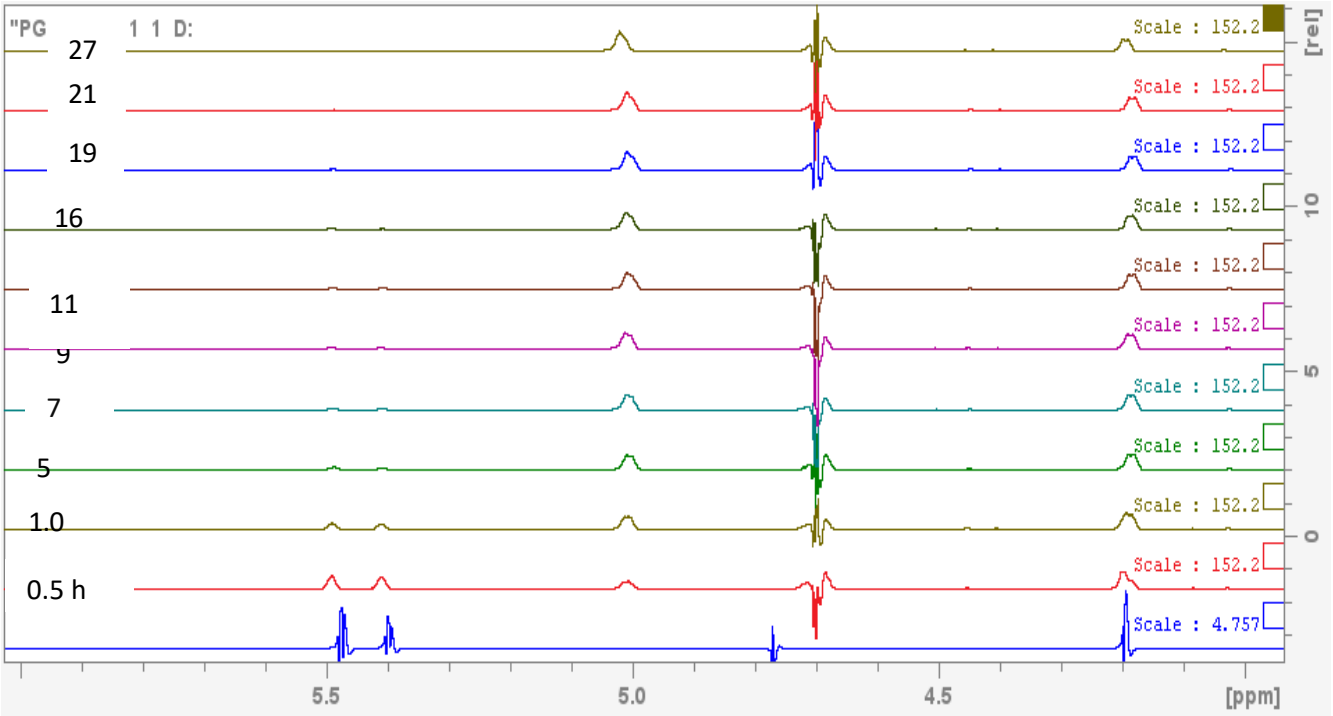

Figure 3.17. ^{1}H NMR of Penicillin G in 0.75 mL of D_2O and 0.25 mL of sodium hypochlorite solution (with water suppression, section between 4-6 ppm) (blue is the standard prior to addition of sodium hypochlorite)

e. Analysis of the rate of degradation of Penicillin G

The ^{1}H NMR time series (Figure 3.17) indicated a rapid degradation process and in order to investigate the rates of degradation further, the signal intensity versus time of selected ^{1}H NMR peaks were analysed. Using the data from the NMR spectra shown in Figure 3.15, the heights of the peak at 1.18 ppm, due to the methyl group of penicilloic acid, and 0.98 ppm, thought to be due to the methyl group of penillic acid, were plotted against reaction time (Figure 3.18). The benzyl proton peak appearing between 3.54-3.57 ppm was used as a reference as it does not change due to the addition of sodium hypochlorite solution.

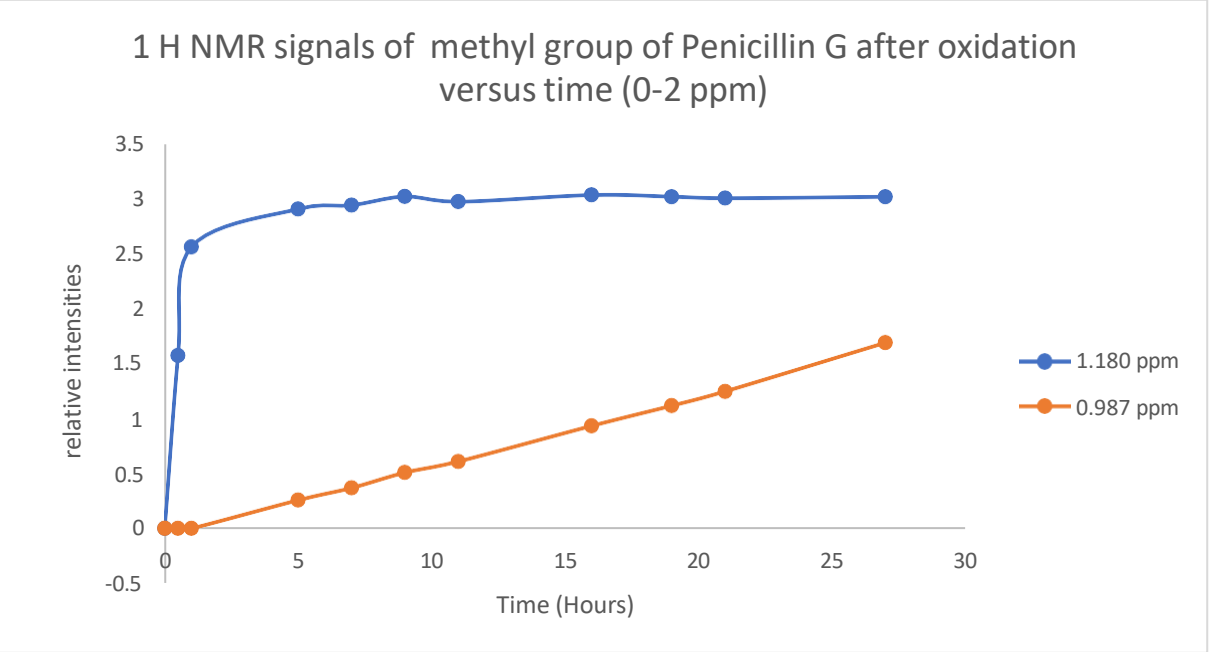

Figure 3.18. Time-dependent changes in ^{1}H NMR signal intensities of methyl group resonances of penicillin G following exposure to sodium hypochlorite, showing the peak at 1.180 ppm (blue) and the peak at 0.9871 ppm (orange)

The data clearly indicate the rapid formation of penicilloic acid (1.18ppm) with significant amounts present after 30 minutes and a steady state concentration reached after 5 hours. As expected, penilloic acid is not formed until 1-5 hours after the addition of sodium hypochlorite and continues to be formed at a steady rate throughout the reaction period. This is consistent with the penilloic acid being a secondary degradation product. Interestingly, the penicilloic acid does not decrease in concentration as the penilloic acid is formed, even though penilloic acid is reported to be a degradation product of penicilloic acid. This may indicate that the penicilloic acid is being formed from penicillin G at the same rate it is being degraded to penilloic acid.

A study by Degelean et al. showed the concentration of Penicillin G degradation products after different time intervals under acidic conditions. Penicilloic acid is formed immediately under acidic conditions and significant concentration is present after 80 minutes which slowly declines over time and is not detectable after 2 days whilst penilloic acid increases in concentration over this time, indicating its formation from penicilloic acid. Whilst there are similarities with the present study with the immediate formation of penicilloic acid and the subsequent formation of penilloic acid, the concentration of penicilloic acid is not observed to decrease over the reaction time period.

Using the data from the NMR spectra shown in Figure 3.17, the area under peaks at 5.35 ppm and 5.40 ppm, due to the protons on the lactam ring of penicillin G were plotted against reaction time (Figure 3.19). The benzyl proton peak appearing between 3.54-3.57 ppm was used as a reference as it does not change due to the addition of sodium hypochlorite.

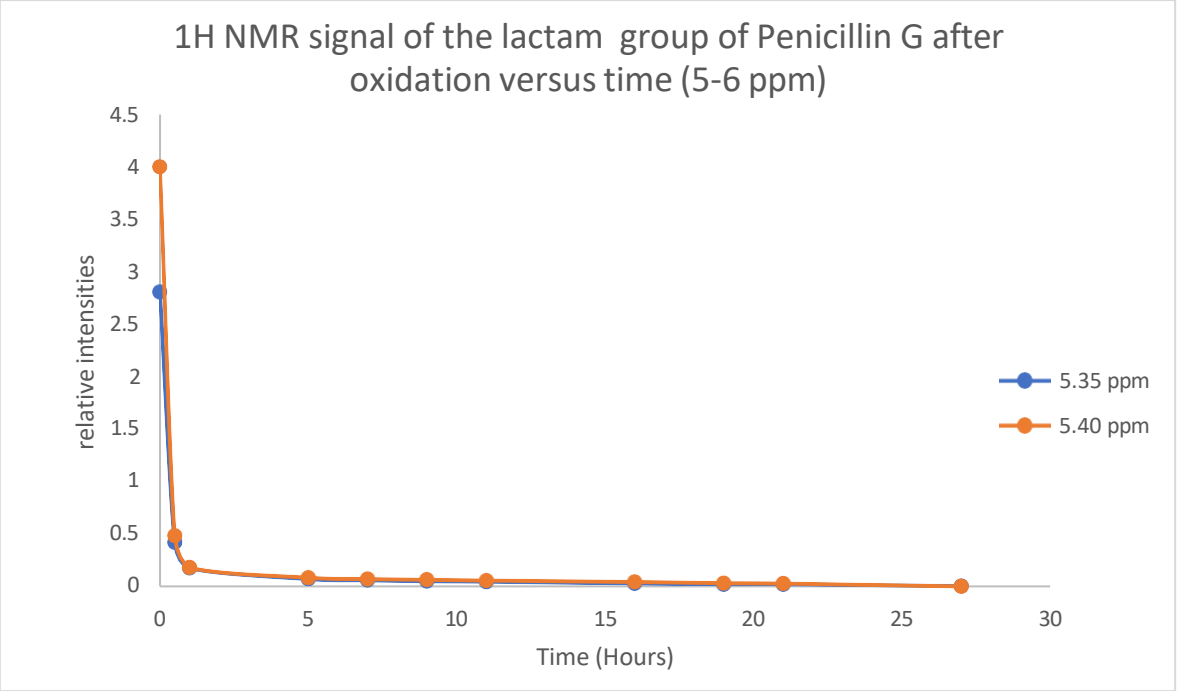

Figure 3.19. Time-dependent changes in ^{1}H NMR signal intensities of penicillin G following exposure to sodium hypochlorite solution, showing resonances at 5.35 ppm (blue) and 5.40 ppm (orange), corresponding to chemically distinct proton environments of penicillin G discussed in the main text

After Penicillin G reaction with sodium hypochlorite, an immediate change is observed as both peaks decrease in intensity and cannot be detected after 10 hours. The decrease in concentration of both peaks implies the complete degradation of Penicillin G. This is

consistent with the degradation of Penicillin G under acidic conditions after 100 minutes all of the Penicillin G had been degraded (Degelaen et al., 1979).

The NMR analysis of the degradation of Penicillin G upon reaction with sodium hypochlorite indicated that the reaction is almost immediate, and that no penicillin G was present in solution after 10 hours and that by-products including penicilloic acid and penilloic acid were formed under these conditions that is consistent with the well-known instability of β-lactam antibiotics, which readily undergo ring-opening reactions and oxidative transformations in aqueous environments. These findings therefore support previously reported behaviour of β-lactam antibiotics under oxidative or aqueous conditions and confirm that Penicillin G is highly susceptible to rapid structural transformation. (Canzani and Aldeek, 2017, Berkani et al., 2022)

3.2.2 Amoxicillin

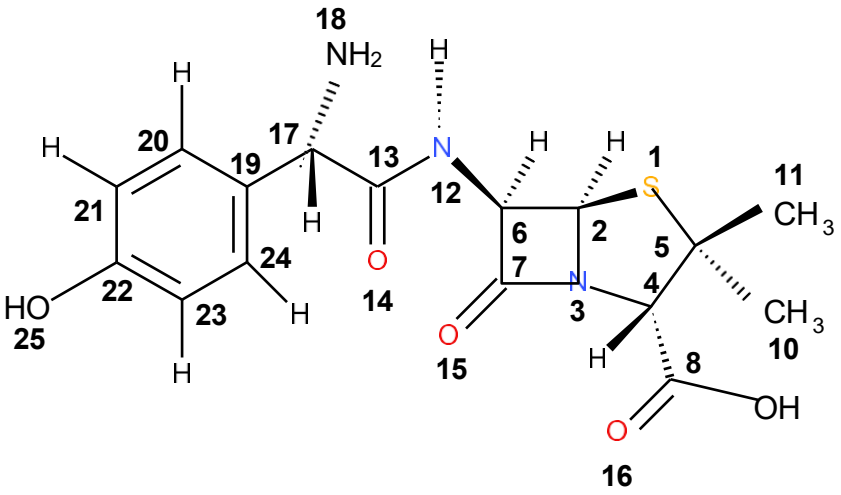

Figure 3.20. Detailed structure of Amoxicillin (structure drawn by the author)

Amoxicillin is a beta-lactam antibiotic belonging to the penicillin class. Its structure consists of β-lactam ring, a thiazolidine ring and hydroxylated phenyl group, and an amino group (-NH_2) and an amide group exo to the cyclic structures.

a. Nuclear Magnetic Resonance (NMR) spectra for Amoxicillin

A range of NMR spectra of Amoxicillin in D_2O using an approximately 10 mg mL^{-1}solution and were run as follows: ^1H water suppression; ^1H-^1H correlation spectroscopy (COSY); ^{13}C with proton decoupling; 1H-^{13}C Heteronuclear Single Quantum Coherence (HSQC) that can be seen below in Figures 3.21 - 3.24.

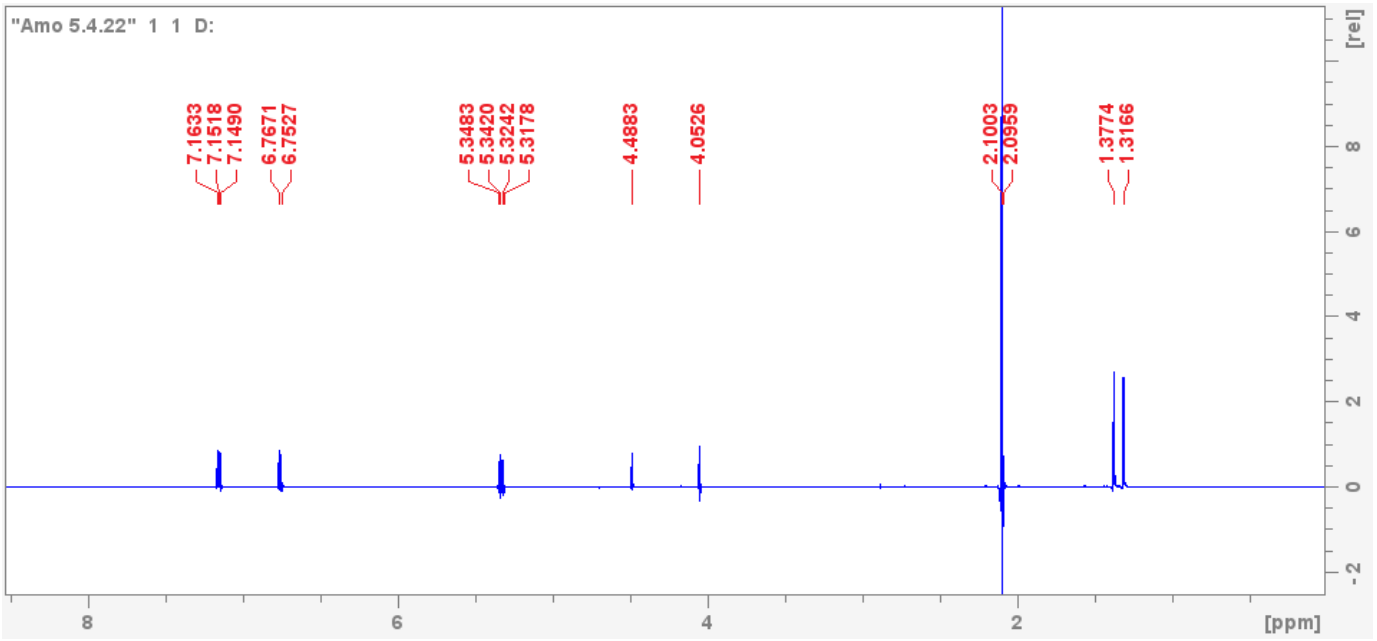

Figure 3.21. ^{1}H NMR of Amoxicillin in D_2O (with water suppression NMR spectra)

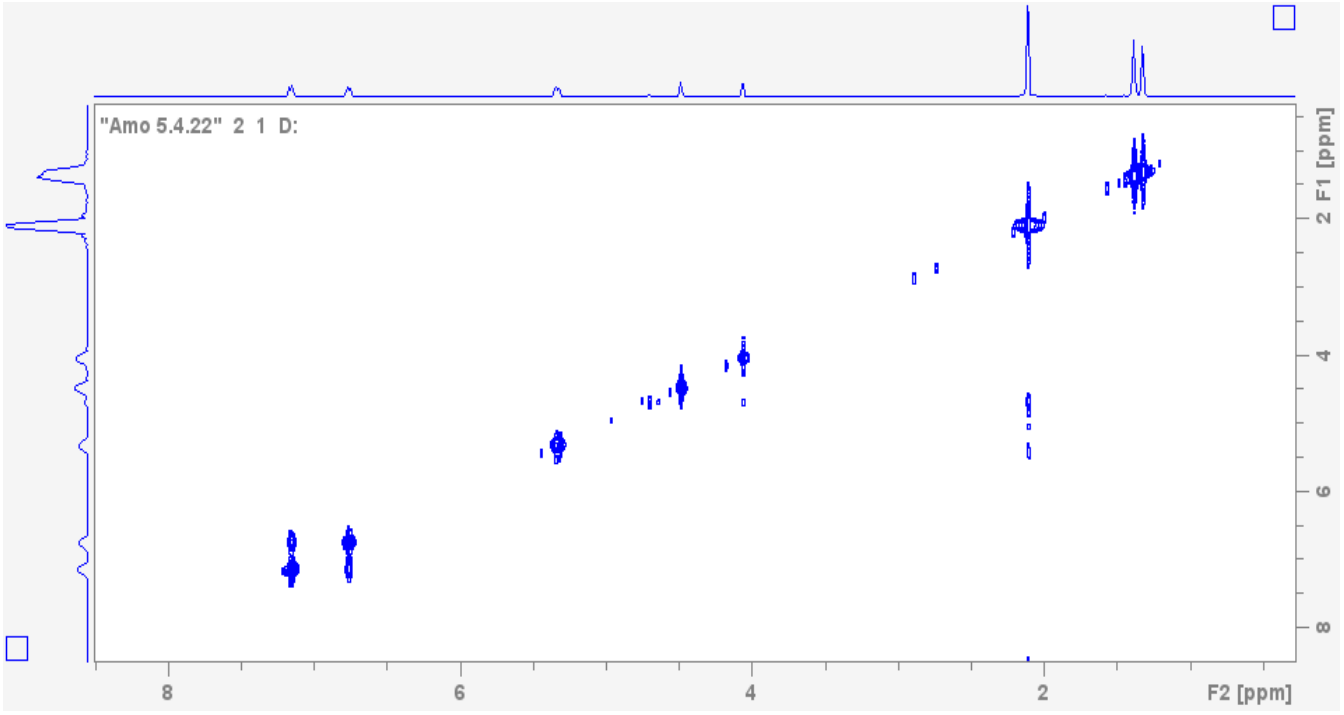

Figure 3.22. ^{1}H-^{1}H COSY NMR spectra of Amoxicillin in D_2O (with water suppression)

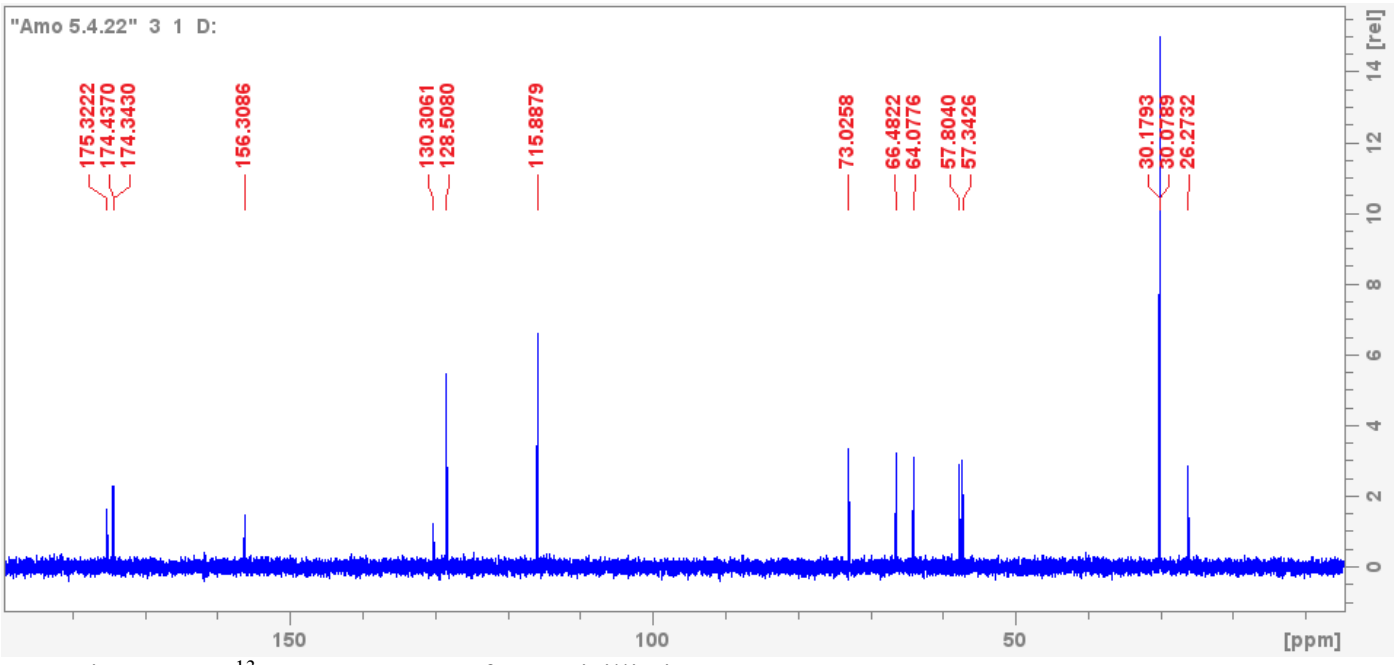

Figure 3.23. ^{13}C NMR spectra of Amoxicillin in D_2O

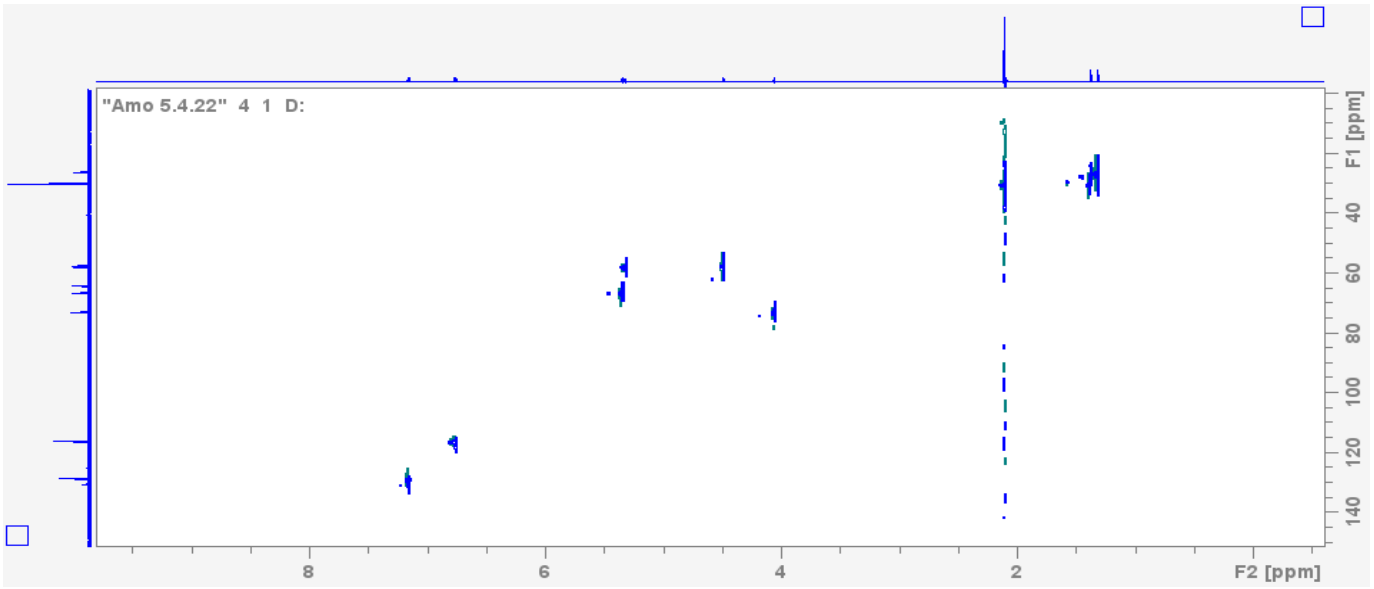

Figure 3.24. ^{1}H-^{13}C COSY (HSQC) NMR spectrum of Amoxicillin on D_2O

After running NMR spectroscopy of Amoxicillin using different methods, it was possible to assign the peaks for both the protons and the carbons in Amoxicillin and that can be seen in the tables below.

Table 3.3. Assignments of proton NMR peaks for Amoxicillin

Assignments	**Protons in Amoxicillin**
Aromatic protons (20-24)	7.16 – 6.75
Methine protons of the lactam ring (2 and 6)	5.34 - 5.31
Methine proton of the thiazolidine ring (4)	4.48
Methine attached to amino group (17)	4.05
Methyl protons attached to the thiazolidine ring (10 and 11)	1.38 – 1.32

*The signal from the hydroxyl proton is expected to appear in the region of 10 ppm and amide proton about 8 ppm- these are not detected as D_2O was used as the solvent

The table below (Table 3.4) show the peak assignments of the protons and the carbons in Amoxicillin. In case of ^{1}H NMR of Amoxicillin, the chemical shift frequencies ranging from 0 to 8ppm was observed. Obvious functionalities, such as the aromatic protons (~7-8ppm) and methyl protons (~1-2ppm) were identified. The ^{1}H and ^{13}C NMR data were consistent with that previously reported (Bisson-Boutelliez et al., 2010, Gozlan et al., 2013).

Table 3.4. Assignments of ^{13}C peaks for Amoxicillin

Assignments	**Carbons in Amoxicillin**
Carbonyl carbon of amide (13)	175.3
Carbonyl carbon of the lactam ring (7)	174.4
Carbonyl carbon of the carboxylate group (8)	174.3
Aromatic carbons (19-24)	130.3 -115.9
Methylene carbon of the thiazolidine ring (4)	73.0
Methine carbon common to the lactam and thiazolidine ring (2)	66.5
Quaternary carbon of the thiazolidine ring (5)	64.0
Methine carbon of the lactam ring adjacent to the amide group (6)	57.8
Methylene carbon adjacent to the aromatic ring (17)	57.3
Methyl carbons attached to the thiazolidine ring (10 and 11)	30.2 – 26.3

The tables above show the peak assignments of the protons and the carbons in Amoxicillin. In case of ^{1}H NMR of Amoxicillin, the chemical shift frequencies ranging from 0 to 8ppm was observed. Obvious functionalities, such as the aromatic protons (~7-8ppm) and methyl protons (~1-2ppm) were identified. The ^{1}H and ^{13}C NMR data were

consistent with that previously reported (Bisson-Boutelliez et al., 2010, Gozlan et al., 2013).

b. The Effect of UV irradiation on Amoxicillin in the solid state

The effect of UV light on Amoxicillin was studied in this experiment to determine if it causes degradation of the antibiotic. Amoxicillin in quartz cuvettes was left under UV irradiation(300-800nm) using an accelerated weatherability chamber for 2 days. A ^{1}H NMR spectrum was run to determine if any degradation had occurred (Figure 3.25).

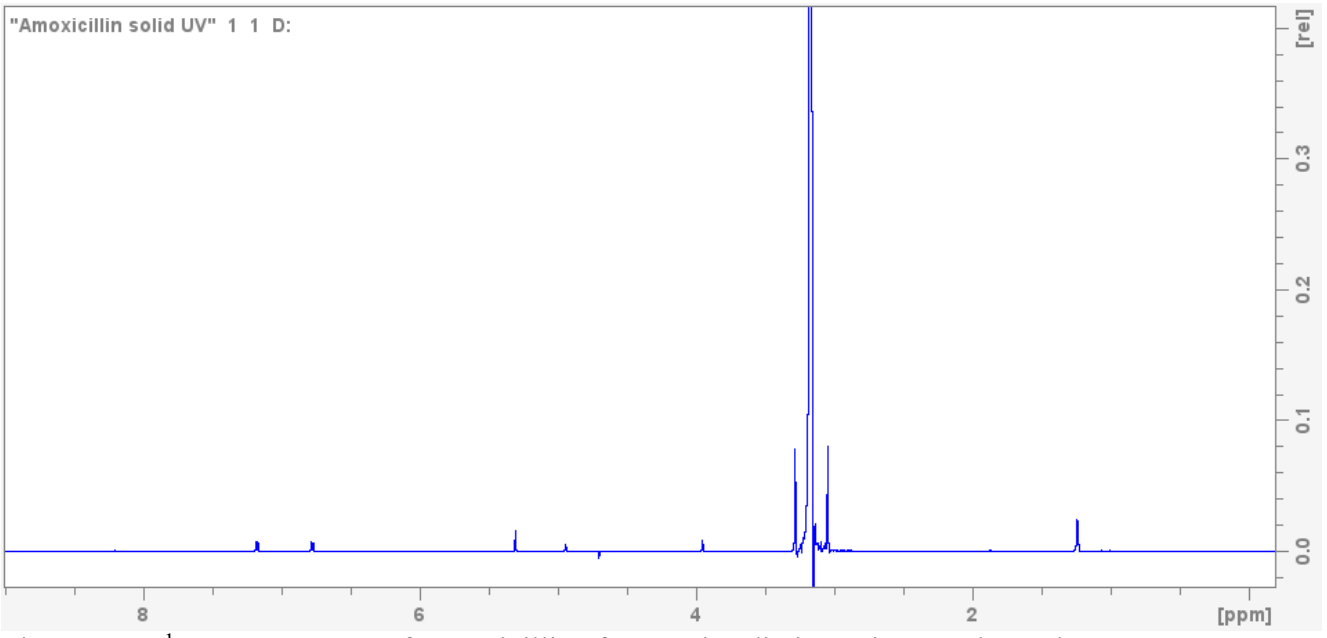

Figure 3.25. ^{1}H NMR spectra of Amoxicillin after UV irradiation using accelerated weatherability chamber over 2 days.

The ^{1}H spectrum of Amoxicillin after irradiation using the UV light was identical with that of the pure antibiotic (Figure 3.21) which clearly indicates that under these conditions no degradation had occurred.

Given that no degradation was observed using the Amoxicillin in solid form, it was considered to test Amoxicillin in solution as this is a more common way of wastewater treatment practices using the UV irradiation.

c. The Effect of UV irradiation on Amoxicillin in solution

The UV irradiation of Amoxicillin in solution was conducted by employing a UV-visible spectrophotometer, where Amoxicillin in solution was irradiated under UV light for 24 hours. ^{1}H NMR spectra of the samples were run at intervals of: 30 minutes, then after one hour, two and 24 hours of UV irradiation (Figure 3.26)

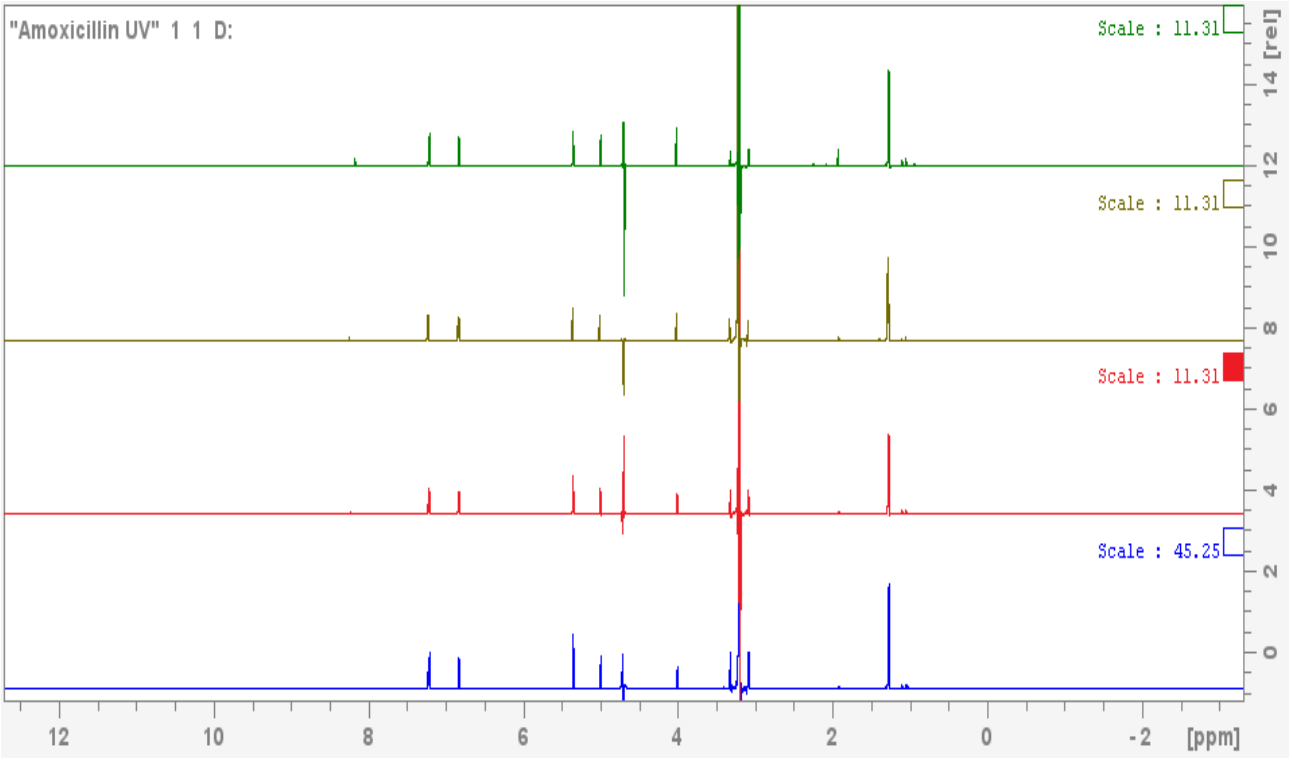

Figure 3.26. ^{1}H NMR spectra of Amoxicillin under UV irradiation with wavelength ranging from 200- 450 nm over time (Blue 30min, red 1 h, brown 2 h and green 24 h)

The UV irradiation showed no effect on Amoxicillin as there are no shifts, or changes, to the signals of the protons in the spectra. This indicates that, under the low-irradiance UV exposure conditions provided by the spectrophotometer-based setup employed in this study, no detectable photochemical transformation of amoxicillin occurred. This is consistent with a previous study that showed UV irradiation alone had an insignificant effect on Amoxicillin degradation, while the addition of persulfate, or hydrogen peroxide, increased the degradation of Amoxicillin significantly due to the generation of hydroxyl radical and sulfate (Zhang et al., 2019).

In conclusion, given that no degradation of Amoxicillin was observed in both solid form and in solution (approximately 10 mg mL^{-1}) after UV irradiation using different instruments, wavelengths and exposure times, that is consistent with reports in the literature

indicating that Amoxicillin exhibits limited photodegradation under certain UV conditions used in this experiment and therefore, it was decided to study the effect of sodium hypochlorite on Amoxicillin, as it's the most common disinfectant product used in wastewater treatment practices.

d. Effect of Sodium hypochlorite on Amoxicillin

In this experiment, in order to monitor the degradation of Amoxicillin, sodium hypochlorite solution was added to an aqueous solution of Amoxicillin (approximately 10 mg mL^{-1}) and ^{1}H NMR spectra were recorded at regular intervals as shown in Figure 3.27. Here, it is to be noted that a couple of drops of formic acid were added to the solution to effect complete dissolution.

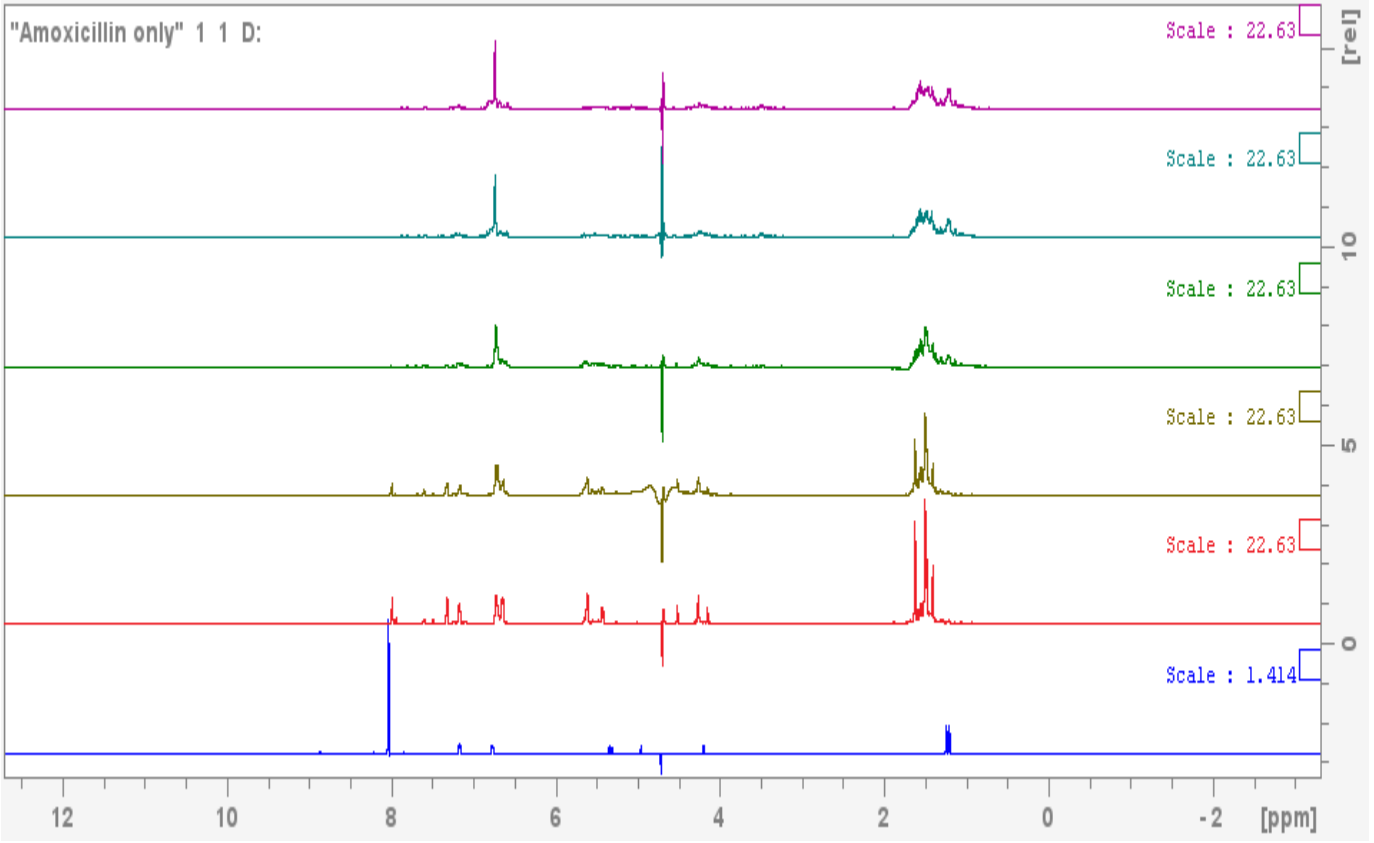

Figure 3.27. ^{1}H NMR of Amoxicillin in 0.75 mL of D_2O and 0.25 mL of sodium hypochlorite solution (with water suppression NMR spectra) over two days (blue is the standard prior to addition of sodium hypochlorite, starting from red that shows half an hour after the addition of sodium hypochlorite, brown 1.5-h, green is 7 h, light blue 19 hand purple 28 h)

The initial spectrum (blue trace) represents the intact structure of Amoxicillin, followed by spectra taken at 0.5 hours (red), 1.5 hours (brown), 7 hours (green), 19 hours (light blue), and 28 hours (purple) after oxidant addition. Two drops of formic acid were included to ensure complete dissolution. Obvious differences were observed almost

immediately following the addition of sodium hypochlorite (Figure 3.27). Significant changes occurred in the methyl region (1–2 ppm), β-lactam region (5–5.5 ppm), and the aromatic region (6.5–7.5 ppm), indicating rapid degradation of Amoxicillin. This is similar to the behaviour seen with Penicillin G in earlier experiments. The most immediate observation after the addition of sodium hypochlorite, was the rapid disappearance of the β-lactam proton signals (~5.3–5.5 ppm) within the first 30 minutes, suggesting cleavage of the β-lactam ring. Likewise, the singlet near 1.5 ppm, assigned to methyl groups on the thiazolidine ring, began to shift and decrease in intensity. These changes demonstrate early-stage degradation of both the β-lactam and thiazolidine rings.

Notably, a new peak emerged at 4.51 ppm almost immediately after the addition of sodium hypochlorite, suggesting the formation of an early degradation product. After approximately 7 hours, a second new peak appeared at 3.48 ppm, indicating the formation of additional degradation products. Based on their timing and chemical shifts, they are consistent with Amoxicillin penicilloic acid (4.51 ppm) and Amoxicillin penilloic acid (3.48 ppm), both of which are common degradation products reported in literature (Gozlan et al., 2013). These findings suggest that β-lactam ring hydrolysis is the first degradation step, followed by further rearrangement of the molecule. These newly emerging peaks are also consistent with intermediates such as compounds **1** and **3** in Figure 3.29, which represent hydrolytic cleavage products of the β-lactam ring and early-stage degradation derivatives of Amoxicillin(Siciliano et al., 2021).

Another significant transformation was observed in the aromatic region between 6.5–7.5 ppm. Initially, the untreated Amoxicillin spectrum displayed two distinct doublets, characteristic of the symmetrical substitution on the phenyl ring. After the addition of sodium hypochlorite, these signals split into four doublets, suggesting that substitution reactions had taken place on the ring. By 6 hours post-treatment, these aromatic signals disappeared entirely, pointing to further degradation or transformation of the aromatic ring.

Although earlier interpretations suggested possible oxidation of the phenol group, this is not supported by the data. Instead, the changes observed are more consistent with chlorine substitution on the aromatic ring. This interpretation aligns with the type of reactivity expected from sodium hypochlorite and with the appearance of new NMR signals, particularly the loss in the aromatic protons.

These findings are consistent with degradation pathways reported in the literature. Gozlan et al. (2010, 2013) and Lamm et al. (2009) identified penicilloic acid and penilloic acid as primary degradation products of Amoxicillin, resulting from β-lactam ring hydrolysis. In this study, the disappearance of β-lactam-associated signals (5–5.5 ppm) and the emergence of the 4.51 ppm signal suggest the formation of penicilloic acid, while the 3.48 ppm signal is likely attributable to penilloic acid.

Previous studies show that the main products that are formed by degradation of Amoxicillin in solution are Amoxicillin penicilloic acid, Amoxicillin penilloic acid, diketopiperazine amoxicillin and hydroxyphenylglyl amoxicillin (Lamm et al., 2009, Gozlan et al., 2013, Gozlan et al., 2010, Deshpande et al., 2004b, Connor et al., 1994b, Yang et al., 2020, Pérez-Parada et al., 2011, Bisht et al., 2024) (Figure 3.28). However, the distribution of degradation products reported in the literature is not always consistent, as several studies indicate that the products formed depend strongly on experimental conditions such as pH, oxidant type, irradiation conditions, and analytical technique employed. In the present study no evidence was found in the NMR data for more complex degradation products such as diketopiperazine Amoxicillin, although these have been detected in other analytical studies (Lamm et al., 2009). By 28 hours, all the original Amoxicillin peaks had disappeared from the spectrum, which suggests that the parent compound had fully broken down. However, there were still some small, broad signals present, most likely from the degradation products. These were difficult to interpret due to their low intensity and overlapping nature.

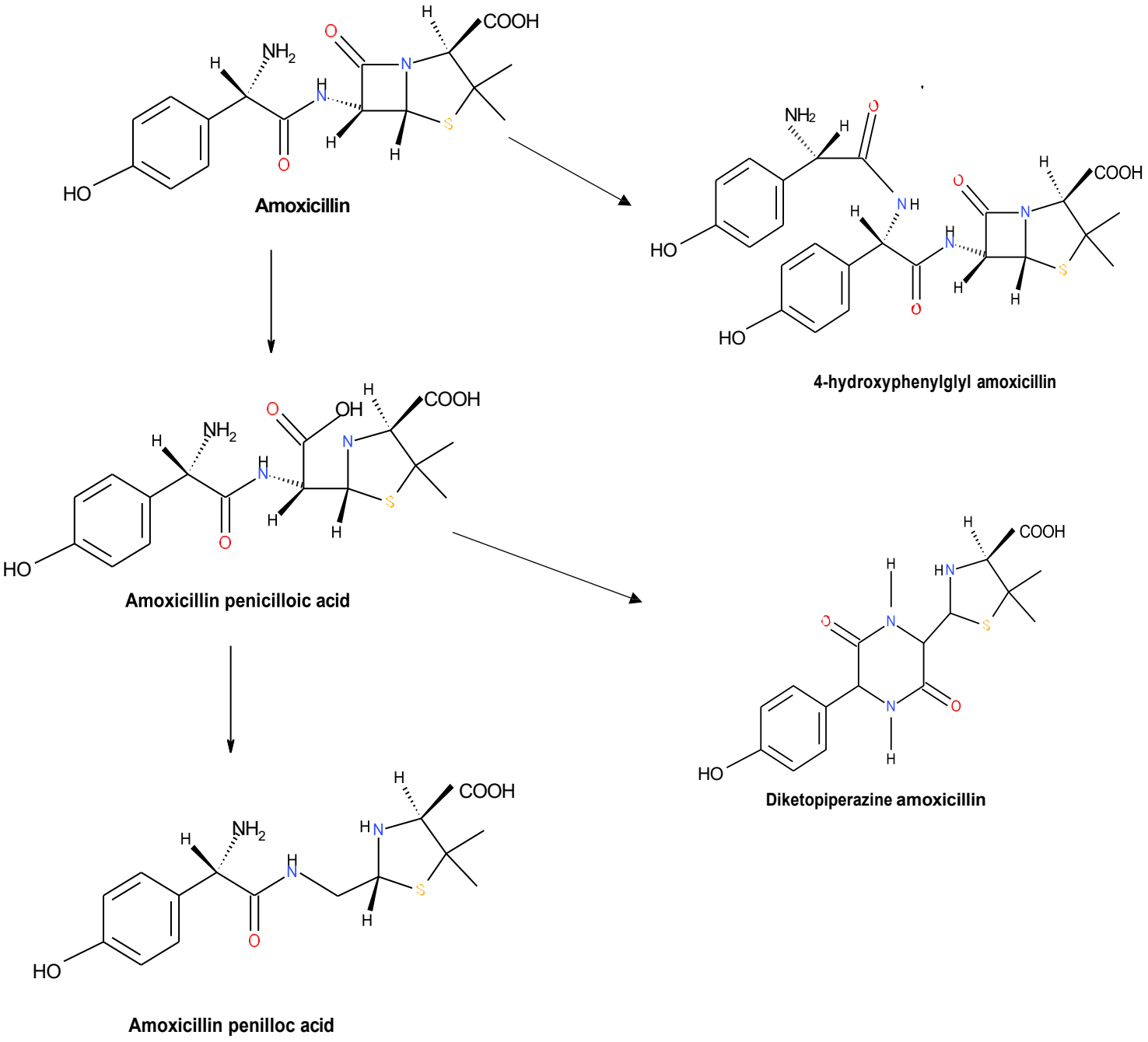

Figure 3.28. Suggested degradation pathway of amoxicillin in aqueous medium (according to (Gozlan et al., 2010, Gozlan et al., 2013))

Although phenol oxidation was considered, no clear evidence supported this pathway. Instead, the shifts and eventual disappearance of these signals are more possibly attributed to substitution reactions, likely involving chlorine. This interpretation is strongly supported by the oxidation transformation products identified in Figure 3.29, which outlines 16 possible oxidative by-products of Amoxicillin following treatment with sodium hypochlorite (reproduced from Siciliano et al., 2021). Figure 3.29 is reproduced to provide literature context for the observed NMR trends and does not imply direct identification of these transformation products in the present study. For example, chlorinated compounds such as structures 9 and 10 (chlorophenols), and structure 16 (a highly oxidised, multifunctional degradation product), correlate well with the observed shifts and eventual disappearance of the aromatic proton signals in the NMR spectra. Moreover, structures 1 through 5 represent hydrolysed or rearranged products of the β-lactam and thiazolidine rings, aligning with the early loss of key proton signals in those regions (1.3–1.5 ppm and ~5.3 ppm). The NMR data thus directly supports the presence of several degradation pathways, including β-lactam hydrolysis, chlorine substitution on the aromatic ring, and advanced oxidative fragmentation.

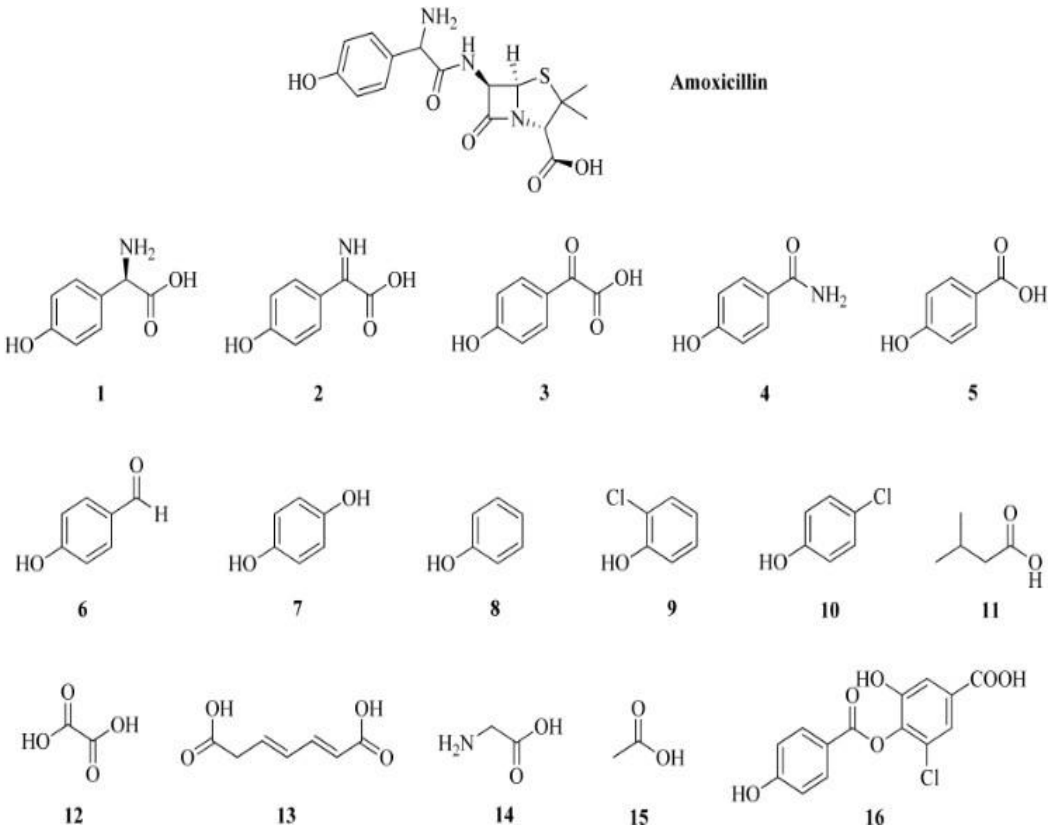

Figure 3.29. Proposed degradation pathway of Amoxicillin in aqueous solution following sodium hypochlorite treatment, showing 16 possible by-products (reproduced from Siciliano et al., 2021). Numbered compounds correspond to transformation products as assigned in the original publication

Legend: Numbered compounds (1–16) correspond to transformation products of amoxicillin as identified and labelled by Siciliano et al. (2021)

In conclusion, the ^{1}H NMR analysis in this case clearly demonstrates that Amoxicillin undergoes rapid and extensive degradation upon exposure to sodium hypochlorite. The earliest transformations involved the loss of β-lactam and thiazolidine ring protons, along with emergence of new peaks indicating specific degradation products. Changes in the aromatic region suggest substitution reactions, most likely involving chlorine. These experimental findings are consistent with previously reported degradation pathways, confirming the molecule's high sensitivity to oxidative treatment (Siciliano et al., 2021). Although NMR provided valuable structural information, the inability to establish a reliable internal standard limited the use of this technique for kinetic analysis. The degradation products identified here will be explored further and validated using HPLC/MS in the next section.

e. Analysis of the rate of degradation of Amoxicillin

Due to the rapid and extensive degradation of Amoxicillin after the addition of sodium hypochlorite, and the absence of a stable internal reference to compare other peaks with, accurate quantification of degradation kinetics via ^{1}H NMR was not feasible in this study. While in case of Penicillin G a consistent reference signal allowed semi-quantitative tracking, the same approach could not be applied for Amoxicillin.

Initially, the intensity of the aromatic proton signal at 7.16 ppm (precisely measured at 7.1646 ppm) was considered for degradation monitoring. However, this peak did not diminish consistently over time and never approached baseline, making it unsuitable for quantification. While a signal near 8 ppm was also visible, this was confirmed to originate from formic acid (used to aid dissolution) and was thus not usable as a reference.

Peak intensities were initially assessed using the Bruker® TopSpin 4.4.10 software, where hovering over each peak displayed its height. However, because of the shifting baselines, spectral overlaps and the complexity of degradation products forming over time, none of the peaks proved stable or consistent enough to be used for reliable intensity plotting.

As a result, while qualitative observations clearly indicate rapid degradation that is evidenced by the disappearance and shifting of peaks in key regions such as the methyl (1–2 ppm), β-lactam (5–5.5 ppm), and aromatic (6.5–7.5 ppm) zones and therefore, a quantitative degradation curve could not be constructed from the NMR data.

In this experiment, and consistent with previous studies, it can be concluded that Amoxicillin undergoes rapid degradation immediately upon chlorination (Gozlan et al., 2013; Siciliano et al., 2021), with no significant further transformations observed over extended time periods. The disappearance of key NMR signals and the eventual absence of any measurable spectrum after 28 hours suggest complete molecular breakdown. As NMR provides only limited structural detail on the complex mixture of degradation products, a more detailed mass spectrometric analysis is required to identify and characterise the major by-products formed. This is addressed in the following chapter through LC/MS analysis.

3.2.3 Ciprofloxacin

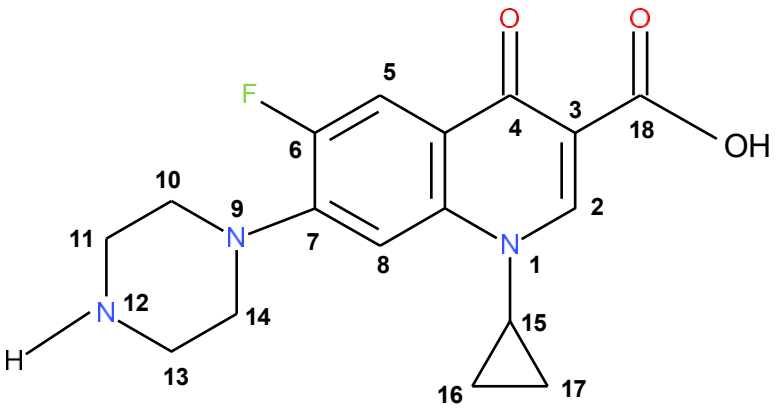

Figure 3.30. Detailed structure of Ciprofloxacin (structure drawn by the author)

Ciprofloxacin consists of 1-cyclopropyl-6-fluoro-1,4-dihydro-4-oxo-7-(1-piperazinyl)-3-quinolinecarboxylic acid. The peak assignments of protons, which are of particular interest in the current study were studied using NMR.

a. Nuclear Magnetic Resonance (NMR) spectra for Ciprofloxacin

A range of NMR spectra of Ciprofloxacin in water were run as follows, ^{1}H water suppression; ^{1}H-^{1}H correlation spectroscopy (COSY); ^{13}C with proton decoupling; ^{1}H-^{13}C (Heteronuclear Single Quantum Coherence (HSQC) and ^{19}F NMR of Ciprofloxacin can be seen below in Figures 3.31 – 3.35.

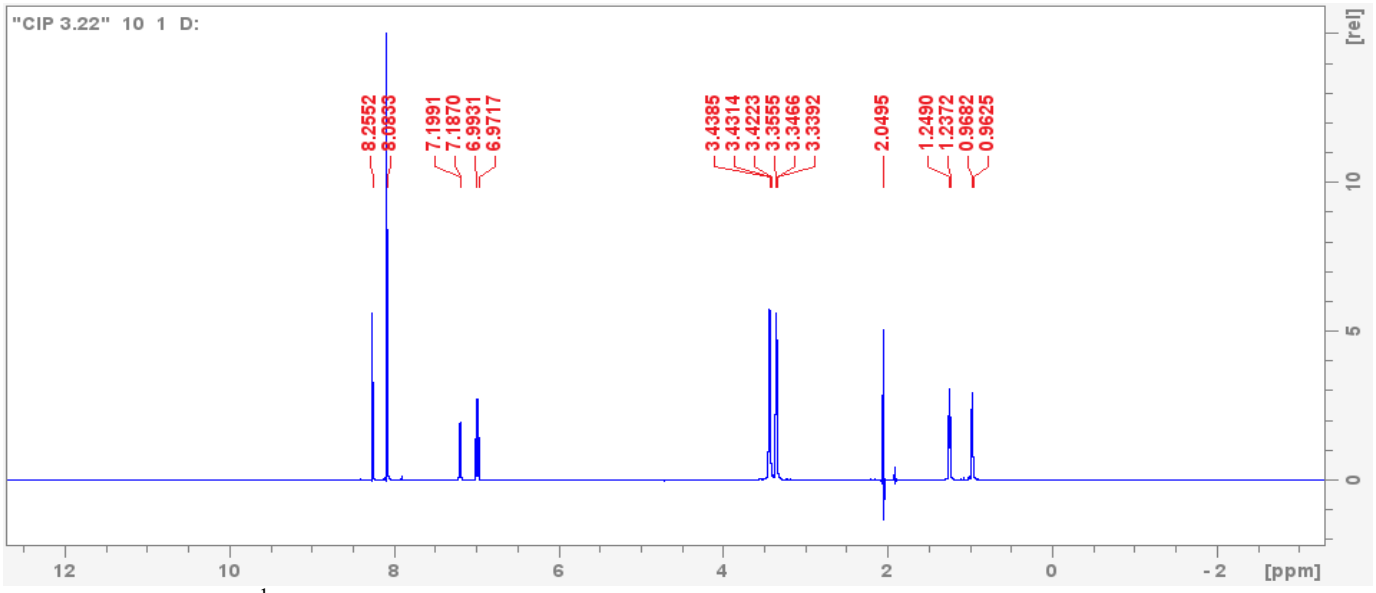

Figure 3.31. ^{1}H NMR of Ciprofloxacin in D_2O (with water suppression)

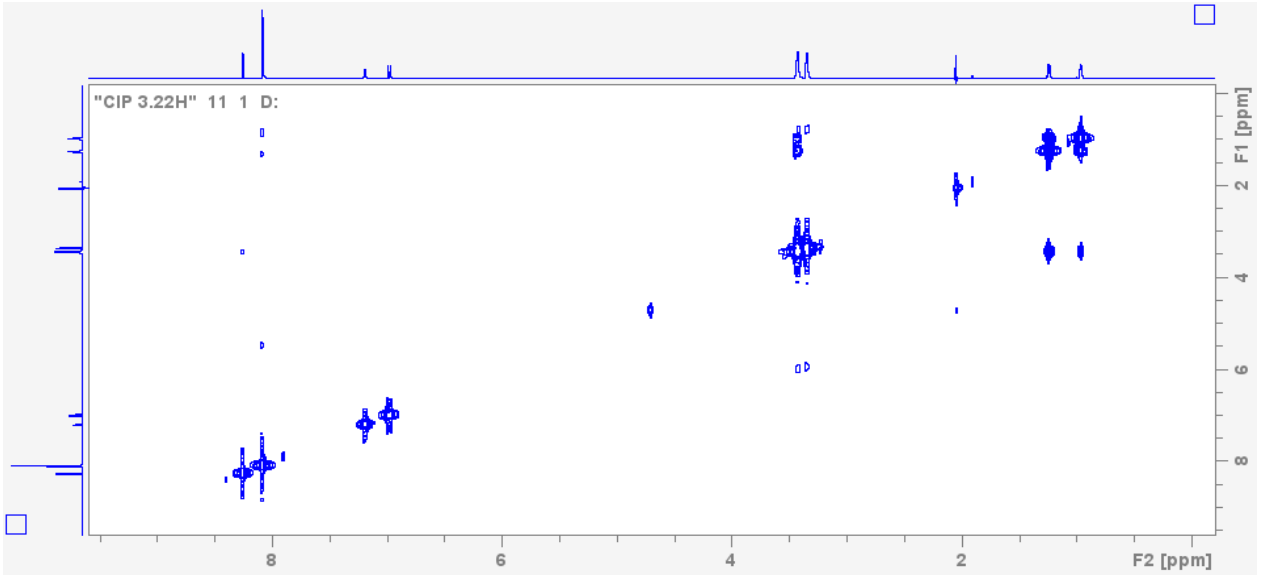

Figure 3.32. ^{1}H-^{1}H COSY NMR spectra of Ciprofloxacin in D_2O (with water suppression)

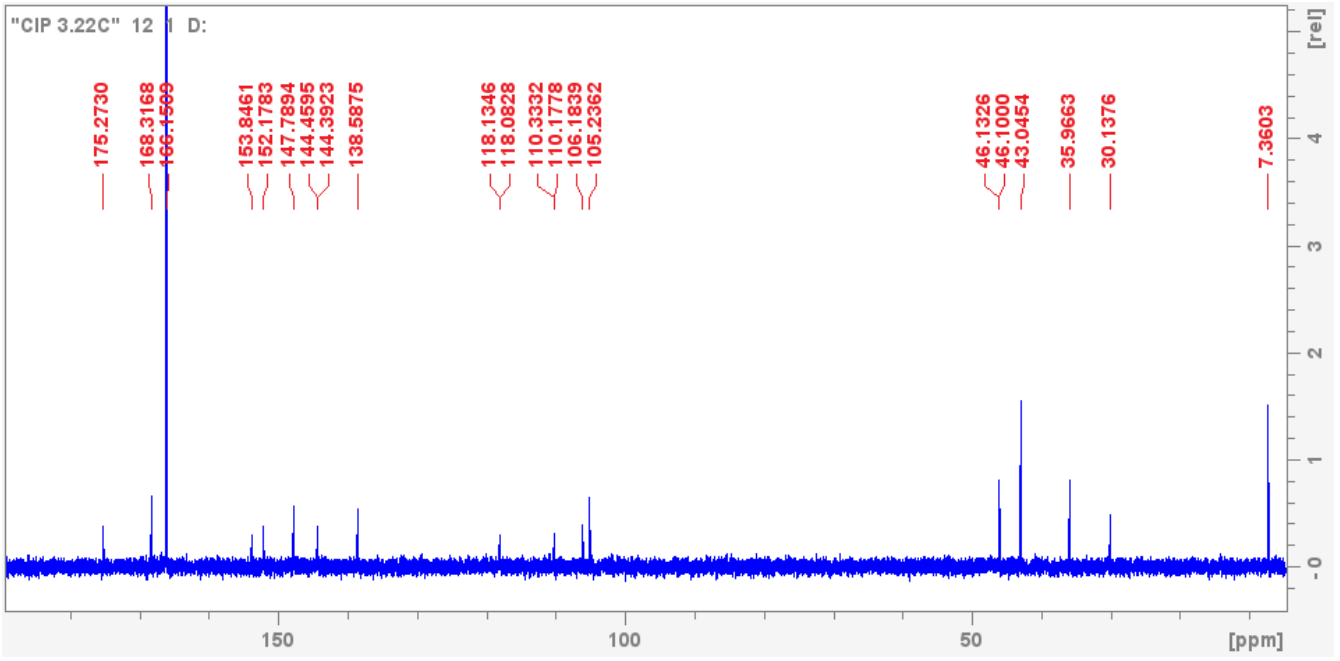

Figure 3.33. ^{13}C NMR spectra of Ciprofloxacin in D_2O

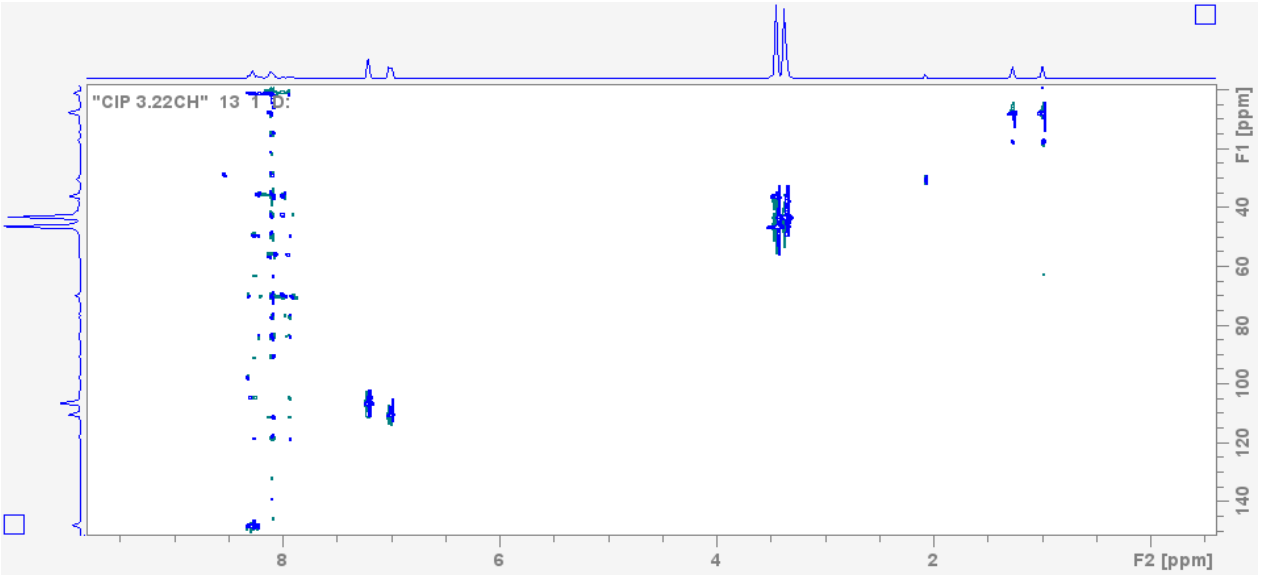

Figure 3.34. ^{1}H-^{13}C COSY (HSQC) NMR spectrum of Ciprofloxacin in D_2O

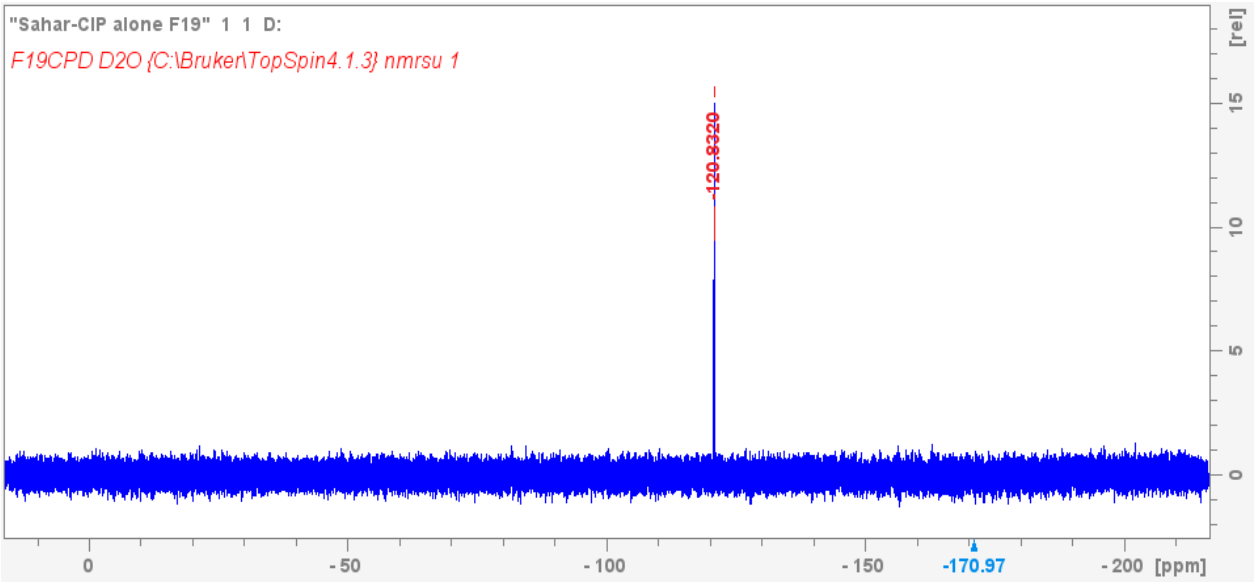

Figure 3.35. ^{19}F NMR of Ciprofloxacin in D_2O (with water suppression)

After running NMR spectroscopy of Ciprofloxacin using different methods, it was possible to assign the peaks for both the hydrogens and the carbons in Ciprofloxacin and that can be seen in the tables below.

Table 3.5. Assignments of proton NMR peaks for Ciprofloxacin

Assignments	**Protons in Ciprofloxacin**
Vinyl proton (2,3)	8.2
Aromatic protons (5,8)	7.19 – 6.97
Methine protons of the diaza ring (10,11,13,14)	3.44 – 3.34
Methylene protons attached to the cyclopropyl ring (15,16,17)	1.25 – 0.96

Table 3.6. Assignments of ^{13}C peaks for Ciprofloxacin

Assignments	**Carbons in Ciprofloxacin**
Vinyl carbons (2,3)	147.8 + 106.1
Carbonyl carbon of the ketonic group (4)	175.2
carbonyl carbon of the carboxylic group (18)	166.0
Aromatic carbons (5a,5,6.7,8,8a)	152 + 144.4 + 138.0 + 118 + 110 + 106.0
-CH_2 of the piperazine group (10,14)	46.0
-CH_2 of the piperazine group (11,13)	43.0
-CH of cyclopropyl group (15)	35.96
-CH_2 of cyclopropyl group (16,17)	7.4

The tables above show all the peak assignments of the hydrogens and the carbons in Ciprofloxacin. In case of ^{1}H NMR of Ciprofloxacin, the chemical shift frequencies ranging from 0 to 8.5 ppm were observed. Obvious functionalities, such as the aromatic protons (~7-8ppm) and the protons of the piperazine ring (~2-4 ppm) were also identified. Furthermore, in case of ^{13}C NMR spectrum of Ciprofloxacin the frequency shifts range from 0 to 200 ppm. The NMR data was consistent with that previously reported (Trefi et al., 2007) (Zięba et al., 2004, Dr. Holzgrabe, 2010).

b. The effect of UV irradiation on Ciprofloxacin in the solid state

The effect of UV light on Ciprofloxacin (solid state) was studied in order to determine if it causes degradation of the antibiotic. Ciprofloxacin in quartz cuvettes was left in a UV irradiation chamber (300-800 nm) using an accelerated weatherability instrument for 2 days. An ^{1}H NMR spectrum was then run on the irradiated sample in order to determine if any degradation had occurred (Figure 3.36).

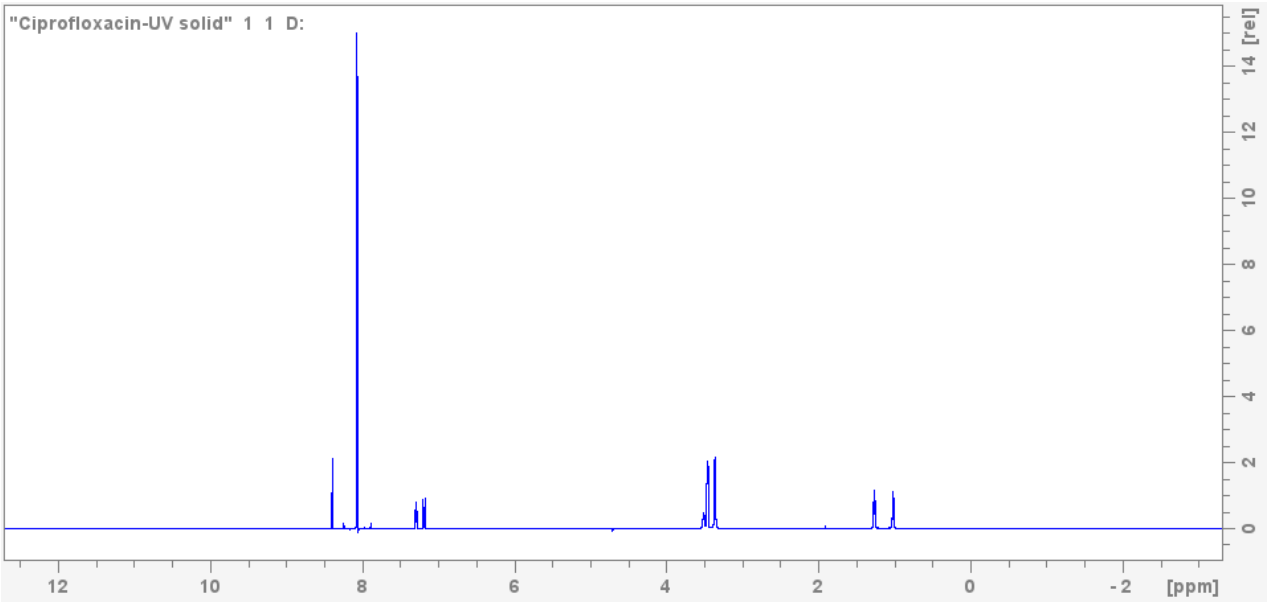

Figure 3.36. ^{1}H NMR spectra of Ciprofloxacin being irradiated using accelerated weatherability chamber over 2 days.

The ^{1}H NMR spectrum of ciprofloxacin following UV irradiation was identical to that of the pure compound, indicating that no observable photochemical transformation occurred under the applied exposure conditions. This outcome is consistent with the fact that the accelerated weatherability chamber used in this study does not emit UVC radiation and primarily provides UVB/UVA wavelengths. Moreover, effective UV-induced degradation requires absorption of photons by the compound, and the absence of detectable changes suggests limited overlap between the emission spectrum of the UV source and the UV–Visible absorption characteristics of ciprofloxacin under the conditions employed.

Given that no degradation was observed using the Ciprofloxacin in the solid state, it was considered to test Ciprofloxacin in solution as this is more common with wastewater treatment employing UV irradiation. The UV irradiation experiments were investigative in nature and confirmed that direct UV exposure under the low-fluence conditions employed was insufficient to induce measurable transformation of the compound. This outcome, while expected, provided a useful comparative baseline and supported the importance on hypochlorite-based oxidation, which is more relevant to wastewater disinfection.

c. The Effect of UV irradiation on Ciprofloxacin in solution

The UV irradiation was repeated in solution by employing UV-visible spectrophotometer (wavelength ranging from 430-275 nm) where, Ciprofloxacin in solution was irradiated under UV light for 24 hours. ^{1}H NMR spectra of the sample were run at intervals of: 30 minutes, then after one hour, two and 24 hours of UV irradiation (figure 3.37).

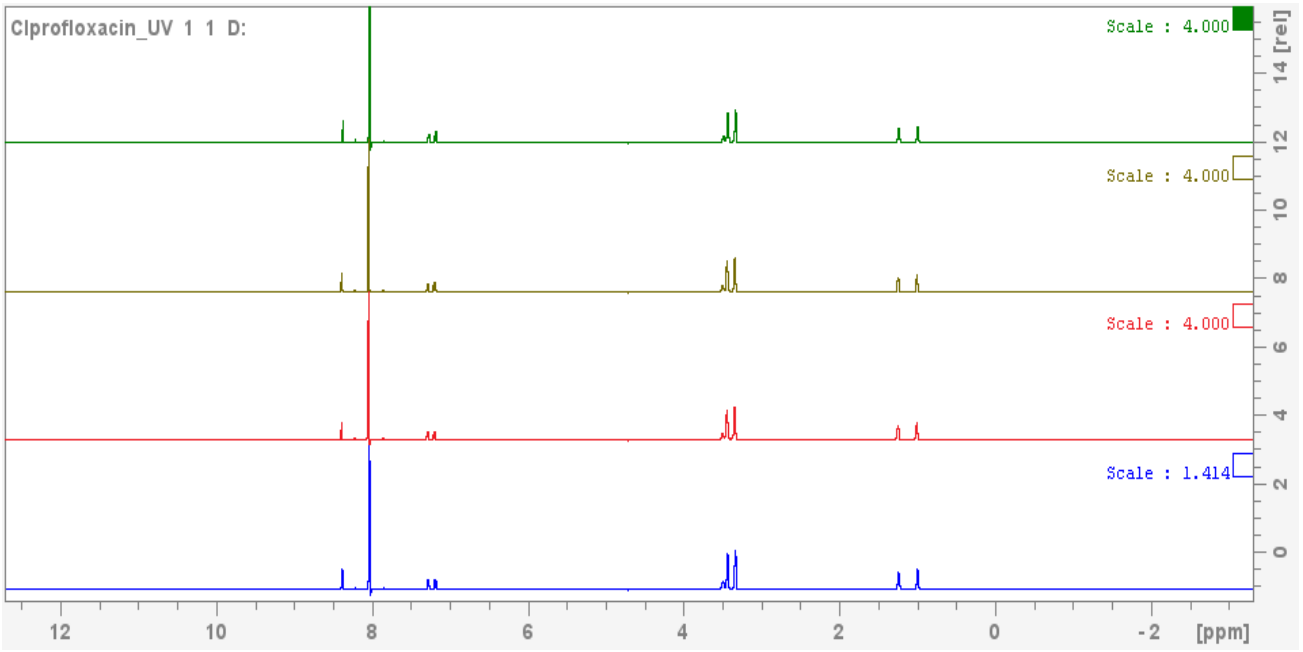

Figure 3.37. ^{1}H NMR spectra of Ciprofloxacin under UV irradiation run at intervals of: 30 minutes (blue), then after one hour (red), two (brown) and 24 hours (green) using the UV visible spectrophotometer instrument with wavelength ranging from 275 - 400 nm

It may be noted here that the UV irradiation under the applied UV exposure conditions, specifically within the 275–400 nm wavelength range and at the low irradiance associated with the spectrophotometer-based irradiation setup, no detectable changes in the resonance frequencies of the structural groups of ciprofloxacin were observed. This indicates that, at the UV dose and wavelengths employed in this study, no measurable photochemical transformation occurred andtherefore, no degradation has taken place and hence, UV irradiation is not appropriate for Ciprofloxacin degradation.

In conclusion, given that no observable degradation of Ciprofloxacin was identified in both solid form and in solution after UV irradiation using different instruments, wavelengths and exposure times, it was decided to study the effect of sodium hypochlorite solution on Ciprofloxacin, as it is the most common disinfectant product used in wastewater treatment practices (Lee et al., 2007, Kim et al., 2020).

d. Effect of Sodium hypochlorite on Ciprofloxacin

In order to monitor the degradation of Ciprofloxacin, sodium hypochlorite solution was added to an aqueous solution and ^{1}H NMR spectra of the Ciprofloxacin solution were recorded at regular time intervals (Figure 3.38).

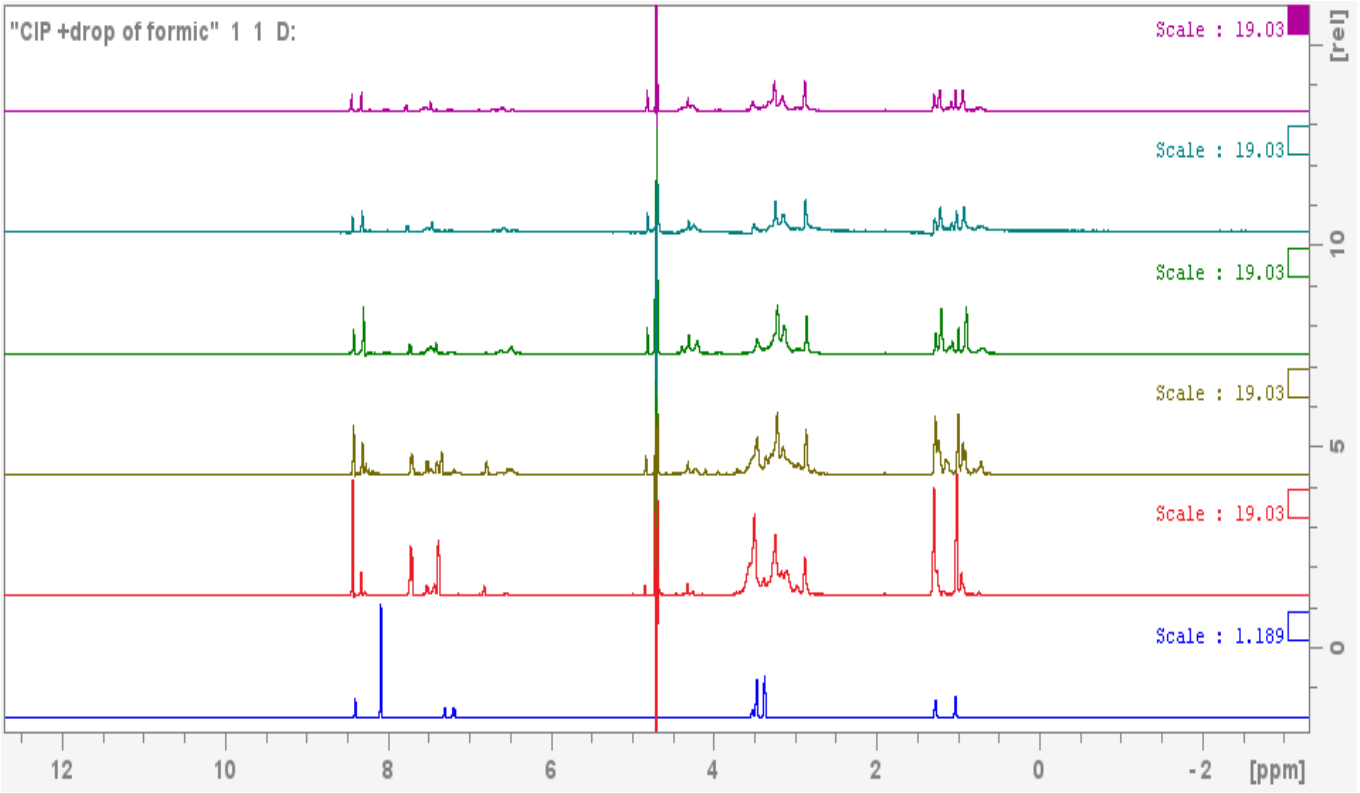

Figure 3.38. ^{1}H NMR of Ciprofloxacin in 0.75 mL of D_2O and 0.25 mL of sodium hypochlorite solution (with water suppression NMR spectra) over two days (blue is the standard prior to addition of sodium hypochlorite, starting from red that shows half an hour after the addition of sodium hypochlorite, brown 1 h, green is 7 h, baby blue 20 h and purple 29 h).

To monitor the degradation of Ciprofloxacin, sodium hypochlorite solution was added to an aqueous solution of the antibiotic, and ^{1}H NMR spectra were recorded over a two-day period (Figure 3.38). The reference spectrum was recorded prior to treatment, followed by spectra collected at 30 minutes, 1 hour, 7 hours, 20 hours, and 29 hours after the addition of sodium hypochlorite.

Immediately after exposure, significant changes were observed in the ^{1}H NMR spectra. The CH_2 signals of the piperazine ring (~3.0–3.6 ppm) broadened and gradually disappeared, indicating oxidative degradation or cleavage of the ring structure. Aromatic

proton signals in the 7–8 ppm range also diminished and eventually vanished, suggesting substitution or modification of the quinolone ring. In addition, new peaks appeared between 5 and 7 ppm, which may be attributed to polar degradation products such as chlorinated intermediates. These signals are unlikely to represent aldehydes, as such species would typically appear further downfield and would be expected to undergo rapid oxidation under bleach treatment.

The effect of sodium hypochlorite on Ciprofloxacin was also studied using ^{19}F NMR. (Figure 3.39)

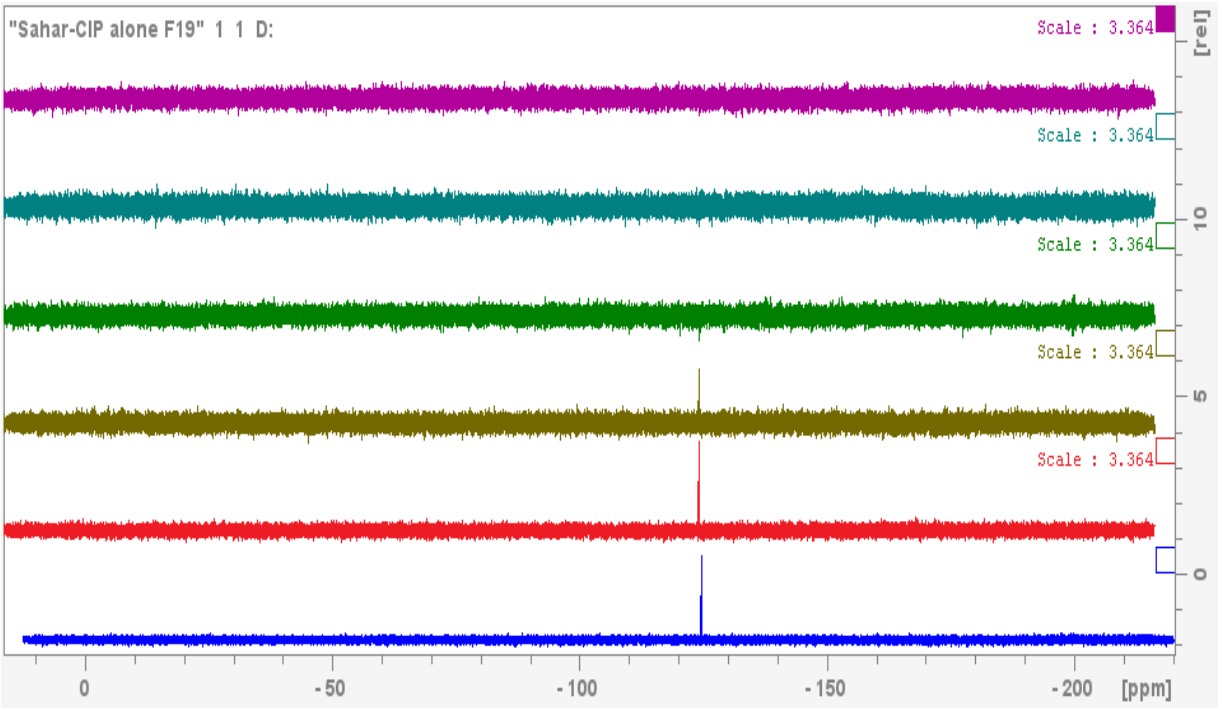

Figure 3.39 NMR spectra of ^{19}F Ciprofloxacin in 0.75 cm^3 of D_2O and 0.25 cm^3 of sodium hypochlorite solution over two days (blue is the standard prior to addition of sodium hypochlorite, starting from red that shows half an hour after the addition of sodium hypochlorite, brown 1 h, green is 7 h, baby blue 20 h and purple 29 h).

The ^{19}F NMR (Figure 3.39) provided further evidence of structural changes in Ciprofloxacin. A small shift in the fluorine signal was detected shortly after sodium hypochlorite was added, followed by a gradual drop in intensity. After extended exposure, the ^{19}F signal disappeared completely. This suggests that the fluorine atom was no longer bound within the quinolone ring and was likely released as free fluoride ion in solution.

In the current study, ^{1}H NMR spectra of Ciprofloxacin recorded prior to the addition of sodium hypochlorite revealed characteristic aromatic proton signals between ~7.0–7.5 ppm (Figure 3.38) and can be attributed to the quinolone ring. After treatment with

sodium hypochlorite, these signals progressively diminished and eventually disappeared over time, particularly in the 7.0–8.5 ppm region. Simultaneously, new downfield signals appeared, indicating the formation of polar oxidative byproducts, such as hydroxylated derivatives. The ^{19}F NMR spectra showed a gradual loss of the fluorine signal until it became undetectable, suggesting cleavage of the C–F bond at the C-6 position of the quinolone ring.

The ^{1}H NMR data also showed that the piperazine ring was significantly affected. Before the addition of sodium hypochlorite, the piperazine -CH_2 protons appeared as broad multiplets around 3.0–3.6 ppm. After chlorine treatment, a notable reduction in intensity was observed in this region, and a new signal emerged at approximately 4.2 ppm, suggesting oxidative ring cleavage and possible formation of carboxylic acid-containing degradation products. This pattern supports the conclusion that the piperazine ring is a primary site of oxidative attack during the degradation process.

In contrast, the cyclopropyl group remained unaffected. The corresponding protons consistently appeared as multiplets between 0.9–1.5 ppm throughout the experiment, with no noticeable change in chemical shift or intensity. This suggests that the cyclopropyl ring is stable under the oxidative conditions applied in this study and does not participate in the degradation pathway.

These findings align with previously reported degradation pathways of Ciprofloxacin under oxidative conditions using sodium hypochlorite. Several studies have demonstrated that sodium hypochlorite can induce transformations such as hydroxylation of the quinolone ring, cleavage of the C–F bond at C-6 (Kim et al., 2020, Holzgrabe, 2015), and piperazine ring opening (Gou et al., 2021, Kim et al., 2020). The observed defluorination and aromatic signal loss are consistent with known mechanisms of oxidative degradation. Although many studies involve combined treatments such as UV/sodium hypochlorite to enhance degradation efficiency (Figure 3.39) (Keen and Linden, 2013, Deng et al., 2019, Jia et al., 2021, Kim et al., 2020), the current results confirm that sodium hypochlorite alone is sufficient to induce key structural changes in Ciprofloxacin. These include piperazine ring oxidation, modification of the quinolone core, and removal of the fluorine atom, all of which contribute to the formation of structurally altered byproducts.

Although the degradation pathway illustrated in Figure 3.40 was proposed under UV/chlorine conditions, many of the structural transformations, such as piperazine ring cleavage, carboxyl removal, and defluorination, are also consistent with the degradation patterns observed in this study using sodium hypochlorite alone.

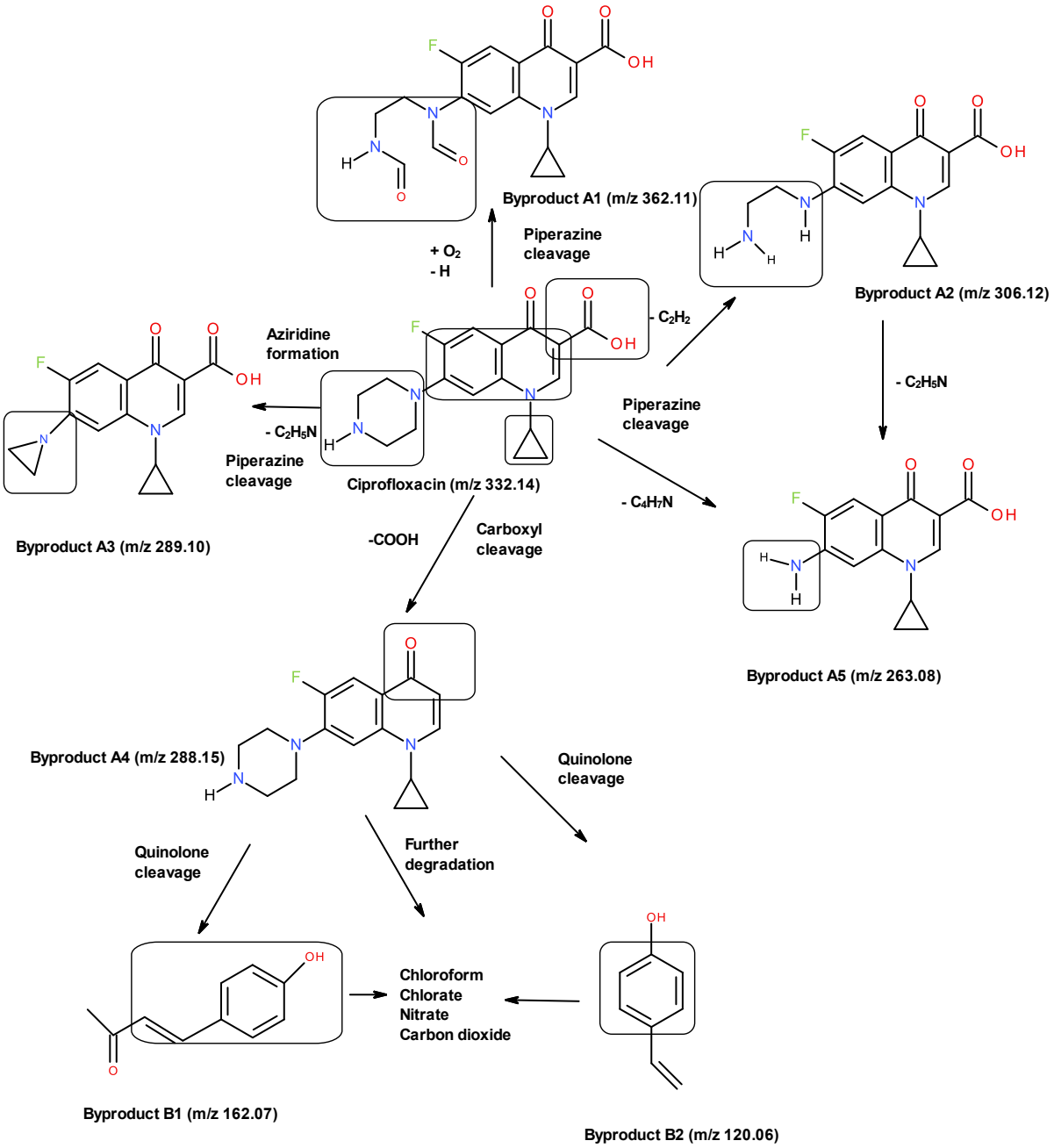

Figure 3.40 Proposed degradation pathways of ciprofloxacin during combined UV-LED irradiation and chlorine exposure, employing UVC-LED light (~275 nm) under the fluence conditions reported by Kim et al. (2020)

The degradation pathways illustrated in Figure 3.40 provide further context for the transformations observed in this study. Although the conditions described in Kim et al. (2020) involved UV-enhanced chlorination, many of the proposed byproducts, such as those formed through piperazine cleavage (A1, A2), quinolone core breakdown (B1, B2) and carboxyl group removal (A4), are all consistent with the NMR evidence reported here (Kim et al., 2020). The observed loss of piperazine signals, disappearance of aromatic protons, and defluorination all support the likelihood of similar intermediate structures forming under sodium hypochlorite treatment alone.

In conclusion, ^{1}H and ^{19}F NMR analyses clearly demonstrate that Ciprofloxacin underwent extensive structural degradation following exposure to sodium hypochlorite. The complete disappearance of piperazine -CH_2 signals, loss of aromatic proton resonances, and the eventual absence of the fluorine signal all indicate that the parent compound was no longer intact. These spectral changes reflect the cleavage of the piperazine ring, substitution or breakdown of the quinolone core, and defluorination at the C-6 position. The emergence of new downfield signals also supports the formation of highly polar degradation products. The cyclopropyl group remained unchanged, consistent with its chemical stability under oxidative conditions (Kim et al., 2020). While several studies similarly report significant degradation of Ciprofloxacin under oxidative conditions, the extent and pathways of transformation are known to vary depending on factors such as oxidant concentration, reaction time and pH, and some reports describe only partial structural modification rather than complete loss of key functional groups. Overall, the NMR evidence in the present work suggests near complete degradation of Ciprofloxacin over the two-day period. These findings will be further explored in the following chapter using LC/MS to help identify the resulting byproducts.

e. Analysis of the rate of degradation of Ciprofloxacin

Although the original intention was to monitor the intensity of selected NMR signals over time and plot their changes following sodium hypochlorite treatment, this approach proved to be unreliable in this experiment. Due to the absence of a stable internal reference and the progressive loss or overlap of key analytical peaks, the spectral data could not support accurate quantitative tracking of signal intensities.

Nevertheless, qualitative assessment of the NMR spectra provided clear time-dependent insights into the degradation of Ciprofloxacin. For example, the ^{19}F signal decreased rapidly and had completely disappeared by the fourth spectrum in Figure 3.39, which

corresponds to 8 hours after sodium hypochlorite addition. This indicates that defluorination occurred relatively early in the degradation process

Similarly, ^{1}H NMR signals associated with the piperazine ring and aromatic protons diminished in intensity or vanished completely over time, confirming progressive structural degradation. These visual spectral changes reflect the ongoing oxidative breakdown of the molecule, consistent with the degradation patterns discussed earlier in this chapter.

The NMR findings presented in this section provide clear evidence that Ciprofloxacin undergoes extensive structural degradation upon exposure to sodium hypochlorite. Key functional groups such as the piperazine ring and fluorinated quinolone core were particularly affected, while the cyclopropyl ring remained intact. Although the precise structures of the resulting transformation products could not be fully determined using NMR alone, the progressive disappearance of the signals and emergence of new resonances strongly support ongoing oxidative degradation. To further investigate the identities of these degradation products and validate the proposed pathways, complementary analysis using LC/MS was conducted, as detailed in the following section.

3.2.4 Some concluding remarks for NMR studies

a. The effect of UV irradiation on the three antibiotics:

To assess the photostability of Penicillin G, Amoxicillin, and Ciprofloxacin, two UV irradiation methods were used: solid-state exposure in a UV-visible weatherability chamber, and solution-state irradiation via a UV-1900 spectrophotometer. The irradiation wavelength ranges applied for each antibiotic were selected based on the operational output ranges of the respective UV sources and on conditions commonly reported in previous UV exposure studies, rather than on compound-specific absorption spectra. For the purposes of this study, only wavelengths within the ultraviolet region (≤400 nm) are considered relevant. Antibiotic-specific wavelength ranges based on literature values were applied: Penicillin G (190–300 nm), Amoxicillin (200–450 nm), and Ciprofloxacin (275–430 nm). Samples were exposed for 30 minutes, 1 hour, 2 hours, and overnight, followed by ^{1}H NMR analysis at each time point.

The NMR spectra of all three antibiotics showed virtually no changes after UV exposure. This indicated that the chemical environments of their key functional groups remained

largely unaffected, even after extended irradiation. It is recognised that effective photochemical transformation requires absorption of incident photons, and therefore the absence of observable UV-induced changes under the applied conditions likely reflects limited spectral overlap between the UV sources employed and the basic absorption characteristics of the antibiotics, rather than definitive photostability. As a result, UV irradiation alone was not considered a significant degradation pathway for these compounds, and further analysis by LC/MS was not pursued.

b. The effect of sodium hypochlorite solution on the three antibiotics:

In contrast, treatment with sodium hypochlorite induced clear and time-dependent chemical changes in all three antibiotics, as observed by NMR. For Penicillin G, the disappearance of characteristic methyl resonances (0–2 ppm) and the emergence of new peaks at ~3.3 and 5.0 ppm suggested major structural changes, likely involving β-lactam ring opening. These findings warranted further investigation by LC/MS to confirm degradation products.

Amoxicillin showed rapid and extensive degradation. Major spectral changes were observed in the aromatic region and β-lactam-associated signals. After 48 hours of exposure, no identifiable ^{1}H NMR peaks of the parent compound remained, indicating complete breakdown and supporting a detailed LC/MS study to track resulting byproducts.

Ciprofloxacin also demonstrated clear evidence of oxidative degradation. Loss of signals associated with the piperazine and aromatic regions, the appearance of new resonances, and the disappearance of the ^{19}F signal after 8 hours confirmed significant transformation, including defluorination. Notably, the cyclopropyl ring remained intact. These NMR changes reflected structural changes in the quinolone and piperazine rings and were consistent with known degradation patterns under oxidative conditions.

While UV light had little effect on the stability of these antibiotics, sodium hypochlorite triggered extensive chemical transformation across all three structures. These findings highlight the importance of understanding oxidant-antibiotic interactions in environmental and water treatment contexts. As noted by Cheng et al. (2022), deeper insight into such degradation mechanisms is essential for evaluating the broader implications of chlorine-based disinfection practices (Cheng et al., 2022).

Overall, NMR spectroscopy proved highly valuable in monitoring the chemical transformations of each antibiotic, allowing for real-time tracking of structural changes(Kan et al., 1973, Holzgrabe, 2015, Daletos et al., 2017). These insights form the basis for the detailed LC/MS investigations that follow, which aim to identify and characterize the resulting degradation products more specifically (Choudhury et al., 2017, Aldeek et al., 2016).

3.3 High-performance liquid chromatography/Mass spectrometry (HPLC/MS) analysis of Penicillin G, Amoxicillin and Ciprofloxacin

As stated earlier, sodium hypochlorite (NaOCl) is widely used as a water disinfectant due to its broad-spectrum biocidal activity and strong oxidizing agent (da Cruz Nizer et al., 2020). In practice, NaOCl is the most common chlorinating agent used in wastewater and drinking water treatment, however, NaOCl disinfection can form various toxic by-products and degradation intermediates (Luongo et al., 2020). Regarding antibiotics, NaOCl can oxidize β-lactam antibiotics and other drug residues that contributes to their transformation in treated waters (Luongo et al., 2020).

In this study, High-performance liquid chromatography/mass spectrometry (HPLC/MS) was employed as another analytical approach to detect and characterize antibiotics and their transformation products. In this experiment HPLC/MS (triple-quadrupole) been used to study the effect of sodium hypochlorite on Penicillin G and its degradation.

3.3.1 HPLC/MS analysis of Penicillin G

As described in the experimental section, a stock solution was prepared by dissolving 10 mg of Penicillin G in 100 mL of commercial LC/MS-grade water. This concentration is higher than typically reported levels of antibiotics in real wastewater effluents, which are generally in the ng/L to low µg/L range, but was selected to enable reliable detection and characterisation of transformation products under controlled laboratory conditions. To initiate oxidative degradation, two drops of 12.5% sodium hypochlorite (NaOCl) solution were added to the solution under gentle stirring. The oxidant was applied at a nominal level based on volumetric addition of the commercial stock solution, and free or residual chlorine concentrations were not independently quantified. For LC/MS analysis, 1 mL of this reaction mixture was then diluted with 99 mL of LC/MS-grade water, yielding a final concentration of 1 ppm, which was determined to provide optimal chromatographic and spectrometric response.

Chromatographic separation was performed using a Waters Acquity® UPLC BEH C18 column (100 × 2.1 mm, 1.7 μm particle size). The mobile phase consisted of:

- Solvent A: commercial LC/MS-grade water with 0.1% formic acid
- Solvent B: commercial LC/MS-grade acetonitrile with 0.1% formic acid

The gradient began with 1% solvent B, creating a highly aqueous environment suitable for retaining polar degradation products. The injection volume was 1 μL, with a flow rate of 0.2 mL/min and a total run time of 7 minutes per sample.

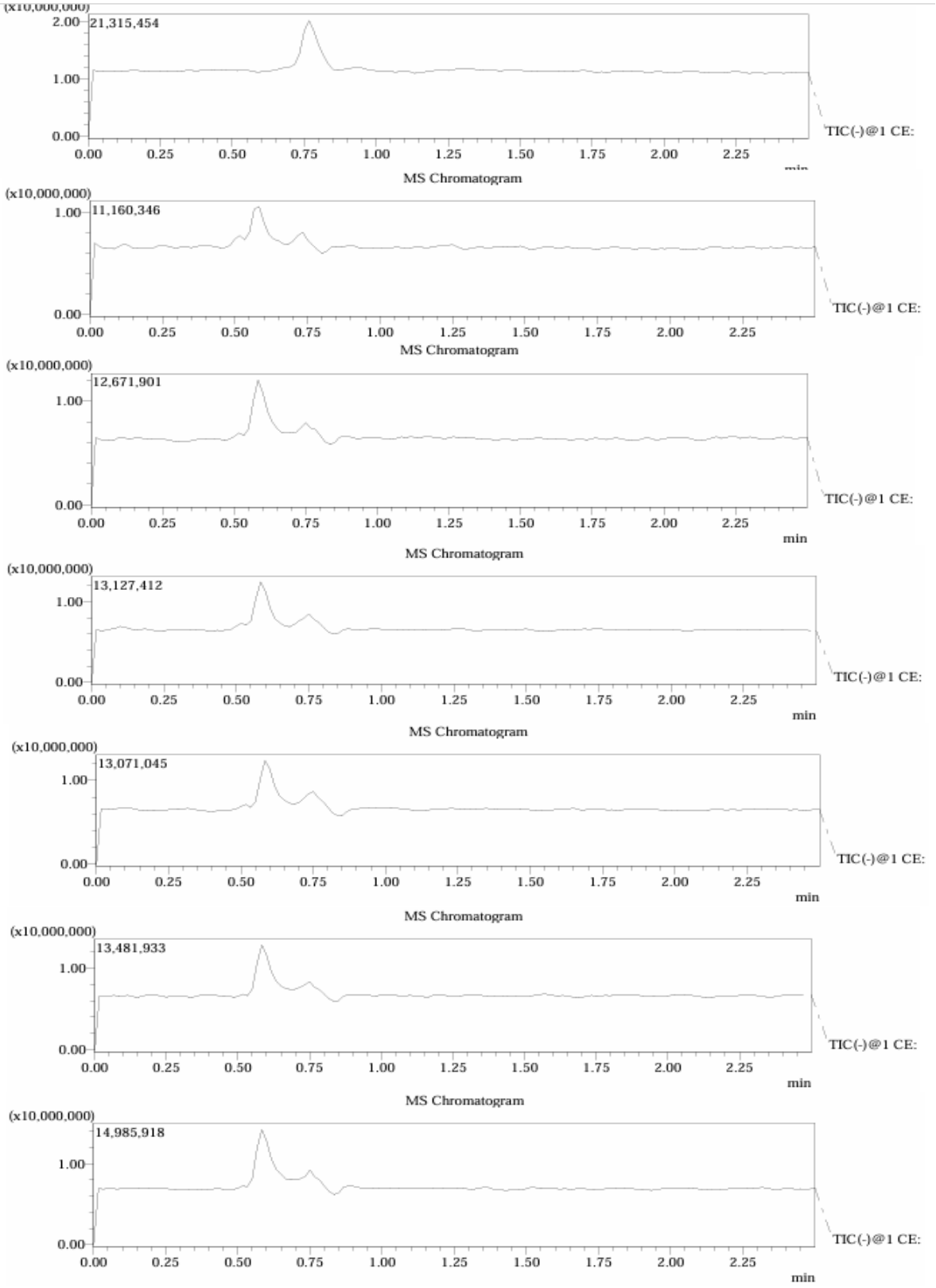

Figure 3.41. Total ion chromatograms (TICs) of Penicillin G before and after sodium hypochlorite b(NaOCl) solution treatment, monitored over a 24-hour period. The chromatograms are shown in sequential order: top trace: Penicillin G only (2:00 pm, untreated), second: 0 h post NaOCl addition, third: 1 h, fourth: 2 h fifth: 3 h sixth: 4 h bottom trace: 24 h analyzed using HPLC/MS in negative ion mode

The prepared sample was analysed using an HPLC/MS system operating in negative ionisation mode. A total of six sequential runs were conducted at 1-hour intervals, followed by a final run at 24 hours to monitor longer-term degradation of Penicillin G under oxidative conditions.

The first figure above (3.41) presents the Total Ion Chromatograms (TICs) obtained across all timepoints (Figure 3.41), demonstrating the progressive formation of degradation products. Each chromatogram shows total ion current plotted against retention time for a given run, highlighting time-resolved changes in signal intensity and peak profile. A noticeable decline in the intensity of the main parent peak with RT of 0.8 minutes, accompanied by the emergence of new peaks at 0.65 minutes and 0.75 minutes, clearly indicates the time-dependent degradation of Penicillin G following the addition of sodium hypochlorite solution.

The dominant peak at around 0.80 minutes in the untreated sample (Figure 3.41) represents the intact Penicillin G compound before any degradation has occurred. After the addition of sodium hypochlorite, the intensity of this peak gradually decreases over time, which clearly shows that Penicillin G is breaking down. By the 3-to-4-hour timepoints, the peak has almost completely disappeared, and by 24 hours, it is fully gone, confirming that the parent compound has been fully degraded. During this process, the shape of the peak becomes broader, and some small new peaks begin to appear nearby, suggesting the formation of degradation products. These small changes, along with slight variations in total ion signal, reflect the instability of the intermediates and the ongoing breakdown process. By the end of the 24 hours, the original peak is no longer visible, and instead, new peaks appear at earlier retention times, likely corresponding to smaller, more polar breakdown products that can possibly be from hydrolysis, ring opening, or oxidative modifications (Aldeek et al., 2016, Mitsumori et al., 1977).

The HPLC/MS chromatographic data strongly support the hypothesis that sodium hypochlorite acts as a potent oxidizing agent, initiating multiple breakdown pathways. These findings align with previous reports of Penicillin G degradation under chlorination and oxidative stress (Li et al., 2008b, Wang et al., 2021, Canzani and Aldeek, 2017, Dexter and van der Veen, 1978).

To gain a more detailed understanding of Penicillin G degradation under sodium hypochlorite treatment, five key ions were selected and monitored across all timepoints during the LC/MS analysis. These ions, m/z 365, 307, 289, 202, and 157, were chosen

based on their consistent detection, reported relevance in the literature, and alignment with proposed degradation pathways. Each transition ion corresponds to a specific structural transformation, ranging from β-lactam ring opening (m/z 365 and 289) to side-chain cleavage (m/z 307), thiazolidine ring breakdown (m/z 202), and formation of low-mass, likely chlorinated terminal fragments (m/z 157). By tracking their presence and intensity over time, it becomes possible to reconstruct the degradation sequence of Penicillin G and distinguish between temporary intermediates and stable end-products. The following sections present the time-resolved extracted ion chromatograms (EICs) for each ion, along with detailed interpretations based on their detection patterns, structural implications, and correlation with NMR findings.

The ion m/z 365 corresponds to the deprotonated form of Penicilloic acid, which forms through β-lactam ring hydrolysis of Penicillin G. It is commonly identified in both NMR and LC/MS studies as a key intermediate in the degradation of β-lactam antibiotics (Mitsumori et al., 1977, Aldeek et al., 2016) (Figure 3.42). In this study, m/z 365 was monitored across all timepoints following sodium hypochlorite addition.

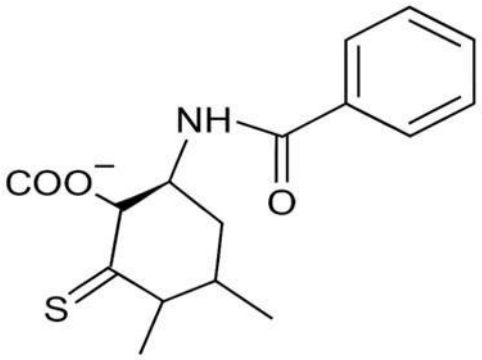

Penicilloic acid

Figure 3.42. Structure of Penicilloic acid, formed by β-lactam ring hydrolysis of Penicillin G. It corresponds to the detected ion at m/z 365(Aldeek et al., 2016)

Detected ion m/z 365

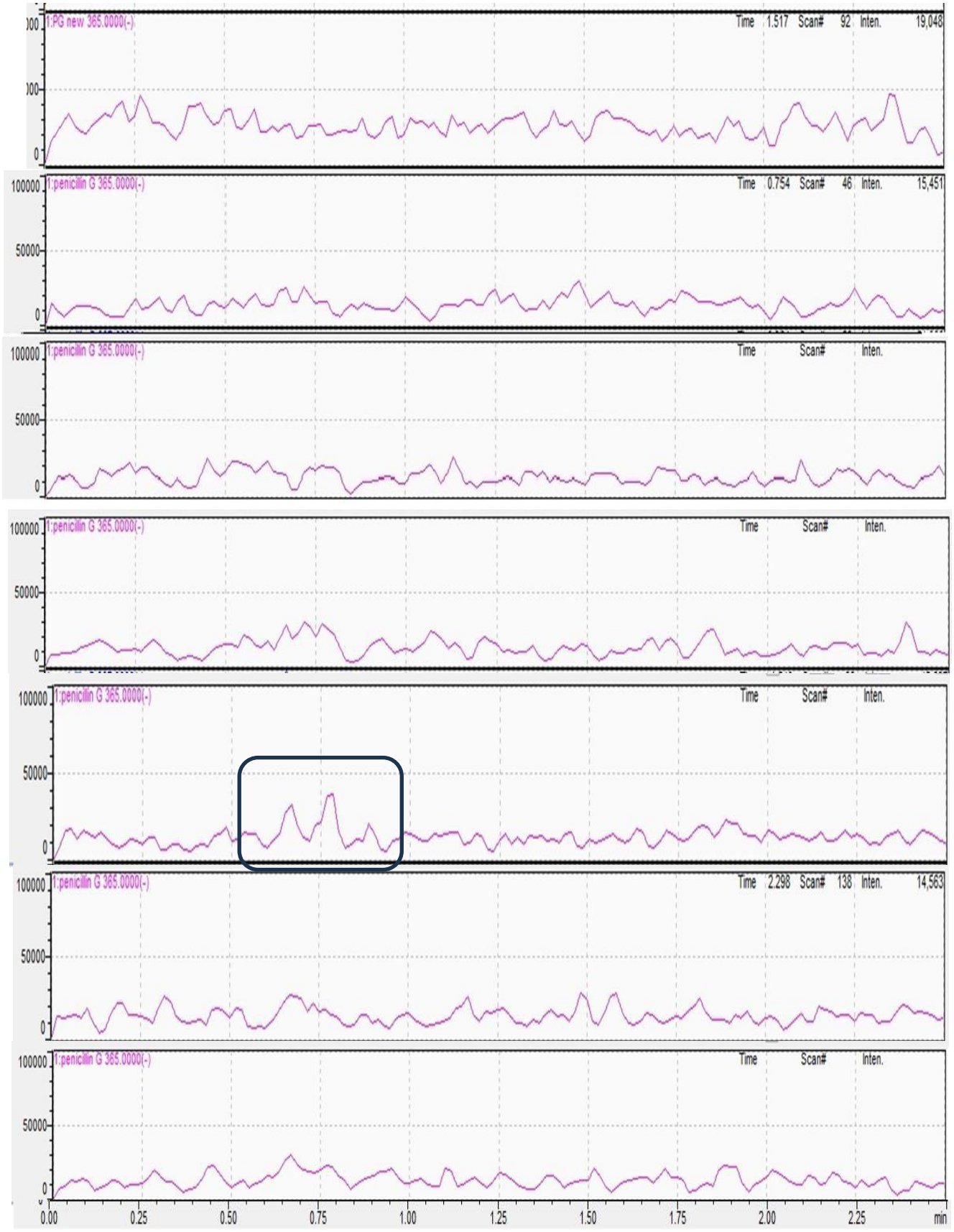

Figure 3.43. Extracted ion chromatograms (EICs) of m/z 365 (Penicilloic acid) collected during HPLC/MS monitoring of Penicillin G degradation after addition of sodium hypochlorite solution. The traces are shown in chronological order as follows: first trace: Penicillin G only (no NaOCl), second: 0 h after NaOCl addition third: 1 h, fourth: 2 h, fifth: 3 h, sixth: 4 h, seventh: 24 h. All runs were recorded in negative ion mode, with intensity plotted against retention time (0.00–2.50 min)

Visual inspection of the extracted ion chromatograms revealed that m/z 365 was absent in the baseline (Penicillin G only) and in the early timepoints (0–2 h). It was detected only at the 3-hour timepoint and disappeared again by the 4-hour and 24-hour marks. This transient detection supports its identity as a short-lived intermediate rather than a stable byproduct. The delayed appearance of Penicilloic acid suggests that β-lactam hydrolysis occurs as a mid-stage event in the overall degradation process. Its disappearance after 3 hours may be due to further oxidation or ring cleavage, leading to smaller fragments such as m/z 289 or m/z 202. The NMR data supports this assignment, as Penicilloic acid–like structures were also observed during intermediate stages of degradation, particularly after the β-lactam proton signal had vanished.

Following the disappearance of the parent ion at m/z 365, a new fragment ion emerged at m/z 307, indicating a subsequent stage in the degradation sequence and reflecting further breakdown of the Penicilloic acid–like structure.

Detected ion m/z 307

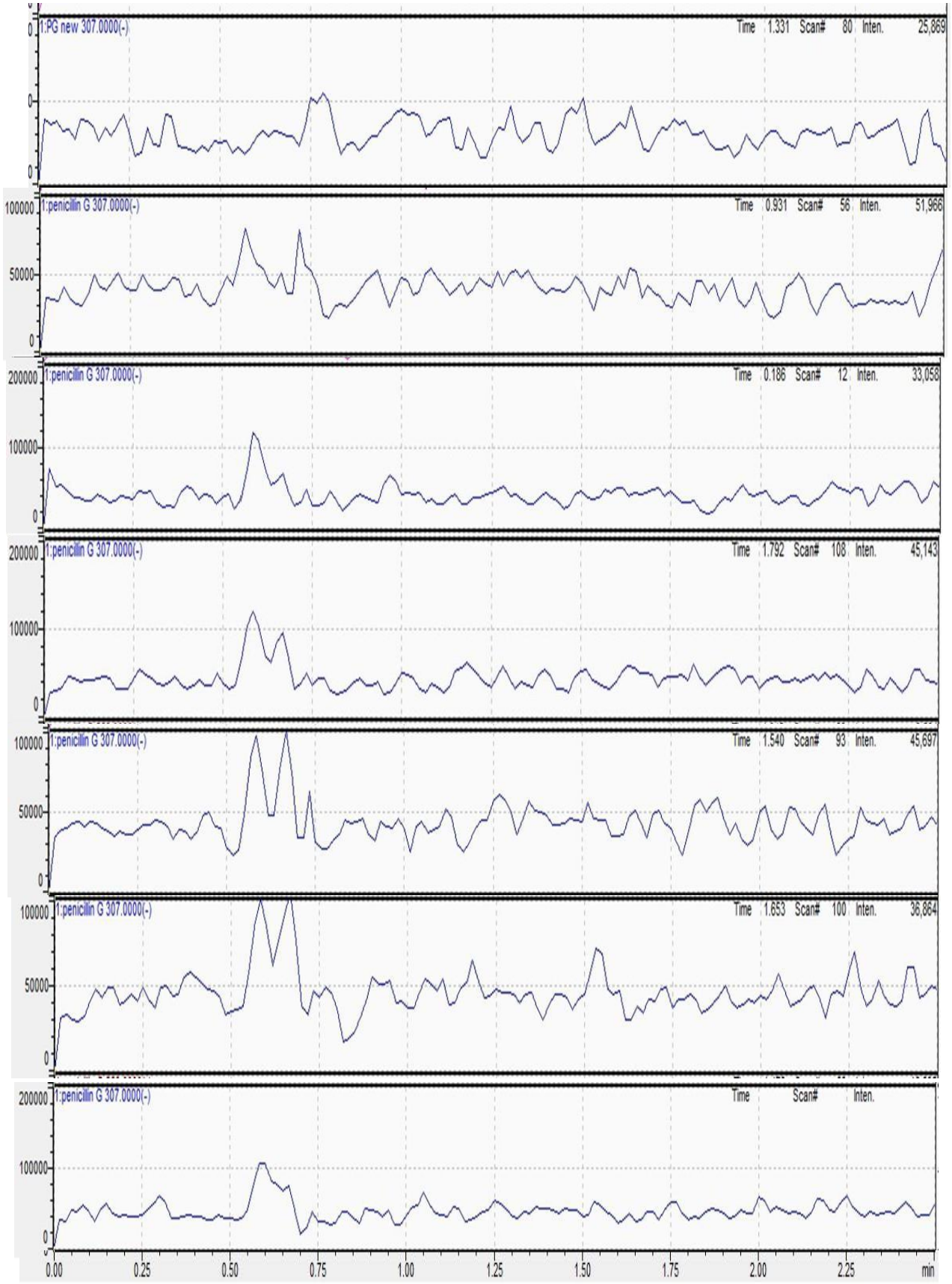

Figure 3.44. Extracted ion chromatograms (EICs) of m/z 307 collected during HPLC/MS monitoring of Penicillin G degradation after sodium hypochlorite addition. The traces are shown in chronological order as follows: first trace: Penicillin G only (no NaOCl), second: 0 h after NaOCl addition third: 1 h fourth: 2 h, fifth: 3 h, sixth: 4 h, seventh: 24 h. All runs were recorded in negative ion mode, with intensity plotted against retention time (0.00–2.50 min)

The ion m/z 307 is a characteristic fragment associated with the early-stage degradation of Penicillin G and is believed to result from partial side chain cleavage, or the loss of water from Penicilloic acid like structures (Aldeek et al., 2016). It was not detected in the baseline chromatogram of Penicillin G alone, confirming that m/z 307 is not a native fragment of the intact parent compound under neutral conditions. Following the addition of sodium hypochlorite, the ion appeared immediately at the 0-hour timepoint, indicating rapid onset of degradation. It remained consistently present throughout the first four hours, suggesting that m/z 307 represents a relatively stable intermediate formed during the oxidative breakdown of the molecule. By the 24-hour mark, however, the ion was no longer detectable, implying that it had been further degraded into smaller species such as penilloic acid (m/z 202) or terminal fragments like m/z 157. This behaviour aligns with previously reported chlorination pathways in which Penicillin G undergoes side-chain and β-lactam ring modifications under oxidative stress, resulting in intermediate products such as m/z 307 that gradually degrade into smaller, possibly chlorinated, low-mass fragments like m/z 157(Canzani and Aldeek, 2017, Aldeek et al., 2016).

As the degradation progressed, another prominent ion, m/z 289, began to emerge, indicating continued structural breakdown beyond the stage represented by m/z 307 and reflecting further cleavage of the Penicillin G framework.

Detected ion m/z 289

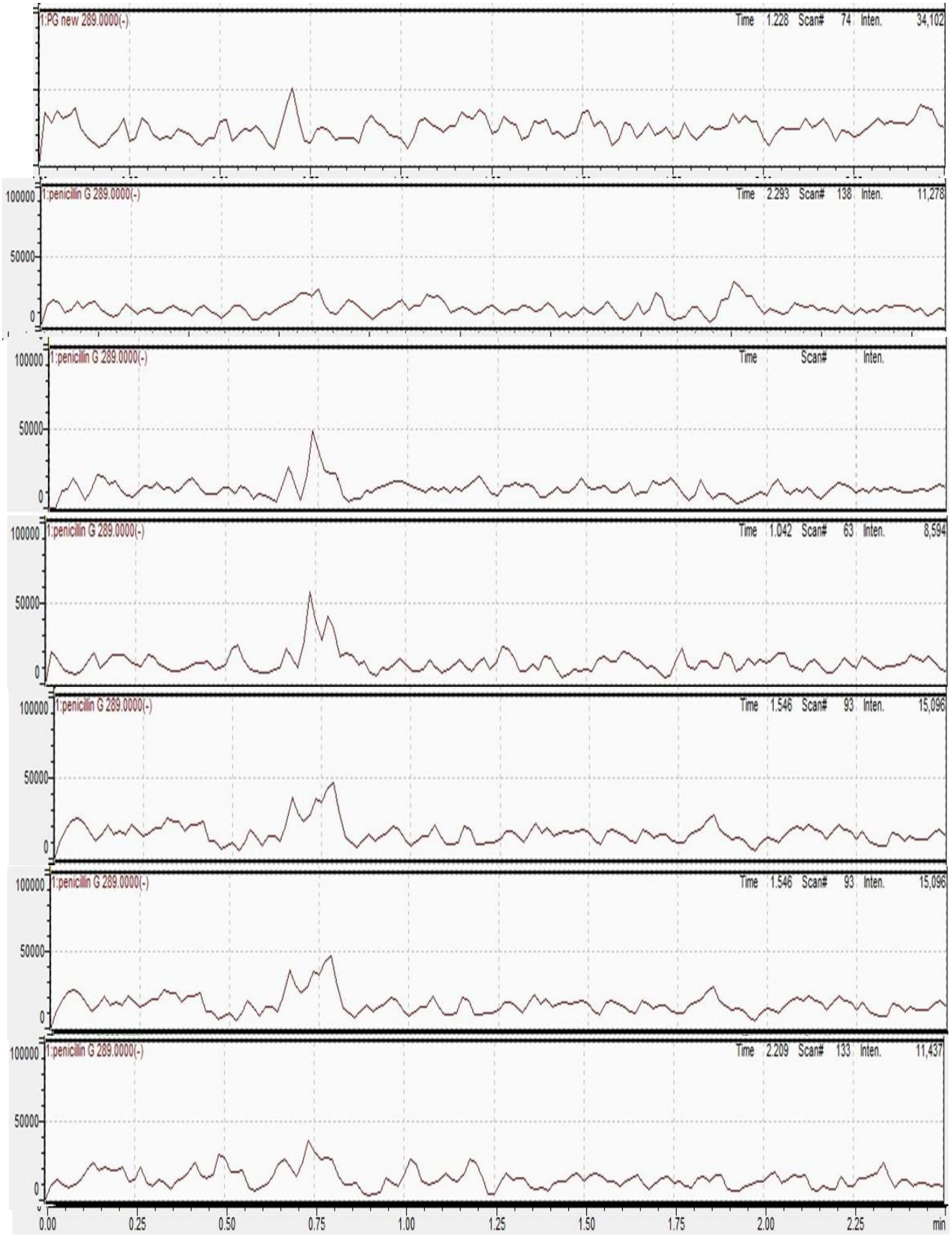

Figure 3.45. Extracted ion chromatograms (EICs) of m/z 289 collected during LC/MS monitoring of Penicillin G degradation after addition of sodium hypochlorite (NaOCl) solution. The traces are shown in chronological order as follows: first trace: Penicillin G only (no NaOCl), second: 0 h after NaOCl addition third: 1 h fourth: 2 h, fifth: 3 h, sixth: 4 h, seventh: 24 h. All runs were recorded in negative ion mode, with intensity plotted against retention time (0.00–2.50 min)

The ion m/z 289 is widely reported in the literature (Canzani and Aldeek, 2017) as a key intermediate in the oxidative degradation of Penicillin G (Aldeek et al., 2016). It is typically associated with β-lactam ring opening, resulting in Penicilloic acid like structures where further loss of side chains or minor rearrangements may generate this fragment. In the present study, m/z 289 was not detected immediately after sodium hypochlorite addition; however, this was first observed at 1 hour and persisted through to the 4-hour timepoint. Its delayed appearance, relative to penilloic acid (m/z 202), may reflect either differences in ionisation efficiency, or slightly slower structural rearrangement pathways. Nevertheless, its consistent presence during the intermediate phase of degradation and disappearance by 24 hours strongly support its identity as a transient but significant intermediate. The formation of m/z 289 provides further evidence for β-lactam ring hydrolysis, in agreement with the NMR findings, and confirms that this ion plays a central role in the progression of Penicillin G degradation under chlorination conditions (Li et al., 2008b, Timm et al., 2019).

Following the formation of m/z 289, the appearance of m/z 202 marked a further stage of degradation, representing more extensive fragmentation of the Penicillin G backbone and the possible formation of penilloic acid derivatives (Figure 3.46).

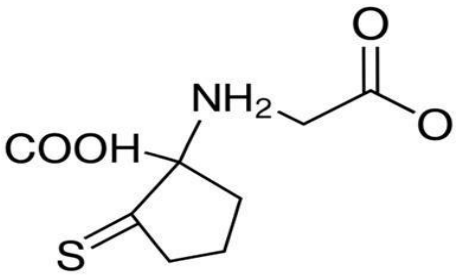

Penilloic acid

Figure 3.46. Structure of penilloic acid, a stable terminal degradation product of Penicillin G, corresponding to m/z 202 (Aldeek et al., 2016)

Detected ion m/z 202

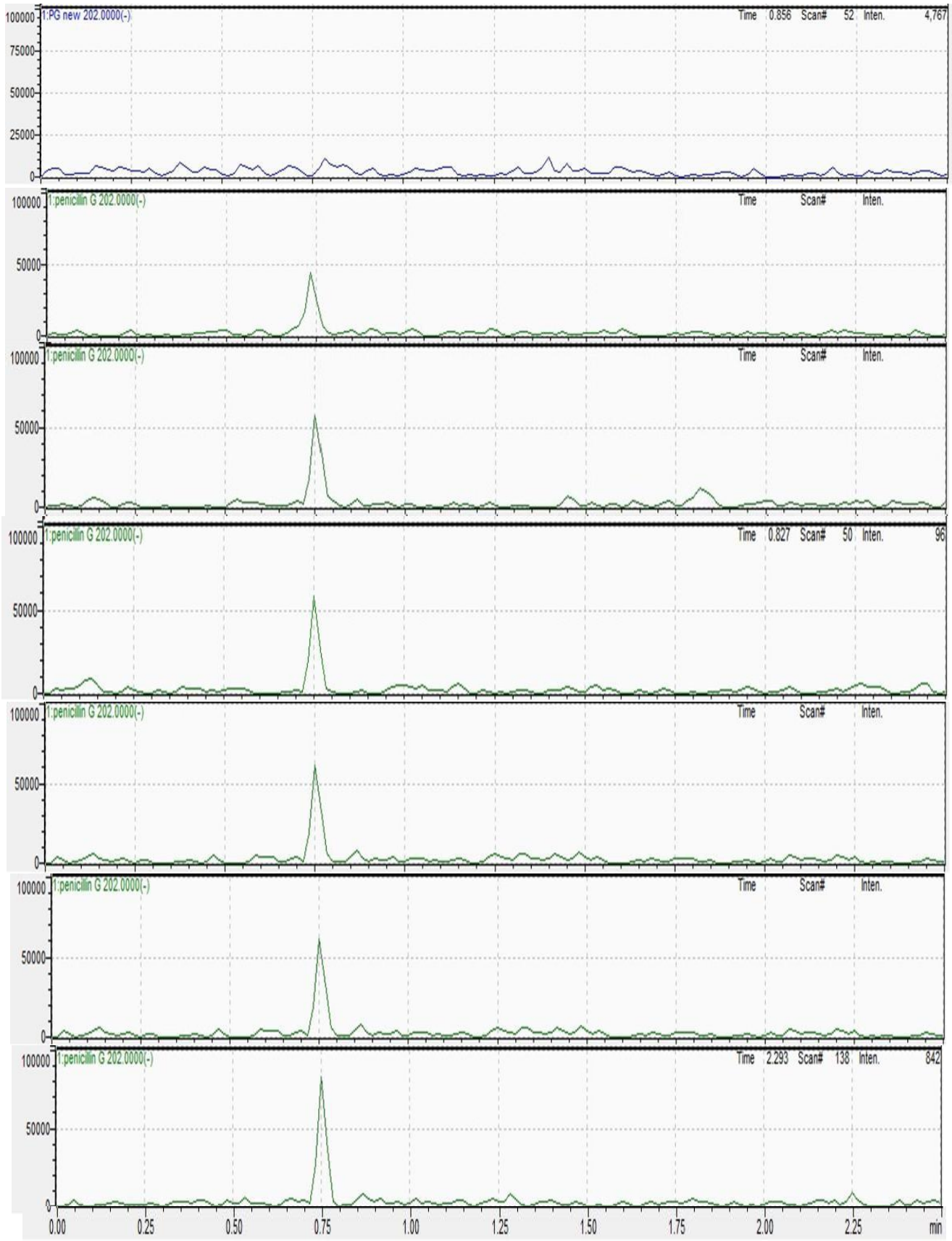

Figure 3.47. Extracted ion chromatograms (EICs) of m/z 202 collected during LC/MS monitoring of Penicillin G degradation after addition of sodium hypochlorite (NaOCl). The traces are shown in chronological order as follows: first trace: Penicillin G only (no NaOCl), second: 0 h after NaOCl addition third: 1 h fourth: 2 h, fifth: 3 h, sixth: 4 h, seventh: 24 h. All runs were recorded in negative ion mode, with intensity plotted against retention time (0.00–2.50 min)

The ion m/z 202 was not present in the untreated Penicillin G sample but appeared immediately following the addition of sodium hypochlorite at the 0-hour timepoint. It remained consistently detectable across all following chromatograms, including the 24-hour timepoint, indicating its stability and persistence throughout the degradation process. This ion corresponds to penilloic acid, a well-documented degradation product formed through cleavage of the thiazolidine ring following β-lactam ring hydrolysis. Its immediate formation suggests that structural breakdown of Penicillin G begins rapidly after exposure to sodium hypochlorite, and that penilloic acid forms early and remains unchanged over time, likely due to its chemical stability under oxidative conditions. The continued presence of m/z 202, even after the complete disappearance of intermediate ions such as m/z 365 and 289, highlights its role as a major terminal degradation product. This observation is fully consistent with ^{1}H NMR findings (Degelaen et al., 1979, Aldeek et al., 2016), where penilloic acid like signals remained prominent throughout the degradation experiment supporting a shared structural pathway across both HPLC/MS and NMR analyses.

While ^{1}H NMR observations suggest that penicilloic acid forms prior to penilloic acid through a stepwise degradation pathway, HPLC/MS data revealed that m/z 202, attributed to penilloic acid, appeared immediately following sodium hypochlorite addition and was consistently present at all different timepoints. This suggests that penilloic acid may form via multiple simultaneous routes, some of which do not rely on the prior accumulation of Penicilloic acid. One possible explanation is that penilloic acid is generated rapidly in small quantities through direct cleavage mechanisms, such as β-lactam and thiazolidine ring opening under strong oxidative conditions (Aldeek et al., 2016, Postigo and Richardson, 2014). In contrast, penicilloic acid (m/z 365) may accumulate later in the process and be less efficiently ionised under HPLC/MS conditions, making it appear only briefly in the chromatographic profile (Aldeek et al., 2015, Ho et al., 2011, Aldeek et al., 2016). This highlights a key difference between NMR and HPLC/MS that indicates, while NMR captures the structural development of the bulk mixture, HPLC/MS is more sensitive to low concentration and early forming polar species. Overall, the two methods offer complementary perspectives on the degradation pathway, revealing penilloic acid as a persistent and a major end product, regardless of the specific intermediates formed along the pathway.

While m/z 202 reflected ongoing fragmentation of the core structure, the appearance of m/z 157 marked the formation of stable, low-mass chlorinated structure, likely indicative of final-stage degradation products in the HPLC/MS profile.

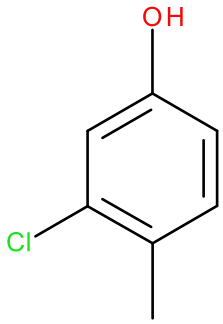

Figure 3.48. Proposed structure of 2-chlorobenzoic acid, a terminal chlorinated degradation product of Penicillin G corresponding to m/z 157.

Detected ion m/z 157

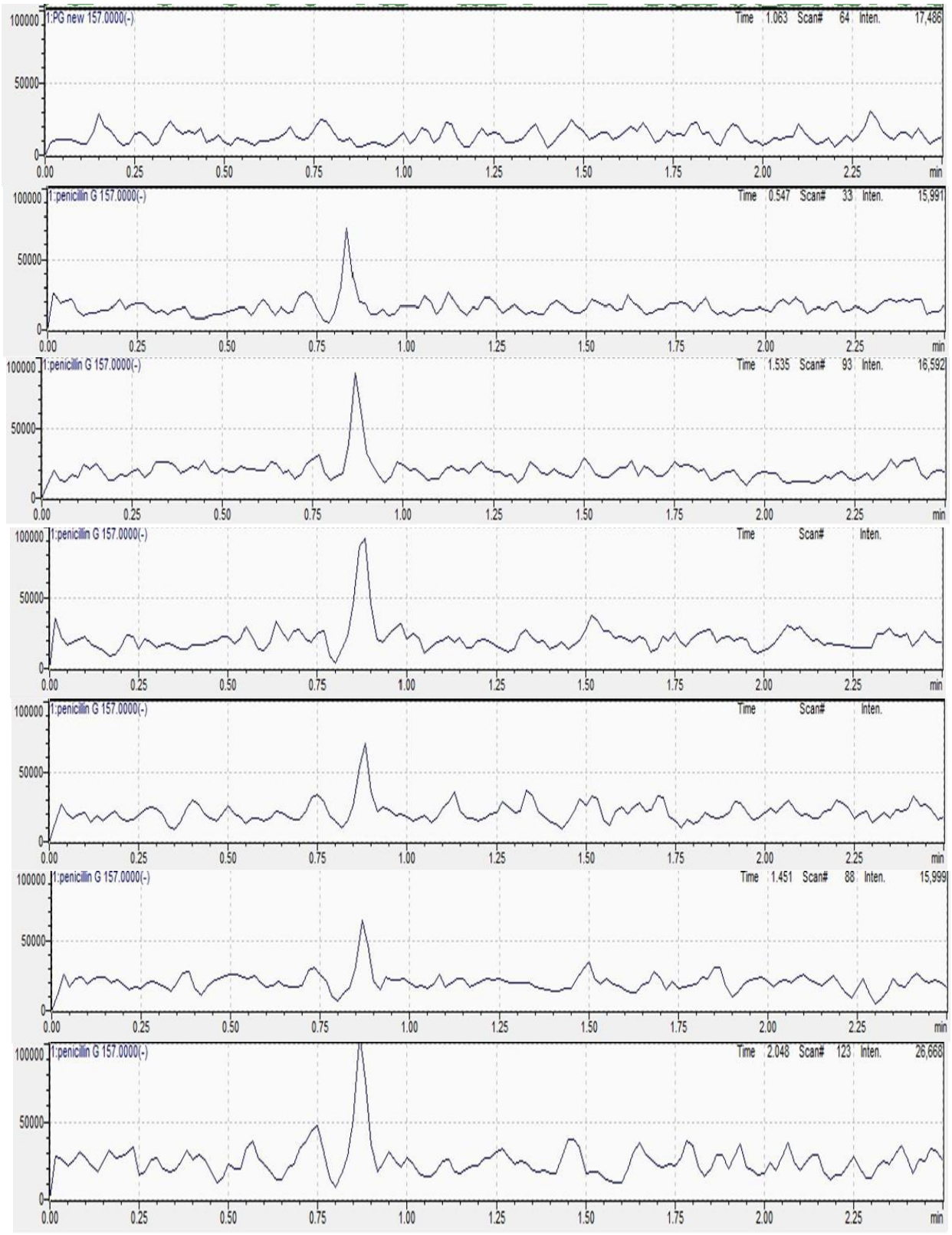

Figure 3.49. Extracted ion chromatograms (EICs) of m/z 157collected during HPLC/MS monitoring of Penicillin G degradation after addition of sodium hypochlorite (NaOCl)solution. The traces are shown in chronological order as follows: first trace: Penicillin G only (no NaOCl), second: 0 h after NaOCl addition third: 1 h fourth: 2 h, fifth: 3 h, sixth: 4 h, seventh: 24 h. All runs were recorded in negative ion mode, with intensity plotted against retention time (0.00–2.50 min)

The ion m/z 157 was not observed in the untreated Penicillin G sample but appeared immediately after the addition of sodium hypochlorite at 0 hr. It persisted at all following timepoints and increased steadily in intensity, becoming one of the most prominent ions by the 24-hour run. The early appearance and sustained accumulation of m/z 157 suggest that it is a stable terminal degradation product, likely resulting from extensive oxidative cleavage of both the β-lactam and thiazolidine rings. This ion may originate from highly polar or chlorinated fragments formed during late-stage breakdown of penilloic acid, or other intermediates. Its consistent presence and progressive dominance support the idea that m/z 157 represents a final chlorinated end-product, particularly under continued oxidative exposure. These results complement the NMR findings (Degelaen et al., 1979), which showed general signal loss and broadening over time, consistent with full molecular breakdown.

The persistence and increasing intensity of m/z 157 over time suggest that it may represent a terminal chlorinated degradation product. Given that sodium hypochlorite is a strong oxidizing and chlorinating agent, it is reasonable that m/z 157 corresponds to a halogenated fragment, potentially derived from the aromatic ring of Penicillin, G or from byproducts owing ring cleavage. Such chlorinated species have been widely reported in the oxidative degradation of β-lactam antibiotics, particularly under advanced oxidation or disinfection conditions (Ali and Maafa, 2024, Zhang et al., 2017a, Aldeek et al., 2016). The persistence of this ion at later timepoints supports its classification as a final, environmentally stable transformation product, emphasizing the need to identify and assess such compounds in water treatment research.

A further indication of oxidative transformation was obtained by closely monitoring the isotopic distribution of the ion m/z 157, particularly its relationship with m/z 155 and m/z 159. In the early timepoints following the addition of sodium hypochlorite, both m/z 157 and m/z 155 were observed as singlets, with m/z 155 consistently appearing alongside m/z 157 at comparable retention times. However, in the 24-hour post-treatment run, a different isotopic pattern was evident, where m/z 155 and 157 formed a well-defined doublet with an intensity ratio of approximately 3:1. This ratio corresponds to the natural abundance of chlorine isotopes (^{35}Cl: ^{37}Cl), strongly indicating the formation of a monochlorinated degradation product (Figure 3.50). Additionally, the occasional appearance of m/z 159 further supports the presence of multiple chlorinated species. Together, these findings offer considerable HPLC/MS evidence of chlorination occurring as a result of sodium hypochlorite treatment and align with expected degradation pathways under oxidative conditions.

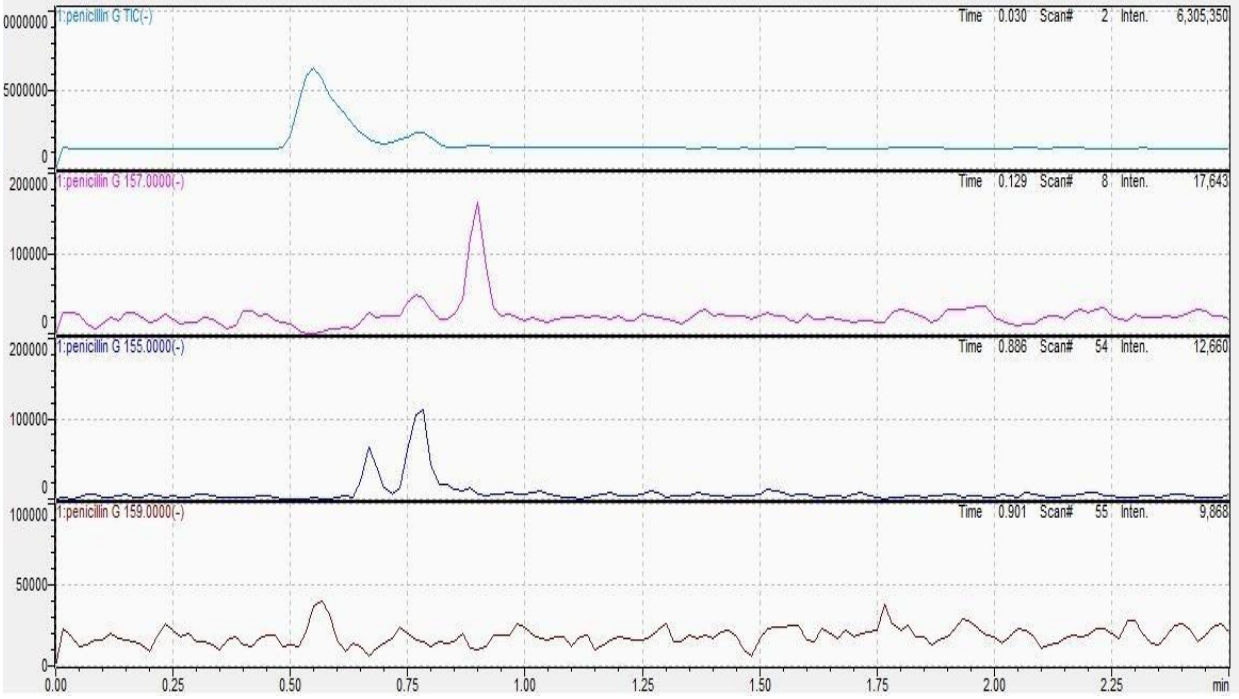

Figure 3.50. Extracted ion chromatograms of Penicillin G, 24 hours post oxidation with sodium hypochlorite solution, showing the appearance of m/z 155 and 157 as a doublet at the same retention time. The observed intensity ratio (~3:1) corresponds to the natural isotopic distribution of ^{35}Cl and ^{37}Cl, confirming the presence of a monochlorinated degradation product. All runs were recorded in negative ion mode, with intensity plotted against retention time (0.00–2.50 min)

While the HPLC/MS data clearly demonstrate the time-dependent degradation of Penicillin G, it is essential to relate these findings back to the structural transformations previously identified via NMR. In the above NMR section, the formation of penicilloic acid and penilloic acid was strongly supported by the emergence of characteristic signals at 1.18 ppm and 1.0 ppm, respectively. The detection of m/z 289 in the HPLC/MS results

aligns with the formation of Penicilloic acid, a primary β-lactam ring opened product, reinforcing the correlation between both techniques (Zhang et al., 2017a, Degelaen et al., 1979).

Interestingly, while penilloic acid was clearly detected in NMR, it appeared even earlier in HPLC/MS as m/z 202, with immediate and sustained presence across all timepoints. This suggests penilloic acid may form through multiple degradation routes, potentially bypassing Penicilloic acid in certain pathways. The difference in timing between NMR and HPLC/MS likely reflects their respective sensitivities such as, NMR captures the main species in solution, while HPLC/MS can detect transient or low-abundance fragments (Petrovic et al., 2005, Branch et al., 1987).

Moreover, no distinct ion could be confidently assigned to penillic acid, despite its identification in the NMR spectra. Its absence may be due to rapid degradation, poor ionisation, or overlap with other fragments. However, the detection of smaller ions such as m/z 229, 192, and 157 supports the hypothesis of progressive cleavage of the thiazolidine ring, sulfur elimination, and aromatic ring chlorination, all of which are consistent with known degradation routes under oxidative conditions (Li et al., 2008b, Aldeek et al., 2016).

The HPLC/MS chromatographic data (Figure 3.41) clearly demonstrate that Penicillin G undergoes rapid and extensive degradation following the addition of sodium hypochlorite solution. In the untreated control sample (top chromatogram), a sharp and intense parent peak appears at an early retention time of approximately 0.80 minutes, corresponding to the intact Penicillin G molecule. This peak significantly diminishes within the first hour after oxidant addition, reflecting the compound's rapid susceptibility to oxidative degradation. By the 24-hour timepoint, the original peak is either completely absent or significantly reduced, and a series of smaller peaks begins to appear throughout the chromatographic window, suggesting the formation of various degradation products. These changes indicate a multi-step degradation pathway involving β-lactam hydrolysis, thiazolidine ring cleavage, and sulfur oxidation, consistent with previously reported mechanisms for the oxidative transformation of β-lactam antibiotics (Deshpande et al., 2004a, Li et al., 2008b). The reduction in parent peak intensity, coupled with the appearance of multiple low-intensity peaks at similar or slightly earlier retention times, confirms the breakdown of Penicillin G and the emergence of more polar, lower-mass fragments over time.

Mass spectrometric fragmentation data further supports this transformation as, m/z 365 (penicilloic acid) appeared transiently, the m/z 307 was consistently detected in early to mid-stage degradation, the m/z 289 remained prominent as a stable intermediate, and m/z 202 persisted throughout, consistent with penilloic acid. The persistent detection of m/z 157, thoughtfully identified as 2-chlorobenzoic acid, suggests terminal chlorinated products may also form under continued oxidative stress.

Taken together, these results confirm that sodium hypochlorite induces irreversible, multi -step and rapid degradation of Penicillin G, involving different transformations by-products, including β-lactam ring opening, thiazolidine ring cleavage, oxidation, and chlorination. The combination of HPLC/MS and NMR data provides a complementary and comprehensive understanding of Penicillin G's degradation behaviour, highlighting the potential of sodium hypochlorite as a powerful oxidant in advanced oxidation processes (AOPs) used for pharmaceutical removal from water.

3.3.2 HPLC/MS analysis of Amoxicillin

As mentioned earlier, the oxidative degradation of Amoxicillin by sodium hypochlorite solution was investigated using HPLC/MS in negative ion mode. For this, a stock solution was prepared by dissolving 10 mg of Amoxicillin in 100 mL of HPLC/MS-grade water, followed by the addition of two drops of methanol to assist with solubility. The solution was then sonicated for 10 minutes to ensure complete dissolution. To initiate the degradation process, two drops of 12.5% sodium hypochlorite were added to the solution. This mixture was subsequently serially diluted to a final concentration of 0.1 ppm: first, 1 mL of the treated solution was added to 99 mL of HPLC/MS-grade water; then, 1 mL of that diluted solution was added to 9 mL of water. This final concentration was selected as it produced the most consistent and informative chromatographic results.

Chromatographic separation was carried out using a Waters Acquity® UPLC BEH C18 column (100 × 2.1 mm, 1.7 µm particle size). The mobile phase consisted of Solvent A: LC/MS-grade water with 0.1% formic acid, and Solvent B: LC/MS-grade acetonitrile with 0.1% formic acid. The gradient started at 1% B, creating a highly aqueous environment ideal for retaining polar degradation products. Each sample was injected at 1 µL, with a flow rate of 0.2 mL/min and a total run time of 7 minutes.

The HPLC/MS runs were performed hourly over the first 6 hours after sodium hypochlorite addition, with a final run at 24 hours. Each run was conducted over a total

of 7 minutes, but the retention time window was cropped to 0–2.5 minutes for analysis and figure presentation, as all significant peaks appeared within this timeframe. This adjustment improved visual clarity and allowed for more focused comparison of changes in the early eluting regions. The resulting chromatograms are presented in Figure 3.51, showing the gradual degradation of Amoxicillin and the emergence of new transformation products following sodium hypochlorite treatment.

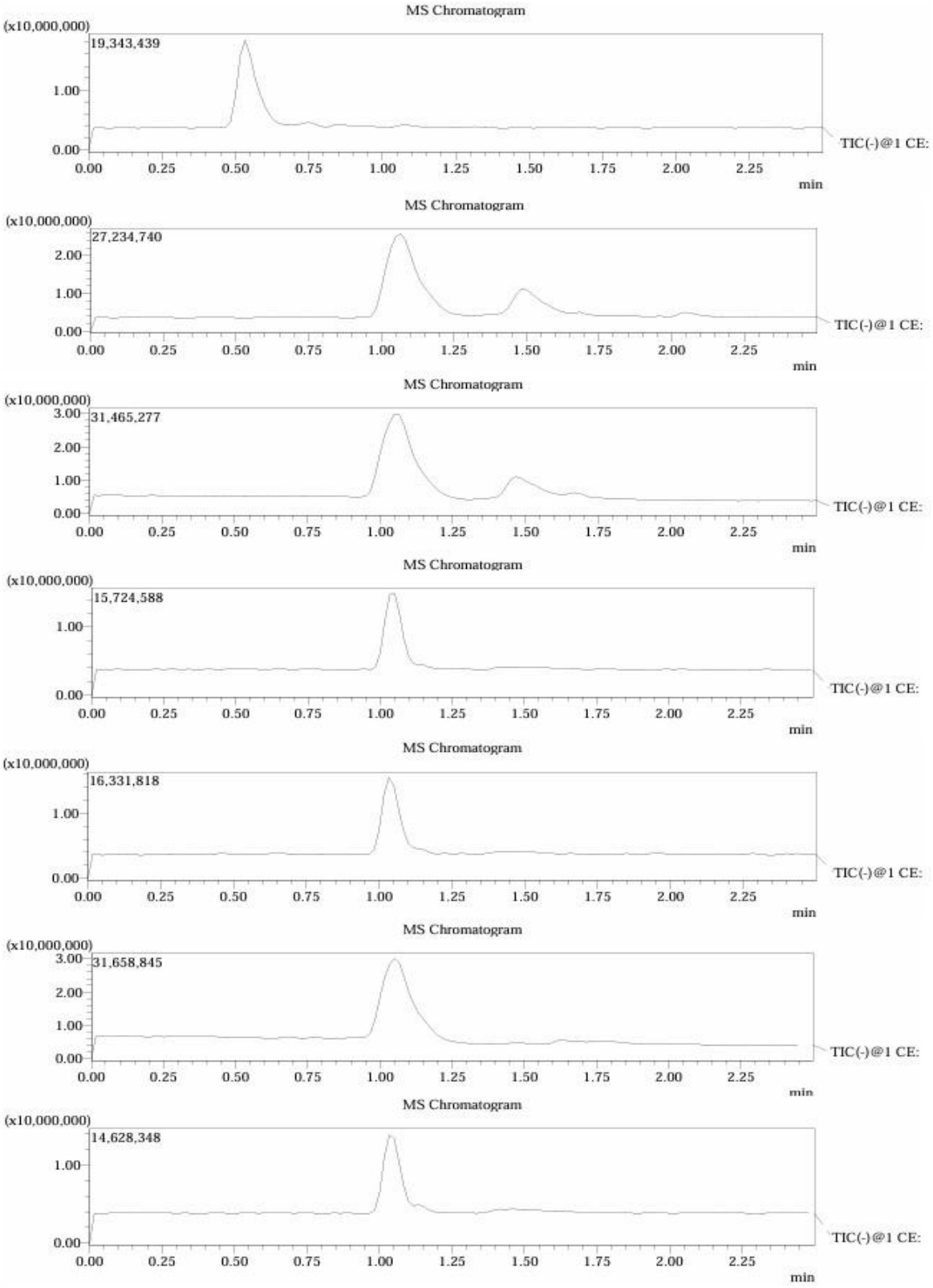

Figure 3.51. Total ion chromatograms (TICs) of Amoxicillin before and after addition sodium hypochlorite (NaOCl) solution, monitored over a 24-hour period. The chromatograms are shown in sequential order: top trace: Amoxicillin only (untreated), second: 0 h post-NaOCl addition, third: 1 h, fourth: 2 h fifth: 3 h, sixth: 4 h and bottom trace: 24 h analyzed using LC/MS in negative ion mode

Figure 3.51 presents the Total Ion Chromatograms (TICs) of Amoxicillin before and after the addition of sodium hypochlorite (NaOCl), monitored over a 24-hour period. The chromatograms are arranged in chronological order, beginning with the untreated Amoxicillin sample (Amoxicillin only, no oxidant), followed by sequential runs taken hourly after NaOCl addition, and concluding with the 24-hour sample collected the next day.

Each trace represents the total ion current (TIC) plotted as a function of retention time, recorded under negative ion mode. In the untreated control, a sharp and dominant peak appears at approximately 0.54 minutes, corresponding to the intact Amoxicillin molecule. Upon NaOCl addition, this peak drops sharply, showing that the parent compound is rapidly degraded. At the same time, new peaks emerge at later retention times (1.0–1.5 minutes), indicating the formation of less polar transformation products.

By 1 hour post NaOCl addition, the parent ion is almost completely absent, and by 24 hours, it has fully disappeared. The peaks seen at later retention times reflect stable intermediate products rather than very early, highly polar fragments. These HPLC/MS observations align with the ^{1}H NMR findings, which showed near-instant β-lactam ring cleavage and a shift toward new degradation products after exposure to sodium hypochlorite.

In order to gain a clearer picture of how Amoxicillin breaks down after the addition of sodium hypochlorite solution and building on the NMR findings for Amoxicillin (Figures 3.28 and 3.29 from the NMR section), which confirmed penicilloic acid and penilloic acid as major degradation products and outlined up to 20 possible transformation pathways from the literature, the HPLC/MS analysis was designed to target ions representing these and other reported products (Table 3.7). A comprehensive screening was carried out for all expected ions, including those linked to β-lactam ring hydrolysis, rearrangements, aromatic ring breakdown, cyclisation (diketopiperazine, reported in literature) and chlorinated phenol formation (Table 3.7).

Table 3.7. Targeted ions for Amoxicillin in negative ion mode HPLC/MS, showing proposed compounds, degradation pathways, and rationale for inclusion. These ions were selected based on NMR findings (Figures 3.28–3.29) and published literature on Amoxicillin oxidation and β-lactam degradation pathways

Ion (m/z)	**Proposed compound**	**Source/pathway**	**Rationale**
364–365	Amoxicillin $[M–H]^-$	Parent molecule	Confirms presence and disappearance of intact drug
382–383	Penicilloic acid $[M–H]^-$	β-lactam ring hydrolysis (DP1)	Major NMR products
371	Penilloic acid $[M–H]^-$	Rearrangement product (DP2)	Expected in NMR pathway and Confirmed in LC/MS runs
340-341	Diketopiperazine $[M–H]^-$	Cyclisation product (DP3)	Reported in Literature (Ali and Maafa, 2024, Gozlan et al., 2010, Gozlan et al., 2013)
152	Hydroxybenzaldehyde	Aromatic breakdown (DP6)	Reported in Literature (Ali and Maafa, 2024, Gozlan et al., 2010, Gozlan et al., 2013)
138	Hydroquinone	Aromatic breakdown (DP7)	Minor NMR by-product
127/158	4-chlorophenol/chlorophenol	Chlorinated aromatic fragments (DP9–DP10)	Seen in chlorination studies
89	Oxalic acid	Final oxidation product (DP12)	Indicates extensive oxidation

While the full group of ions listed in Table 3.7 was examined, only four degradation-related ions-- m/z 364 (Amoxicillin), 383 (penicilloic acid), 371 (penilloic acid), and 341 (diketopiperazine), were consistently detected across the runs. These ions therefore form the basis of the HPLC/MS interpretation for Amoxicillin, providing a clear picture of its major degradation pathways under sodium hypochlorite treatment. By monitoring these ions across all timepoints using extracted ion chromatograms (EICs), the progression from the parent compound to intermediate and final degradation products could be followed.

These results also support the NMR findings discussed in earlier where Amoxicillin showed rapid and extensive degradation after the addition of sodium hypochlorite, and are in good agreement with previously reported chlorination studies (Ali and Maafa, 2024, Gozlan et al., 2010, Gozlan et al., 2013).

Furthermore, to explore these findings in more depth, each of the four detected ions was examined individually across all timepoints. Extracted ion chromatograms (EICs) were generated for m/z 364 (Amoxicillin), 383 (penicilloic acid), 371 (penilloic acid), and 341 (diketopiperazine) to track their appearance, retention times, and intensity changes over the 24-hour degradation period. This ion-specific approach allows a step-by-step reconstruction of Amoxicillin's degradation sequence, highlighting which products form immediately, which persist, and which disappear as oxidation progresses.

Detected ion m/z 364

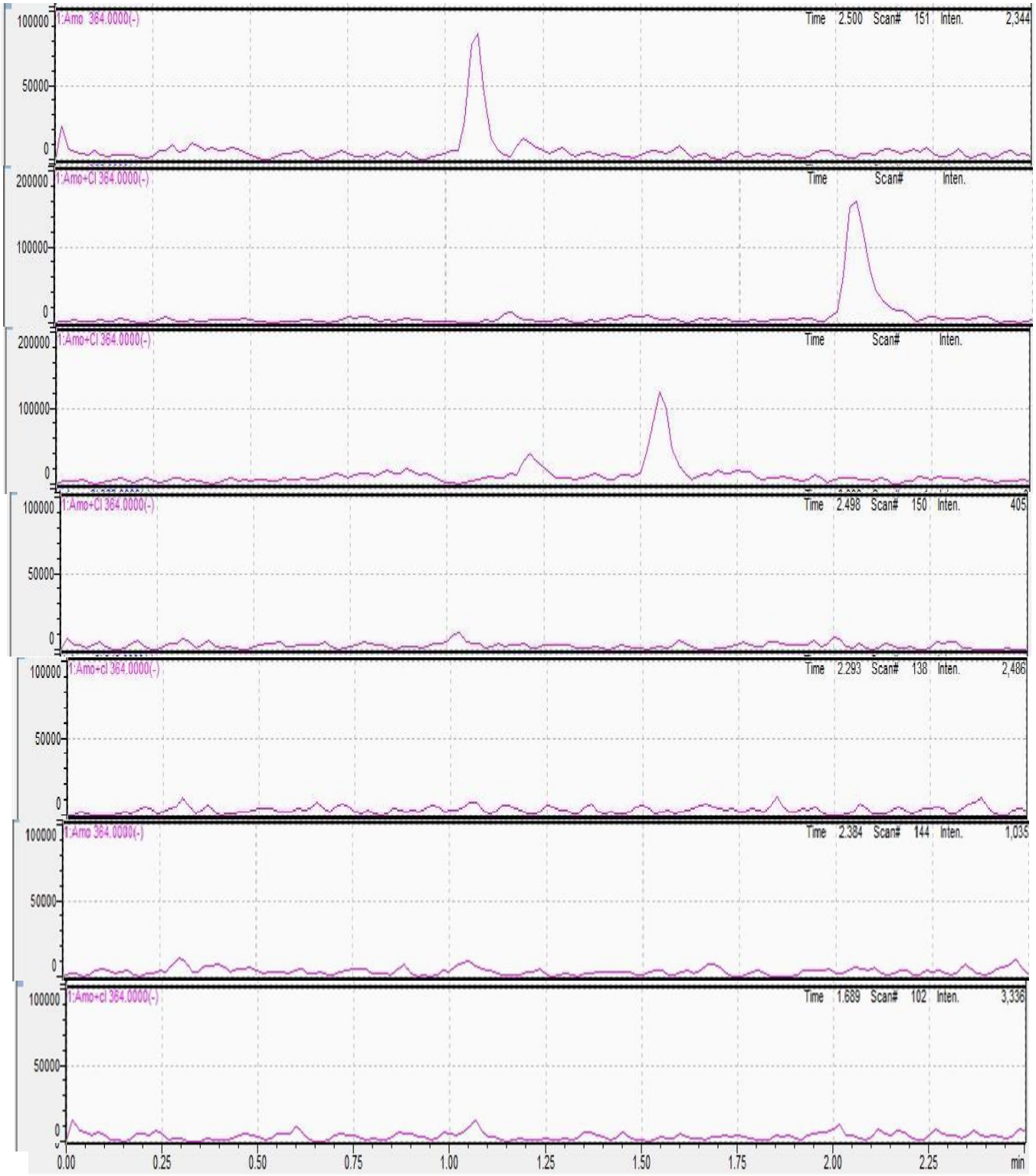

Figure 3.52. Extracted ion chromatograms (EICs) of m/z 364 collected during HPLC/MS monitoring of Amoxicillin degradation after addition of sodium hypochlorite (NaOCl)solution. The traces are shown in chronological order as follows: first trace: Amoxicillin only (no NaOCl), second: 0 h after NaOCl addition, third: 1 h, fourth: 2 h, fifth: 3 h, sixth: 4 h, seventh: 24 h (next day). All runs were recorded in negative ion mode, with intensity plotted against retention time (0.00–2.50 min)

The ion m/z 364 represents the deprotonated molecular ion $[M–H]^-$ of intact Amoxicillin, In the untreated sample, it appeared as a sharp and intense peak at ~1.10 minutes, confirming the presence of the parent compound prior to degradation.

Following the addition of sodium hypochlorite, m/z 364 was still detected at the 0-hour and 1-hour timepoints, but the retention time shifted slightly, and the signal intensity was noticeably reduced. This change indicates the presence of an isomeric or rearranged species with the same mass-to-charge ratio or may suggests that some of the parent compound persisted briefly after oxidant exposure (Yang et al., 2020).

From the 2-hour timepoint onwards, m/z 364 disappeared entirely, consistent with rapid oxidative breakdown of the β-lactam structure (Ali and Maafa, 2024). This disappearance is fully aligned with the ^1H NMR findings in the above NMR section, where the Amoxicillin signature signals vanished shortly after the addition of sodium hypochlorite confirming the parent drug's inherent instability under oxidative conditions (Siciliano et al., 2021).

As the parent Amoxicillin signal (m/z 364) diminished and ultimately disappeared, new ions began to emerge that reflect the initial stages of β-lactam ring opening. The most prominent of these was m/z 383, corresponding to Amoxicillin penicilloic acid which is the first major hydrolysis product of Amoxicillin (Gozlan et al., 2013, Gozlan et al., 2010).

Detected ion m/z 383

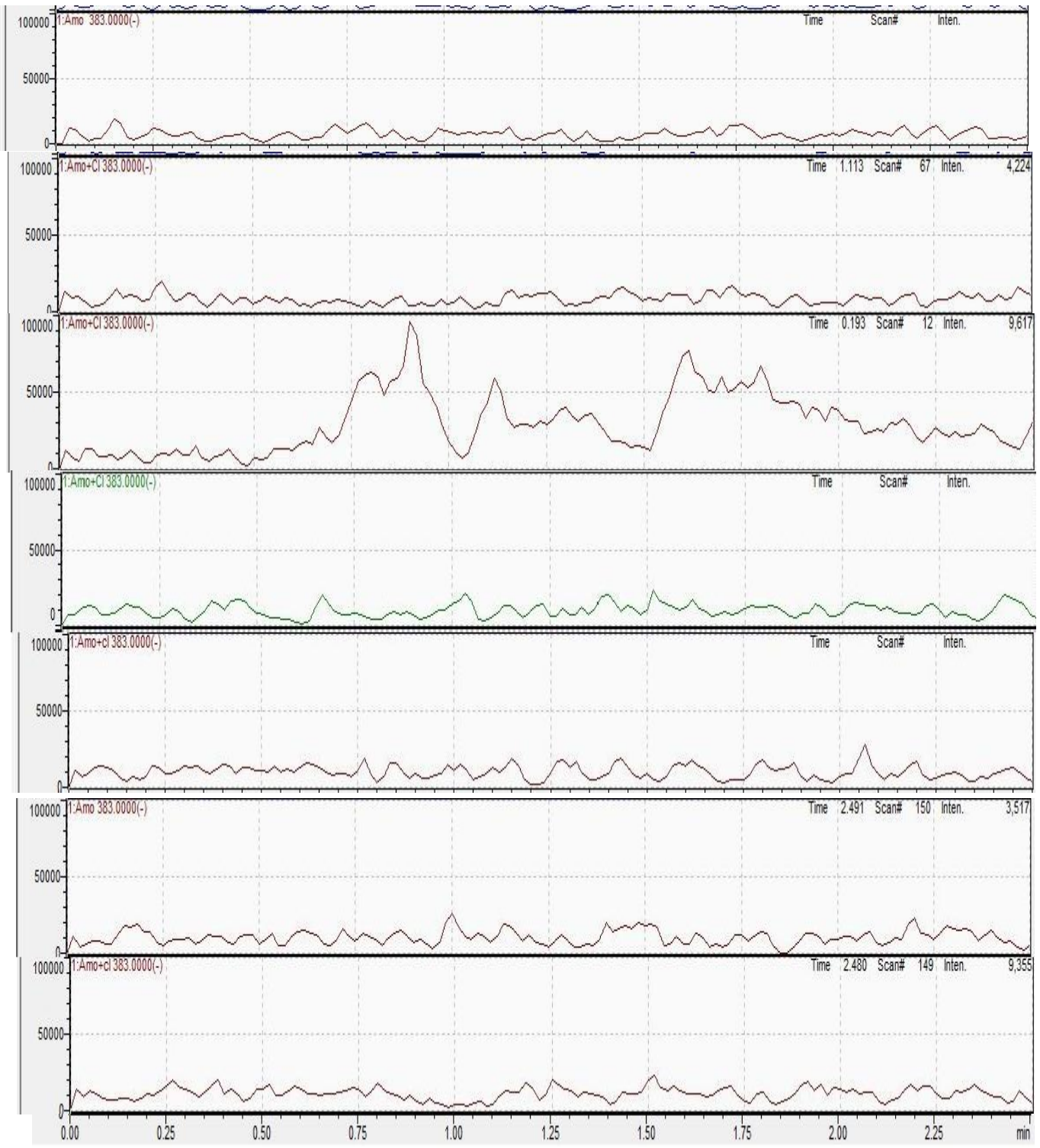

Figure 3.53. Extracted ion chromatograms (EICs) of m/z 383 collected during HPLC/MS monitoring of Amoxicillin degradation after addition of sodium hypochlorite (NaOCl) solution. The traces are shown in chronological order as follows: first trace: Amoxicillin only (no NaOCl), second: 0 h after chlorination, third: 1 h, fourth: 2 h, fifth: 3 h, sixth: 4 h, seventh: 24 h (next day). All runs were recorded in negative ion mode, with intensity plotted against retention time (0.00–2.50 min)

The ion m/z 383 corresponds to the deprotonated molecular ion $[M–H]^-$ of penicilloic acid, the primary β-lactam ring-opened product formed upon hydrolysis (Gozlan et al., 2010). This ion was absent in the untreated Amoxicillin chromatogram and at 0 hours after NaOCl addition. It first appeared at the 1-hour timepoint (Figure 3.53), showing a distinct peak at ~0.19 minutes, but then disappeared in all the following runs. This brief detection suggests that penicilloic acid formed rapidly after sodium hypochlorite addition but was highly unstable, quickly breaking down into further degradation products. The detection of m/z 383 provides direct mass spectrometric confirmation of the β-lactam ring cleavage also evidenced by the ^1H NMR data, where the β-lactam proton signals disappeared, and new downfield resonances were attributed to ring-opened species. Together, these findings highlight penicilloic acid as a short-lived but critical intermediate in Amoxicillin's degradation pathway (Siciliano et al., 2021, Gozlan et al., 2010).

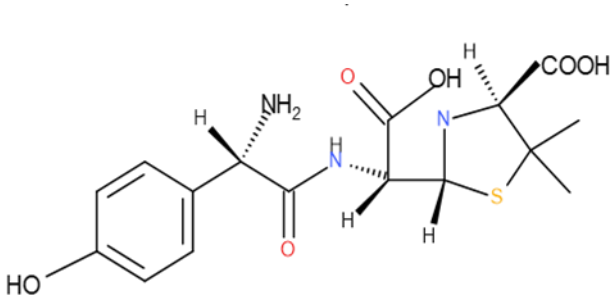

Figure 3.54. Chemical structure of penicilloic acid, a primary degradation product of Amoxicillin. Formation of Amoxicillin penicilloic acid (detected as m/z 383 in HPLC/MS) results from β-lactam ring hydrolysis after the addition of sodium hypochlorite solution, consistent with NMR findings (Siciliano et al., 2021)

As penicilloic acid (m/z 383) appeared briefly and then diminished, another key product began to dominate the profile, the m/z 371, corresponding to Amoxicillin penilloic acid, which formed quickly and persisted as the most stable degradation product in this study.

Detected ion m/z 371

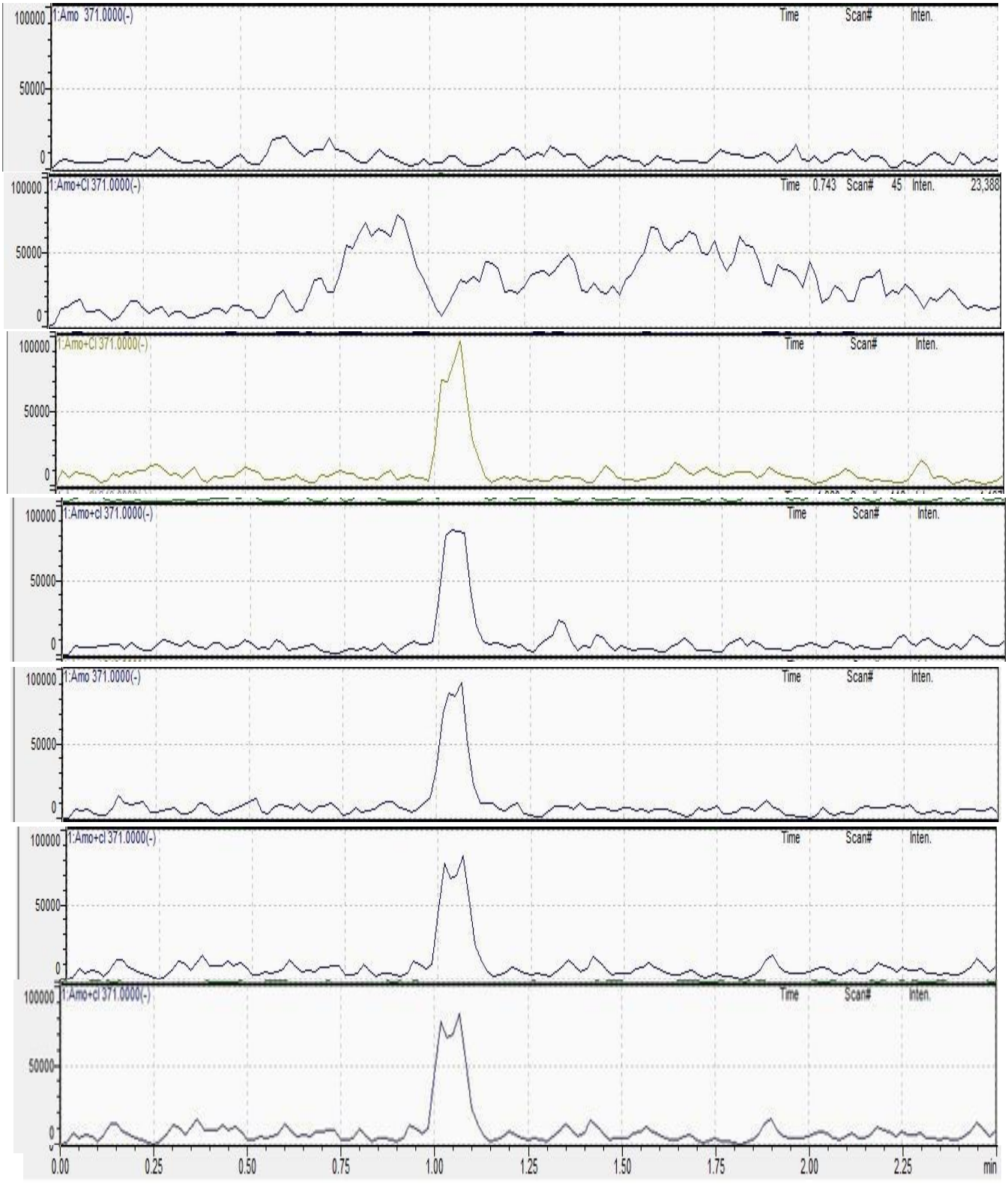

Figure 3.55. Extracted ion chromatograms (EICs) of m/z 371 collected during HPLC/MS monitoring of Amoxicillin degradation after addition of sodium hypochlorite (NaOCl) solution. The traces are shown in chronological order as follows: first trace: Amoxicillin only (no NaOCl), second: 0 h after chlorination, third: 1 h, fourth: 2 h, fifth: 3 h, sixth: 4 h, seventh: 24 h (next day). All runs were recorded in negative ion mode, with intensity plotted against retention time (0.00–2.50 min)

The ion m/z 371 corresponds to the deprotonated molecular ion [M–H] ⁻ of penilloic acid, a rearrangement product formed from penicilloic acid (Gozlan et al., 2013). A very low-intensity signal for m/z 371 was already detectable immediately after sodium hypochlorite addition (0 hr), but a sharp, well-defined peak emerged at the 1-hour timepoint and persisted through all subsequent runs, including the 24-hour sample (Figure 3.55). This detection pattern suggests that penilloic acid begins forming almost immediately but becomes the dominant and most stable degradation product within the first hour of oxidation. The persistence of m/z 371 aligns closely with the NMR results discussed earlier, where penilloic acid resonances became prominent after initial β-lactam ring opening. Together, these findings confirm Amoxicillin penilloic acid as the primary long-lived product of Amoxicillin degradation under sodium hypochlorite treatment 1(Gozlan et al., 2013, Siciliano et al., 2021).

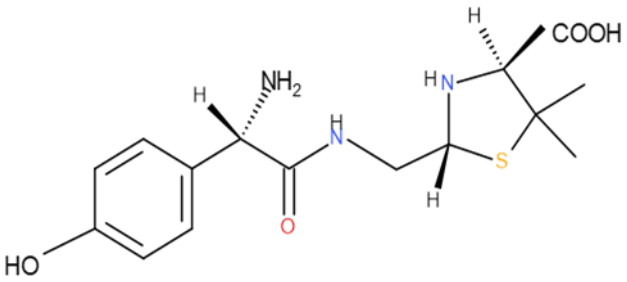

Figure 3.56. Chemical structure of Amoxicillin penilloic acid, a secondary degradation product of Amoxicillin. Penilloic acid (detected as m/z 371 in HPLC/MS) is formed through rearrangement following initial β-lactam ring hydrolysis

Alongside these ring-opened products, a minor cyclisation product was also observed, the m/z 341, associated with the formation of diketopiperazine, though its appearance was brief and limited.

Detected ion m/z 341

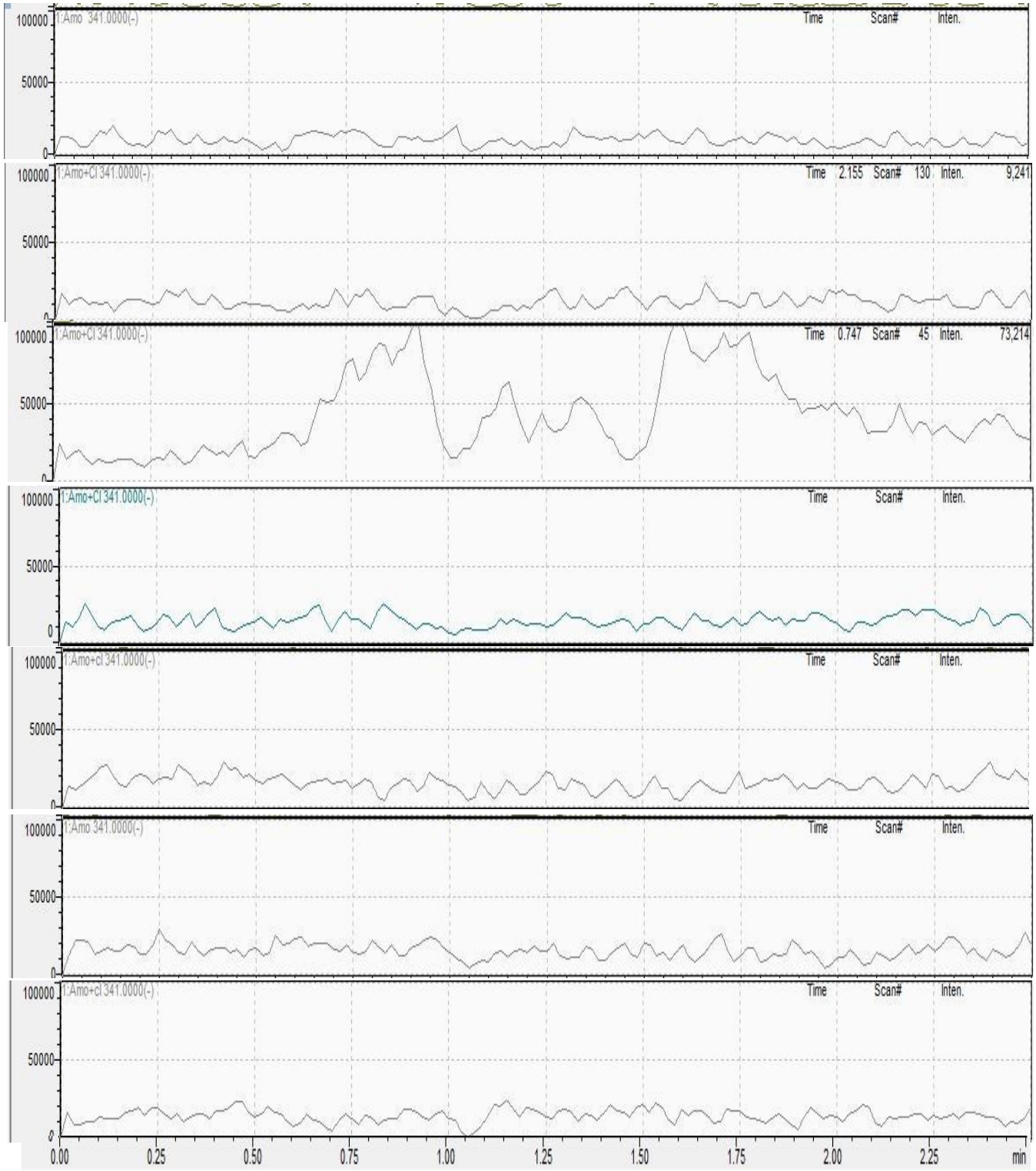

Figure 3.57. Extracted ion chromatograms (EICs) of m/z 341 collected during HPLC/MS monitoring of Amoxicillin degradation after addition of sodium hypochlorite (NaOCl) solution. The traces are shown in chronological order as follows: first trace: Amoxicillin only (no NaOCl), second: 0 h after NaOCl addition, third: 1 h, fourth: 2 h, fifth: 3 h, sixth: 4 h, seventh: 24 h (next day). All runs were recorded in negative ion mode, with intensity plotted against retention time (0.00–2.50 min)

The ion m/z 341 is associated with diketopiperazine, a cyclisation product of Amoxicillin reported in the literature (Gozlan et al., 2010, Siciliano et al., 2021, Gozlan et al., 2013, Lamm et al., 2009). In this study, m/z 341 was not present in the untreated Amoxicillin sample or at 0 hours after the addition of sodium hypochlorite. It first appeared at the 1-hour timepoint as two broad, diffuse peaks (Figure 3.57). Although these signals were large, they lacked the sharp definition of a typical chromatographic peak and were absent in all the other following runs. This behaviour suggests that m/z 341 may represent a transient or unstable intermediate, or possibly overlapping low-intensity signals from minor products, forming briefly during the early stages of oxidation (Siciliano et al., 2021, Pérez-Parada et al., 2011). Its brief appearance indicates that, under the conditions used here, diketopiperazine formation is minimal and not a major degradation pathway for Amoxicillin. Importantly, diketopiperazine was not observed in the NMR data either, further supporting the conclusion that its formation is minimal and not a major degradation pathway for Amoxicillin under the conditions used here.

In summary, HPLC/MS analysis of Amoxicillin after the addition of sodium hypochlorite revealed a rapid and largely sequential degradation pathway. The parent ion (m/z 364) disappeared within two hours, confirming the rapid breakdown of the intact molecule. A short-lived signal for penicilloic acid (m/z 383) was detected only at 1 hour, while penilloic acid (m/z 371) emerged almost immediately and persisted as the dominant and most stable product throughout the 24-hour study. Diketopiperazine (m/z 341) was observed only briefly as diffuse peaks at 1 hour, indicating that cyclisation is a minor and transient side reaction under these conditions.

Moreover, these findings support the NMR observations, where Amoxicillin underwent rapid β-lactam ring opening and rearrangement and confirm that penilloic acid is the primary long-lived degradation product of Amoxicillin in the presence of sodium hypochlorite. Together, the HPLC/MS and NMR results support the conclusion that Amoxicillin is highly reactive under oxidative conditions, breaking down into a mixture of smaller, more polar, and possibly rearranged fragments over time (Gozlan et al., 2013).

While many studies have proposed chemical structures for the degradation products of Amoxicillin under oxidative conditions that includes the β-lactam ring opening, side-chain loss, and chlorine substitution (Siciliano et al., 2021, Yang et al., 2020, Gozlan et al., 2013), only partial structural identification was possible in the present study. Penicilloic acid and penilloic acid were confirmed as key degradation products, supported by both HPLC/MS and NMR data. However, for many of the other fragment ions

detected, structural assignment was not feasible with the available data. This reflects the more complex and challenging degradation profile of Amoxicillin compared to Penicillin G, and highlights the need for further targeted analyses to fully characterise all breakdown products (Gozlan et al., 2010).

3.3.3 HPLC/MS analysis of Ciprofloxacin

The oxidative degradation of Ciprofloxacin by sodium hypochlorite solution was investigated using high-performance liquid chromatography/mass spectrometry (HPLC/MS) in positive ion mode. The analysis aimed to characterise degradation behaviour over time and identify transformation products resulting from treatment using sodium hypochlorite solution.

As described earlier, a stock solution was prepared by dissolving 10 mg of Ciprofloxacin in 100 mL of a pre-sonicated standard solution consisting of 500 mL of HPLC/MS-grade acetonitrile and 0.5 mL of formic acid. Two additional drops of formic acid were added to assist with solubility, and the solution was sonicated for 10 minutes to ensure full dissolution. The degradation reaction was initiated by adding two drops of 12.5% sodium hypochlorite solution. Following this, a serial dilution was performed to achieve a final concentration of 1 ppm (by adding 1 mL of the treated solution to 99 mL of the standard solution), which provided optimal chromatographic results.

Chromatographic separation was carried out using a Waters Acquity® UPLC BEH C18 column (100 × 2.1 mm, 1.7 µm), with solvent A as LC/MS-grade water (0.1% formic acid) and solvent B as LC/MS-grade acetonitrile (0.1% formic acid). The gradient began at 20% solvent B, favouring retention of polar degradation products. The injection volume was 2 µL, with a flow rate of 0.4 mL/min, and each sample run lasted 6 minutes. Samples were analysed at 1-hour intervals during the first 6 hours after the addition of sodium hypochlorite, followed by a final run at 24 hours to monitor time-dependent degradation trends. The total ion chromatograms (TICs) shown in Figure 20 demonstrate the progressive degradation of Ciprofloxacin after exposure to sodium hypochlorite.

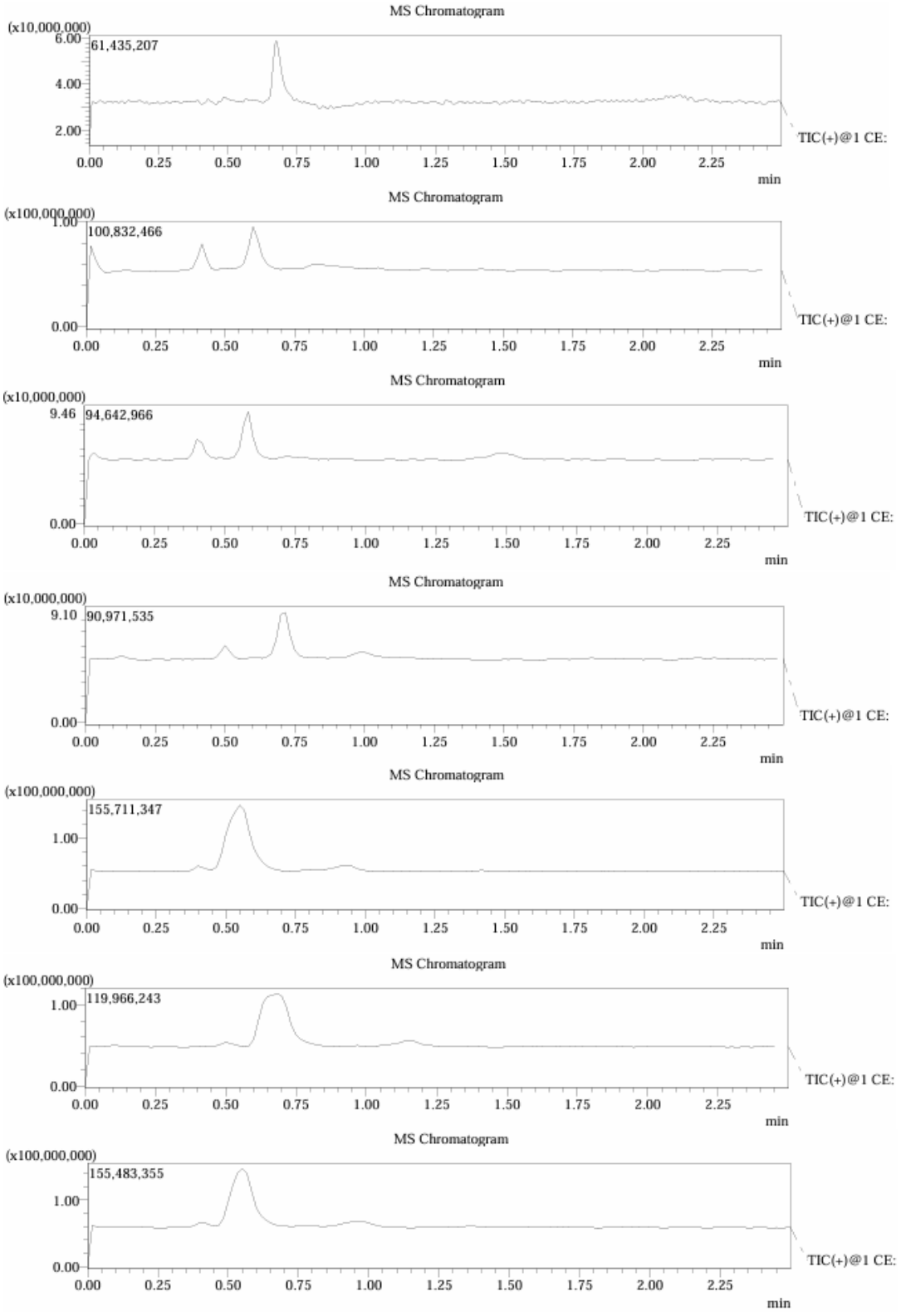

Figure 3.58. Total ion chromatograms (TICs) of Ciprofloxacin before and after addition of sodium hypochlorite (NaOCl) solution, monitored over a 24-hour period. The chromatograms are shown in sequential order: top trace: Ciprofloxacin only (untreated), second: 0 h post NaOCl addition, third: 1 h, fourth: 2 h fifth: 3 h, sixth: 4 h and bottom trace: 24 h analyzed using HPLC/MS in positive ion mode

The HPLC/MS chromatograms in Figure 3.58, show the degradation profile of Ciprofloxacin following sodium hypochlorite treatment, tracked over a 24-hour period. The top trace represents Ciprofloxacin alone (untreated), which shows a strong and sharp peak at ~0.70 minutes, corresponding to the intact parent compound.

After the addition of sodium hypochlorite, the 0-hour chromatogram (second trace) shows a slightly shifted peak at ~0.6 minutes, indicating a potential immediate chemical response or rearrangement triggered by the oxidant. Despite this shift, a dominant peak remains visible across all timepoints, suggesting that the parent compound, or a closely related transformation product persists.

From 1 to 4 hours post-treatment, the main peak remained prominent, with only minor variations in shape and intensity, indicating limited and gradual degradation. By the 24-hour mark, the peak was still present, though slightly broader and of reduced intensity, consistent with partial oxidation or the formation of stable by-products.

These results from this study suggest that Ciprofloxacin is more resistant to degradation by sodium hypochlorite than the β-lactam antibiotics examined. The persistent parent peak throughout the 24-hour period supports the interpretation that much of the parent compound remained intact, or that degradation produced structurally similar fragments with comparable retention and ionisation behaviour. This observation is consistent with the ^{1}H NMR data (NMR section), which also showed gradual changes rather than complete breakdown, and aligns with reports in the literature where fluoroquinolones, including Ciprofloxacin, demonstrate slower and less extensive chlorination reactivity compared to β-lactams (Kennedy Neth et al., 2019, Matta et al., 2018, Wang et al., 2017).

To gain a deeper understanding of the degradation process, the HPLC/MS data were examined by tracking fragment ions that correspond to degradation products proposed in the NMR study (Figure 3.40) and reported in the literature (Dodd et al., 2005, Deng et al., 2019). All relevant masses were screened, but only seven ions including, m/z 332, 306, 362, 324, 298, 288, and 263, were consistently detected across the runs and therefore selected for interpretation.

These ions represent a combination of the intact parent compound (m/z 332) and likely transformation products arising from the opening of the piperazinyl, oxygen insertion, and other oxidative modifications. Monitoring the retention time and behaviour of these ions at each timepoint provided clearer insight into how Ciprofloxacin transforms after

the addition of sodium hypochlorite. The interpretation of these ions, linked to both NMR findings and published degradation pathways, is presented in the following section.

Detected ion m/z 332

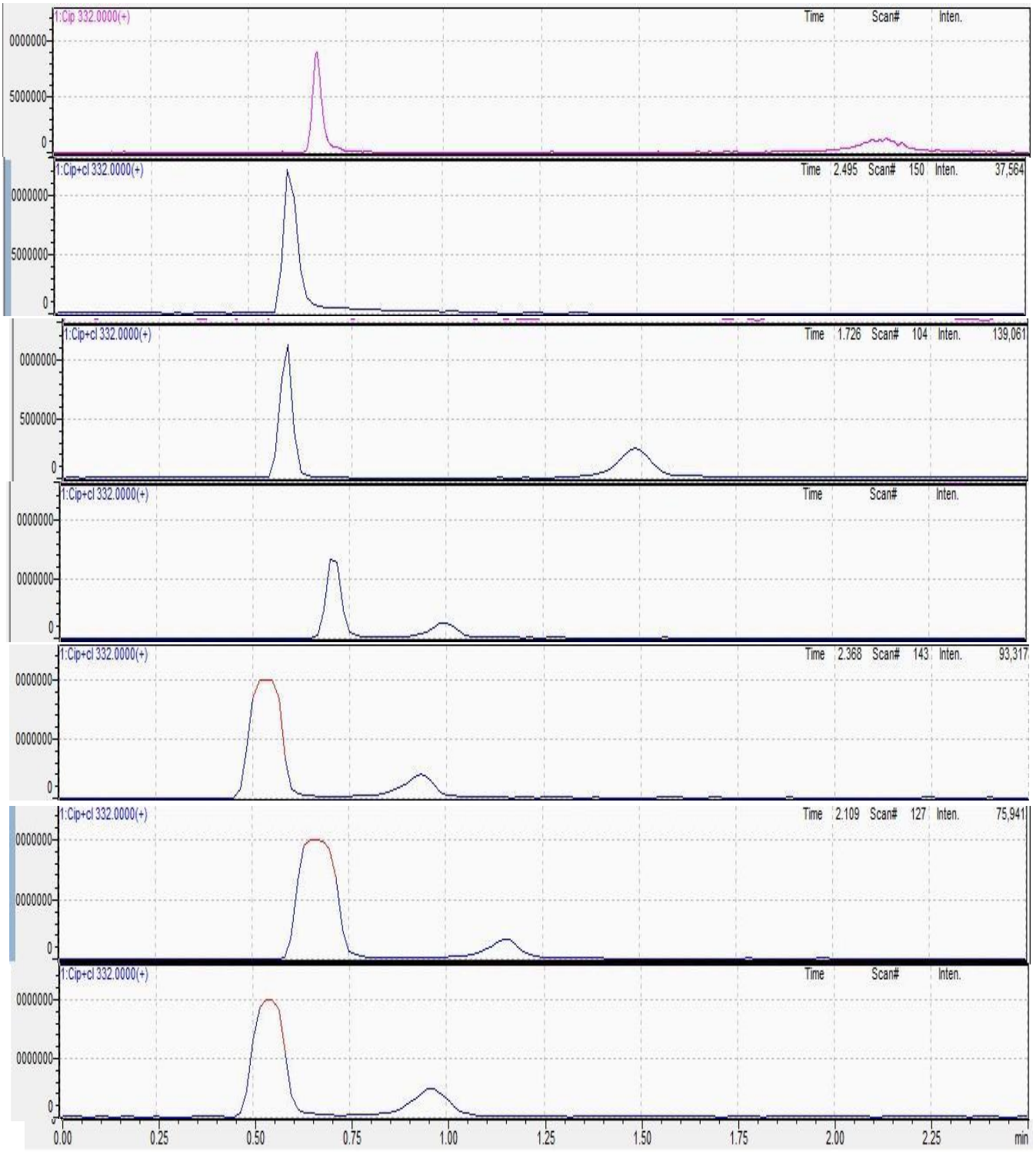

Figure 3.59. Extracted ion chromatograms (EICs) of m/z 332 collected during HPLC/MS monitoring of Ciprofloxacin degradation after addition of sodium hypochlorite (NaOCl) solution n. The traces are shown in chronological order as follows: first trace: Ciprofloxacin only (no NaOCl), second: 0 h after NaOCl addition, third: 1 h, fourth: 2 h, fifth: 3 h, sixth: 4 h, seventh: 24 h (next day). All runs were recorded in positive ion mode, with intensity plotted against retention time (0.00–2.50 min)

The ion m/z 332, corresponding to the $[M+H]^+$ protonated parent ion of Ciprofloxacin, was consistently detected across all timepoints, including in the untreated sample. In the Ciprofloxacin only chromatogram, it appeared as a sharp, intense peak at approximately 0.70 minutes, confirming the presence of the intact molecule. Following the addition of sodium hypochlorite, the m/z 332 signal remained visible at all timepoints, though with a slightly earlier retention time of ~0.60 minutes and minor changes in peak intensity and shape (Figure 3.59).

This consistent detection suggests that either the parent compound is relatively stable under oxidative conditions, or that structurally similar transformation products with the same nominal mass are being formed. The slight shift in retention time suggests that the addition of sodium hypochlorite altered the sample matrix, for example, by changing pH or ionic strength, which in turn could have slightly influenced the chromatographic behaviour and shifted the peak retention time (Deng et al., 2019).

Ciprofloxacin's parent ion (m/z 332) was consistently detected across all timepoints, gradually decreasing in intensity over the 24-hour period but never fully disappearing. This persistence reflects the stability of Ciprofloxacin's core structure (the quinolone ring system with its attached cyclopropyl group) which resisted oxidative attack under treatment with lower strength sodium hypochlorite solution used (12.5 vol%). While the more reactive piperazine ring underwent fragmentation, generating products such as m/z 362, 306 and 289, the central quinolone structure stayed largely intact, explaining why m/z 332 continued to be detected throughout the experiment. The persistence of m/z 332 across all timepoints supports the idea that Ciprofloxacin degrades more slowly than β-lactam antibiotics. Its partial resistance to oxidation under the conditions used aligns with previous reports in the literature that describe fluoroquinolones as more chemically stable, often requiring harsher oxidative conditions for full breakdown (Sayed et al., 2016, Matta et al., 2018, Gou et al., 2021, Kim et al., 2020, Keen and Linden, 2013, Kennedy Neth et al., 2019, Wang et al., 2017, Zhou et al., 2011).

Although the parent ion (m/z 332) remained the dominant peak, the first clear evidence of molecular alteration was the emergence of m/z 306, indicating the early stages of piperazine ring oxidation and fragmentation.

Detected ion m/z 306

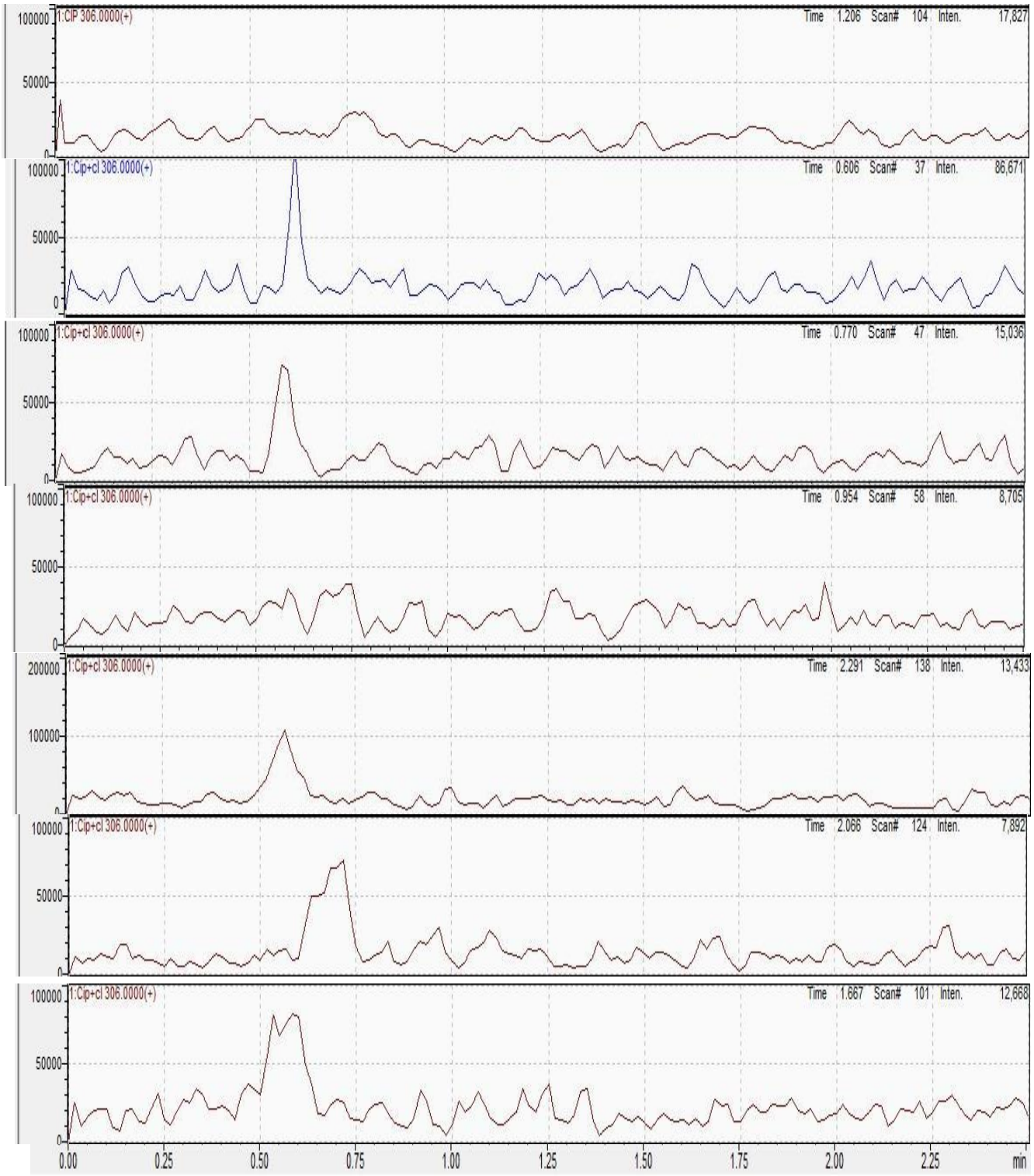

Figure 3.60. Extracted ion chromatograms (EICs) of m/z 306 collected during HPLC/MS monitoring of Ciprofloxacin degradation after addition of sodium hypochlorite (NaOCl) solution. The traces are shown in chronological order as follows: first trace: Amoxicillin only (no NaOCl), second: 0 h after NaOCl addition, third: 1 h, fourth: 2 h, fifth: 3 h, sixth: 4 h, seventh: 24 h (next day). All runs were recorded in positive ion mode, with intensity plotted against retention time (0.00–2.50 min)

The ion m/z 306 was one of the earliest transformation products detected following sodium hypochlorite addition. It appeared immediately after treatment and was present across most following timepoints, though generally at lower intensity than the parent ion. Its consistent presence suggests that it represents a primary oxidative modification rather than a minor by-product (Figure 3.60).

In the literature, m/z 306 has been linked to partial cleavage or oxidation of the piperazine ring in Ciprofloxacin (Kennedy Neth et al., 2019, Deng et al., 2019). The HPLC/MS detection of m/z 306 is consistent with the ^{1}H NMR findings, which indicated disruption of the piperazine ring. Literature reports also describe m/z 306 as resulting from the loss of C_2H_2 from the parent molecule (Kim et al., 2020, Kennedy Neth et al., 2019), reflecting partial piperazine ring cleavage. The formation of m/z 306 therefore likely reflects an early step in Ciprofloxacin's degradation pathway, where the more reactive piperazine ring undergoes oxidative attack, while the quinolone core remains largely intact (Kennedy Neth et al., 2019). Its detection throughout the experiment indicates that m/z 306 may serve as a relatively stable intermediate formed during the first stages of breakdown. The proposed structure of this fragment is shown below in Figure 3.61.

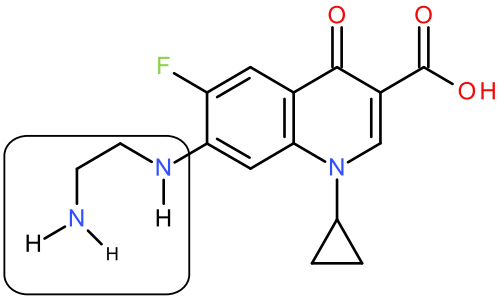

Figure 3.61. Proposed structure of the m/z 306 degradation product of Ciprofloxacin, redrawn based on NMR data obtained in this study and literature-reported fragmentation pathways (Kim et al., 2020, Kennedy Neth et al., 2019). The fragment corresponds to the parent molecule following the loss of C_2H_2 from the piperazine ring

In addition to m/z 306, another key fragment detected after the addition of sodium hypochlorite was m/z 362, which appeared shortly after exposure and provides further evidence of early oxidative changes to the piperazine ring.

Detected ion m/z 362

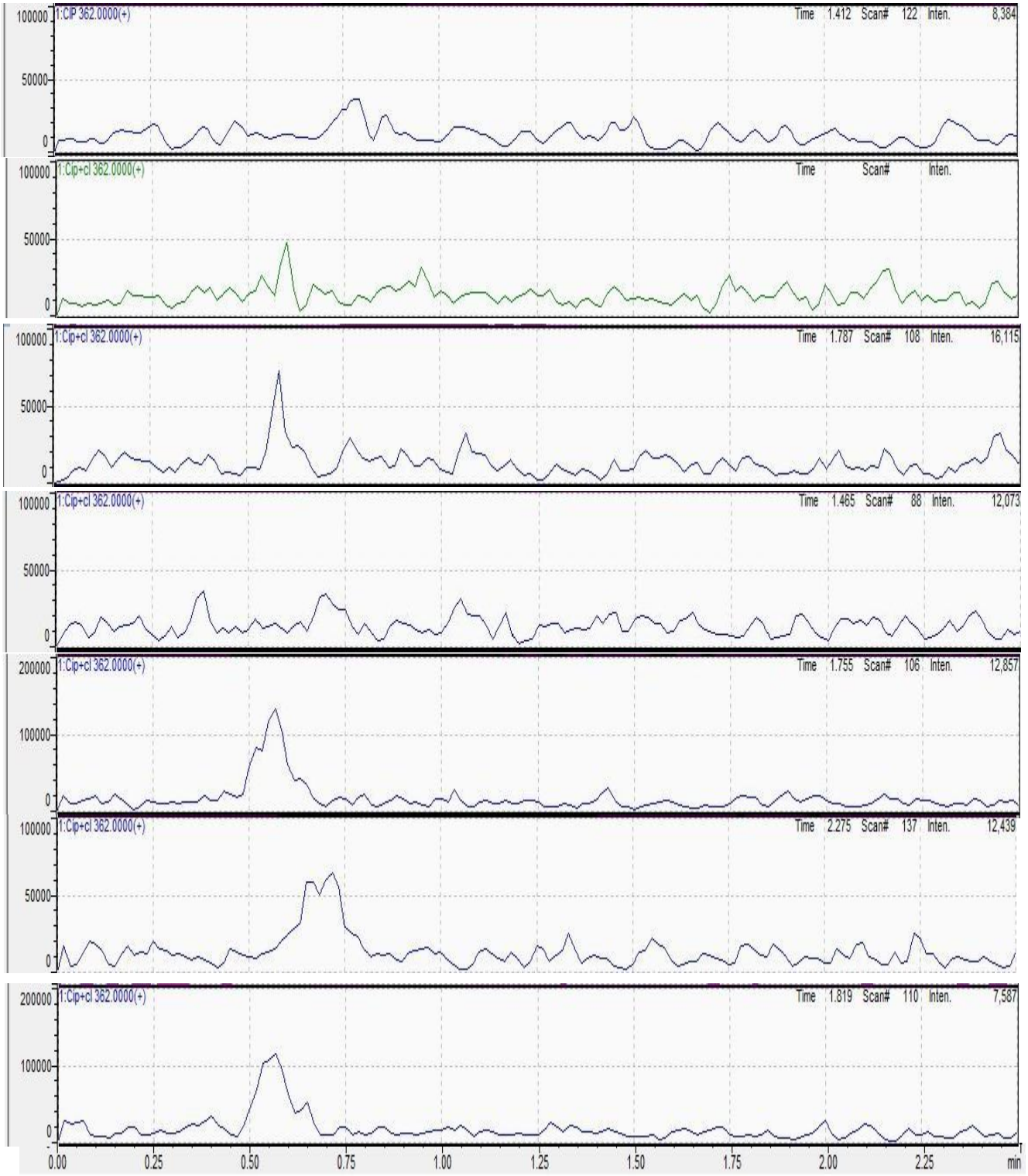

Figure 3.62. Extracted ion chromatograms (EICs) of m/z 362 collected during HPLC/MS monitoring of Ciprofloxacin degradation after addition of sodium hypochlorite (NaOCl) solution. The traces are shown in chronological order as follows: first trace: Ciprofloxacin only (no NaOCl), second: 0 h after NaOCl addition, third: 1 h, fourth: 2 h, fifth: 3 h, sixth: 4 h, seventh: 24 h (next day). All runs were recorded in positive ion mode, with intensity plotted against retention time (0.00–2.50 min)

The extracted ion chromatogram (EIC) of m/z 362 revealed that this oxidised ciprofloxacin product appeared immediately after the addition of sodium hypochlorite solution and reached its highest intensity at the 1-hour timepoint. This early and noticeable peak indicates that oxidation of ciprofloxacin occurs rapidly once sodium hypochlorite solution is introduced (Figure 3.62).

Following this peak, the signal intensity progressively declined at later timepoints, confirming that m/z 362 is a transient intermediate rather than a stable end product. By the 24-hour run, the EIC trace displayed only a low-intensity, irregular peak, indicating that most of this oxidised species had further degraded or transformed into secondary products (Figure 3.62).

The ion at m/z 362 was observed following the initial piperazine cleavage event (m/z 306) and corresponds to an oxidised ciprofloxacin product. Kim et al. (2020) through NMR studies have characterised this transformation and assigned it to the structure shown in Figure 3.63, where the piperazine ring undergoes further oxidation, incorporating two oxygen atoms ($+O_2$) with loss of two hydrogens (-H), resulting in a +30 Da mass shift from the parent ciprofloxacin ion (m/z 332) (Kim et al., 2020, Kennedy Neth et al., 2019). This modification indicates that after sodium hypochlorite initiates cleavage of the piperazine bond, it rapidly promotes N-oxide formation or hydroxylation on the remaining piperazine ring (Kennedy Neth et al., 2019).

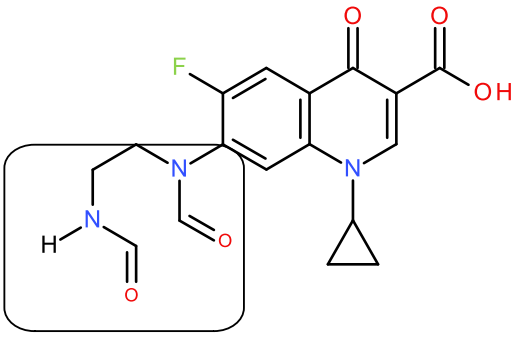

Figure 3.63. Redrawn proposed structure of the m/z 362 degradation product of Ciprofloxacin as reported by Kim et al. (2020)

The consistent but short-lived presence of m/z 362 across the time-series runs supports its role as a transient but significant intermediate in the degradation process, which then enables downstream reactions, including the formation of further sodium hypochlorite-derived products such as m/z 324(Kennedy Neth et al., 2019, Kim et al., 2020).

Detected ion m/z 324

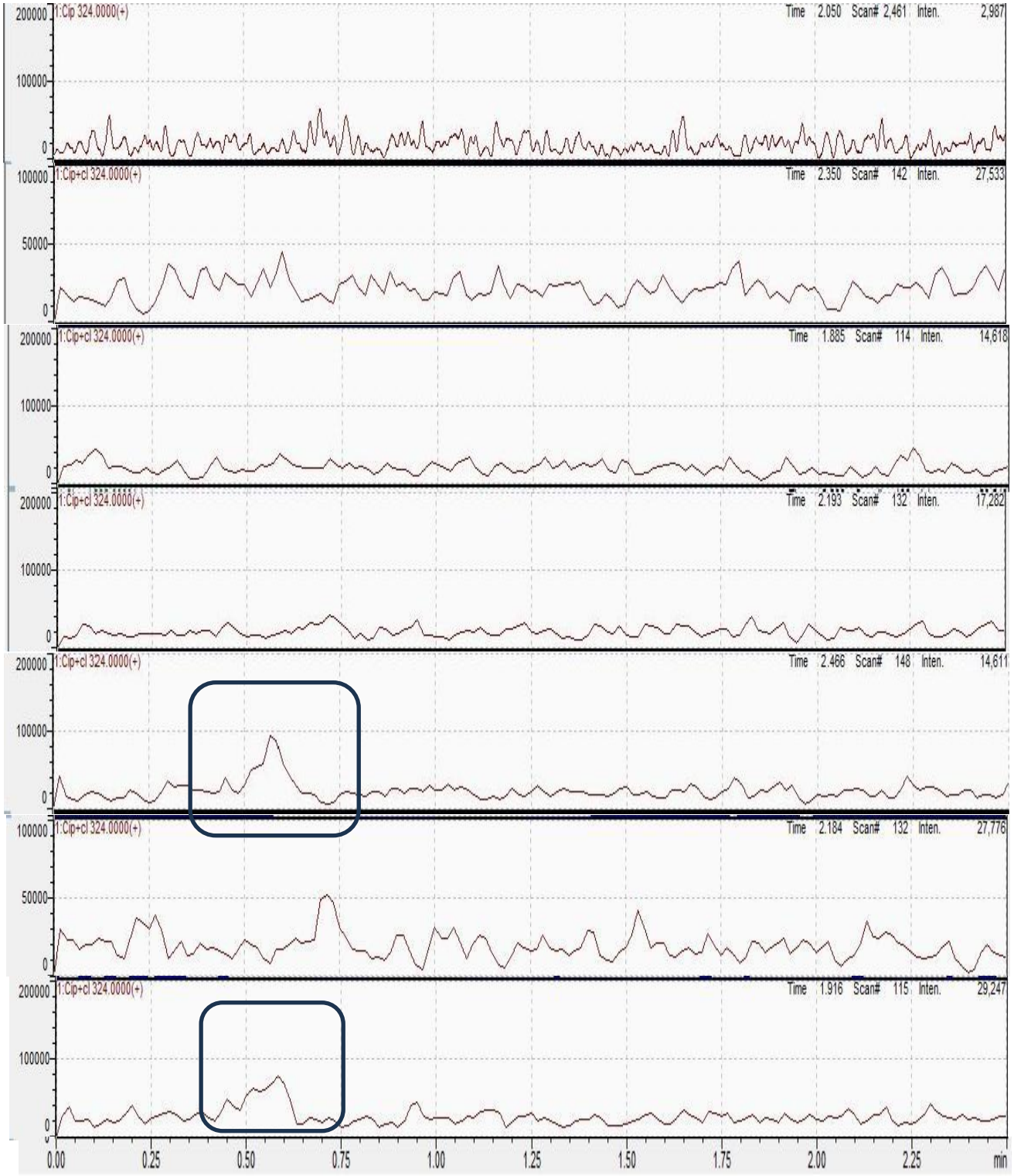

Figure 3.64. Extracted ion chromatograms (EICs) of m/z 324 collected during HPLC/MS monitoring of Ciprofloxacin degradation after addition of sodium hypochlorite (NaOCl) solution. The traces are shown in chronological order as follows: first trace: Ciprofloxacin only (no NaOCl), second: 0 h after NaOCl addition, third: 1 h, fourth: 2 h, fifth: 3 h, sixth: 4 h, seventh: 24 h (next day). All runs were recorded in positive ion mode, with intensity plotted against retention time (0.00–2.50 min)

The ion m/z 324 was not detected in the Ciprofloxacin-only sample and did not appear during the early stages following sodium hypochlorite treatment. It first appeared after 3 hours of NaOCl addition and remained present in the 24-hour sample, showing a consistent retention time of approximately 0.58 minutes (Figure 3.64).

Its delayed appearance suggests that m/z 324 is a later-stage degradation product, most likely formed through the gradual transformation of either the parent compound or earlier intermediates. Its persistence and stable retention time indicate that, once formed, it is a stable byproduct of the oxidation process (Kennedy Neth et al., 2019).

In support of this, a study by Kennedy Neth et al. (2019) proposed a degradation pathway where the piperazinyl ring of Ciprofloxacin undergoes ring opening and addition of a double-bonded oxygen, forming an intermediate with m/z 334, which can then undergo chlorine substitution at the carboxyl group to yield a product with m/z 324 (Figure 3.65). While this exact structure cannot be confirmed from the present data, the timing and persistence of m/z 324 observed here are consistent with this proposed degradation mechanism (Kennedy Neth et al., 2019).

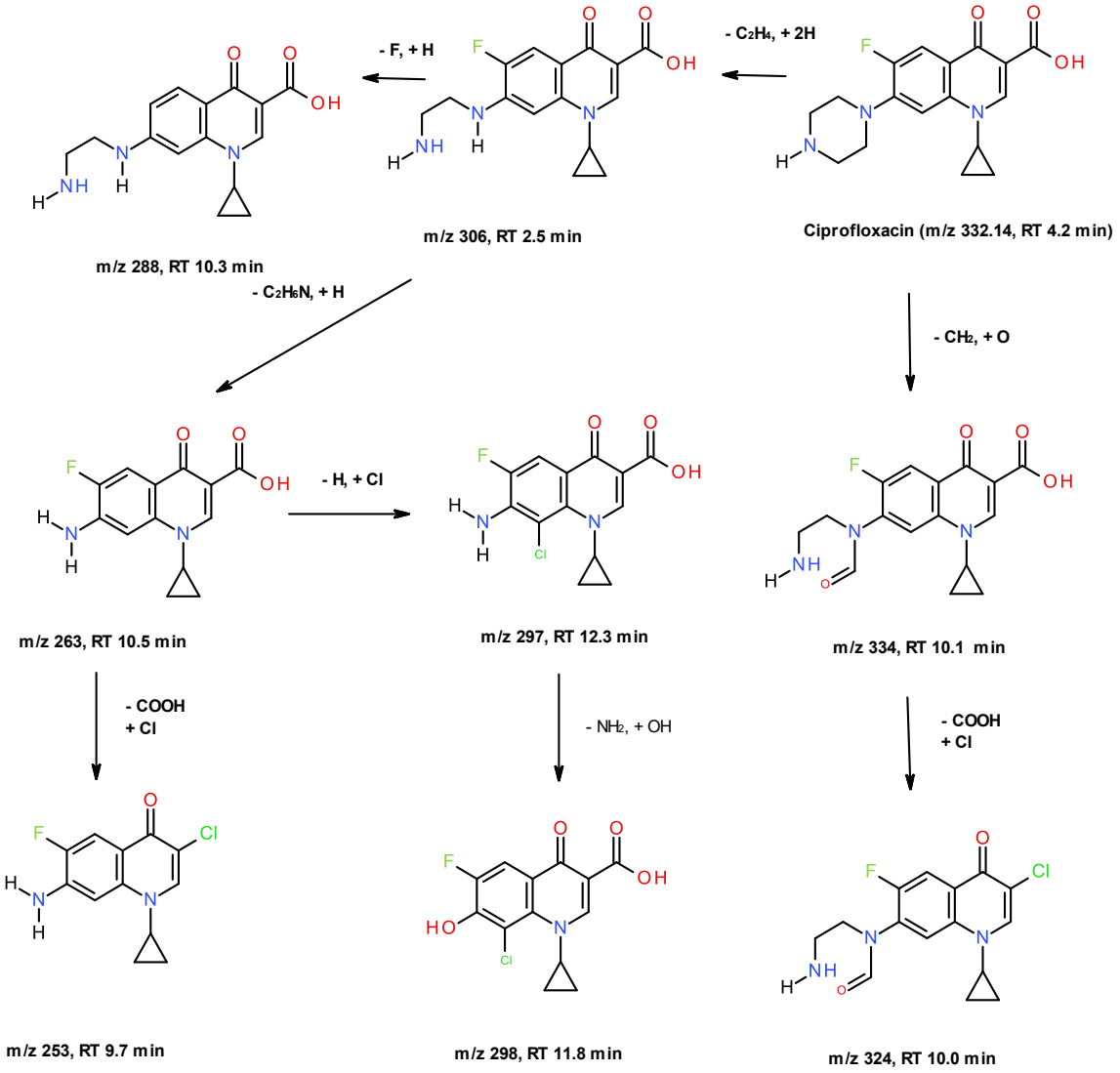

Figure 3.65. Proposed ciprofloxacin degradation pathway reproduced from Kennedy et al. (2019)

Kennedy et al. developed this pathway under different experimental parameters, but it provides a valuable framework for interpreting the present study's HPLC/MS findings.

Alongside these transformations, another notable fragment ion, m/z 298, was also detected. Its appearance indicates a further breakdown step in the ciprofloxacin structure, building upon the earlier intermediates and by-products already identified.

Detected ion m/z 298

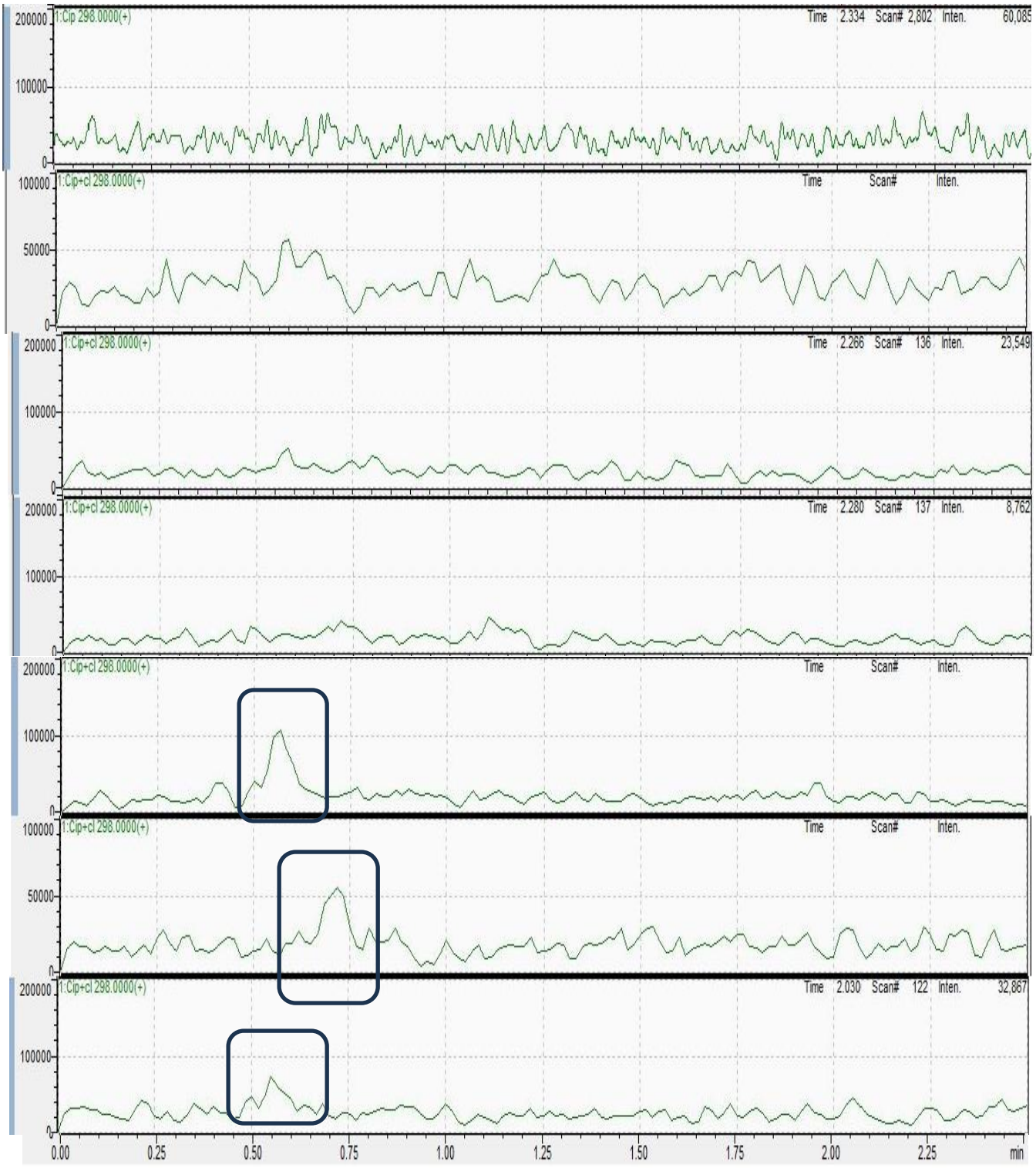

Figure 3.66. Extracted ion chromatograms (EICs) of m/z 298 collected during HPLC/MS monitoring of Ciprofloxacin degradation after addition of sodium hypochlorite (NaOCl)

solution. The traces are shown in chronological order as follows: first trace: Ciprofloxacin only (no NaOCl), second: 0 h after NaOCl addition, third: 1 h, fourth: 2 h, fifth: 3 h, sixth: 4 h, seventh: 24 h (next day). All runs were recorded in positive ion mode, with intensity plotted against retention time (0.00–2.50 min)

The ion m/z 298 was not detected in the Ciprofloxacin-only chromatogram, nor in the early timepoints after sodium hypochlorite was added. It only began to appear after 4 hours of NaOCl addition, showing up as a peak at around 0.58 minutes, and remained visible in the 24-hour run (Figure 3.66).

Because this ion appears relatively late in the degradation timeline, it likely represents a secondary or later-stage product, possibly forming after continued oxidation or transformation of earlier intermediates. Its consistent presence from the 4-hour mark onwards suggests that once it forms, it is stable enough to persist, but it does not form immediately after oxidation begins.

The fact that m/z 298 was not seen in the untreated sample, or in the first few hours, supports the idea that it is not a simple fragment of the parent compound, but more likely a distinct degradation product formed further along the pathway. While some studies (Kennedy Neth et al., 2019) suggest this ion may be associated with cleavage of the piperazine ring or side-chain modifications, no structural confirmation could be made in this study, and no clear correlation with NMR results was observed.

Interestingly, Kennedy Neth et al. (2019) also reported the detection of an ion with m/z 298 during chlorination of fluoroquinolones. Their study also suggested that it forms from a further transformation of m/z 297, where the primary aromatic amine is substituted by a hydroxyl group, resulting in a more oxidised structure (Kennedy Neth et al., 2019). This proposed pathway helps explain the late appearance of m/z 298 in the current results, supporting the idea that it likely forms after multiple transformation steps from the original Ciprofloxacin molecule. Although the exact structure could not be confirmed, its detection aligns well with progressive oxidative degradation, as described in the literature (Figure 3.65) (Kennedy Neth et al., 2019, Zhou et al., 2011).

Following the detection of m/z 298, a further minor fragment, m/z 288, was observed, indicating continued structural breakdown of the ciprofloxacin framework beyond the initial oxidation and piperazine cleavage events.

Detected ion m/z 288

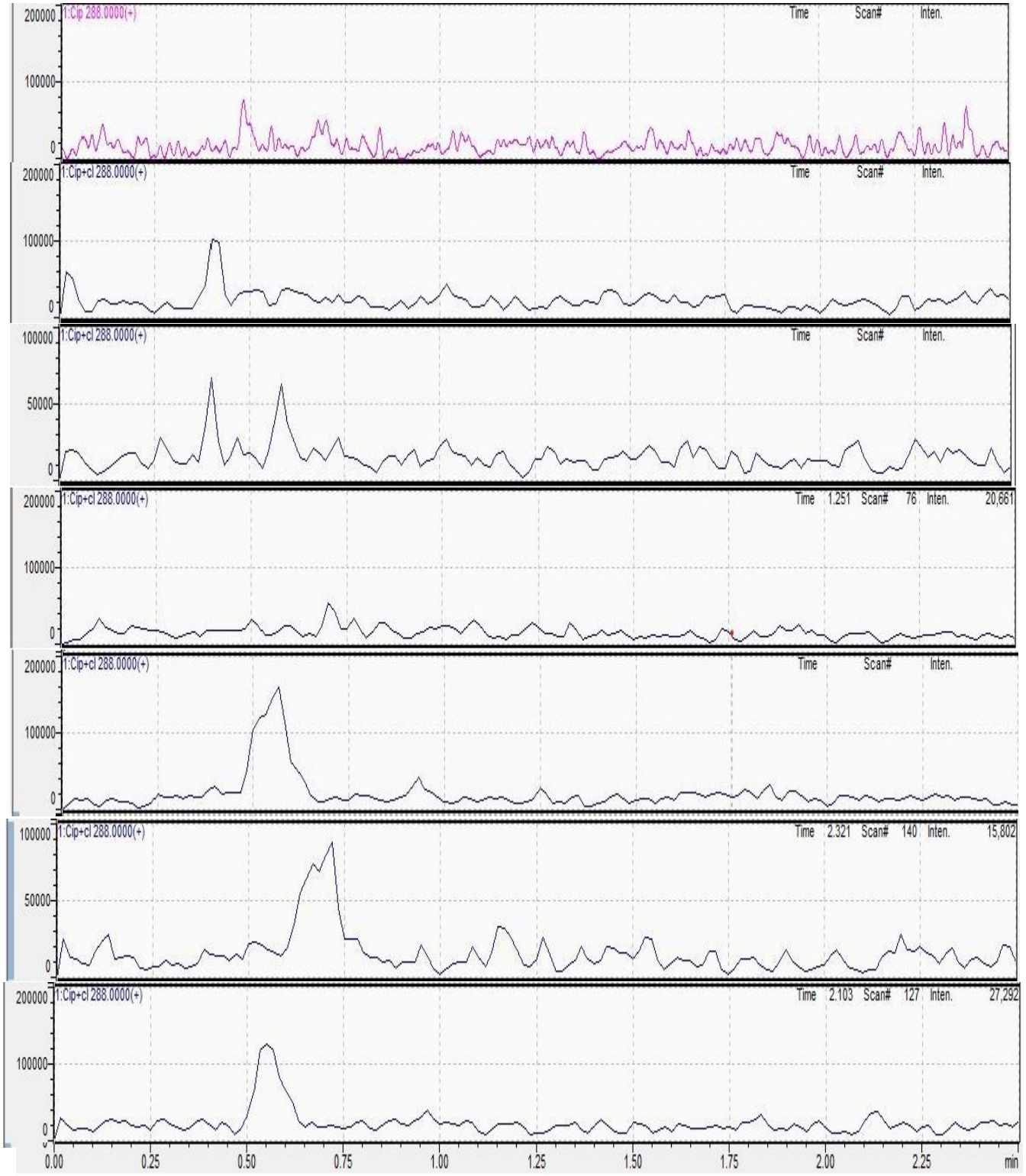

Figure 3.67. Extracted ion chromatograms (EICs) of m/z 288 collected during HPLC/MS monitoring of Ciprofloxacin degradation after addition of sodium hypochlorite (NaOCl) solution. The traces are shown in chronological order as follows: first trace: Ciprofloxacin only (no NaOCl), second: 0 h after NaOCl addition, third: 1 h, fourth: 2 h, fifth: 3 h, sixth: 4 h, seventh: 24 h (next day). All runs were recorded in positive ion mode, with intensity plotted against retention time (0.00–2.50 min)

The ion m/z 288 was not detected in the Ciprofloxacin-only sample, indicating that it is not an in-source MS fragment of the parent molecule but rather a product formed only after oxidative treatment. It was first observed immediately after sodium hypochlorite was added, appearing as a clear peak at around 0.42 minutes, and it continued to be detected throughout the oxidation timeline. The peak was still visible at 1 hour, 2 hours, and was most prominent at 3 hours, suggesting it may be an intermediate product formed relatively early during the degradation process. By 24 hours, the peak was still present but noticeably reduced in intensity, indicating that this product may begin to break down further over time (Figure 3.67).

The delayed appearance and gradual decline in signal intensity point to m/z 288 being a transient degradation product, possibly formed from one or more earlier intermediates (Kennedy Neth et al., 2019). In support of this, Kennedy Neth et al. (2019) proposed that m/z 288 may originate from a precursor ion m/z 306, which results from the loss of two carbon and two hydrogen atoms from the piperazinyl ring (Figure 3.65). The product m/z 306 can then undergo defluorination, where the fluorine atom is lost, yielding m/z 288 (Figure 3.65). Although structural confirmation of this product was not possible in the current study, the observed timing and consistent retention of m/z 288 support its formation via this sequential oxidative pathway (Kennedy Neth et al., 2019, Wang et al., 2017).

Beyond m/z 288, the chromatograms revealed the emergence of m/z 263, signifying an additional step in the breakdown sequence and pointing to further fragmentation of the ciprofloxacin structure after the addition of sodium hypochlorite.

Detected ion m/z 263

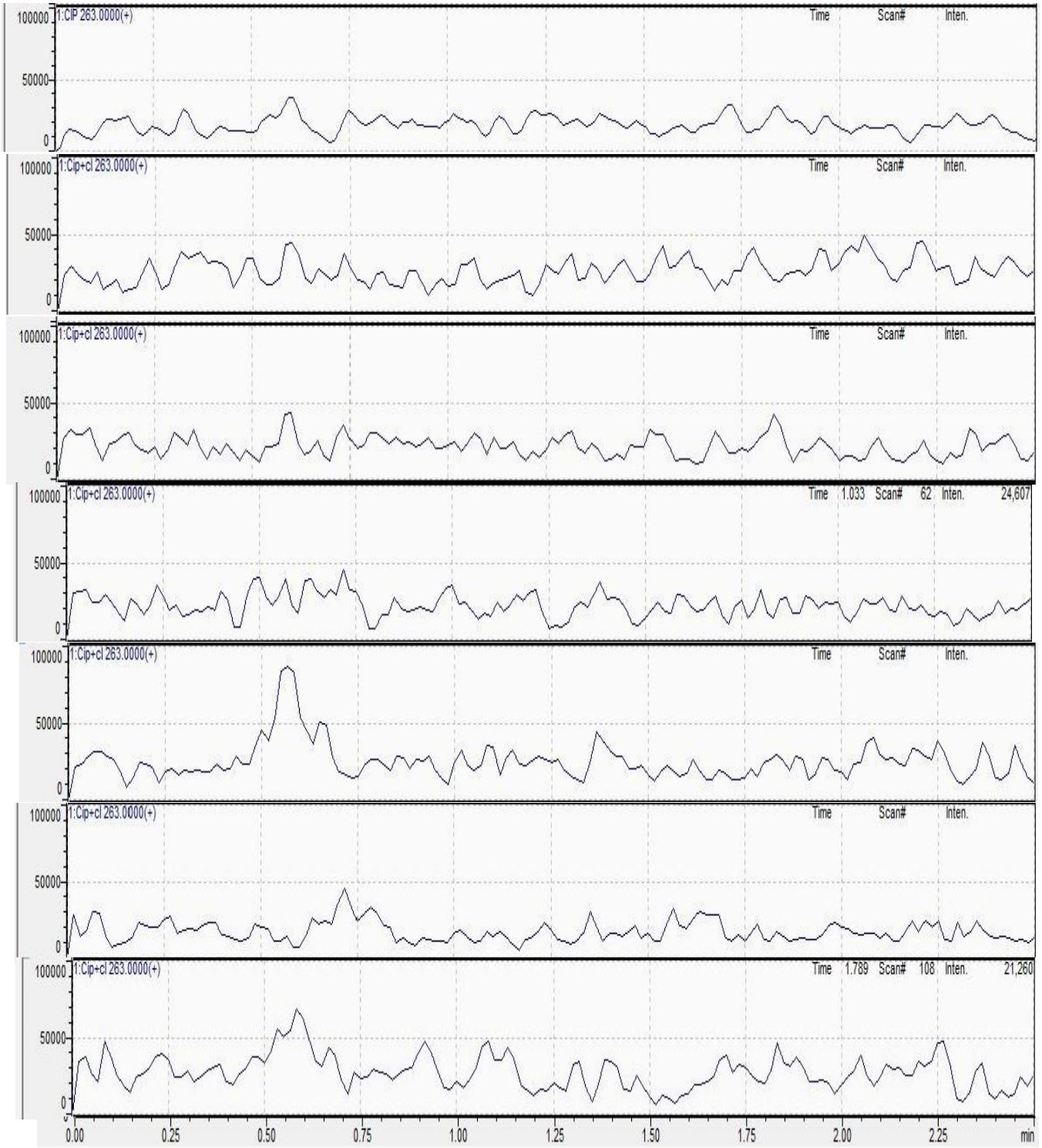

Figure 3.68. Extracted ion chromatograms (EICs) of m/z 263 collected during HPLC/MS monitoring of Ciprofloxacin degradation after addition of sodium hypochlorite (NaOCl) solution. The traces are shown in chronological order as follows: first trace: Ciprofloxacin only (no NaOCl), second: 0 h after chlorination, third: 1 h, fourth: 2 h, fifth: 3 h, sixth: 4 h, seventh: 24 h (next day). All runs were recorded in positive ion mode, with intensity plotted against retention time (0.00–2.50 min)

The ion m/z 263 was not detected in the untreated Ciprofloxacin sample or during the first two hours after sodium hypochlorite addition. It first appeared at the 3-hour timepoint as a clear peak but was absent in all subsequent runs, suggesting it is a transient degradation product formed during the intermediate stages of oxidation (Figure 3.68).

The formation of m/z 263 is well supported in the literature. Kennedy et al. (2019) and other studies of fluoroquinolone chlorination report this ion as a key byproduct arising from stepwise piperazine ring cleavage and partial quinolone core modification (Kennedy Neth et al., 2019, Kim et al., 2020). Similarly, the proposed degradation pathway in Figure 3.40 from the NMR section identifies m/z 263 as a fragment produced after the combined loss of piperazine substituents and subsequent oxidative rearrangement.

Moreover, the brief detection of m/z 263 in this study indicates that it may be a short-lived intermediate that either rapidly transforms into smaller products or other species not resolved under the conditions used here. Its transient nature aligns with NMR observations, where piperazine ring degradation signals were strong, but complete disassembly of the quinolone core remained limited.

The sequential transformations described above are visually summarised in Figure 3.65, adapted from Kennedy et al. (2019). While Kennedy et al.2019 conducted their work under different experimental parameters and observed their products at different retention times, their pathway provides valuable context for interpreting the suite of degradation products identified in this study.

In conclusion, the HPLC/MS analysis of Ciprofloxacin following the addition of sodium hypochlorite solution revealed a multi-step degradation sequence involving both transient intermediates and stable by-products. The parent compound, m/z 332, disappeared rapidly after treatment, confirming immediate structural reactivity. Early fragmentation produced m/z 306, linked to piperazine ring cleavage and corroborated by NMR evidence (Figure 3.40). Oxidation yielded m/z 362, a transient but significant intermediate peaking at one hour, which subsequently declined as further breakdown occurred.

Later in the sequence, m/z 324 emerged as a stable sodium hypochlorite-derived by-product, persisting through the 24-hour period. Additional lower-mass fragments, the m/z 298, m/z 288, and m/z 263, were also detected, indicating continued molecular disintegration as ciprofloxacin underwent complete oxidative degradation.

The pathway proposed by Kennedy et al. (2019) (Figure 3.65) provides valuable context for these findings. Although Kennedy's study employed different experimental conditions

and retention times, the overall sequence of transformations they describe, from piperazine ring cleavage, through oxidation, to the appearance of stable by-products, aligns closely with the degradation products detected here. Together, the LC/MS data and supporting NMR evidence highlight ciprofloxacin's susceptibility to rapid and extensive breakdown following sodium hypochlorite addition.

It is also worth noting that the extent of degradation observed in this study may be influenced by the relatively mild oxidative conditions applied. Previous research has shown that more aggressive or prolonged chlorine exposure can lead to greater structural breakdown, including defluorination and further ring transformations (Zhou et al., 2011, Kennedy Neth et al., 2019). The partial degradation and absence of certain expected fragments, particularly those involving the fluorine group or cyclopropyl ring, could reflect the limitations of the current treatment conditions. However, the ions detected provide valuable insight into the early and intermediate stages of Ciprofloxacin degradation, even under moderate oxidative stress.

3.4 Correlations of analytical findings using the NMR and HPLC/MS techniques

Understanding the degradation behaviour of pharmaceutical compounds under oxidative treatment requires multiple analytical techniques to capture both structural and compositional changes (Postigo and Richardson, 2014). In this study, two complementary analytical tools namely, Nuclear Magnetic Resonance (NMR) spectroscopy and high-performance liquid chromatography/mass spectrometry (HPLC/MS), were applied to capture these changes during treatment with sodium hypochlorite solution.

The NMR spectroscopic analyses provide real-time, direct and non-destructive analysis of proton and carbon environments, making it ideal for detecting changes in key functional groups (i.e., loss of β-lactam rings, loss of methyl groups and etc) and the formation of intermediate product during degradation processes (Daletos et al., 2017, Branch et al., 1987). It also enables the identification of ring-opening events, structural substitution and new group insertions that occur under oxidative stress (Dr. Holzgrabe, 2010, Vafaei et al., 2020, Mitsumori et al., 2006, Padfield and Kellaway, 1974, Kan et al., 1973, Holzgrabe, 2015, Connor et al., 1994a, Acosta, Branch et al., 1987).

On the other hand, HPLC/MS runs confirmed the degradation trends observed by NMR with greater sensitivity and specificity, while also provided the detection of very low-concentration with high-sensitivity degradation products including polar and halogenated fragments that

NMR could not easily resolve (Samanidou et al., 2007, Matta et al., 2018, Choudhury et al., 2017). By following the appearance and disappearance of selected m/z values over time, it was possible to link these signals to specific structural breakdown events seen in NMR.

Therefore, the combined application of ^{1}H NMR and LC/MS techniques offered a comprehensive view of the oxidative degradation behaviours of Penicillin G, Amoxicillin, and Ciprofloxacin following the addition of sodium hypochlorite solution. This chapter integrates the data for all three compounds, aligning NMR-observed structural changes with HPLC/MS-detected fragments and assessing how both techniques complement one another. Each method provided different, but complementary information regarding the degradation mechanisms and the identification of shared and different transformation pathways.

Moreover, by comparing the specific transformation products formed and the degradation trends through each technique, a more integrated understanding of the underlying chemical transformation pathways can be developed under controlled laboratory conditions. In this chapter the combined interpretation of both techniques used highlights not only the sequence of degradation events for each molecule but also demonstrates the oxidative behavioural effect of sodium hypochlorite on β-lactam antibiotics versus fluoroquinolones under the experimental conditions employed, without implying direct correspondence to behaviour in real environmental matrices

3.4.1 Correlation between NMR and LC/MS findings: Penicillin G

The degradation of Penicillin G was monitored using both NMR and HPLC/MS techniques to provide a complementary understanding of the molecular transformations using NaOCl. The combined interpretation of these results reveals a high degree of agreement between the structural changes shown by NMR and the fragmentation patterns observed in HPLC/MS.

The ^{1}H NMR analysis clearly demonstrated that Penicillin G undergoes rapid and significant degradation upon exposure to sodium hypochlorite solution. Key analytical signals included the methyl peaks at 1.18 ppm and 0.98 ppm, and the β-lactam proton signal around 5.0–5.3 ppm which underwent substantial changes. The immediate formation of new peaks at 1.18 ppm was assigned to penicilloic acid, while the delayed emergence of a peak at 0.98 ppm was allocated to penilloic acid, consistent with prior literature (Mitsumori et al., 1977, Degelaen et al., 1979). These findings support a two-

step degradation pathway where the initial step is the hydrolysis of the β-lactam ring followed by further rearrangement.

These observations were directly confirmed by HPLC/MS analyses, which showed the disappearance of the parent ion m/z 365 over time, accompanied by the emergence of degradation fragments. The emergence of four key ions over time: m/z 307, 289, 202, and 157, suggest secondary degradation processes involving oxidation of the thiazolidine ring and ring cleavage. Each ion associates with a specific stage in Penicillin G's breakdown, where the m/z 365 represents the intact parent molecule before major structural changes, the m/z 307 reflects side-chain cleavage events following β-lactam hydrolysis, the m/z 289 is associated with the formation of penicilloic acid that matches the NMR peak at 1.18 ppm, the m/z 202 indicates thiazolidine ring breakdown, that is consistent with those arrangements in the ring region detected using NMR, and finally the m/z 157 represents low-mass chlorinated oxidative fragments formed in the later stages of degradation. These key ions detected in this study, align with the chemical shifts observed in the NMR of β-lactam and methyl regions, and supports the interpretation that multiple degradation products are formed sequentially (Zhang et al., 2017a).

More importantly, the m/z 289 fragment was identified as penicilloic acid, in agreement with the peak at 1.18 ppm in the NMR spectra. Although penilloic acid was identified from the NMR data, its corresponding mass ion could not be confidently identified in the HPLC/MS spectra. This absence can be due to its low ionization efficiency, instability under electrospray conditions, or overlapping fragmentation patterns with other degradation products.

In summary, both NMR and HPLC/MS techniques in this study confirm the degradation of Penicillin G through rapid β-lactam ring cleavage and other transformations, including the loss of methyl groups, thiazolidine ring disruption, and eventual production of smaller oxidative fragments. The early appearance of penicilloic acid is a common feature detected by both methods, while the later-stage formation of penilloic acid was observed primarily through NMR. The minor differences between the techniques reflect their complementary nature, where NMR provides detailed structural insights for intact and early-stage degradation products, while HPLC/MS detects fragmentation patterns and provides precise mass-based identification of transformation products (Dr. Holzgrabe, 2010, Branch et al., 1987, Postigo and Richardson, 2014). Together, the two methods used in this study provided a clearer and complimentary picture of Penicillin G degradation pathways under oxidative conditions.

The degradation behaviour observed for Penicillin G in this study is consistent with established literature pathways for β-lactam breakdown. Several studies have shown that sodium hypochlorite solution rapidly hydrolyses the β-lactam ring of Penicillin G, producing penicilloic acid as the primary product, followed by further rearrangements to penilloic acid and other derivatives (Mitsumori et al., 1977, Degelaen et al., 1979, Zhang et al., 2017a). The NMR findings here confirmed both penicilloic and penilloic acid formation, while HPLC/MS detected key ions such as m/z 289 that align with these intermediates, along with lower-mass fragments (m/z 202, 157) suggesting thiazolidine ring breakdown and secondary oxidation. Although HPLC/MS did not allow structural confirmation of every fragment detected, the combination of NMR and HPLC/MS findings supports the conclusion that β-lactam antibiotics are highly susceptible to oxidative treatment using sodium hypochlorite solution (Gozlan et al., 2013, Zhang et al., 2017a, Simazaki D, 2008, Mitsumori et al., 1977).

3.4.2 Correlation between NMR and LC/MS findings: Amoxicillin

The degradation of Amoxicillin under sodium hypochlorite treatment was examined using NMR spectroscopy and HPLC/MS to provide complementary insights into its breakdown pathway (Gozlan et al., 2013, Gozlan et al., 2010, Branch et al., 1987). Both techniques showed that Amoxicillin was highly unstable upon exposure to sodium hypochlorite, but they revealed this instability in different ways.

The degradation patterns observed for Amoxicillin using HPLC/MS generally support the structural changes identified through NMR analysis. Both techniques indicate rapid hydrolysis of the β-lactam ring, evidenced by the loss of the characteristic β-lactam signals in the ^{1}H NMR spectra and the disappearance of the parent ion in HPLC/MS within the first hour of sodium hypochlorite exposure.

In addition, ^{1}H NMR analysis demonstrated that Amoxicillin degraded immediately after the addition of NaOCl. The disappearance of the β-lactam proton signal (5.0–5.5 ppm) and significant changes in the aromatic region indicated rapid β-lactam hydrolysis and rearrangement of the molecule. Two new indicative peaks were observed, one at 4.51 ppm, assigned to amoxicilloic acid (i.e. a derivative of penicilloic acid), and another at 3.48 ppm, assigned to amoxicillinoic acid (i.e. a derivative of penilloic acid). These findings are consistent with degradation pathways reported in the literature stating that penicilloic acid and penilloic acid identified as primary degradation products of

Amoxicillin resulting from the hydrolysis of the β-lactam ring (Gozlan et al., 2010, Gozlan et al., 2013, Lamm et al., 2009). The NMR data from this study match these reports closely, confirming penicilloic acid formation immediately after the addition of sodium hypochlorite, and penilloic acid as a later-stage degradation product.

Furthermore, HPLC/MS analysis strongly supported and complimented the NMR findings. The parent ion m/z 364 diminished rapidly within the first hour after the addition of sodium hypochlorite solution, indicating immediate structural disruption. Several major ions were then detected (i.e., m/z 383, 371 and 341), providing further insight into Amoxicillin's breakdown. The first ion m/z 383, was identified as Amoxicillin penicilloic acid, the primary product of β-lactam ring hydrolysis and its early appearance correlates directly with the NMR peak at 4.51 ppm, confirming the formation of this intermediate. The m/z 371 ion identification is associated with Amoxicillinpenilloic acid, a rearrangement product of penicilloic acid. Its delayed but clear detection confirms the later-stage NMR signal at 3.48 ppm. Finally, the m/z 341 ion, that is assigned to diketopiperazine, a well-documented degradation product of Amoxicillin that forms via intramolecular cyclisation (Lamm et al., 2009, Gozlan et al., 2010) and Its detection suggests that in addition to hydrolysis, ring-closure reactions also play a role in the molecule's degradation.

The above-mentioned HPLC/MS results provided a time-resolved profile of Amoxicillin's degradation that complements the NMR data. While NMR clearly tracked the structural rearrangements, HPLC/MS identified specific ions and confirmed the molecular masses of the key intermediates.

In addition, minor Amoxicillin by-products detected by NMR were not clearly visible in HPLC/MS, likely due to their low ionisation efficiency or instability under electrospray conditions. However, the alignment between the major NMR-detected products (penicilloic and penilloic acid) and the LC/MS ions (m/z 383 and 371) demonstrates strong agreement between the two techniques.

The proposed degradation pathways of Amoxicillin (Figures 3.28 and 3.29, NMR section) show the range of potential by-products that can form under sodium hypochlorite treatment, including β-lactam ring hydrolysis products, phenyl derivatives, and other oxidative fragments (Siciliano et al., 2021, Gozlan et al., 2013). The NMR data obtained in this study align closely with this pathway, showing clear evidence for the formation of Amoxicillin penicilloic acid and Amoxicillin penilloic acid as major intermediates.

In summary, NMR and HPLC/MS results align in confirming Amoxicillin's extreme susceptibility to oxidative degradation under sodium hypochlorite treatment. Additionally, NMR highlighted the rapid β-lactam ring cleavage and formation of Amoxicillin penicilloic acid and Amoxicillin penilloic acid, while LC/MS tracked the loss of the parent ion (m/z 364) and identified the major by-products (m/z 383, 371, and 341) that form during breakdown. Together, the two methods provide a comprehensible interpretation of Amoxicillin's degradation pathway, demonstrating that β-lactam antibiotics rapidly undergo hydrolysis and rearrangement under oxidative conditions (Postigo and Richardson, 2014, Zhang et al., 2017a, Siciliano et al., 2021).

3.4.3 Correlation between NMR and HPLC/MS findings: Ciprofloxacin

The combined use of ^{1}H and ^{19}F NMR, and HPLC/MS techniques provided complementary insights into the degradation behaviour of Ciprofloxacin under NaOCl treatment. Both techniques showed evidence of transformation, but together they confirm that Ciprofloxacin was far less reactive than the β-lactam antibiotics studied.

NMR analysis of Ciprofloxacin revealed slow but clear chemical changes. The ^{1}H NMR spectra showed diminishing aromatic signals between 7.0–8.5 ppm after the addition of sodium hypochlorite, indicating oxidative modification of the quinolone ring. The piperazine -CH_2 protons (3.0–3.6 ppm) also lost intensity, with the emergence of a new peak around 4.2 ppm, suggesting oxidative ring opening and formation of polar degradation products. On the other hand, the cyclopropyl ring remained unchanged, with no shift or intensity loss in its 0.9–1.5 ppm multiples. The ^{19}F NMR spectra showed a gradual reduction of the fluorine signal over time, suggesting that defluorination may occur slowly under the experimental conditions.

In addition, HPLC/MS analysis supported and complimented these observations while providing a clearer timeline for the breakdown process. The parent ion, m/z 332 (Ciprofloxacin $[M+H]^{+}$), persisted across all timepoints, including after 24 hours, showing only a slight decrease in intensity that highlights Ciprofloxacin's relative stability.

Furthermore, seven ions were consistently detected and selected for interpretation: m/z 332, 306, 362, 324, 298, 288, and 263. These represent the intact parent compound and a series of transformation products, where m/z 306 was detected immediately after the addition of sodium hypochlorite solution and this fragment reflects piperazine ring

cleavage, a finding strongly supported by NMR (Figure 3.29), where significant piperazine signal loss was observed.

The m/z 362 ion shows an oxidised ciprofloxacin intermediate, formed through the incorporation of two oxygen atoms ($+O_2$) and the loss of one hydrogen atom (-H). It peaked at 1 hour, then declined, behaving as a transient but significant intermediate. The m/z 324 ion that appeared later in the time series and persisted through to 24 hours. Literature (Kennedy Neth et al., 2019) connects this ion with further structural modification of the quinolone core, and its stability here suggests that it is a late-stage oxidation by-product.

The m/z 298 and m/z 288 ions that are lower-mass fragments indicate further breakdown of the piperazine side chain and the quinolone ring. Their delayed appearance, and lower intensity, point to a gradual oxidative fragmentation process (Kennedy Neth et al., 2019). The final detected ion, m/z 263, relates to the smallest major fragment observed, consistent with piperazine ring cleavage and advanced stages of oxidative breakdown (Figure 3.64) (Kennedy Neth et al., 2019).

These HPLC/MS results complement the NMR findings, showing that the piperazine ring is the primary site of attack, while the cyclopropyl ring remains unaffected, and NMR confirms that the fluorine atom is gradually removed. Significantly, in this study the cyclopropyl group remained unchanged in the ^{1}H NMR spectra, and no corresponding LC/MS fragments were identified that suggest cleavage or transformation of this ring. This confirms its chemical stability under oxidative conditions, consistent with previously reported findings in the literature (Zhou et al., 2011, Wang et al., 2017, Kennedy Neth et al., 2019). The persistent parent ion m/z 332 and the continued presence of structurally related fragments suggest that degradation is partial, producing intermediates that remain chemically similar to Ciprofloxacin even after 24 hours.

Overall, the combined NMR and HPLC/MS data provide a comprehensive picture of Ciprofloxacin degradation. The degradation pathway of Ciprofloxacin observed in this study aligns with published literature on fluoroquinolone oxidation using sodium hypochlorite solution but reflects the milder conditions applied here. Previous studies (Kennedy Neth et al., 2019, Wang et al., 2017, Zhou et al., 2011) have shown that Ciprofloxacin undergoes piperazinyl ring opening, quinolone core modifications, and chlorine substitution, producing ions such as m/z 324 (Kennedy Neth et al., 2019). The same ion was detected in this study, supporting the idea that similar pathways are

occurring. The NMR analysis also confirmed that defluorination occurred over time, evidenced by the gradual loss of the fluorine signal, whereas HPLC/MS did not capture fragment ions that could confirm this process. The persistence of the parent ion (m/z 332) and structurally similar intermediates suggests that degradation was only partial under the

Table 3.8. Summary of correlations between NMR and HPLC/MS findings for Penicillin G, Amoxicillin and Ciprofloxacin following the addition of sodium hypochlorite solution. The table highlights the parent ions, key HPLC/MS-detected fragments, NMR observations, and overall interpretations for each antibiotic

Antibiotic	**Parent Ion (HPLC/MS)**	**Key HPLC/MS Ions Detected**	**Key NMR Observations**	**Overall Interpretation**
Penicillin G	m/z 365	m/z 307, 289, 202, 157	Rapid disappearance of β-lactam proton signal; new peaks at 1.18 ppm (penicilloic acid) and 0.98 ppm (penilloic acid); thiazolidine ring changes	Immediate β-lactam ring hydrolysis followed by side-chain cleavage and thiazolidine ring breakdown, producing stable low-mass oxidative fragments
Amoxicillin	m/z 364	m/z 383, 371, 341	Immediate loss of β-lactam signal; peaks at 4.51 ppm (penicilloic acid) and 3.48 ppm (penilloic acid) detected	Highly unstable, rapid β-lactam hydrolysis with formation of penicilloic/penilloic acids and diketopiperazine, near complete breakdown after sodium hypochlorite addition
Ciprofloxacin	m/z 332	m/z 306, 362, 324, 298, 288, 263	Gradual loss of piperazine ring (3.0–3.6 ppm); new peak ~4.2 ppm (oxidation); slow defluorination in ^{19}F NMR; cyclopropyl ring unchanged	Partial degradation; piperazine ring is main site of attack, parent compound persists after 24 h, showing Ciprofloxacin is more resistant than β-lactams

conditions tested. Taken together, the combined NMR and HPLC/MS findings confirm that while Ciprofloxacin is susceptible to sodium hypochlorite oxidation, mainly at the piperazine ring with associated defluorination; however, it remains significantly more resistant to full structural breakdown than the β-lactam antibiotics studied.

3.5 Summary

As summarised in Table 3.8., the combined use of ^{1}H and ^{19}F NMR spectroscopy and HPLC/MS provided a comprehensive, complementary perspective on the oxidative degradation of Penicillin G, Amoxicillin, and Ciprofloxacin under sodium hypochlorite treatment. By correlating structural information from NMR with compositional data from LC/MS, this study was able to track both how these molecules change at the functional group level and what molecular fragments emerge during the process.

For the β-lactam antibiotics, Penicillin G and Amoxicillin, both NMR and LC/MS confirmed their high susceptibility to sodium hypochlorite oxidation. NMR revealed almost immediate β-lactam ring opening, side-chain rearrangements, and the formation of penicilloic and penilloic acid derivatives. The HPLC/MS data approved these observations, showing the rapid disappearance of the parent ions (m/z 365 for Penicillin G and m/z 364 for Amoxicillin) and the emergence of key degradation fragments. For Penicillin G, ions such as m/z 307 and 289 reflected β-lactam hydrolysis and thiazolidine ring breakdown. For Amoxicillin, LC/MS confirmed m/z 383 (penicilloic acid), m/z 371 (penilloic acid) and m/z 341 (diketopiperazine), supporting the NMR findings while adding time-resolved evidence for these transformations. Together, these results show that the β-lactam core is highly vulnerable to oxidative stress, with sodium hypochlorite causing almost complete breakdown into smaller, often more polar fragments within just a few hours (Hou and Poole, 1971, Deshpande et al., 2004a).

In contrast, Ciprofloxacin showed noticeable different behaviour. Furthermore, NMR showed gradual changes in the quinolone ring and significant attack on the piperazine ring, while the cyclopropyl ring remained intact. The ^{19}F NMR spectra confirmed defluorination, with the fluorine signal gradually diminishing and ultimately disappearing over the 24-hour period. In addition, the HPLC/MS findings supported these observations, but also highlighted Ciprofloxacin's relative stability where the parent ion m/z 332 persisted throughout the experiment with only slight loss of intensity. Seven key ions were tracked, m/z 306, 362, 324, 298, 288, and 263, which together represent partial

oxidation and fragmentation, particularly at the piperazine ring. However, the absence of deeper fragmentation signals and the continued presence of the parent ion confirm that Ciprofloxacin is far more resistant to sodium hypochlorite degradation than theβ-lactams (Zhou et al., 2011, Wang et al., 2017, Kennedy Neth et al., 2019).

Overall, these correlations highlight both the power and necessity of combining NMR and HPLC/MS. Here, the NMR provided real-time insight into functional group changes, intermediate formation and bond cleavage, while LC/MS tracked the molecular fragments and end products, even those too small or too transient for NMR detection. The two methods reinforced each other's findings, where NMR verified the structural changes suggested by HPLC/MS fragment ions, while HPLC/MS provided additional confirmation of NMR-identified products such as penicilloic acid and penilloic acid.

From a laboratory perspective, these findings provide useful insight into the relative oxidative reactivity of different antibiotic classes toward sodium hypochlorite. The β-lactam antibiotics degraded rapidly under sodium hypochlorite treatment, suggesting that common disinfection processes could effectively break down this class of antibiotics in water systems (Postigo and Richardson, 2014, Deshpande et al., 2004a). However, it is acknowledged that such behaviour may differ significantly in real or simulated wastewater effluents, where high chlorine demand and the presence of competing organic and inorganic elements would likely influence transformation efficiency.

Nevertheless, Ciprofloxacin's persistence, even after 24 hours, indicates that fluoroquinolones may remain intact or transform into stable intermediates under similar treatment conditions, consistent with reports that prolonged exposures are required for complete breakdown (Kennedy Neth et al., 2019, Zhou et al., 2011). This partial degradation means that some structurally related transformation products could persist in treated water, raising questions about their potential environmental impacts (Kennedy Neth et al., 2019).

In conclusion, integrating the NMR and HPLC/MS data offered a detailed and comprehensive understanding of the antibiotic degradation pathways. For β-lactams, both methods confirmed rapid breakdown and identified shared transformation products. For Ciprofloxacin, the combined data revealed slower, incomplete degradation, with partial modification of the piperazine ring, retention of the cyclopropyl ring, and evidence from NMR that defluorination occurred over time. These findings highlight how using both techniques together can resolve complex degradation patterns, offering valuable insights for analytical chemistry as well as for developing effective water treatment strategies.

CHAPTER 4: MAIN CONCLUSIONS AND SUGGESTIONS FOR FUTURE WORK

In this chapter, some preliminary conclusions (i.e. the summary of the research programme) is provided. This is followed by a section on some suggestions for further work.

4.1 Main Conclusions

This thesis investigated the oxidative degradation behaviour of three representative antibiotics, Penicillin G, Amoxicillin, and Ciprofloxacin, using a combined analytical approach of high-field NMR spectroscopy and HPLC/MS technique.

In the early stages of the study, UV irradiation experiments were conducted on both solid and solution forms of the antibiotics in order to assess potential photochemical effects under the irradiation conditions available. However, no measurable structural changes were observed under the conditions tested, as revealed by NMR analyses. This outcome is attributed to the relatively low irradiance and wavelength ranges employed, which limited effective photon absorption by the antibiotics and therefore did not favour photochemical transformation. This finding led the focus of the research to shift toward oxidation using sodium hypochlorite (NaOCl) solution, which produced clear, quantifiable transformations, through both the techniques.

The NMR spectroscopic analyses provided real-time structural information, revealing key molecular events such as β-lactam ring opening in Penicillin G and Amoxicillin, piperazine ring oxidation in Ciprofloxacin, and the appearance of intermediates like penicilloic and penilloic acids. Furthermore, HPLC/MS analyses complemented these findings, in several relevant places, by tracking the loss of parent ions and the emergence of identifiable degradation products over time.

The combined evidence confirmed that β-lactam antibiotics (Penicillin G and Amoxicillin) degrade rapidly and extensively under NaOCl treatment, with almost complete breakdown into smaller, more polar fragments within hours. In contrast, Ciprofloxacin displayed slower, partial degradation: the piperazine ring was attacked, forming transient intermediates and later-stage by-products, but the cyclopropyl ring remained intact and the parent ion persisted even after 24 hours.

By correlating NMR and HPLC/MS data, this work provides one of the most comprehensive analyses to date of antibiotic transformation of the selected compounds under sodium hypochlorite treatment, showing that β-lactams are highly susceptible, while fluoroquinolones are significantly more resistant. These findings have clear implications for water treatment practices, as while sodium hypochlorite effectively degrades certain antibiotic classes, better

or combined approaches may be required to address persistent compounds like Ciprofloxacin.

4.2 Suggestions for Future Work

If further time and resources were available, several avenues could expand and deepen this research:

- UV Irradiation: re-evaluation

  While initial UV experiments under the tested conditions produced no measurable structural changes, further work using longer exposure times, different wavelengths, or combined UV–oxidant treatments could clarify whether UV plays a role in antibiotic breakdown. Careful control and reporting of wavelength, irradiance, and dose would be critical to ensure meaningful comparison with operational water treatment systems.

- Structural confirmation of minor by-products

  Use high-resolution MS/MS and isotopic labelling to confirm the identities of low-abundance fragments (say, for example, penilloic acid in HPLC/MS).

- Comparative oxidation studies

  Examine other oxidants (UV/H_2O_2, ozone, etc.) alongside sodium hypochlorite solution to evaluate their efficiencies and formation of by-product profiles.

- Extended antibiotic scope

  Include additional antibiotic classes with known antimicrobial resistance properties (such as, sulfonamides, macrolides, etc) to compare degradation behaviour across structures.

- Toxicological assessment

  Investigate whether intermediates (particularly from Ciprofloxacin) retain antibacterial activity, or present ecotoxicological risks.

- Real-world testing

  Simulate municipal wastewater treatment conditions (temperature, variable pH and chlorine residuals) to identify the environmental implications.

REFERENCES

ACOSTA, R. *Nuclear Magnetic Resonance Spectroscopy. [electronic resource]*, MDPI AG. Available at: https://www.mdpi.com/

ALDEEK, F., CANZANI, D., STANDLAND, M., CROSSWHITE, M. R., HAMMACK, W., GERARD, G. & COOK, J.-M. 2016. Identification of Penicillin G Metabolites under Various Environmental Conditions Using UHPLC-MS/MS. *Journal of Agricultural and Food Chemistry,* 64**,** 6100-6107.

ALDEEK, F., ROSANA, M. R., HAMILTON, Z. K., CROSSWHITE, M. R., BURROWS, C. W., SINGH, S., GERARD, G., HAMMACK, W. & COOK, J. M. 2015. LC-MS/MS Method for the Determination and Quantitation of Penicillin G and Its Metabolites in Citrus Fruits Affected by Huanglongbing. *J Agric Food Chem,* 63**,** 5993-6000.

ALI, M. A. & MAAFA, I. M. 2024. Photodegradation of Amoxicillin in Aqueous Systems: A Review. *International Journal of Molecular Sciences,* 25**,** 9575.

ALLEN, H. K., DONATO, J., WANG, H. H., CLOUD-HANSEN, K. A., DAVIES, J. & HANDELSMAN, J. 2010. Call of the wild: antibiotic resistance genes in natural environments. *Nature reviews. Microbiology,* 8**,** 251-259.

ALPERT, P. T. 2017. Superbugs: Antibiotic Resistance Is Becoming a Major Public Health Concern. *Home Health Care Management and Practice,* 29**,** 130-133.

ARIZA, A., MAYORGA, C., FERNANDEZ, T., BARBERO, N., MARTÍN-SERRANO, A., PÉREZ-SALA, D., SÁNCHEZ-GÓMEZ, F., BLANCA, M., TORRES, M. & MONTANEZ, M. 2015. Hypersensitivity reactions to β-lactams: relevance of hapten-protein conjugates.

ASHOK, A. & KHEDIKAR, I. 2016. *Overview of Water Disinfection by UV Technology -A Review*.

BATCHELOR, F. R., DEWDNEY, J. M. & GAZZARD, D. 1965. Penicillin Allergy: The Formation of the Penicilloyl Determinant. *Nature,* 206**,** 362-364.

BEN SALEM, I., MEZNI, M., BOULILA, A., HAMDI, M. & SAIDI, M. 2016. Removal of Penicillin G and Erythromycin with Ionizing Radiation Followed by Biological Treatment. *Current Microbiology,* 73.

BERENDONK, T. U., MANAIA, C. M., MERLIN, C., FATTA-KASSINOS, D., CYTRYN, E., WALSH, F., BÜRGMANN, H., SØRUM, H., NORSTRÖM, M., PONS, M.-N., KREUZINGER, N., HUOVINEN, P., STEFANI, S., SCHWARTZ, T., KISAND, V., BAQUERO, F. & MARTINEZ, J. L. 2015. Tackling antibiotic resistance: the environmental framework. *Nature reviews. Microbiology,* 13**,** 310-317.

BISHT, B., AHMAD, W., NANDA, M., HUSSAIN, A., JAISWAL, K. K., VLASKIN, M. S., VERMA, M., DE FARIAS NEVES, F. & KUMAR, V. 2024. Algal remediation of toxic chlorinated derivatives of amoxicillin and ampicillin via direct and indirect photodegradation in water treatment. *Journal of Water Process Engineering,* 68**,** 106422.

BISSON-BOUTELLIEZ, C., FONTANAY, S., FINANCE, C. & KEDZIEREWICZ, F. 2010. Preparation and physicochemical characterization of amoxicillin beta-cyclodextrin complexes. *AAPS PharmSciTech,* 11**,** 574-81.

BOUND, J. P. & VOULVOULIS, N. 2004. Pharmaceuticals in the aquatic environment—a comparison of risk assessment strategies. *Chemosphere,* 56**,** 1143-1155.

BRANCH, S. K., CASY, A. F. & OMINDE, E. M. A. 1987. Application of 1H nuclear magnetic resonance spectroscopy to the analysis of β-lactam antibiotics and their common degradation products. *Journal of Pharmaceutical and Biomedical Analysis,* 5**,** 73-103.

CANZANI, D. & ALDEEK, F. 2017. Penicillin G's function, metabolites, allergy, and resistance. 1**,** 28-40.

CHANG, C.-J. & HEM, S. L. 1979. Carbon-13 Magnetic Resonance Spectroscopy of Drugs III: Penicillins. *Journal of Pharmaceutical Sciences,* 68**,** 64-69.

CHEN, D., CHENG, Y., ZHOU, N., CHEN, P., WANG, Y., LI, K., HUO, S., CHENG, P., PENG, P., ZHANG, R., WANG, L., LIU, H., LIU, Y. & RUAN, R. 2020a. Photocatalytic degradation of organic pollutants using TiO2-based photocatalysts: A review. *Journal of Cleaner Production,* 268.

CHEN, D., CHENG, Y., ZHOU, N., CHEN, P., WANG, Y., LI, K., HUO, S., CHENG, P., PENG, P., ZHANG, R., WANG, L., LIU, H., LIU, Y. & RUAN, R. 2020b. Photocatalytic degradation of organic pollutants using TiO2-based photocatalysts: A review. *Journal of Cleaner Production,* 268**,** 121725.

CHEN, Y.-D., DUAN, X., ZHOU, X., WANG, R., WANG, S., REN, N.-Q. & HO, S.-H. 2021. Advanced oxidation processes for water disinfection: Features, mechanisms and prospects. *Chemical Engineering Journal,* 409**,** 128207.

CHENG, X., WANG, S., HUANG, W., WANG, F., FANG, S., GE, R., ZHANG, Q., ZHANG, L., DU, W., FANG, F., FENG, Q., CAO, J. & LUO, J. 2022. Current status of hypochlorite technology on the wastewater treatment and sludge disposal: Performance, principals and prospects. *Science of The Total Environment,* 803**,** 150085.

CHENG, Y., CHEN, Y., LU, J., NIE, J. & LIU, Y. 2018. Fenton treatment of bio-treated fermentation-based pharmaceutical wastewater: removal and conversion of organic pollutants as well as estimation of operational costs. *Environmental Science and Pollution Research,* 25**,** 12083-12095.

CHOUDHURY, H., GORAIN, B., PAUL, A., SARKAR, P., DAN, S., CHAKRABORTY, P. & PAL, T. K. 2017. Development and Validation of an LC-MS/MS-ESI Method for Comparative Pharmacokinetic Study of Ciprofloxacin in Healthy Male Subjects. *Drug Res (Stuttg),* 67**,** 94-102.

CHOWDHURY, P. & VIRARAGHAVAN, T. 2009. Sonochemical degradation of chlorinated organic compounds, phenolic compounds and organic dyes : A review. *Science of the total environment.* Kidlington: Elsevier.

CONNOR, S. C., EVERETT, J. R., JENNINGS, K. R., NICHOLSON, J. K. & WOODNUTT, G. 1994a. High resolution 1H NMR spectroscopic studies of the metabolism and excretion of ampicillin in rats and amoxycillin in rats and man. *J Pharm Pharmacol,* 46**,** 128-34.

CONNOR, S. C., EVERETT, J. R., JENNINGS, K. R., NICHOLSON, J. K. & WOODNUTT, G. 1994b. High Resolution 1H NMR Spectroscopic Studies of the Metabolism and Excretion of Ampicillin in Rats and Amoxycillin in Rats and Man. *Journal of Pharmacy and Pharmacology,* 46**,** 128-134.

CUTLER, T. D. & ZIMMERMAN, J. J. 2011. Ultraviolet irradiation and the mechanisms underlying its inactivation of infectious agents. *Animal health research reviews,* 12**,** 15-23.

DA CRUZ NIZER, W. S., INKOVSKIY, V. & OVERHAGE, J. 2020. Surviving Reactive Chlorine Stress: Responses of Gram-Negative Bacteria to Hypochlorous Acid. *Microorganisms,* 8.

DALETOS, G., ANCHEEVA, E., ORFALI, R. S., WRAY, V. & PROKSCH, P. 2017. Structure Elucidation of Antibiotics by NMR Spectroscopy. *In:* SASS, P. (ed.) *Antibiotics: Methods and Protocols.* New York, NY: Springer New York.

DEGELAEN, J. P., LOUKAS, S. L., FEENEY, J., ROBERTS, G. C. K. & BURGEN, A. S. V. 1979. A nuclear magnetic resonance study of the degradation of penicillin G in acidic solution. *Journal of the Chemical Society, Perkin Transactions 2***,** 86-90.

DENG, J., WU, G., YUAN, S., ZHAN, X., WANG, W. & HU, Z.-H. 2019. Ciprofloxacin degradation in UV/chlorine advanced oxidation process: Influencing factors, mechanisms and degradation pathways. *Journal of Photochemistry and Photobiology A: Chemistry,* 371**,** 151-158.

DESHPANDE, A., BAHETI, K. & CHATTERJEE, N. 2004a. Degradation of β-lactam antibiotics. *Current Science,* 87.

DESHPANDE, A. D., BAHETI, K. G. & CHATTERJEE, N. R. 2004b. Degradation of β-lactam antibiotics. *Current Science,* 87**,** 1684-1695.

DEXTER, D. D. & VAN DER VEEN, J. M. 1978. Conformations of penicillin G: crystal structure of procaine penicillin G monohydrate and a refinement of the structure of potassium penicillin G. *Journal of the Chemical Society, Perkin Transactions 1***,** 185-190.

DODD, M. C., KOHLER, H.-P. E. & VON GUNTEN, U. R. S. 2009. Oxidation of Antibacterial Compounds by Ozone and Hydroxyl Radical: Elimination of Biological Activity during Aqueous Ozonation Processes. *Environmental Science & Technology,* 43**,** 2498-2504.

DODD, M. C., SHAH, A. D., VON GUNTEN, U. & HUANG, C.-H. 2005. Interactions of Fluoroquinolone Antibacterial Agents with Aqueous Chlorine: Reaction Kinetics, Mechanisms, and Transformation Pathways. *Environmental Science & Technology,* 39**,** 7065-7076.

DR. HOLZGRABE, U. 2010. Quantitative NMR Spectroscopy in Pharmaceutical R&D. *Progress in nuclear magnetic resonance spectroscopy,* 57**,** 229-40.

EL NAJJAR, N. H., DEBORDE, M., JOURNEL, R. & VEL LEITNER, N. K. 2013. Aqueous chlorination of levofloxacin: Kinetic and mechanistic study, transformation product identification and toxicity. *Water Research,* 47**,** 121-129.

ELDER, D. P., KUENTZ, M. & HOLM, R. 2016. Antibiotic Resistance: The Need For a Global Strategy. *Journal of Pharmaceutical Sciences,* 105**,** 2278-2287.

ETAFA TASISA, Y., KUMAR SARMA, T., KRISHNARAJ, R. & SARMA, S. 2024. Band gap engineering of titanium dioxide (TiO2) nanoparticles prepared via green route and its visible light driven for environmental remediation. *Results in Chemistry,* 11**,** 101850.

EZEUKO, A. S., OJEMAYE, M. O., OKOH, O. O. & OKOH, A. I. 2021. Technological advancement for eliminating antibiotic resistance genes from wastewater: A review of their mechanisms and progress. *Journal of Environmental Chemical Engineering,* 9**,** 106183.

FAN, Z., WANG, S. & HOU, G. 2010. Chlorination Disinfection By-Products and Its Control in Drinking Water.

FERREIRA, L. C., CASTRO-ALFÉREZ, M., NAHIM-GRANADOS, S., POLO-LÓPEZ, M. I., LUCAS, M. S., LI PUMA, G. & FERNÁNDEZ-IBÁÑEZ, P. 2020. Inactivation of water pathogens with solar photo-activated persulfate oxidation. *Chemical Engineering Journal,* 381.

GAMARRA-GÜERE, C. D., DIONISIO, D., SANTOS, G. O. S., VASCONCELOS LANZA, M. R. & DE JESUS MOTHEO, A. 2022. Application of Fenton, photo-Fenton and electro-Fenton processes for the methylparaben degradation: A comparative study. *Journal of Environmental Chemical Engineering,* 10**,** 106992.

GARCIA-MUNOZ, P., VALENZUELA, L., WEGSTEIN, D., SCHANZ, T., LOPEZ, G. E., RUPPERT, A. M., REMITA, H., BLOH, J. Z. & KELLER, N. 2023. Photocatalytic Synthesis of Hydrogen Peroxide from Molecular Oxygen and Water. *Topics in Current Chemistry,* 381**,** 15.

GOMES, J., COSTA, R., QUINTA-FERREIRA, R. M. & MARTINS, R. C. 2017. Application of ozonation for pharmaceuticals and personal care products removal from water. *Science of the Total Environment,* 586**,** 265-283.

GOU, Y., CHEN, P., YANG, L., LI, S., PENG, L., SONG, S. & XU, Y. 2021. Degradation of fluoroquinolones in homogeneous and heterogeneous photo-Fenton processes: A review. *Chemosphere,* 270**,** 129481.

GOZLAN, I., ROTSTEIN, A. & AVISAR, D. 2010. Investigation of an amoxicillin oxidative degradation product formed under controlled environmental conditions. *Environmental Chemistry,* 7**,** 435-442.

GOZLAN, I., ROTSTEIN, A. & AVISAR, D. 2013. Amoxicillin-degradation products formed under controlled environmental conditions: Identification and determination in the aquatic environment. *Chemosphere,* 91**,** 985-992.

HAN, J., LI, W., YANG, Y., ZHANG, X., BAO, S., ZHANG, X., ZHANG, T. & LEUNG, K. M. Y. 2024. UV-Based Advanced Oxidation Processes for Antibiotic Resistance Control: Efficiency, Influencing Factors, and Energy Consumption. *Engineering,* 37**,** 27-39.

HERRAIZ-CARBONÉ, M., COTILLAS, S., LACASA, E., SAINZ DE BARANDA, C., RIQUELME, E., CAÑIZARES, P., RODRIGO, M. A. & SÁEZ, C. 2021. A review on disinfection technologies for controlling the antibiotic resistance spread. *Science of The Total Environment,* 797**,** 149150.

HIJNEN, W., BEERENDONK, E. & MEDEMA, G. J. 2006a. Inactivation credit of UV radiation for viruses, bacteria and protozoan (oo) cysts in water: a review. *Water research,* 40**,** 3-22.

HIJNEN, W. A. M., BEERENDONK, E. F. & MEDEMA, G. J. 2006b. Inactivation credit of UV radiation for viruses, bacteria and protozoan (oo)cysts in water: A review. *Water Research,* 40**,** 3-22.

HILLER, C. X., HÜBNER, U., FAJNOROVA, S., SCHWARTZ, T. & DREWES, J. E. 2019. Antibiotic microbial resistance (AMR) removal efficiencies by conventional and advanced wastewater treatment processes: A review. *Science of The Total Environment,* 685**,** 596-608.

HO, H. P., LEE, R. J., CHEN, C. Y., WANG, S. R., LI, Z. G. & LEE, M. R. 2011. Identification of new minor metabolites of penicillin G in human serum by multiple-stage tandem mass spectrometry. *Rapid Commun Mass Spectrom,* 25**,** 25-32.

HODGES, B. C., CATES, E. L. & KIM, J.-H. 2018. Challenges and prospects of advanced oxidation water treatment processes using catalytic nanomaterials. *Nature Nanotechnology,* 13**,** 642-650.

HOLZGRABE, U. 2015. Quantitative NMR Spectroscopy in Pharmaceutical R&D. *eMagRes.*

HOMEM, V. & SANTOS, L. 2011. Degradation and removal methods of antibiotics from aqueous matrices – A review. *Journal of Environmental Management,* 92**,** 2304-2347.

HOU, J. P. & POOLE, J. W. 1971. β-Lactam Antibiotics: Their Physicochemical Properties and Biological Activities in Relation to Structure. *Journal of Pharmaceutical Sciences,* 60**,** 503-532.

HUBER, M. M., GÖBEL, A., JOSS, A., MCARDELL, C. S., SIEGRIST, H., VON GUNTEN, U., HERMANN, N., LÖFFLER, D., TERNES, T. A. & RIED, A. 2005. Oxidation of pharmaceuticals during ozonation of municipal wastewater effluents: A pilot study. *Environmental Science and Technology,* 39**,** 4290-4299.

ISSAKA, E., AMU-DARKO, J. N.-O., YAKUBU, S., FAPOHUNDA, F. O., ALI, N. & BILAL, M. 2022. Advanced catalytic ozonation for degradation of pharmaceutical pollutants—A review. *Chemosphere,* 289**,** 133208.

JIA, Z., LV, R., GUO, L., ZHANG, J., LI, R., LIU, J. & FAN, C. 2021. Rapid degradation of ciprofloxacin over BiOCl: Insight into the molecular structure transformation and antibacterial activity elimination. *Separation and Purification Technology,* 257**,** 117872.

JONES, K. E., PATEL, N. G., LEVY, M. A., STOREYGARD, A., BALK, D., GITTLEMAN, J. L. & DASZAK, P. 2008. Global trends in emerging infectious diseases. *Nature,* 451**,** 990-993.

JOSEPH, C. G., LI PUMA, G., BONO, A. & KRISHNAIAH, D. 2009. Sonophotocatalysis in advanced oxidation process: A short review. *Ultrasonics sonochemistry.* Kidlington: Elsevier.

JUÁREZ, R. 2021. *Ozonation in Advanced Wastewater Treatment : Practical Aspects and Development of a Prediction Tool for Pharmaceutical Removal.* Lund University.

JUNG, Y. J., KIM, W. G., YOON, Y., KANG, J.-W., HONG, Y. M. & KIM, H. W. 2012. Removal of amoxicillin by UV and UV/H2O2 processes. *Science of the Total Environment,* 420**,** 160-167.

KAMALI, M., AMINABHAVI, T. M., V. COSTA, M. E., UL ISLAM, S., APPELS, L. & DEWIL, R. 2023. Heterogeneous Advanced Oxidation Processes (HE-AOPs) for the Removal of Pharmaceutically Active Compounds—Pros and Cons. *In:* KAMALI, M., AMINABHAVI, T. M., V. COSTA, M. E., UL ISLAM, S., APPELS, L. & DEWIL, R. (eds.) *Advanced Wastewater Treatment Technologies for the Removal of Pharmaceutically Active Compounds.* Cham: Springer International Publishing.

KAN, L. S., SCHWEIGHARDT, F. K., KAO, S. & LI, N. C. 1973. NMR study of interaction between several penicillins and nucleosides. *Journal of Magnetic Resonance (1969),* 9**,** 239-246.

KEEN, O. S. & LINDEN, K. G. 2013. Degradation of antibiotic activity during UV/H2O2 advanced oxidation and photolysis in wastewater effluent. *Environmental Science and Technology,* 47**,** 13020-13030.

KENNEDY NETH, N. L., CARLIN, C. M. & KEEN, O. S. 2019. Emerging investigator series: transformation of common antibiotics during water disinfection with chlorine and formation of antibacterially active products. *Environmental Science: Water Research & Technology,* 5**,** 1222-1233.

KENNEDY NETH, N. L., KEEN, O. S. & CARLIN, C. M. 2017. Doxycycline transformation and emergence of antibacterially active products during water disinfection with chlorine. *Environmental Science: Water Research and Technology,* 3**,** 1086-1094.

KHEIROLOMOOM, A., KAZEMI-VAYSARI, A., ARDJMAND, M. & BARADAR-KHOSHFETRAT, A. 1999. The combined effects of pH and temperature on penicillin G decomposition and its stability modeling. *Process Biochemistry,* 35**,** 205-211.

KIM, H.-J., YOON, H.-W., LEE, M.-A., KIM, Y.-H. & LEE, C. J. 2022. Impact of UV-C Irradiation on Bacterial Disinfection in a Drinking Water Purification System. *Journal of microbiology and biotechnology,* 33**,** 1-8.

KIM, T.-K., KIM, T., PARK, H., LEE, I., JO, A., CHOI, K. & ZOH, K.-D. 2020. Degradation of ciprofloxacin and inactivation of ciprofloxacin resistant E. faecium during UV-LED (275 nm)/chlorine process. *Chemical Engineering Journal,* 394**,** 124803.

KRASNER, S. W., WEINBERG, H. S., RICHARDSON, S. D., PASTOR, S. J., CHINN, R., SCLIMENTI, M. J., ONSTAD, G. D. & THRUSTON JR, A. D. 2006. Occurrence of a New Generation of Disinfection Byproducts. *Environmental Science & Technology,* 40**,** 7175-7185.

LAMM, A., GOZLAN, I., ROTSTEIN, A. & AVISAR, D. 2009. Detection of amoxicillin-diketopiperazine-2', 5' in wastewater samples. *Journal of environmental science and health. Part A, Toxic/hazardous substances & environmental engineering,* 44**,** 1512-7.

LE PAGE, G., GUNNARSSON, L., SNAPE, J. & TYLER, C. R. 2017. Integrating human and environmental health in antibiotic risk assessment: A critical analysis of protection goals, species sensitivity and antimicrobial resistance. *Environment International,* 109**,** 155-169.

LEVY, S. B. & MARSHALL, B. 2004. Antibacterial resistance worldwide: causes, challenges and responses. *Nature Medicine,* 10**,** S122.

LI, D., YANG, M., HU, J., ZHANG, Y., CHANG, H. & JIN, F. 2008a. Determination of penicillin G and its degradation products in a penicillin production wastewater treatment plant and the receiving river. *Water research,* 42 1-2**,** 307-17.

LI, D., YANG, M., HU, J., ZHANG, Y., CHANG, H. & JIN, F. 2008b. Determination of penicillin G and its degradation products in a penicillin production wastewater treatment plant and the receiving river. *Water Research,* 42**,** 307-317.

LI, M., WEI, D. & DU, Y. 2016. Genotoxicity of quinolone antibiotics in chlorination disinfection treatment: formation and QSAR simulation. *Environmental Science and Pollution Research,* 23**,** 20637.

LIMA, L. M., SILVA, B. N. M. D., BARBOSA, G. & BARREIRO, E. J. 2020. β-lactam antibiotics: An overview from a medicinal chemistry perspective. *European Journal of Medicinal Chemistry,* 208**,** 112829.

LINSEBIGLER, A. L., LU, G. & YATES, J. T., JR. 1995. Photocatalysis on TiO2 Surfaces: Principles, Mechanisms, and Selected Results. *Chemical Reviews,* 95**,** 735-758.

LIU, S.-S., QU, H.-M., YANG, D., HU, H., LIU, W.-L., QIU, Z.-G., HOU, A.-M., GUO, J., LI, J.-W., SHEN, Z.-Q. & JIN, M. 2018. Chlorine disinfection increases both intracellular and extracellular antibiotic resistance genes in a full-scale wastewater treatment plant. *Water Research,* 136**,** 131-136.

LUONGO, G., PREVITERA, L., LADHARI, A., DI FABIO, G. & ZARRELLI, A. 2020. Peracetic Acid vs. Sodium Hypochlorite: Degradation and Transformation of Drugs in Wastewater. *Molecules* [Online], 25.

MANAIA, C. M., ROCHA, J., SCACCIA, N., MARANO, R., RADU, E., BIANCULLO, F., CERQUEIRA, F., FORTUNATO, G., IAKOVIDES, I. C., ZAMMIT, I., KAMPOURIS, I., VAZ-MOREIRA, I. & NUNES, O. C. 2018. Antibiotic resistance in wastewater treatment plants: Tackling the black box. *Environment International,* 115**,** 312-324.

MAO, S. 2007. Titanium Dioxide Nanomaterials: Synthesis, Properties,Modifications, and Applications. *Chemical Reviews; 107; Other Information: Journal Publication Date: 2007.*

MATTA, M. K., CHOCKALINGAM, A., GANDHI, A., STEWART, S., XU, L., SHEA, K., PATEL, V. & ROUSE, R. 2018. LC-MS/MS based quantitation of ciprofloxacin and its application to antimicrobial resistance study in Balb/c mouse plasma, urine, bladder and kidneys. *Analytical Methods,* 10**,** 1237-1246.

MICHAEL, I., RIZZO, L., MCARDELL, C. S., MANAIA, C. M., MERLIN, C., SCHWARTZ, T., DAGOT, C. & FATTA-KASSINOS, D. 2013. Urban wastewater treatment plants as hotspots for the release of antibiotics in the environment: A review. *Water Research,* 47**,** 957-995.

MISHRA N. S, R. R., KUILA A, RANI A, MUKHERJEE P, NAWAZ A, PICHIAH S 2017. A Review on Advanced Oxidation Processes for Effective Water Treatment. *Curr World Environ,* 12(3).

MITSUMORI, F., ARATA, Y., FUJIWARA, S., MURANAKA, M. & HORIUCHI, Y. 1977. NMR Study of Spontaneous Degradation of Penicillin G in Aqueous Solution. *Bulletin of the Chemical Society of Japan,* 50**,** 3164-3166.

MITSUMORI, F., ARATA, Y., FUJIWARA, S., MURANAKA, M. & HORIUCHI, Y. 2006. NMR Study of Spontaneous Degradation of Penicillin G in Aqueous Solution. *Bulletin of the Chemical Society of Japan,* 50**,** 3164-3166.

NAHIM-GRANADOS, S., RIVAS-IBÁÑEZ, G., ANTONIO SÁNCHEZ PÉREZ, J., OLLER, I., MALATO, S. & POLO-LÓPEZ, M. I. 2020. Synthetic fresh-cut wastewater disinfection and decontamination by ozonation at pilot scale. *Water Research,* 170**,** 115304.

NEYENS, E. & BAEYENS, J. 2003. A review of classic Fenton's peroxidation as an advanced oxidation technique. *Journal of Hazardous Materials,* 98**,** 33-50.

O'NEIL, J. 2015. Review on antimicrobial resistance. Tackling a Crises for the Health and Wealth of Nations.

OU, H.-S., YE, J.-S., MA, S., WEI, C.-H., GAO, N.-Y. & HE, J.-Z. 2016. Degradation of ciprofloxacin by UV and UV/H2O2 via multiple-wavelength ultraviolet light-emitting diodes: Effectiveness, intermediates and antibacterial activity. *Chemical Engineering Journal,* 289**,** 391-401.

PADFIELD, J. M. & KELLAWAY, I. W. 1974. Effect of Solvents on NMR Spectra of Penicillins. *Journal of Pharmaceutical Sciences,* 63**,** 143-144.

PÉREZ-PARADA, A., AGÜERA, A., GÓMEZ-RAMOS, M. D. M., GARCÍA-REYES, J. F., HEINZEN, H. & FERNÁNDEZ-ALBA, A. R. 2011. Behavior of amoxicillin in wastewater and river water: identification of its main transformation products by liquid chromatography/electrospray quadrupole time-of-flight mass spectrometry. *Rapid Communications in Mass Spectrometry,* 25**,** 731-742.

PETROVIC, M., HERNANDO, M., DÍAZ-CRUZ, S. & BARCELO, D. 2005. Liquid Chromatography–Tandem Mass Spectrometry for the Analysis of Pharmaceutical Residues in Environmental Samples: A Review. *Journal of chromatography. A,* 1067**,** 1-14.

PICHEL, N., VIVAR, M. & FUENTES, M. 2019. The problem of drinking water access: a review of disinfection technologies with an emphasis on solar treatment methods. *Chemosphere,* 218**,** 1014-1030.

PIGNATELLO, J. J., OLIVEROS, E. & MACKAY, A. 2006. Advanced Oxidation Processes for Organic Contaminant Destruction Based on the Fenton Reaction and Related Chemistry. *Critical Reviews in Environmental Science and Technology,* 36**,** 1-84.

POSTIGO, C. & RICHARDSON, S. D. 2014. Transformation of pharmaceuticals during oxidation/disinfection processes in drinking water treatment. *Journal of Hazardous Materials,* 279**,** 461-475.

PRADA-VÁSQUEZ, M. A., ESTRADA-FLÓREZ, S. E., SERNA-GALVIS, E. A. & TORRES-PALMA, R. A. 2021. Developments in the intensification of photo-Fenton and ozonation-based processes for the removal of contaminants of emerging concern in Ibero-American countries. *Science of The Total Environment,* 765**,** 142699.

PRADO, J. & ESPLUGAS, S. 1999. Comparison of different advanced oxidation processes involving ozone to eliminate atrazine. *Ozone : science & engineering.* Philadelphia, PA: Taylor & Francis.

PRUDEN, A. 2014. Balancing water sustainability and public health goals in the face of growing concerns about antibiotic resistance. *Environmental Science and Technology,* 48**,** 5-14.

PULLERITS, K., AHLINDER, J., HOLMER, L., SALOMONSSON, E., ÖHRMAN, C., JACOBSSON, K., DRYSELIUS, R., FORSMAN, M., PAUL, C. J. & RÅDSTRÖM, P. 2020. Impact of UV irradiation at full scale on bacterial communities in drinking water. *npj Clean Water,* 3**,** 11.

RECKHOW, D. A., LINDEN, K. G., KIM, J., SHEMER, H. & MAKDISSY, G. 2010. Effect of UV treatment on DBP formation. *Journal-American Water Works Association,* 102**,** 100-113.

RIZZO, L., MANAIA, C., MERLIN, C., SCHWARTZ, T., DAGOT, C., PLOY, M. C., MICHAEL, I. & FATTA-KASSINOS, D. 2013. Urban wastewater treatment plants as hotspots for antibiotic resistant bacteria and genes spread into the environment: A review. *Science of the Total Environment,* 447**,** 345-360.

SAMANIDOU, V. F., NISYRIOU, S. A. & PAPADOYANNIS, I. N. 2007. Development and validation of an HPLC method for the determination of penicillin antibiotics residues in bovine muscle according to the European Union Decision 2002/657/EC. *Journal of Separation Science,* 30**,** 3193-3201.

SANGANYADO, E. & GWENZI, W. 2019. Antibiotic resistance in drinking water systems: Occurrence, removal, and human health risks. *Science of The Total Environment,* 669**,** 785-797.

SANTOS-LOPEZ, A., MARSHALL, C. W., SCRIBNER, M. R., SNYDER, D. J. & COOPER, V. S. 2019. Evolutionary pathways to antibiotic resistance are dependent upon environmental structure and bacterial lifestyle. *ELife,* 8.

SAYED, M., ISMAIL, M., KHAN, S., TABASSUM, S. & KHAN, H. 2016. Degradation of ciprofloxacin in water by advanced oxidation process: Kinetics study, influencing parameters and degradation pathways. 1**,** 1-13.

SICILIANO, A., GUIDA, M., LIBRALATO, G., SAVIANO, L., LUONGO, G., PREVITERA, L., FABIO, G. & ZARRELLI, A. 2021. Amoxicillin in Water: Insights into Relative Reactivity, Byproduct Formation, and Toxicological Interactions during Chlorination. *Applied Sciences,* 11**,** 1076.

SIMAZAKI D, F. J., MANABE S, MATSUDA M, ASAMI M, KUNIKANE S 2008. Removal of selected pharmaceuticals by chlorination, coagulation-sedimentation and powdered activated carbon treatment. *Water Sci Technol.,* 58(5):1129-1135.

SIRÉS, I., BRILLAS, E., OTURAN, M. A., RODRIGO, M. A. & PANIZZA, M. 2014. Electrochemical advanced oxidation processes: today and tomorrow. A review. *Environmental Science and Pollution Research,* 21**,** 8336-8367.

SZABÓ, L., TÓTH, T., RÁCZ, G., TAKÁCS, E. & WOJNÁROVITS, L. 2016. Drugs with susceptible sites for free radical induced oxidative transformations: the case of a penicillin. *Free Radical Research,* 50**,** 26-38.

TIMM, A., BOROWSKA, E., MAJEWSKY, M., MEREL, S., ZWIENER, C., BRÄSE, S. & HORN, H. 2019. Photolysis of four β-lactam antibiotics under simulated environmental conditions: Degradation, transformation products and antibacterial activity. *Science of The Total Environment,* 651**,** 1605-1612.

TORRES-PALMA, R. A. & SERNA-GALVIS, E. A. 2018. Chapter 7 - Sonolysis. *In:* AMETA, S. C. & AMETA, R. (eds.) *Advanced Oxidation Processes for Waste Water Treatment.* Academic Press.

TREFI, S., GILARD, V., MALET-MARTINO, M. & MARTINO, R. 2007. Generic ciprofloxacin tablets contain the stated amount of drug and different impurity profiles: A 19F, 1H and DOSY NMR analysis. *Journal of Pharmaceutical and Biomedical Analysis,* 44**,** 743-754.

USLU, G., DEMIRCI, A. & REGAN, J. M. 2015. Efficacy of pulsed UV-light treatment on wastewater effluent disinfection and suspended solid reduction. *Journal of Environmental Engineering (United States),* 141.

VAFAEI, N., MARAT, K., ESKIN, M. N. A., REMPEL, C. B., JONES, P. J. H. & SCANLON, M. G. 2020. Nuclear magnetic resonance spectroscopy: a versatile tool for qualitative and quantitative analysis of an emulsifier mixture of soybean oil. *Journal of the American Oil Chemists' Society,* 97**,** 125-133.

VALLEJO, M., FRESNEDO SAN ROMÁN, M., ORTIZ, I. & IRABIEN, A. 2015. Overview of the PCDD/Fs degradation potential and formation risk in the application of advanced oxidation processes (AOPs) to wastewater treatment. *Chemosphere,* 118**,** 44-56.

VARMA, K. S., TAYADE, R. J., SHAH, K. J., JOSHI, P. A., SHUKLA, A. D. & GANDHI, V. G. 2020. Photocatalytic degradation of pharmaceutical and pesticide compounds (PPCs) using doped TiO2 nanomaterials: A review. *Water-Energy Nexus,* 3**,** 46-61.

VECITIS, C. D., SCHNOOR, M. H., SAIFUR RAHAMAN, M., SCHIFFMAN, J. D. & ELIMELECH, M. 2011. Electrochemical Multiwalled Carbon Nanotube Filter for Viral and Bacterial Removal and Inactivation. *Environmental science & technology.* Washington, DC: American Chemical Society.

VENIERI, D., KARAPA, A., PANAGIOTOPOULOU, M. & GOUNAKI, I. 2020. Application of activated persulfate for the inactivation of fecal bacterial indicators in water. *Journal of Environmental Management,* 261.

VENTER, H. 2019. Reversing resistance to counter antimicrobial resistance in the World Health Organisation's critical priority of most dangerous pathogens. *Bioscience reports,* 39.

VON SONNTAG, C. & VON GUNTEN, U. 2012. *Chemistry of ozone in water and wastewater treatment*, IWA publishing.

VOUKKALI, I. & ZORPAS, A. A. 2015. Disinfection methods and by-products formation. *Desalination and Water Treatment,* 56**,** 1150-1161.

WANG, B. & WANG, Y. 2022. A comprehensive review on persulfate activation treatment of wastewater. *Science of The Total Environment,* 831**,** 154906.

WANG, H., HU, C., LIU, L. & XING, X. 2017. Interaction of ciprofloxacin chlorination products with bacteria in drinking water distribution systems. *Journal of Hazardous Materials,* 339**,** 174-181.

WANG, J. & BAI, Z. 2017. Fe-based catalysts for heterogeneous catalytic ozonation of emerging contaminants in water and wastewater. *Chemical Engineering Journal,* 312**,** 79-98.

WANG, J., CHU, L., WOJNÁROVITS, L. & TAKÁCS, E. 2020. Occurrence and fate of antibiotics, antibiotic resistant genes (ARGs) and antibiotic resistant bacteria (ARB) in municipal wastewater treatment plant: An overview. *Science of The Total Environment,* 744**,** 140997.

WANG, J. & WANG, S. 2018. Activation of persulfate (PS) and peroxymonosulfate (PMS) and application for the degradation of emerging contaminants. *Chemical Engineering Journal,* 334**,** 1502-1517.

WANG, J. & ZHUAN, R. 2020. Degradation of antibiotics by advanced oxidation processes: An overview. *Science of The Total Environment,* 701**,** 135023.

WANG, P., LIU, S., WANG, X., CONG, Q. & LU, J. 2021. Assessment of the efficiency of synergistic photocatalysis on penicillin G biodegradation by whole cell Paracoccus sp. *Journal of Biological Engineering,* 15**,** 25.

WELTZIEN, H. U. & PADOVAN, E. 1998. Molecular features of penicillin allergy. *Journal of investigative dermatology,* 110**,** 203-206.

WILLACH, S., LUTZE, H. V., LÖPPENBERG, K., LÜLING, M., TERHALLE, J., WOLBERT, J. B., JOCHMANN, M. A., SCHMIDT, T. C., ECKEY, K. & KARST, U. 2017. Degradation of sulfamethoxazole using ozone and chlorine dioxide - Compound-specific stable isotope analysis, transformation product analysis and mechanistic aspects. *Water Research,* 122**,** 280-289.

XIAO, R., WEI, Z., CHEN, D. & WEAVERS, L. K. 2014. Kinetics and mechanism of sonochemical degradation of pharmaceuticals in municipal wastewater. *Environmental Science and Technology,* 48**,** 9675-9683.

XIAO, S., CHENG, M., ZHONG, H., LIU, Z., LIU, Y., YANG, X. & LIANG, Q. 2020. Iron-mediated activation of persulfate and peroxymonosulfate in both homogeneous and heterogeneous ways: A review. *Chemical Engineering Journal,* 384**,** 123265.

YANG, L., WANG, X., ZHU, D., ZHANG, Q., XI, T., LIU, D., NIU, J., HUANG, F., ZHAO, Y., QI, Z. & ZHAO, Z. 2020. Mechanism of Amoxicillin Degradation in Water Treated by Atmospheric-Pressure Air Microplasma. *IEEE Transactions on Plasma Science,* 48**,** 953-960.

YANG, W. & WU, T. 2019. Investigation of Matrix Effects in Laboratory Studies of Catalytic Ozonation Processes. *Industrial & Engineering Chemistry Research,* 58**,** 3468-3477.

YUKSEK, G., OKUTMAN TAS, D., UBAY COKGOR, E., INSEL, G., KIRCI, B. & ERTURAN, O. 2016. Effect of eco-friendly production technologies on wastewater characterization and treatment plant performance. *Desalination and Water Treatment,* 57**,** 27924-27933.

ZHANG, K., ZHOU, X., DU, P., ZHANG, T., CAI, M., SUN, P. & HUANG, C.-H. 2017a. Oxidation of β-lactam antibiotics by peracetic acid: Reaction kinetics, product and pathway evaluation. *Water Research,* 123**,** 153-161.

ZHANG, Y., RONG, C., SONG, Y., WANG, Y., PEI, J., TANG, X., ZHANG, R. & YU, K. 2017b. Oxidation of the antibacterial agent norfloxacin during sodium hypochlorite disinfection of marine culture water. *Chemosphere,* 182**,** 245-254.

ZHANG, Y., XIAO, Y., ZHONG, Y. & LIM, T.-T. 2019. Comparison of amoxicillin photodegradation in the UV/H2O2 and UV/persulfate systems: Reaction kinetics, degradation pathways, and antibacterial activity. *Chemical Engineering Journal,* 372**,** 420-428.

ZHOU, H., OUYANG, Q., PENG, M. & LI, W. 2011. Investigation on the reaction of ciprofloxacin and chlorine. *Zhongshan Daxue Xuebao/Acta Scientiarum Natralium Universitatis Sunyatseni,* 50**,** 79-84.

ZHUANG, Y., REN, H., GENG, J., ZHANG, Y., ZHANG, Y., DING, L. & XU, K. 2015. Inactivation of antibiotic resistance genes in municipal wastewater by chlorination, ultraviolet, and ozonation disinfection. *Environmental Science and Pollution Research,* 22**,** 7037-7044.

ZIĘBA, A., MAŚLANKIEWICZ, A. & SITKOWSKI, J. 2004. 1H, 13C and 15N NMR spectra of ciprofloxacin. *Magnetic Resonance in Chemistry,* 42**,** 903-904.

ZIEMBOWICZ, S. & KIDA, M. 2022. Limitations and future directions of application of the Fenton-like process in micropollutants degradation in water and wastewater treatment: A critical review. *Chemosphere,* 296**,** 134041.

ALDEEK, F., CANZANI, D., STANDLAND, M., CROSSWHITE, M. R., HAMMACK, W., GERARD, G. & COOK, J.-M. 2016. Identification of Penicillin G Metabolites under Various Environmental Conditions Using UHPLC-MS/MS. *Journal of Agricultural and Food Chemistry,* 64**,** 6100-6107.

ANDERSEN, N. H., EATON, H. L., NGUYEN, K. T., HARTZELL, C., NELSON, R. J. & PRIEST, J. H. 1988. 2D NMR studies of aminoglycoside antibiotics. Use of relayed coherence transfer for 1H resonance assignment and in situ structure elucidation of amikacin derivatives in reaction mixtures. *Biochemistry,* 27**,** 2782-90.

BERKANI, M., SMAALI, A., KADMI, Y., ALMOMANI, F., VASSEGHIAN, Y., LAKHDARI, N. & ALYANE, M. 2022. Photocatalytic degradation of Penicillin G in aqueous solutions: Kinetic, degradation pathway, and microbioassays assessment. *Journal of Hazardous Materials,* 421**,** 126719.

BRANCH, S. K., CASY, A. F. & OMINDE, E. M. A. 1987. Application of 1H nuclear magnetic resonance spectroscopy to the analysis of β-lactam antibiotics and their common degradation products. *Journal of Pharmaceutical and Biomedical Analysis,* 5**,** 73-103.

CANZANI, D. & ALDEEK, F. 2017. Penicillin G's function, metabolites, allergy, and resistance. 1**,** 28-40.

CHOUDHURY, H., GORAIN, B., PAUL, A., SARKAR, P., DAN, S., CHAKRABORTY, P. & PAL, T. K. 2017. Development and Validation of an LC-MS/MS-ESI Method for Comparative Pharmacokinetic Study of Ciprofloxacin in Healthy Male Subjects. *Drug Res (Stuttg),* 67**,** 94-102.

DALETOS, G., ANCHEEVA, E., ORFALI, R. S., WRAY, V. & PROKSCH, P. 2017. Structure Elucidation of Antibiotics by NMR Spectroscopy. *In:* SASS, P. (ed.) *Antibiotics: Methods and Protocols.* New York, NY: Springer New York.

DEIMEL, L. P., MOYNIÉ, L., SUN, G., LEWIS, V., TURNER, A., BUCHANAN, C. J., BURNAP, S. A., KOBRAS, C. M., STRACY, M., STRUWE, W. B., BALDWIN, A. J., NAISMITH, J., DAVIS, B. G. & SATTENTAU, Q. J. 2023. Haptenic adducts of β-lactam antibiotics elicit antibody responses with narrow clonality and specificity. *bioRxiv***,** 2023.11.02.565155.

DR. HOLZGRABE, U. 2010. Quantitative NMR Spectroscopy in Pharmaceutical R&D. *Progress in nuclear magnetic resonance spectroscopy,* 57**,** 229-40.

HOLZGRABE, U. 2015. Quantitative NMR Spectroscopy in Pharmaceutical R&D. *eMagRes.*

KAN, L. S., SCHWEIGHARDT, F. K., KAO, S. & LI, N. C. 1973. NMR study of interaction between several penicillins and nucleosides. *Journal of Magnetic Resonance (1969),* 9**,** 239-246.

KIM, T.-K., KIM, T., PARK, H., LEE, I., JO, A., CHOI, K. & ZOH, K.-D. 2020. Degradation of ciprofloxacin and inactivation of ciprofloxacin resistant E. faecium during UV-LED (275 nm)/chlorine process. *Chemical Engineering Journal,* 394**,** 124803.

L. RIAZ, M. A., Q. YANG, R. SAFEER, A. SIKANDAR, H. ULLAH, A. SHAHAB, W. YUAN, Q. WANG, 2020. Antibiotics and antimicrobial resistance eenes [electronic resource] : environmental occurrence and treatment technologies / Muhammad Zaffar Hasmi, editor. Springer.

LEE, H.-B., PEART, T. E. & SVOBODA, M. L. 2007. Determination of ofloxacin, norfloxacin, and ciprofloxacin in sewage by selective solid-phase extraction, liquid chromatography with fluorescence detection, and liquid chromatography–tandem mass spectrometry. *Journal of Chromatography A,* 1139**,** 45-52.

LEVY, S. B. & MARSHALL, B. 2004. Antibacterial resistance worldwide: causes, challenges and responses. *Nature Medicine,* 10**,** S122.

MANAIA, C. M. 2017. Assessing the Risk of Antibiotic Resistance Transmission from the Environment to Humans: Non-Direct Proportionality between Abundance and Risk. *Trends in Microbiology,* 25**,** 173-181.

MANAIA, C. M., ROCHA, J., SCACCIA, N., MARANO, R., RADU, E., BIANCULLO, F., CERQUEIRA, F., FORTUNATO, G., IAKOVIDES, I. C., ZAMMIT, I., KAMPOURIS, I., VAZ-MOREIRA, I. & NUNES, O. C. 2018. Antibiotic resistance in wastewater treatment plants: Tackling the black box. *Environment International,* 115**,** 312-324.

MATTA, M. K., CHOCKALINGAM, A., GANDHI, A., STEWART, S., XU, L., SHEA, K., PATEL, V. & ROUSE, R. 2018. LC-MS/MS based quantitation of ciprofloxacin and its application to antimicrobial resistance study in Balb/c mouse plasma, urine, bladder and kidneys. *Analytical Methods,* 10**,** 1237-1246.

MITSUMORI, F., ARATA, Y., FUJIWARA, S., MURANAKA, M. & HORIUCHI, Y. 1977. NMR Study of Spontaneous Degradation of Penicillin G in Aqueous Solution. *Bulletin of the Chemical Society of Japan,* 50**,** 3164-3166.

NETH, N., CARLIN, C. & KEEN, O. 2019. Emerging investigator series: Transformation of common antibiotics during water disinfection with chlorine and formation of antibacterially active products. *Environmental Science: Water Research & Technology,* 5.

PETROVIC, M., HERNANDO, M., DÍAZ-CRUZ, S. & BARCELO, D. 2005. Liquid Chromatography–Tandem Mass Spectrometry for the Analysis of Pharmaceutical Residues in Environmental Samples: A Review. *Journal of chromatography. A,* 1067**,** 1-14.

SAMANIDOU, V. F., NISYRIOU, S. A. & PAPADOYANNIS, I. N. 2007. Development and validation of an HPLC method for the determination of penicillin antibiotics residues in bovine muscle according to the European Union Decision 2002/657/EC. *Journal of Separation Science,* 30**,** 3193-3201.

SANGANYADO, E. & GWENZI, W. 2019. Antibiotic resistance in drinking water systems: Occurrence, removal, and human health risks. *Science of The Total Environment,* 669**,** 785-797.

SAWA, R., TAKAHASHI, Y., SAWA, T., NAGANAWA, H. & TAKEUCHI, T. 1994. Aldecalmycin, a new antimicrobial antibiotic from Streptomyces. II. Structure elucidation by NMR studies. *J Antibiot (Tokyo),* 47**,** 1273-9.

SHAH, A. D. 2009. Antibiotics in water treatment: the role of water quality conditions on their fate and removal during chlorination and nanofiltration.

SICILIANO, A., GUIDA, M., LIBRALATO, G., SAVIANO, L., LUONGO, G., PREVITERA, L., FABIO, G. & ZARRELLI, A. 2021. Amoxicillin in Water: Insights into Relative Reactivity, Byproduct Formation, and Toxicological Interactions during Chlorination. *Applied Sciences,* 11**,** 1076.

ZIĘBA, A., MAŚLANKIEWICZ, A. & SITKOWSKI, J. 2004. 1H, 13C and 15N NMR spectra of ciprofloxacin. *Magnetic Resonance in Chemistry,* 42**,** 903-904.